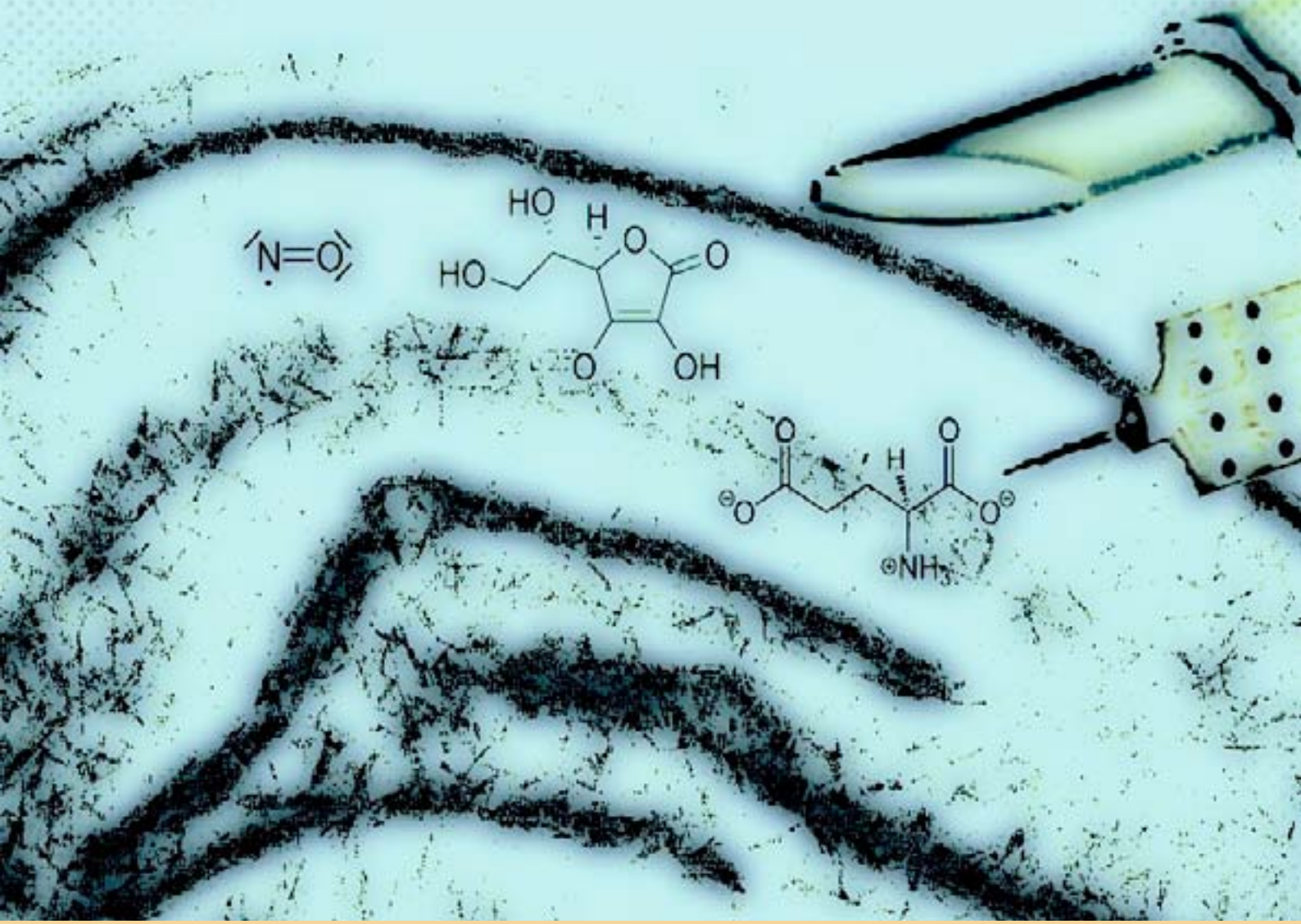

Nuno Ricardo Esteves Ferreira

The interplay of ascorbic acid, nitric oxide and nitrite in the brain and its role on the regulation of cerebral blood flow: an in vivo electrochemical study

Tese de Doutoramento em Ciências Farmacêuticas, área de especialização em Bioquímica, orientada pelos Professores Doutores João António Nave Laranjinha e Rui Manuel Silva Gomes Barbosa e apresentada à Faculdade de Farmácia da Universidade de Coimbra

Setembro 2015

· U C ·

Universidade de Coimbra

The interplay of ascorbic acid, nitric oxide and nitrite in the brain and its role on the regulation of cerebral blood flow: an *in vivo* electrochemical study

Nuno Ricardo Esteves Ferreira

Tese apresentada à
Faculdade de Farmácia da Universidade de Coimbra
para prestação de provas de Doutoramento em Farmácia,
na área de especialização em Bioquímica.

Este trabalho foi realizado no Centro de Neurociências e Biologia Celular e na Faculdade de Farmácia da Universidade de Coimbra sob orientação científica do Prof. Doutor João António Nave Laranjinha e do Prof. Doutor Rui Manuel Silva Gomes Barbosa

This work was supported by the fellowship SFRH/BD/65396/2009 and projects PEst-C/SAU/LA0001/2013-2014, PTDC/SAU-BEB/103228 and PTDC/BBB-BQB/3217/2012 funded by Fundação para a Ciência e Tecnologia

Agradecimentos

Acknowledgements

Os últimos cinco anos têm sido uma grande viagem em que passei momentos únicos. Para além da riquíssima vivência académica e profissional, tive também a felicidade de poder ser pai e de viver junto dos que mais amo. Estes fatores moldaram decisivamente a minha forma de encarar a ciência, tornando-me uma pessoa mais serena e focada na concretização dos seus objetivos. É por isso que neste momento me quero dirigir a todos aqueles que direta ou indiretamente contribuíram para este percurso que agora se conclui.

Desde logo, um agradecimento especial aos meus orientadores científicos Doutor João Laranjinha e Doutor Rui Barbosa por me terem trazido de volta ao ambiente académico, pela contínua motivação e pelo contributo determinante para o desenvolvimento científico deste trabalho. Obrigado por me contagiarem com o vosso entusiasmo, disponibilidade, espírito crítico e a genuína curiosidade característica de quem está na ciência. Foram vocês que me fizeram sempre acreditar neste projeto mesmo nos momentos em que a dúvida se instala e também me souberam manter os pés assentes no chão nos momentos de euforia.

Quero também agradecer aos meus amigos e colegas do laboratório Redox Biology and Brain Sensing – Ana, Cátia, Bárbara, Ricardo, Cassilda, Cândida, Gianni, João, Carla, Miguel, Marcelo, Sérgio. Foi convosco que partilhei o meu dia-a-dia e foram o meu suporte (científico e pessoal) para que o trabalho chegasse a bom porto. Aos docentes e auxiliares dos laboratórios de Bioquímica e Métodos Instrumentais de Análise da Faculdade de Farmácia da Universidade de Coimbra, um agradecimento pela gentileza com que sempre fui tratado.

Finalmente, o maior agradecimento vai para a minha família. À Elsa, ao Afonso, à Francisca e à Carolina desculpem pelos momentos em que devia estar convosco e não estive para poder apresentar hoje este trabalho. Vocês mostraram-me uma dimensão do amor que eu julgava não existir e são uma fonte de inspiração contínua e orgulho para mim. Aos meus pais, os melhores pais que alguma vez poderia imaginar, agradeço o amor incondicional e apoio, foram vocês que fizeram de mim o que sou hoje. À minha irmã um obrigado pelo carinho de sempre e pelo incentivo. Aos meus sogros e cunhados obrigado pelo apoio, afeto e disponibilidade.

Obrigado!

Index of illustrations

Index of tables

Contents

Abreviations and Symbols

20-HETE	20-hydroxyeicosatetraenoic acid
7-NI	7-nitroindazole
AA	arachidonic acid
ADMA	asymmetrical dimethyl L-arginine
AMPA	amino-3-hydroxy-5-methylisooxazole-4-propionic acid
ANLSH	astrocyte-neuron lactate shuttle hypothesis
AP	antero-posterior
ATP	adenosine-5'-triphosphate
BH_4	tetrahydrobiopterin
BSA	bovine serum albumin
CA	*cornu ammonis*
Cam	calmodulin
CBF	cerebral blood flow
CcO	cytochrome c oxidase
CFM	carbon fiber microelectrode
cGMP	cyclic guanosine-monophosphate
CI	confidence interval
CNS	central nervous system
CNTs	Carbon nanotubes
COX	cyclooxygenases
DG	dentate gyrus
DHA	dehydroascorbate
DMSO	dimethyl sulfoxide
DNA	Deoxyribonucleic acid
DV	dorso-ventral
EAAT	excitatory amino-acid transporter
ECF	extracellular fluid
EDRF	endothelial derived relaxing factor
EET	epoxyeicosatrienoic acids
eNOS	endothelial nitric oxide synthase
EPR	electron paramagnetic resonance
FAD	flavin adenine dinucleotide
FCV	fast cyclic voltammetry
FMN	flavin adenine mononucleotide
GABA	gamma-aminobutyric acid
GLUT	glucose transpoter
GSH	glutathione
GTP	guanosine-5'-triphosphate
HIF-1α	hypoxia inducible factor 1
iNOS	inducible nitric oxide synthase
iGluR	ionotropic glutamate receptors
ip	intraperitoneal
LDF	laser Doppler flowmetry
L-NHA	N-hydroxy-L-Arginine
L.O.D	limit of detection
LTD	long term depression
LTP	long term potentiation
MEA	Microelectrode array

mGluR	metabotropic glutamate receptor
ML	medio-lateral
mRNA	messenger ribonucleic acid
MWCNT	Multiwall carbon nanotube
NADH	reduced form of nicotinamide adenine dinucleotide
NADPH	reduced form of nicotinamide adenine dinucleotide phosphate
NMDA	N-methyl-D-aspartate
nNOS	neuronal nitric oxide synthase
$^{\bullet}NO$	nitric oxide
NOS	nitric oxide synthase
NVC	neurovascular coupling
OCT	optimal cutting temperature
$ONOO^{-\bullet}$	peroxynitrite
o-PD	*ortho*-phenylenediamine
PBS	phosphate buffer saline
PCB	Printed circuit board
PDE	phosphodiesterases
PDZ	post-synaptic density protein, discs-large, ZO-1
PGE	prostaglandins
PKG	cGMP-dependent protein kinases (also cGK)
PSD-95	post-synaptic density protein-95
PU	Perfusion unit
RNS	reactive nitrogen species
ROS	Reactive oxygen species
SD	spreading depression
SEM	standard error of the mean
sGC	soluble guanylate cyclase
SVCT	sodium-dependent vitamin C transporter
SWCNT	single wall carbon nanotube
SWV	Square wave voltammetry

Abstract

Ascorbate (the major form of ascorbic acid at physiologic pH) is highly concentrated in the brain, reaching 500 µM in the extracellular space and 10 mM intracellularly. It plays critical roles as a reductant, redox signaling molecule and modulator of processes linked to glutamate, the most prevalent excitatory neurotransmitter in the central nervous system (CNS), and whose dysregulation sets the background for neurodegenerative and mental disorders. Apparently, compartmentalization of ascorbate suffers dynamic and transient changes upon neural activity. Evidence suggests that ascorbate is released by a heteroexchange mechanism by which glutamate uptake triggers the outward transport of ascorbate. Thus, the concentration changes in response to neural activity rises the need for ascorbate and glutamate dynamic measurements.

In the brain, stimulation of NMDA glutamate receptors also leads to the activation of neuronal nitric oxide synthase (nNOS) and subsequent production of nitric oxide ($^{\bullet}NO$), a free radical transmitter involved in processes like memory formation, neurovascular coupling (NVC) and neurodegeneration. Available evidence that links ascorbate and $^{\bullet}NO$ metabolism was obtained mainly with *in vitro* systems and the literature is scarce about the dynamics and compartmentalization of ascorbate and $^{\bullet}NO$ upon glutamatergic stimulation *in vivo*. Moreover, the hypothesis that $^{\bullet}NO$ acts as a modulator of ascorbate release may help to understand some of the inconsistencies found with the heteroexchange mechanism for ascorbate release, revealing an additional player in the process of ascorbate release to the extracellular space.

The dynamic interplay between ascorbate, glutamate and $^{\bullet}NO$ is also determinant to satisfy the high energetic demand of the brain the constant supply of O_2 and glucose during neural activity. This is satisfied through the local and transient increase in cerebral blood flow (CBF), via the mechanism of neurovascular coupling (NVC). It has recently been shown that $^{\bullet}NO$ produced by nNOS mediates NVC in hippocampus under physiological conditions. However, when O_2 supply is diminished (e.g., stroke, ageing), this pathway is compromised and, under hypoxic and acidic conditions, extracellular nitrite emerges as a possible source of $^{\bullet}NO$ in the brain, in a process that involves its reduction by ascorbate and is independent of enzymatic control.

Given the above rationale, in the first part of this work we developed a carbon fiber microelectrode (CFM) modified with a composite film of carbon nanotubes and Nafion for ascorbate real time measurements in brain tissue *in vivo*. The CFM exhibited an electrocatalytic activity for ascorbate oxidation by shifting negatively the peak potential to -0.040 V *vs*. Ag/AgCl. Glutamate-evoked changes in ascorbate in the rat hippocampus were biphasic comprising fast and slow components and the estimated basal concentration was 290 µM. In the second part of

this work we coupled the use of the previously developed modified CFMs with ceramic-based Pt microelectrode arrays (MEAs) biosensors for simultaneous measurements of glutamate and ascorbate. *In vivo* experiments showed a delay (c.a 1 s) between the onset of glutamate and ascorbate signals, suggesting that ascorbate is released following the rise in concentration of extracellular glutamate. In the 5th chapter we tested the hypothesis that •NO produced upon NMDA receptor activation is a modulator of ascorbate release to the extracellular space. For that, we used CFMs for dynamic and simultaneous measurements of these substances in the hippocampus. Results showed that ascorbate and •NO signals had a high degree of correlation between them. Combined experiments encompassing direct stimulus with •NO and inhibitors of glutamate uptake and nNOS provided additional evidence supporting the modulator role of •NO in the release of ascorbate to the extracellular space. The observed coupling between •NO and ascorbate points to a functional impact on the activities of both compounds and lays the foundations for new regulatory mechanisms in the brain, although the precise molecular mechanism needs to be clarified.

In the last chapter we tested the possibility of nitrite becoming a non enzymatic source of •NO in the brain in a process that involves its reduction by ascorbate. We used an *in vivo* approach for measurements of •NO, ascorbate and CBF dynamics in the hippocampus. Results showed that the localized microinjection of nitrite in animals submitted to short-term acidosis (in the absence of glutamate stimulus) induced a transient increase of 90% in •NO signals. The maximum peak amplitude of CBF signals also increased 40%. Furthermore, it was observed a decrease in extracellular levels of ascorbate coupled in time with the production of •NO. Local ejection of ascorbate oxidase induced a decrease of 65% in terms of •NO signal maximum amplitude and a decrease of 63% in CBF signals. Results support that reduction of nitrite to •NO by ascorbate occurs in the brain and underlines NVC, being particularly relevant in conditions where the synthesis of •NO from nNOS is impaired due to limited availability of O_2. Finally, we observed a correlation between the supplementation with NO_2^- and NO_3^- and the increase in •NO and CBF signals, suggesting that the intake of food rich in NO_3^- (vegetables and fruit) may have a beneficial impact in brain perfusion, especially in ageing and other disorders that impair NVC.

Resumo

O ascorbato (principal forma do ácido ascórbico ao pH fisiológico) encontra-se em elevadas concentrações no cérebro, atingindo concentrações de 500 µM no espaço extracelular e 10 mM no interior dos neurónios. Esta molécula desempenha um papel muito importante como antioxidante, sinalizador redox e modulador de processos ligados à atividade glutamatérgica. O glutamato é o neurotransmissor excitatório mais prevalente no sistema nervoso central (CNS) e a sua desregulação está na base de diferentes doenças mentais e neurodegenerativas. Aparentemente, a compartimentalização do ascorbato sofre alterações transitórias e dinâmicas durante a atividade neuronal. A literatura sugere que o ascorbato é libertado das células por um mecanismo de "heteroexchange", no qual a internalização do glutamato extracelular se dá à custa da saída de ascorbato para o meio extracelular. Neste sentido, as alterações de concentração em resposta à atividade neuronal levantam a necessidade de efetuar medidas dinâmicas de ascorbato e glutamato.

No cérebro, a estimulação do recetor NMDA do glutamato conduz também à ativação da enzima óxido nítrico sintase neuronal (nNOS) e subsequente produção de óxido nítrico ($^{\bullet}NO$). Este radical livre está implicado em processos como a formação de memória, acoplamento neurovascular (NVC) e neurodegenerescência. A evidência disponível que liga o ascorbato com o $^{\bullet}NO$ foi obtida principalmente em sistemas *in vitro* e a literatura acerca da dinâmica do ascorbato e do $^{\bullet}NO$ após a estimulação *in vivo* com glutamato é escassa. Adicionalmente, a hipótese de que o $^{\bullet}NO$ produzido pode atuar como modulador da libertação de ascorbato ajuda a compreender melhor algumas inconsistências observadas no modelo de "heteroexchange" para a libertação do ascorbato, introduzindo um novo mediador no processo.

A interação dinâmica entre o ascorbato, glutamato e $^{\bullet}NO$ é determinante para satisfazer a elevada necessidade do cérebro em termos do aporte de O_2 e glucose durante a atividade neuronal. Esta é conseguida através do aumento local e transitório do fluxo sanguíneo (CBF), num processo chamado acoplamento neurovascular (NVC). Foi recentemente demonstrado que o $^{\bullet}NO$ produzido pela nNOS é um mediador do NVC no hipocampo em condições fisiológicas. No entanto, quando o aporte de O_2 diminui (por exemplo em situações de acidente vascular cerebral ou envelhecimento), esta via para a produção de $^{\bullet}NO$ fica comprometida e, nas condições hipóxicas e de acidose observadas nestas situações, o nitrito extracelular surge como uma fonte alternativa para a produção de $^{\bullet}NO$ no cérebro, num processo que envolve a sua redução pelo ascorbato e é independente de controlo enzimático.

Tendo em conta este racional, a primeira parte deste trabalho consistiu no desenvolvimento de um microeléctrodo de fibra de carbono (CFM) modificado com um filme compósito de nanotubos de carbono e Nafion para medições *in vivo* e em tempo real de ascorbato no cérebro. O CFM desenvolvido mostrou uma atividade catalítica para a oxidação do ascorbato, tendo desviado o valor de potencial de oxidação do ascorbato para -0.040 V *vs* Ag/AgCl. A estimulação com glutamato induziu alterações bifásicas na concentração extracelular do ascorbato e concentração basal de ascorbato extracelular foi estimada em 290 µM. Na segunda parte do trabalho os CFMs anteriormente desenvolvidos foram utilizados em conjunto com biossensores de glutamato (MEAs) para medidas simultâneas de ascorbato e glutamato. As experiências *in vivo* mostraram um atraso de c.a. de 1s entre o início do sinal de glutamato e de ascorbato, sugerindo que este é libertado para o espaço extracelular na sequência do aumento da concentração de glutamato. No 5º capítulo testámos a hipótese de que o •NO produzido após a ativação do recetor NMDA é um modulador da libertação de ascorbato para o espaço extracelular. Foram usados CFMs para realizar medidas simultâneas e dinâmicas destas duas substâncias no hipocampo. Os resultados mostraram que os sinais de ascorbato e •NO têm um elevado grau de correlação entre si. Foram também realizadas experiências que envolveram o estímulo direto com •NO e inibidores da re-captação do glutamato e da enzima nNOS que evidenciaram o papel modulador do •NO na libertação do ascorbato. O acoplamento observado entre o •NO e ascorbato aponta para um impacto funcional na atividade dos dois compostos e lança as bases para novos mecanismos reguladores no cérebro, ainda que sejam necessários estudos adicionais para esclarecer o mecanismo molecular.

No último capítulo testou-se a hipótese do nitrito ser uma fonte de •NO no cérebro através da sua redução pelo ascorbato. As experiências *in vivo* envolveram a medição dinâmica de •NO, ascorbato e CBF no hipocampo. Os resultados mostraram que a microinjeção local de nitrito em animais submetidos a acidose transitória levou a um aumento de 90% dos sinais de •NO e de 40% dos sinais de CBF. Adicionalmente, observou-se um decréscimo nos níveis extracelulares de ascorbato concomitante com o aumento de •NO. A ejeção local de ascorbato oxidase levou a um decréscimo de 65% nos sinais de •NO e 63% nos sinais de CBF. Os resultados suportam a redução do nitrito a •NO através do ascorbato no cérebro, constituindo-se como um processo alternativo para suporte do NVC, especialmente em situações em que a síntese de •NO através da nNOS esta comprometida devido à falta de O_2. Finalmente, foi observada uma correlação entre a suplementação com NO_2^- e NO_3^- e o incremento nos sinais de •NO e CBF, sugerindo que a ingestão de alimentos ricos em nitratos (fruta e vegetais) pode ser benéfica na perfusão cerebral, especialmente durante o envelhecimento e outras patologias que alterem o NVC.

1. INTRODUCTION

1.1. Ascorbic acid: Physico-chemical and biological properties

Ascorbic acid (Figure 1.1) is a water-soluble, hexonic sugar acid, with a molecular weight of 176.13.

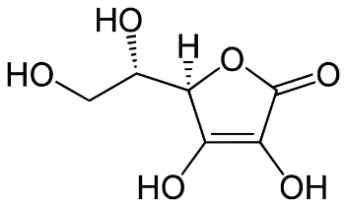

Figure 1.1. *Ascorbic acid chemical structure.*

It has two dissociable protons in –OH groups, with pK_a values of 4.2 and 11.8 (M DAVIES 1991), and, thus, is a monovalent anion, ascorbate, at physiological pH (Figure 1.2). Ascorbate is an excellent reducing agent and readily undergoes two consecutive, one-electron oxidations to form ascorbyl radical ($Asc^{\bullet -}$) and dehydroascorbic acid (DHA). The ascorbyl radical is relatively unreactive due to resonance stabilization of the unpaired electron; dismutating to ascorbate and DHA ($k_{obs}=2\times10^5\,M^{-1}\,s^{-1}$, pH 7.0).

$2\,Asc^{\bullet -} + H^+ \leftrightarrows$ Ascorbate $^-$ + Dehydroascorbic acid (**equation 1.1)**

These properties make ascorbate an effective donor antioxidant with an univalent redox potential of 282 mV (Buettner 1993, Du, Cullen et al. 2012). Most oxidizing free radicals (substances that have one unpaired electron) generated by biological systems can lead to the one-electron oxidation of ascorbate to form the ascorbyl radical, the reason why ascorbate is considered the ultimate reductant in the biological milieu (Buettner 1993). Thus, detection of ascorbyl radical by electron-spin resonance has been proposed as an index of oxidative cascades in vivo. This radical intermediate is also formed in enzymatic reactions that involve ascorbate as an electron donating co-factor.

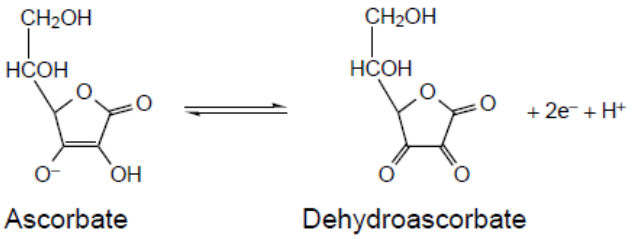

Figure 1.2. *Molecular structure of L-ascorbic acid as the monovalent anion, ascorbate, and its oxidation product, dehydroascorbate (DHA) (formed by the loss of two electrons and a proton).*

Ascorbate oxidizes readily, with the rate of oxidation dependent on pH and accelerated by catalytic metals (Buettner and Jurkiewicz 1996). In the absence of catalytic metals, the spontaneous oxidation of ascorbate is quite slow at pH 7.0 (Buettner 1988). In an air-saturated phosphate buffer (pH 7.0), it has been estimated that the observed pseudo-first-order rate constant for the autoxidation of ascorbate is on the order of 10^{-7}– 10^{-6} s^{-1} at pH 7.0 (Buettner 1988), consistent with a rate constant of ≈300 M^{-1} s^{-1} for the true autoxidation of ascorbate (Du, Cullen et al. 2012). Thus, true autoxidation is indeed very slow and in most laboratory settings, oxidation of ascorbate is catalyzed by adventitious catalytic metals in the buffers as well as metals that enter the buffer for laboratory equipment (Buettner 1988, Buettner 1990). In near-neutral buffers with contaminating metals, the oxidation and subsequent loss of ascorbate can be very rapid and this may be a concern when preparing ascorbate solutions.

1.2. Ascorbate and the brain

Only a small number of species of higher organisms is incapable of synthetizing ascorbate, but one of them includes *Homo sapiens* and humans depend for vitamin C mainly on fruit and vegetables, unless a synthetic supplement is taken (M DAVIES 1991). Despite playing several roles in many organs, ascorbate is specially needed in the brain and central nervous system (May 2012). It is one of the most abundant low molecular weight antioxidants in the CNS (Lyrer, Landolt et al. 1991) and its concentrations in mammalian brain are higher than in any other organs except adrenal cortex and the pituitary (Mefford, Oke et al. 1981). Under normal conditions, turnover of ascorbate in brain is about 2% per hour. Under conditions of ascorbate deficiency, however, brain ascorbate content is retained tenaciously, with decreases of less than 2% per day (Rice 2000). Ascorbate concentration is heterogeneous and regional differences in humans (Schaus 1957, Mefford, Oke et al. 1981, Oke, May et al. 1987) and in rodents (Stamford, Kruk et al. 1984, Ferris, Kume-Kick et al. 1995, Harrison, Yu et al. 2008) have been reported, and in more detail within specific brain areas (Basse-Tomusk and Rebec 1991). In the rat, highest levels of ascorbate are found in the amygdala, hippocampus and hypothalamus. In man, nucleus accumbens and hippocampus have the highest concentrations, with lowest levels in substantia nigra, and a gradient of ascorbate concentration has been demonstrated within some brain nuclei, for example those of the thalamus. Although some degree of compartmentalization of intracellular ascorbate must occur, subcellular fractionation of brain homogenates has been unable to demonstrate that ascorbate is concentrated in nerve terminals or vesicles. Assuming even distribution within cells, concentration ranges from 1 to 2.6 mM in fresh brain tissue (Grunewald 1993).

1.2.1. Ascorbate and glutamate

Beyond its antioxidant role, ascorbate is linked to glutamate (Figure 1.3), the major mediator of excitatory signals in the mammalian central nervous system and that is probably in most aspects of normal brain function including cognition, memory and learning (Fonnum 1984, Headley and Grillner 1990). Glutamate also plays major roles in the development of the central nervous system, including synapse induction and elimination, and cell migration, differentiation and death. The total concentration of glutamate in the brain is elevated, but its distribution is uneven. Most neurons, and even glial cells have glutamate receptors in their plasma membranes. Further, glutamate plays a signaling role also in peripheral organs and tissues as well as in endocrine cells (Moriyama, Hayashi et al. 2000).

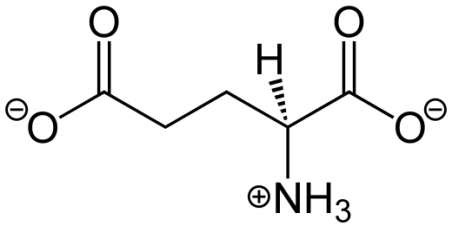

Figure 1.3. *Chemical structure of L-glutamate.*

Glutamate exerts its signaling role by acting on receptors that are located on the surface of the cells expressing them. Glutamate receptors are divided into three families: One family of glutamate receptors is activated by the analogue N-methyl-D-aspartate (NMDA) and these receptors (NR1, NR2A, NR2B, NR2C and NR2D) are collectively referred to as NMDA-receptors. Another family of receptors is activated by α-amino-3-hydroxy-5-methyl-4-isoxazole propionic acid (AMPA) and by kainate. According to their preference for AMPA or kainate, these receptors are further subdivided into AMPA-receptors (GluR1–4) and kainate receptors (GluR5–9, KA1 and KA2). The NMDA and AMPA/kainate receptors are all glutamate gated ion channels (conducting only Na^+ or both Na^+ and Ca^{2+}) and are collectively referred to as ionotropic glutamate receptors. The AMPA receptors open readily upon glutamate exposure, but desensitize quickly (Tang, Dichter et al. 1989, Trussell and Fischbach 1989) and are of low affinity (Patneau and Mayer 1990).

In contrast, the NMDA receptors have much higher affinities and are slowly inactivating. To be activated they need both glutamate binding and an already depolarized membrane. In fact, they require both glutamate and glycine (co-agonist) for activation and have a relatively high Ca^{2+} permeability. In addition, NMDA receptors are characterized by a voltage-sensitive block of the ion channel by extracellular magnesium (Mg^{2+}), which renders the receptor inactive at resting membrane potentials. The third family of glutamate receptors consists of G-protein coupled

receptors, the so-called metabotropic receptors (mGluR1–8) which are subdivided into groups I (mGluR1 and mGluR5), II (mGluR2 and mGluR3) and III (mGluR4, mGluR6, mGluR7 and mGluR8). Group I receptors are coupled to phospholipase C and thereby to inositol triphosphate and diacylglycerol production, whereas groups II and III are negatively coupled to adenylate cyclase (Danbolt 2001).

Usually, L-glutamate concentration in the extracellular fluid (ECF) is around 2 µM (Day, Pomerleau et al. 2006). As a consequence, the concentration gradient of glutamate across the plasma membranes is several thousand-fold. It should be noted that the distribution of glutamate is in a dynamic equilibrium which is highly sensitive to changes in the energy supply. Firstly, glutamate will leak out of the cells if the cells run out of energy. Secondly, there is a rapid turnover of glutamate since it is continuously being released from cells and continuously removed from the extracellular fluid.

Glutamate must be removed from the entire extracellular space because glutamate receptors are found on most of the cellular elements (dendrites, nerve terminals, neuronal cell bodies as well as glial cells). Thus, it is not only a question of keeping a low resting concentration inside the synaptic clefts, but also outside the clefts (extrasynaptically). The only known way to rapidly remove glutamate from the extracellular fluid surrounding the receptors is by cellular uptake. This is accomplished by means of glutamate transporter proteins (present in both neurons and glial cells) which use the electrochemical gradients across the plasma membranes as driving forces for uptake. Because of the high rates of glutamate release, inhibition of glutamate uptake leads to high extracellular levels of glutamate within seconds (Jabaudon, Shimamoto et al. 1999). Originally, these transporters were referred to as the 'sodium-dependent high-affinity transporters' to distinguish them from the 'low-affinity transporters'. However, since their affinities are not particularly high (K_m-values being 1–100 µM) and because they are driven by the gradients of both Na^+ and K^+, the preferred term is now 'sodium and potassium coupled glutamate transporters' or 'excitatory amino acid transporters' (EAATs) (Danbolt 2001).

1.2.2. Ascorbate influx

The observed high levels of ascorbate in the brain are achieved by specific uptake mechanisms, which concentrate it from the bloodstream to cerebrospinal fluid (CSF) and from CSF to intracellular compartment. This uptake involves active, stereospecific, sodium-dependent transport at the choroid plexus by a transporter called SVCT2 (sodium-dependent vitamin C transporter-2, Slc23a2). In rat brain, this process accumulates ascorbate in CSF to a concentration up to 500 µM (Rice 2000, Harrison and May 2009).

Ascorbate can enter neurons and glia from the interstitial space by 1) transport of ascorbate on the SVCT2 and 2) oxidation of ascorbate to DHA and uptake of DHA on the GLUTs and subsequent intracellular reduction. Neurons likely use both mechanisms to maintain intracellular ascorbate, although transport on the SVCT2 contributes the most to amplifying the ascorbate concentration gradient from CSF to neurons (Tsukaguchi, Tokui et al. 1999, Sotiriou, Gispert et al. 2002). In contrast to neurons, ascorbate uptake in supporting glial cells in the brain does not appear to involve the SVCT2 (Berger, Lu et al. 2003). In astrocytes and glial supporting cells lacking the SVCT2, DHA uptake and reduction may be the only mechanism of ascorbate uptake. Although glia may not normally express the SVCT2, oxidant stress due to ischemia-reperfusion injury has been shown to increase SVCT2 mRNA expression in both neurons and glia (Berger, Lu et al. 2003).

1.2.3. Ascorbate efflux

In addition to its movement into neurons and glial cells, ascorbate is also released from both cell types. This release of ascorbate contributes to a homeostatic mechanism for maintaining extracellular rat brain ascorbate at 200-400 μM (Rice 2000). Ascorbate release from astrocytes and neurons has been linked in numerous studies to uptake of glutamate on one or more of its specific transporters (O'Neill, Fillenz et al. 1984, Cammack, Ghasemzadeh et al. 1991, Miele, Boutelle et al. 1994, Sandstrom and Rebec 2007), in a process initiated either by activation of glutamatergic pathways or by direct infusion of glutamate.

1.2.3.1. The heteroexchange mechanism

A heteroexchange model has long been considered to explain the ability of glutamate uptake to cause ascorbate release (Cammack, Ghasemzadeh et al. 1991, Rebec and Pierce 1994). High-affinity transporters for the amino acid neurotransmitters operate in both inward and outward directions (Bernath 1992). Thus, in addition to re-uptake of the neurotransmitter, these carrier proteins also transport either the neurotransmitter itself (homoexchange) or another substance (heteroexchange) in an outward direction. The concept that ascorbate is released by heteroexchange at the glutamate transporter grew out of a series of experiments measuring ascorbate efflux from synaptosomal, homogenate, and mince preparations of brain tissue (Milby, Mefford et al. 1981, Bigelow, Brown et al. 1984, Grunewald and Fillenz 1984). Like established neurotransmitters, ascorbate was found to be released by depolarizing stimuli. However, ascorbate release occurred independently of calcium, indicating that ascorbate release appears to occur from a non-vesicular source. Thus, although neuronal depolarization promotes the release of ascorbate, this process differs from the vesicular release of established neurotransmitters. A critical role for the glutamate transporter emerged from research on synaptosomes prepared from brain regions known to receive dense glutamatergic innervation. Addition of L-, but not D-,

glutamate to cortical, hippocampal, and neostriatal synaptosomes was found to evoke the release of ascorbate, and this effect was blocked by the removal of sodium (Grunewald and Fillenz 1984). Moreover, glutamate-evoked ascorbate release is unaffected by glutamate receptor antagonists but blocked completely by drugs known to prevent the operation of the glutamate transporter (Grunewald and Fillenz 1984). Collectively, these results indicate that the uptake of glutamate is accompanied by the outward transport of ascorbate.

1.2.3.2. Other mechanisms for ascorbate efflux

However, heteroexchange on a single transporter is not supported, since ascorbate does not cause release of radiolabeled glutamate from synaptosomes (Grunewald 1993). The mechanism of glutamate-induced ascorbate release was subsequently elucidated by Wilson and colleagues. It was known from earlier studies that glutamate transport, which also brings sodium into the cell, causes swelling of primary culture astrocytes (Staub, Peters et al. 1993). Wilson's group showed that such astrocyte swelling in turn causes release of ascorbate from the cells, an effect due to opening of volume-sensitive organic anion channels (Siushansian, Dixon et al. 1996). A subsequent paper by the same group (Wilson, Peters et al. 2000) showed clearly that glutamate uptake could be dissociated from ascorbate release by astrocytes in primary culture. Glutamate-induced ascorbate release has also been demonstrated in neuronal cells (May, Li et al. 2006). Additional efflux mechanisms have been proposed for ascorbate as displayed in figure 1.4 (Corti, Casini et al. 2010).

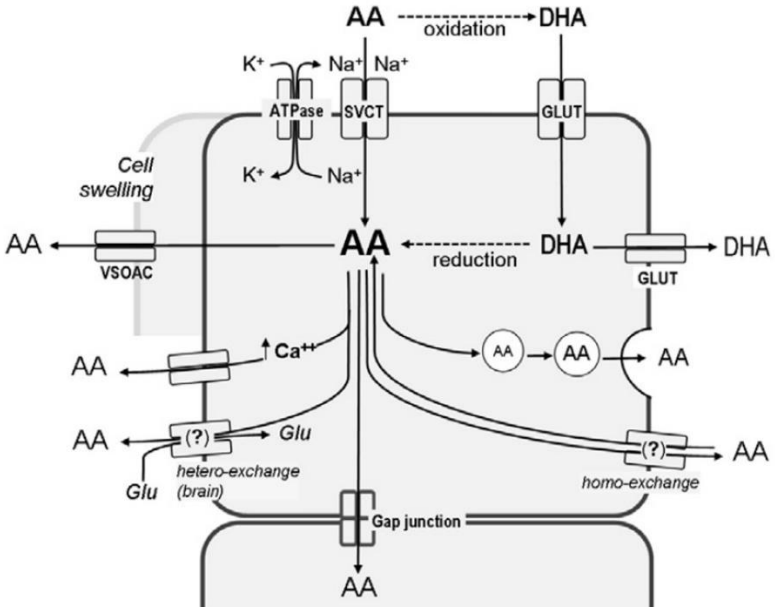

***Figure 1.4**. Ascorbate transport and efflux across cell plasma membrane. Ascorbate can be transported inside cells both as ascorbate and DHA. Ascorbate is transported by means of two sodium-ascorbate co-transporters (SVCT), thanks to the differential concentrations of sodium ion across the plasma membrane maintained by Na^+/K^+-ATPase. DHA is transported by a facilitated-diffusion mechanism mediated by GLUT transporters, and is rapidly reduced to ascorbate intracellularly. In conditions overwhelming the reducing abilities of cells, DHA may also exit the cell through the same GLUT transporters. Several pieces of evidence suggested that, once inside the cells, ascorbate may also be released as such, through as yet not fully characterized mechanisms. A glutamate–ascorbate hetero-exchange (in brain) and an ascorbate–ascorbate homo-exchange (various cell types) have been proposed. Anion channels can mediate ascorbate release and, in particular, a role for volume sensitive anion channels and intracellular Ca^{2+}-sensitive anion channels has been suggested. Finally, the involvement of gap-junction hemichannels and the exocytosis of ascorbate-containing vesicles were also proposed, to justify ascorbate sharing between coupled cells or to explain the release of ascorbate contained in chromaffin granules (Corti, Casini et al. 2010).*

1.2.4. Functions of ascorbate

The functions of this molecule in the CNS and brain are numerous. The high levels of ascorbate and of SVCT2 in a variety of neuronal cell types imply a function for neuronal ascorbate beyond its actions as a cell-specific enzyme cofactor. Importantly, the tenfold difference between ascorbate levels in neurons and glia (Rice and Russo-Menna 1998) is consistent with the estimated tenfold higher rate of oxidative metabolism in neurons compared with glial cells. Its importance as an intracellular antioxidant is further supported by the finding that brain ascorbate (but not glutathione) levels in pond turtles are two to three times higher than in mammals (Rice, Lee et al. 1995).

1.2.4.1. Ascorbate and neurotransmission

Ascorbate is essential for catecholamine biosynthesis in neural tissues, serving as a co-factor for dopamine β- hydroxylase in the conversion of dopamine to norepinephrine (Diliberto and Allen 1980, Diliberto and Allen 1981). Ascorbate has been proposed to function as a neuromodulator of both dopamine and glutamate-mediated neurotransmission (Grunewald 1993, Rebec and Pierce

1994). More recent studies relating ascorbate modulation of glutamate dynamics with changes in rat behavior show that such modulation is complex, since it depends on the site in the brain studied, level of behavioral activity, and level of extracellular ascorbate (Kiyatkin and Rebec 1998, Rebec, Witowski et al. 2005, Sandstrom and Rebec 2007). Ascorbate has been shown to protect neurons from excitotoxicity induced by activation of the NMDA receptor and it prevented glutamate-induced cell damage and death in cultured cerebellar granule cells (Ciani, Groneng et al. 1996, Atlante, Gagliardi et al. 1997). The mechanism(s) by which ascorbate affects neuronal transmission have not been established, but could relate in part to redox changes in the *N*-methyl-D-aspartate (NMDA) receptor (Majewska, Bell et al. 1990), or to direct scavenging of ROS generated by receptor activation.

1.2.4.2. Ascorbate effects on behavior, learning, memory, and locomotion

Animal behavior studies involving ascorbate treatments have focused on two major areas, learning/memory and locomotor activity. Most of the positive effects of ascorbate follow parenteral administration of the vitamin (typically intraperitoneal injection), since much higher effective doses can be given by this route compared to oral administration. Intraperitoneal ascorbate (125 mg/kg) reversed memory deficits in mice induced both by age and scopolamine treatment in a transfer latency task in the elevated plus maze and a passive avoidance task (Parle and Dhingra 2003) and in a habituation-based task in a light-dark paradigm (de Angelis and Furlan 1995). When ascorbate was given orally for 30 days (300mg/kg) in conjunction with vitamin E in aged mice (15 months), it also improved performance on a passive avoidance task. In contrast, long-term low levels of dietary ascorbate did not lead to impairments in learning and memory or anxiety in gulonolactone oxidase knockout mice that are unable to synthesize their own vitamin C (Harrison, Yu et al. 2008) despite an approximately 75% reduction in brain ascorbate. Further, different doses of ascorbate and different dosing regimens used within these experiments rarely reflected a clear pattern of results or obvious dose-response relationships. Notwithstanding the negative results, it seems possible that ascorbate could be a mediator of learning and memory, especially stress related learning, although the exact circumstances under which it has nootropic (cognitive enhancing) abilities are as yet unclear.

1.2.4.3. Ascorbate and neurometabolism

For many years, glucose has been thought to be almost the sole metabolic fuel for brain cells. In the last 15 years, this view has changed. Attention has been focused on the role of monocarboxylates in supporting brain activity, with the ANLSH (Magistretti, Pellerin et al. 1999, Pellerin, Bouzier-Sore et al. 2007) providing a new view of brain energetics. The ANLSH proposes that under resting conditions, neurons consume glucose, while during synaptic activity, they

preferentially consume lactate. During glutamatergic synaptic activity, astrocytes remove glutamate from the synaptic cleft to ensure the success of synaptic transmission (Choi 1988). Glutamate uptake in astrocytes stimulates glucose, glycolysis and lactate efflux (Pellerin and Magistretti 1994, Demestre, Boutelle et al. 1997). Glutamate uptake or activation of glutamate ionotropic receptors stimulates ascorbate release from astrocytes (Wilson, Peters et al. 2000, Portugal, Miya et al. 2009). Ascorbate enters neurons and inhibits glucose consumption (Castro, Pozo et al. 2007) at the same time it stimulates lactate uptake in neurons (Castro, Angulo et al. 2008), that in turn, is metabolized to CO_2 and water to sustain neural function (Fowler 1993, Castro, Pozo et al. 2007). Even though the mechanism of ascorbate effect remains to be understood, the metabolic switch of ascorbate is consistent with the ANLSH and it gives an explanation of how neurons consume lactate when expressing GLUTs and glycolytic enzymes.

1.2.4.4. Excitotoxicity

Another important function of ascorbate might be to prevent redox imbalance from reactive oxygen species (ROS) generated by activation of glutamate receptors (Dykens, Stern et al. 1987, Coyle and Puttfarcken 1993, Lafon-Cazal, Pietri et al. 1993). Both NMDA and kainate can cause depolarization of mitochondria and increased production of superoxide. Ascorbate buffers glutamate-generated ROS and limit consequent cell death in cultured neurons (Ciani, Groneng et al. 1996, Atlante, Gagliardi et al. 1997). An intracellular site of action for these effects was suggested by other studies in brain slices, in which both ascorbate and glutamate-receptor antagonists were shown to inhibit edema formation (Brahma, Forman et al. 2000). There are several possible mechanisms for ascorbate protection against glutamate-induced cell death. Direct scavenging of ROS is likely to have the greatest role, because ascorbate can protect neurons from oxidative damage and decrease levels of glutamate-generated ROS (Sato, Saito et al. 1993, Sharma 1997). In addition, however, glutamate–ascorbate heteroexchange might provide protection by facilitating glutamate uptake or by increasing ascorbate concentration, either of which could minimize excitotoxic consequences of glutamate release (Miele, Boutelle et al. 1994). Finally, ascorbate has also been suggested to decrease NMDA-mediated currents by acting at the redox modulatory site of the NMDA receptor (Majewska, Bell et al. 1990).

1.2.5. Ascorbate recycling

In all of its known functions, ascorbate serves as one-electron donor, generating the ascorbate free radical, or monodehydroascorbate. This one-electron oxidized form of ascorbate is stable and can be detected at 10 nM concentrations in biological fluids by EPR (Coassin, Tomasi et al. 1991, Mehlhorn 1991, Buettner and Jurkiewicz 1993). Ascorbate recycling from both of its oxidized forms occurs largely within cells, although cell-surface reduction of its radical one electron-

oxidized form has been described (May, Qu et al. 2000, VanDuijn, Tijssen et al. 2000). Instead of donation of another hydrogen and electron, the preferred reaction is for two molecules of the ascorbate free radical to dismutate, forming ascorbate and DHA. The latter is unstable at physiologic pH, with a half-life of about 6 min (Winkler 1987). Hydrolysis of the lactone ring irreversibly converts DHA to 2,3-diketo-1-gulonic acid (Bode, Cunningham et al. 1990). Ascorbate loss by DHA decomposition is obviously wasteful of the vitamin, and DHA reduction to ascorbate is rapid and efficient within cells. Mechanisms of GSH-dependent DHA reduction include direct chemical reduction (Winkler, Orselli et al. 1994) and enzyme-dependent reduction with GSH serving as electron donor (Maellaro, Del Bello et al. 1994, Winkler, Orselli et al. 1994, Washburn and Wells 1999). DHA is also reduced to ascorbate with high affinity by both NADH-dependent reductases (Ito, Hayashi et al. 1981, Villalba, Canalejo et al. 1993) and by the NADPH-dependent enzyme thioredoxin reductase (May, Cobb et al. 1998). All these cellular systems provide redundant and efficient mechanisms for recycling of ascorbate from its oxidized forms (May 2012).

1.3. Potential therapeutic functions of vitamin C in neurodegenerative disorders

Neurons appear to be especially sensitive to ascorbate deficiency, and this neuronal sensitivity is most apparent when ascorbate supply is low in conditions in which there is excess oxidant stress. The involvement of reactive oxygen species in neurodegenerative disorders explains the enthusiasm for ascorbate as an antioxidant therapeutic approach, although its complicated interactions with neurotransmitter systems as described above make it difficult to discern the specific mechanisms involved.

1.3.1. Alzheimer's disease

Alzheimer's disease is caused by a combination of genetic and lifestyle factors and it is established that oxidative stress plays a key role in the pathogenesis of the disease contributing to the degeneration of the basal forebrain cholinergic system and general cell death (Montine, Neely et al. 2002, Pratico 2002). Alzheimer's disease patients have been found to have lower plasma ascorbate levels despite adequate nutritional intake (Riviere, Birlouez-Aragon et al. 1998). Positive relationships have been shown between ascorbate supplement use and reduced disease incidence (Morris, Beckett et al. 1998) and also with disease-related markers of oxidative stress, although these beneficial results are not universal (Luchsinger, Tang et al. 2003, Fillenbaum, Kuchibhatla et al. 2005). Interpretation of the data is hindered by the nature of the studies as population or epidemiological studies have high levels of variability inherent in their design.

Despite the large amount of information that can be collected from participants, and complicated statistical techniques that can be used to control for variability in the data, individual differences can still have a significant influence on results. Nevertheless, there is further evidence to support the potential for vitamin C as a therapeutic avenue for Alzheimer's disease (Huang and May 2006).

1.3.2. Parkinson's disease

Parkinson's disease involves severe decreases in dopaminergic signaling in the central nervous system, specifically the motor cortex. Given the range of data presented above concerning the relationship between ascorbate and dopaminergic function it is understandable that ascorbate is being investigated for its therapeutic potential in this disease. Although population studies concerning ascorbate intake show no protection against development of Parkinson's disease (Zhang, Hernan et al. 2002), there are a number of lines of evidence that suggest that ascorbate as a pharmacological agent may be of more benefit. Ascorbate has been shown to improve bioavailability of levodopa (which can then be converted into dopamine) in members of an elderly Parkinson's disease population with low baseline bioavailability for levodopa (Nagayama, Hamamoto et al. 2004).

1.3.3. Huntington's disease

Huntington’s disease (HD) is an autosomal dominant condition caused by an expanded tri-nucleotide (CAG) repeat, which results in the increased length of a poly-glutamine (polyQ) tract in the huntingtin protein (1993). Huntingtin is widely expressed throughout the nervous system, and, accordingly, all brain regions show some atrophy in HD. The most pronounced neuronal pathology, however, strikes the medium spiny neurons of the striatum. In an interesting extension of evidence that striatal ascorbate is essential for normal behavioral output (Rebec and Wang 2001), mice that model HD suffer from a loss of ascorbate in striatal extracellular fluid (Rebec, Barton et al. 2002). In addition, some of the neurological motor signs that these mice display improve upon reversal of the ascorbate deficit (Rebec, Barton et al. 2003). Although these lines of evidence suggest that a deficit in striatal ascorbate release plays a key role in HD, the mechanism underlying this effect is unclear. In view of evidence that ascorbate release is linked to glutamate uptake, it is possible that low extracellular ascorbate simply indicates a glutamate uptake problem. Although a failure of glutamate uptake and the accompanying loss of extracellular ascorbate may comprise critical components of the neuropathological cascade in HD, it is important to recognize that a restoration of striatal ascorbate attenuates both behavioral and firing-rate abnormalities in mouse models of HD (Rebec 2007).

1.4. Ascorbate, nitric oxide and the coupling with glutamate receptor

Besides the close interaction of glutamatergic signaling with ascorbate release, glutamate stimulation also triggers the production of nitric oxide (•NO), a diffusible intercellular messenger with wide-range impact in the brain, ranging from neurotransmission to neurodegeneration and neurovascular coupling (Garthwaite and Boulton 1995, Dawson and Dawson 1998, Lindauer, Megow et al. 1999, Kitaura, Uozumi et al. 2007). •NO and ascorbate have important redox interactions: ascorbate can reduce oxidant stress mechanisms and increase functional •NO synthesis by 1) promoting the degradation of the endogenous NOS inhibitor asymmetrical dimethyl L-arginine (ADMA) (Sydow and Munzel 2003), 2) stabilizing and increasing the synthesis of NOS cofactors (tetrahydrobiopterin, BH_4) (Toth, Kukor et al. 2002), and 3) by inhibiting the arginase pathway that competes for the common NOS substrate L-arginine (Santhanam, Lim et al. 2007).

1.4.1. Nitric oxide biology

•NO is a small free radical synthesized by a family of nitric oxide synthases (NOS). In the brain, •NO is mainly synthesized in synaptic terminals and acts a diffusible intercellular messenger with biological actions that range from neurotransmission to neurodegeneration and neurovascular coupling (Garthwaite and Boulton 1995, Dawson and Dawson 1998, Lindauer, Megow et al. 1999, Kitaura, Uozumi et al. 2007). Its radical nature, small size and hydrophobicity support the notion that •NO lacks specific interactions with receptors and the outcome of these interactions is dictated by its concentration dynamics, ranging from physiological to pathological effects that may ultimately lead to cell death. The very unique •NO signaling results from its particular physical and chemical properties in a biological setting as compared with other signaling molecules.

1.4.2. Physical and chemical properties of nitric oxide: their relevance for the bioactivity

•NO is a gaseous molecule with a water solubility of ≈ 2 mM at 293 K and 1 atm (Zacharia and Deen 2005). •NO can rapidly diffuse in aqueous media due to its small size, having a diffusion coefficient in water between 2.0-4.5 x 10^{-5} cm^2/s. In addition, the small dipolar moment (0.12 D) (Gijsbertsen, Siu et al. 2007) supports that this molecule can easily diffuse across cell membranes. This unusual ability implies that signaling adaptations that are common to the most signaling molecules, including vesicle storage and exocytose, membrane receptor recognition and intracellular uptake would be meaningless in the modulation of •NO signaling processes. The hydrophobicity of •NO results in a much higher solubility in lipid structures like cellular

membranes than in hydrophilic media (Moller, Botti et al. 2005). Interestingly, •NO is oxidized to nitrite by O_2 following the reaction mechanism indicated by equations. 1.2-1.4.

$2\ {}^{\bullet}NO + O_2 \rightarrow 2\ {}^{\bullet}NO_2$ **(equation 1.2)**

${}^{\bullet}NO_2 + {}^{\bullet}NO \rightarrow N_2O_3$ **(equation 1.3)**

$N_2O_3 + H_2O \rightarrow 2\ NO_2^- + 2H^+$ **(equation 1.4)**

This reaction is third order overall and second order relative to •NO, meaning that the •NO half-life depends on its concentration (Kharitonov, Sundquist et al. 1994). Considering a third order rate constant $k = 6.3 \times 10^6\ M^{-2}\ s^{-1}$ in aqueous solution, at physiological levels of the reactants (•NO in nM range and ≈ 20 μM O_2) the reaction is slow but seems to be significantly accelerated in hydrophobic milieu due to preferential partition of both gases in that phase (Liu, Miller et al. 1998). Thus, the lipid environment of cell membranes provides a location where the reaction between •NO and O_2 is favored, with the consequent formation of high nitrogen oxides (note that the reaction in Eq. 1.3 does not occur in the hydrophobic phase), involved in nitrosation and nitration reactions with relevance in physiology and pathology (Hill, Dranka et al. 2010).

The majority of biologically relevant •NO reactions with heme proteins involves ferrous iron (Wink and Mitchell 1998). For instance, the binding of •NO to ferrous heme activates the enzyme soluble guanylyl cyclase (sGC), which is the best characterized signaling target of •NO and inhibits cytochrome c oxidase, a crucial enzyme for mitochondrial respiration (Cooper and Giulivi 2007, Garthwaite 2008). These interactions are both very rapid, with rate constants of $2\text{-}4 \times 10^7\ M^{-1}s^{-1}$ (Cooper 1999). Due to the abundance of hemoglobin in the vasculature, this constitutes the main sink of •NO and affects •NO dynamics at the neighboring tissues.

•NO can readily react with other free radicals but does not easily react with most biological molecules (Hill *et al.*, 2010). Actually, the rapid reaction of •NO with alkoxy or peroxy radicals formed in biological membranes (Eq. 1.6) suggests that, under certain conditions, •NO is an antioxidant, leading to the termination of lipid peroxidation chain reactions in biomembranes and lipoproteins (Rubbo *et al.*, 2002) thereby protecting cells against peroxide and lipoprotein induced cytotoxicity. This effect seems to be important in limiting lipid peroxidation in diseases such as atherosclerosis (Thomas *et al.*, 2008).

${}^{\bullet}LOO + {}^{\bullet}NO \rightarrow LOONO$ **(equation 1.5)**

For opposite reasons, the reaction between •NO and the superoxide radical ($O_2^{\bullet-}$) assumes particular importance in •NO biochemistry (Eq. 1.6). The reported rate constants of this reaction can be up to 1.9 x 10^{10}, meaning that it is limited by how fast the molecules encounter each other (diffusion limited) (Hill, Dranka et al. 2010). The product generated is the strong nitrating and oxidant peroxynitrite, which has been shown to mediate most of the deleterious effects of •NO in cells, including protein and lipid oxidation/nitration and DNA damage (Wink and Mitchell 1998, Thomas, Ridnour et al. 2008).

$^{\bullet}NO + O_2^{\bullet-} \rightarrow ONOO^-$ **(equation 1.6)**

In summary, the unique physical and chemical properties of •NO result in a remarkable range of interactions with biological targets, indicating a singular dynamics of signaling *in vivo.* Next, the processes that determine •NO concentration dynamics and its signaling pathways *in vivo* with special relevance to the brain will be overviewed.

1.4.3. Biosynthesis of nitric oxide

1.4.3.1. Overview of nitric oxide synthase isoforms

In biological systems, •NO is mainly produced by a family of enzymes named nitric oxide synthases (NOS), and they are highly regulated. These enzymes are dimers constituted by an oxygenase and reductase domain, separated by a calmodulin-binding motif which plays a key role in both the structure and function of the enzyme. The oxygenase domain also contains a binding site for BH_4, another important cofactor participating as a redox mediator in the catalytic cycle. NOS use O_2 and NADPH to transform L-arginine to L-citrulline and •NO (Alderton, Cooper et al. 2001). So far, three major members of the NOS family, products of three distinct genes, have been purified and biochemically characterized: neuronal NOS (nNOS, also termed NOS1 or NOS-I), inducible NOS (iNOS, also termed NOS2 or NOS-II) and endothelial NOS (eNOS, also termed NOS3 or NOS-III). A fourth isoform was suggested to exist, the mitochondrial NOS (mtNOS) (Tatoyan and Giulivi 1998). However, it is now assumed as an isoform of nNOS present in the inner mitochondrial membrane. These enzymes have different physiologic functions, their enzymatic activity may be differently regulated and they also exhibit distinct cellular and subcellular localization (Guix, Uribesalgo et al. 2005). Generally, nNOS and eNOS isoforms are Ca^{2+}-calmodulin-dependent enzymes constitutively expressed in mammalian cells (Mungrue, Bredt et al. 2003), that upon activation by Ca^{2+} through transient binding to calmodulin, generate increments of •NO lasting for seconds-minutes. In turn, iNOS regulation depends on de novo synthesis, which occurs following immunological or inflammatory stimulation in macrophages, astrocytes, microglia and other cells,

producing high amounts of •NO lasting, according to current paradigms, for hours or days (Ebadi and Sharma 2003).

1.4.3.2. Nitric oxide synthase catalytic cycle and reaction kinetics

•NO is synthesized by NOS in two cycles consisting in the conversion of L-Arginine to N-hydroxy-L-Arginine (L-NHA) which is then processed to citruline and •NO. In the first catalytic cycle, one O_2 molecule, which binds to the ferrous heme in the active center, and two electrons supplied by NADPH are required to convert L-arginine to L-NHA. In the second cycle, one electron from NADPH and another O_2 molecule are consumed with the consequent formation of •NO and citruline from the intermediate L-NHA that remained bound to the enzyme (Alderton, Cooper et al. 2001, Li and Poulos 2005). Figure 1.5 shows the stoichiometry of the reactions catalyzed by NOS.

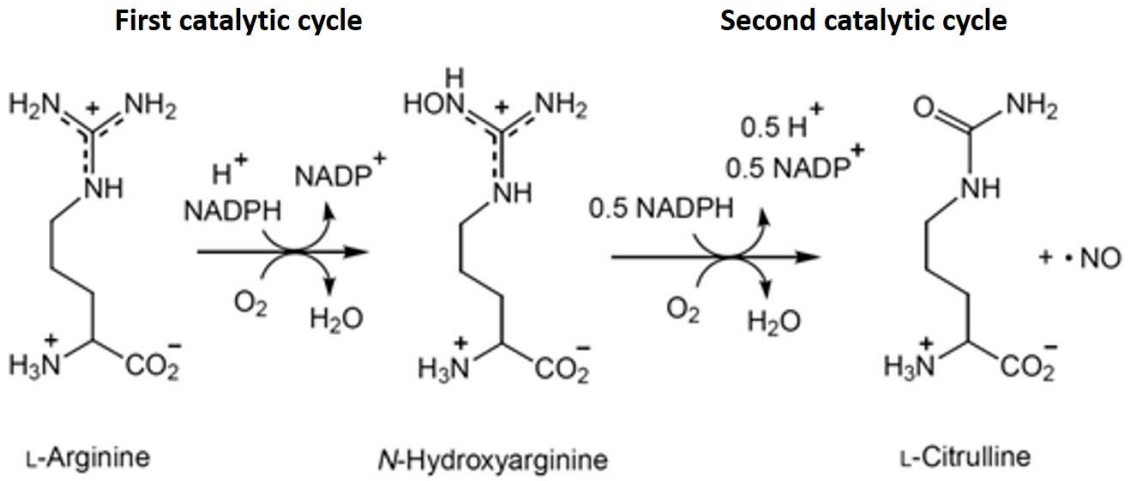

Figure 1.5. *Reactions catalyzed by NOS.*

1.4.4. Nitric oxide synthesis in the brain

The first evidences for a functional link between activation of NMDAr and •NO production in several brain regions (Garthwaite and Boulton 1995) have been reinforced by the demonstration of a physical association between NMDAr and nNOS (Brenman, Chao et al. 1996). Furthermore, co-localization of NMDAr and nNOS has been observed in post-synaptic terminals in the hippocampus (Burette, Zabel et al. 2002). These studies support the notion that a major physiologic trigger for •NO synthesis in the brain is the activation of NMDAr by L-glutamate.

The NMDAr channel allows the flux of Na^+ and K^+ and is also highly permeable to Ca^{2+} (Mayer and Armstrong 2004) but, at resting membrane potentials, extracellular magnesium (Mg^{2+}) ions bind tightly to the NMDAr channel, preventing further ionic flow. A membrane depolarization of sufficient amplitude is required to counteract the driving force that maintains Mg^{2+} ions bound to

the channel. This can be achieved by glutamate activation of AMPAr, which activate much faster than NMDAr. This causes brief depolarizations that last no longer than a few milliseconds, thus allowing Ca^{2+} influx through NMDAr (Blanke and VanDongen 2009). Hence, NMDAr seem to be tuned to integrate and transduce incoming synaptic activity into post-synaptic Ca^{2+} currents. The physical proximity between the NMDAr channel and nNOS accounts for an efficient induction of •NO production following NMDAr activation (Figure 1.6).

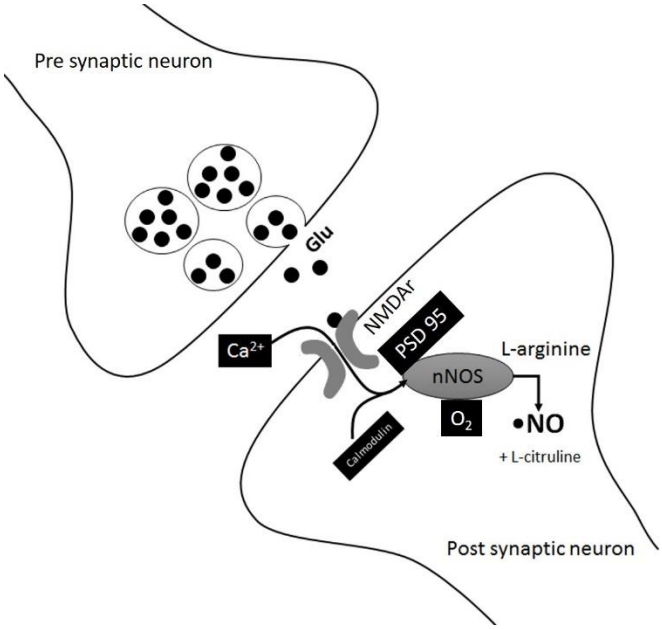

Figure 1.6. *Functional coupling of glutamate NMDA receptor with nitric oxide synthase and •NO signaling pathways. The interaction of NMDA receptor with NOS via PSD-95 facilitates •NO synthesis following Ca^{2+} influx. Adapted from (Ledo, Frade et al. 2004).*

1.4.5. •NO signaling and molecular targets in the brain

•NO is an unconventional neurotransmitter as, unlike the classical neurotransmitters, it is not stored in synaptic vesicles in order to exert its effects as a paracrine messenger, being synthesized on demand by neurons, and its lifetime is not terminated by presynaptic re-uptake or by enzymatic degradation. Furthermore, •NO does not interact specifically with membrane receptors. In turn, its biological effects are determined by its reactivity, rather than protein receptor-ligand interactions (Pacher, Beckman et al. 2007).

The best characterized molecular target for •NO is the soluble guanylate cyclase (sGC). •NO selectively binds to this heterodimeric protein, even in the presence of micromolar concentrations of O_2, to form a stable •NO–heme complex (Stone and Marletta 1995). The formation of such complex is thought to induce a conformational change in the protein leading to enzyme activation and up to 200-fold increase in the synthesis of cGMP from GTP (Stone and Marletta 1994). The •NO-induced cGMP signal is conveyed intracellularly by the activation of several effector

molecules: cGMP-dependent protein kinases (PKGs or cGK), cGMP-regulated phosphodiesterases (PDEs) and cGMP-gated ion channels. It was reported the ability of •NO to promote S-nitrosylation of sGC, leading to a reduction in •NO-stimulated sGC activity (Sayed, Baskaran et al. 2007), thus contributing as a mechanism of •NO signaling termination. However, •NO signaling pathways may involve several other cellular and molecular targets, such as the mitochondria and ion channels.

1.4.6. Nitric Oxide in physiological and pathological pathways

•NO is able to modulate a wide range of physiological processes such as such as learning and memory, neural differentiation and development, nociception, anxiety and neurovascular coupling (Dawson and Dawson 1998). •NO appears to modulate neuronal function by affecting specific ion channels, which, in turn, change the firing rate, the threshold of action potentials and the ability of neurons to respond to excitatory and inhibitory signals (Steinert, Kopp-Scheinpflug et al. 2008). Additionally, there are several lines of evidence suggesting •NO involvement in learning and memory mechanisms through mediation of specific forms synaptic plasticity, namely long term potentiation (LTP) in hippocampus and cerebral cortex and long term depression (LTD) in cerebellum and striatum (Bon and Garthwaite 2003). Additionally, •NO has been shown to participate in the regulation of monoamine-mediated neurotransmission (Kiss and Vizi 2001). Among several other physiological pathways, •NO has also been implicated in the regulation of cerebral blood flow, and more controversially in the coupling of increased local blood flow to neural activity.

Besides its participation in important physiological functions, •NO has also been implicated in pathological processes associated with several neurodegenerative disorders, such as Alzheimer's disease, Parkinson's disease, amyotrophic lateral sclerosis (ALS), Huntington's disease and ischemic brain injury (Guix, Uribesalgo et al. 2005, Knott and Bossy-Wetzel 2009). The pathways by which •NO exerts its pathological role are only partially different from those involved in its physiological actions but are associated to other stress conditions and higher •NO concentrations, globally involving 1) production of RNS and induction of nitrosative stress, 2) S-nitrosylation of protein thiols and nitration, 3) lipid peroxidation, 4) mitochondrial impairment, 5) neuronal damage and 6) inflammation (Contestabile, Monti et al. 2003).

1.4.7. Coupling between neuronal activity and cerebral blood flow – the role of •NO

Despite of comprising only 2% of the body's mass, brain accounts for 20% of resting O_2 consumption (Magistretti, Pellerin et al. 1999, Magistretti 2006). In addition, brain requires a continuous supply of blood flow carrying the substrates necessary to maintain its functional and

structural integrity due to the lack of substrate storage, high metabolic rate and sensitivity to O_2 deprivation, (Iadecola 2004). Cerebrovascular dysregulation has been found to be associated to several pathological conditions, such as Alzheimer's disease, hypertension and stroke due to decrease O_2 and glucose uptake by neurons (Girouard and Iadecola 2006). To sustain a proper neuronal function the increase of blood flow in regions with more intense activity, and thus with more metabolic demands, is satisfied through the local and transient increase in cerebral blood flow (CBF) via a mechanism called functional hyperemia or neurovascular coupling (NVC), thus establishing a tight link between neuronal activity and blood flow. Neurons, glia and blood vessels exhibit a close anatomical and functional coupling, forming the neurovascular unit (Woolsey, Rovainen et al. 1996, del Zoppo and Mabuchi 2003). A very important aspect of the NVC mechanism is the observed coupling in terms of space, time and amplitude between the increase in neuronal activity and CBF (Iadecola 2004). Interestingly, this mechanism was firstly suggested by Roy and Sherrington more than one century ago (Roy and Sherrington 1890) when they observed that "*chemical products of cerebral metabolism…can cause variations of the calibre of the cerebral vessel*" and proposed that the brain possessed an "*intrinsic mechanism by which its vascular supply can be varied locally in correspondence with local variations in functional activity*". Even though there are several evidences suggesting the occurrence of the NVC mechanism, the exact mechanism is still a matter of debate. The search for mediators focused on two distinct lines of research*:* 1) the identification of individual mediators, including ions, neurotransmitters, and metabolic factors and 2) the cellular coordination of the process via intercellular communication among neurons, astrocytes, and vascular cells (Attwell and Iadecola 2002, Iadecola 2004). Nowadays, there is substantial evidence indicating that exogenous glutamate or selective glutamate receptor agonists dilate pial arterioles and/or precapillary microvessels. In contrast to cerebellum, this effect in hippocampus and neocortex does involve NMDA-type glutamate receptors (Fergus and Lee 1997, Lovick, Brown et al. 1999). Because glutamate is not vasoactive in isolated cerebral arteries, it is unlikely that this transmitter is directly responsible for relaxation of vascular smooth muscles and vasodilation. Instead, vasodilation should be mediated by vasoactive factors whose synthesis is triggered by the changes in intracellular Ca^{2+} associated with glutamate receptor activation.

Soon after the identification of $^{\bullet}NO$ as the EDRF and as a neuromodulator (Garthwaite, Charles et al. 1988), it has emerged as a candidate to mediate neurovascular coupling (Iadecola 1993) since it fulfills the characteristics expected for a mediator of the coupling between the neuronal activity and blood flow increases as it is 1) a potent vasodilator, 2) released during enhanced neuronal activity and NMDA receptor activation and 3) a highly diffusible molecule. Further studies support

that •NO, once produced by neurons, is able to reach by diffusion smooth muscle cells of arterioles and induce vasodilation (Ledo, Barbosa et al. 2005). Initial suggestions about the involvement of •NO in the neurovascular coupling arose from the observations that vasoactive actions of glutamate were inhibited by NOS inhibitors, both in hippocampal brain slices (Lovick, Brown et al. 1999) and *in vivo* using a cranial window approach (Faraci and Breese 1993, Pelligrino, Gay et al. 1996). Coherently, similar results were reported when somatosensory stimulation (Dirnagl, Lindauer et al. 1993) was used to evoke NVC, respectively in cerebral and cerebellar cortex. Further supporting the role of •NO in the NVC, CBF changes in cerebellar cortex evoked by electric stimulation were reported to be significantly lower in nNOS-deficient mice (Yang, Zhang et al. 2003). However, authors also reported that those CBF changes were reduced by NOS inhibitors in wild-type mice but not in the knockout, speculating that •NO-independent mechanisms mediate the NVC in mice lacking expression of neuronal NOS. More recently, it has been shown that NVC in hippocampus is mediated via diffusion by neuronal-derived •NO (Faraci and Breese 1993, Lourenco, Santos et al. 2014). In contrast to the reports supporting the •NO involvement in the NVC in regions as cerebellum, cerebral cortex and hippocampus, other reports suggest a secondary role for •NO as modulator of other pathways suggested to mediate the process. Some studies using somatosensory stimulation reported the absence of effect of NOS inhibitors over CBF increases suggesting the lack of •NO-mediated effects (Wang, Kjaer et al. 1993, Greenberg, Sohn et al. 1999). Other studies reported that although •NO is required for NVC, at least in somatosensory cortex, it does not directly mediate the neuron to vessels signals (Lindauer, Megow et al. 1999), but rather act as a modulator of other pathways (Gordon, Mulligan et al. 2007).

The seek for NVC mediators culminated in a current paradigm that establishes astrocytes bridging neuronal activity and changes in CBF (Attwell, Buchan et al. 2010), and the major pathways by which glutamate can regulate CBF during NVC are summarized in figure 1.7.

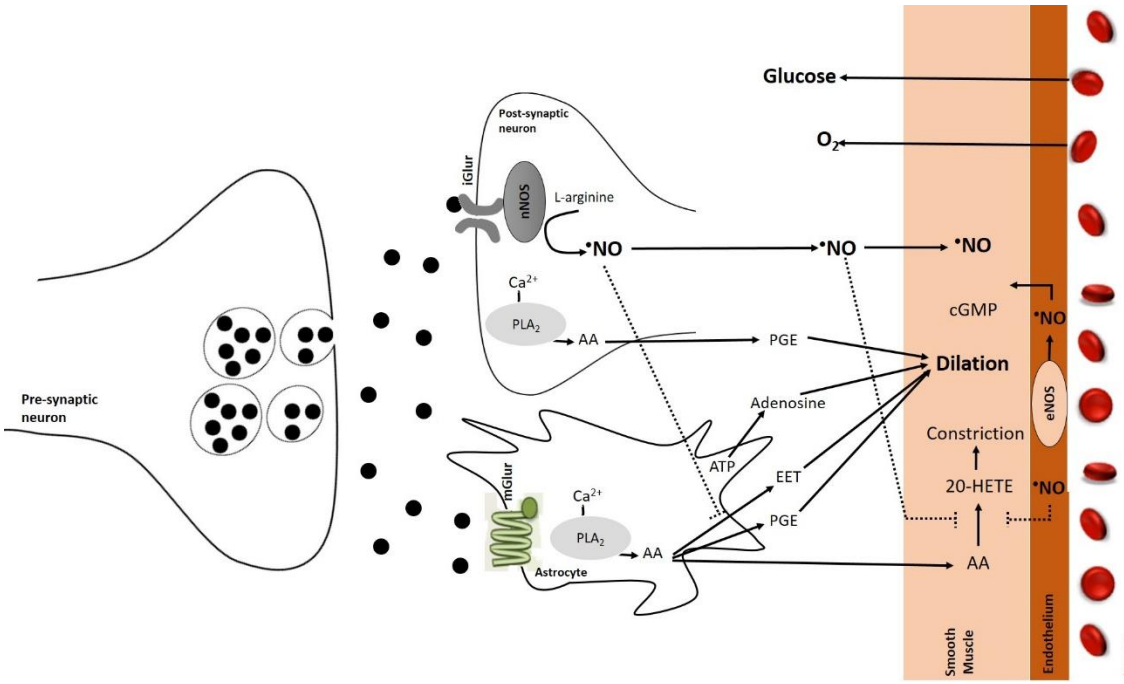

Figure 1.7. *Major pathways by which glutamate, activating neurons and astrocytes, can regulate cerebral blood flow (CBF), controlling the supply of oxygen and glucose. Adapted from (Marques 2011).*

In neurons, glutamate acts on ionotropic glutamate receptors (iGluR), causing nNOS to release •NO, which activates sGC in smooth muscle cells (SMC), promoting dilation. Activation of iGluR, by raising [Ca^{2+}] may also generate arachidonic acid (AA) from phospholipase A_2 (PLA_2), which is converted by COX2 to prostaglandins (PGE) which may also promote vasodilation. In astrocytes, glutamate by activating metabotropic glutamate receptors (mGluR), can generate AA and thus three types of metabolites: prostaglandin (by COX1/3, and COX2 in pathological situations) and EETs (by P450 epoxygenase) in astrocytes, which dilate vessels, and 20-HETE (by ω-hydroxylase) in smooth muscle cells, which constricts vessels. •NO can inhibit the production of both the vasoconstricting 20-HETE and the vasodilating EET. eNOS, activated by flow-induced shear stress, also produces •NO which can regulate CBF. Adenosine derived from the breakdown of ATP utilized by neuronal activity can also promote vasodilation (Attwell, Buchan et al. 2010).

1.4.8. Nitrite and nitric oxide in the central nervous system

Upon its synthesis via NOS, •NO may embark in reactions with biomolecular targets, being ultimately neutralized into the supposedly inert oxidation products nitrite and nitrate (Moncada and Higgs 1993). Both anions have been disregarded as inert products devoid of physiological relevance but it is now accepted that nitrate and nitrite may be stepwisely reduced back to •NO *in vivo* (Benjamin, O'Driscoll et al. 1994, Lundberg, Weitzberg et al. 1994, Zweier, Wang et al. 1995, Gago, Lundberg et al. 2007).This principle has driven the hypothesis that nitrite participates in

hypoxic vasodilation and in the regulation of oxygen consumption at the mitochondrial level. It also predicts a role for nitrite in cytoprotective signaling in the setting of pathological ischaemia and reperfusion (Lundberg, Weitzberg et al. 2008). The bioactivation of nitrate from dietary or endogenous sources requires its initial reduction to nitrite, and because mammals lack specific and effective nitrate reductase enzymes, this conversion is mainly carried out by commensal bacteria in the gastrointestinal tract and on body surfaces (Duncan, Dougall et al. 1995, Lundberg and Govoni 2004). Once nitrite is formed, there are numerous pathways in the body for its further reduction to •NO, involving hemoglobin (Cosby, Partovi et al. 2003), myoglobin (Shiva, Huang et al. 2007), xanthine oxidoreductase (Millar, Stevens et al. 1998), polyphenols (Gago, Lundberg et al. 2007), protons (Benjamin, O'Driscoll et al. 1994) and ascorbate (Carlsson, Wiklund et al. 2001). The generation of •NO by these pathways is greatly enhanced during hypoxia and acidosis, thereby ensuring •NO production in situations for which the oxygen-dependent NOS enzyme activities are compromised (Giraldez, Panda et al. 1997). Interestingly, the l-arginine–NOS pathway is oxygen dependent, whereas the nitrate → nitrite→•NO pathway is gradually activated as oxygen tensions falls. In this sense, NOS-independent •NO formation can be viewed as a back-up system to ensure that there is sufficient •NO formation when oxygen supply is limited, which is analogous to the complementary role of anaerobic glycolysis in energetics.

Presley et al have shown that a high nitrate diet increases the blood flow in specific brain areas in older subjects (Presley, Morgan et al. 2011), introducing the notion that nitrate available from the diet may impact on brain homeostasis. However, the mechanistic details that bridge dietary nitrate and brain function remain largely elusive. As afore mentioned, upon a nitrate load there is an increase of both nitrate and nitrite concentration in blood and tissues, but how (and if) is nitrite converted into •NO in the brain and what is the impact in brain functions such as cognition, neurovascular coupling and memory formation remains to be elucidated. •NO not only regulates oxygen availability in tissues (via mitochondrial actions described above) but also bridges neuronal activity with local changes of blood flow in the microcirculation of the brain, a process known as neurovascular coupling (Attwell and Iadecola 2002). Under hypoxia, it is expectable that the activity of NOS (and, in particular nNOS) is highly attenuated and, consequently, we would expect that the decreased production of •NO translates into subsequent impairment of blood flow and compromised vasodilation. However, apparently, NOS inactivation during hypoxia does not block vasodilation (Millar 1995). This observation adds to several others, including the viability of mice lacking all three isoforms of NOS (Milsom, Fernandez et al. 2012), to suggest the occurrence of alternative and/or complementary pathways to ensure that tissues get the needed amount of •NO, regardless of the functional state of the enzymes usually involved in its synthesis. In this

scenario, the possibility that dietary nitrite/nitrate may contribute to basal levels of •NO signaling emerges as a plausible possibility yet poorly investigated in the brain. This interaction becomes particularly relevant in maintaining the balance between •NO production, oxygen consumption and neurovascular coupling in the brain. Nitrite has shown to increase blood flow preferentially in hypoxic conditions, allowing its increase precisely where it is needed most (Rifkind, Nagababu et al. 2007, Piknova, Kocharyan et al. 2011).

1.4.8.1. Nitric oxide/ nitrite/ ascorbate cycle in the brain

As referred previously, ascorbate is a powerful reducing agent highly concentrated in the brain, both in the extracellular fluid and cells, namely neurons and astrocytes. Ascorbate is present at even higher concentrations in areas such as the hippocampus where •NO has been shown to play critical roles in learning and memory processes and neurovascular coupling (Lourenco, Santos et al. 2014). In addition, there is ascorbate release from neuronal cells to the extracellular fluid upon glutamatergic stimulation. Given the abundance of ascorbate, nitrite pool in the brain (obtained through the diet and /or •NO oxidation) may be reduced back to •NO, emerging as an alternative mechanism for •NO production in the brain completely independent of enzymatic control. This would be particularly important in hypoxia, because (a) the low of oxygen compromises NOS activity and (b) during hypoxia, local pH may drop to values near 6.4 an adequate milieu for •NO production to occur (Pereira, Ferreira et al. 2013). The kinetics and magnitude of nitrite disproportionation have been recently characterized and the corresponding rate law of •NO formation derived. It was observed that the generation and accumulation of •NO from typical nitrite concentrations found in biological tissues increases 100-fold when the pH falls from 7.4 to 5.5. The existence of this enzyme-independent mechanism of •NO formation has important implications in our understanding of how •NO signaling occurs in situations where nNOS activity is compromised (e.g. ischemia, hypoxia, acidosis) (Zweier, Samouilov et al. 1999).

1.5. The choice of hippocampus as the preferred location for recording ascorbate, glutamate and nitric oxide signals in the brain

The hippocampus is part of a functional system called the hippocampal formation, being usually divided in three sub-regions: CA3, CA2, and CA1. (CA - *cornu ammonis*). The other regions of the hippocampal formation include the dentate gyrus (DG), subiculum, and entorhinal cortex (Andersen 2007). On contrary to the synaptic connections between neurons in other brain

regions, the connections that link the various parts of the hippocampal formation are largely unidirectional, as observed in figure 1.8 (Andersen 2007).

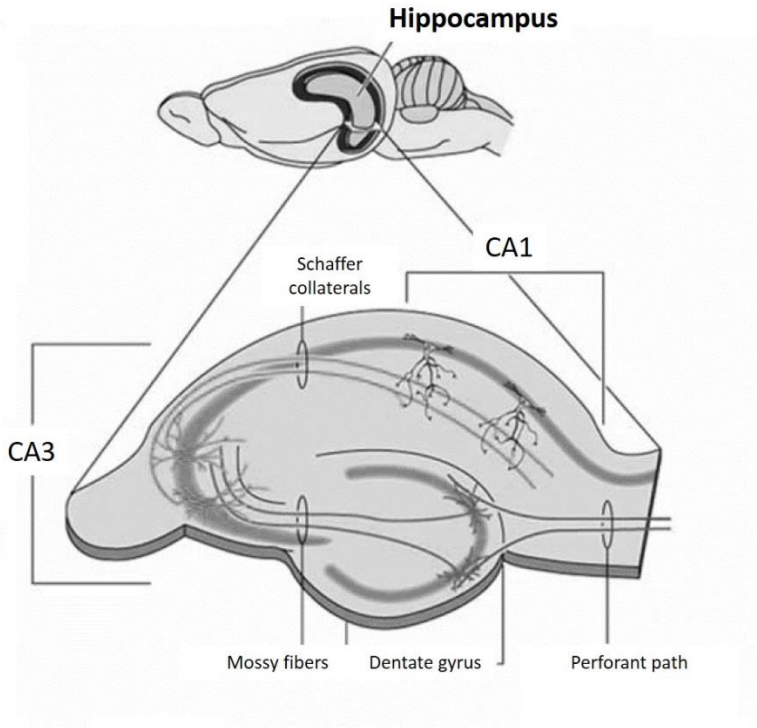

Figure 1.8. *Representation of the rat hippocampus where it is possible to observe the different sub-regions (Ca1, CA2, CA3) and the perforant path, mossy fibers and Schaffer collaterals.*

Although experimental data suggests the involvement of the hippocampal formation in diverse brain functions, two major hippocampal functions have received particular attention. The first is the formation of memories for everyday facts and events that can be consciously recalled, termed declarative memory (Squire 1992). The second concerns its involvement in spatial memory and, more specifically, the formation of cognitive maps and their use in navigation through space (Burgess, Maguire et al. 2002). Thus, the cellular and molecular mechanisms underlying memory formation seem to play a central role in hippocampal functions. Long term potentiation (LTP) appears to be of major importance as a cellular mechanism underlying memory formation. Actually, it is now established that the •NO - cGMP pathway plays a role in LTP in the hippocampus (Garthwaite 2008). The involvement of •NO in LTP supports an important role of this intercellular messenger in the mechanisms of memory formation in the hippocampus. Given that •NO actions depend on its concentration dynamics, the direct measurement of endogenous •NO signals with high spatial and temporal resolution is of great relevance for the understanding of the mechanisms underlying its participation in processes of synaptic plasticity. Other reasons are also important to consider regarding the choice of hippocampus for ascorbate, glutamate and •NO recordings:

1) The relatively simple organization of its principal cell layers coupled with the highly organized laminar distribution of many of its inputs facilitates the interpretation of the results and has encouraged its use as a model system for modern neurobiology.

2) Although some GABAergic interneurons exist, as well as some enervation from other brain regions based on other neurotransmitter systems (dopamine, norepinephrine, serotonine), the principal circuits in the hippocampus are excitatory, using glutamate as the principal neurotransmitter. NMDAr and AMPAr are co-localized in ≈75% of Schaffer Collaterals synapses and in all mossy fiber synapses (Takumi *et al.*, 1999). Since nNOS frequently co-localizes with NMDAr (Burette *et al.*, 2002), the hippocampus seems to be one of the best equipped brain regions towards endogenous •NO synthesis.

3) The hippocampus is one of the brain areas where ascorbate exists in higher concentrations and ascorbate has shown to have a positive impact in studies related with memory and learning. Taking into account its involvement in glutamatergic mechanisms of release and uptake and its redox interactions with •NO, this brain area is a natural hotspot to study the dynamic interplay between these substances.

1.6. Direct measurement of ascorbate, glutamate and •NO *in vivo* in the brain

There are some aspects about ascorbate, glutamate and •NO that make their direct and dynamic measurement important:

1) Although the brain contains the highest concentration of ascorbate in the body, its regional asymmetric distribution within different areas and the concentration change in response to neural activity raises the need for its dynamic measurement upon neurotransmitter stimulation.
2) Since glutamate has rapid clearance kinetics, being able to sample closer to the synaptic cleft is necessary to study neuronal glutamate.
3) It has been conceptualized that changes in extracellular glutamate levels are coupled to fluctuations in extracellular ascorbate levels, perhaps via a heteroexchange mechanism involving the glutamate transporter proteins (O'Neill, Fillenz et al. 1984, Cammack, Ghasemzadeh et al. 1992, Miele, Boutelle et al. 1994, Walker, Galley et al. 1995).
4) •NO signals, having different amplitude, time course and spatial distribution may thus encode different signaling messages, possibly mediated by different biological targets. Paradoxically, in spite of being one of the most studied endogenous molecules during the

last decades, the exceedingly majority of studies are of qualitative and phenomenological nature, lacking the critical quantitative information on •NO dynamics.

Therefore, the monitoring of these molecules concentration profiles *in vivo* is a critical piece of knowledge to understand the mechanisms by which they affect cell and tissue function in the brain.

Several analytical techniques can be used to measure these substances in biological preparations. However, for monitoring them in the rat brain *in vivo*, some key analytical features are desirable:

1) Good detection limit, especially in the case of •NO (whose concentration *in vivo* is thought to lie in the nanomolar range) and glutamate (whose basal extracellular concentration *in vivo* is in the low µM);
2) High temporal resolution to allow reliable monitoring of fast concentration variations which are likely to occur;
3) High spatial resolution for analysis of the spatial properties of signals within a particular brain region;
4) Minimal tissue damage.

On the basis of these requirements, one of the best analytical approaches for *in vivo* monitoring of in the brain is currently provided by electrochemical techniques coupled to microelectrodes. This methodology has several inherent advantages over other techniques, including a great versatility of possible usages, allowing measurements in intact tissue *in vitro* and *in vivo* and the possibility to directly measure ascorbate, glutamate and/or •NO with high temporal and spatial resolution, high sensitivity, low detection limit and little invasiveness due to the small size of the microelectrodes. The most common electrode materials used are carbon and noble metals, such as platinum (Ciszewski and Milczarek 2003). Carbon fiber microelectrodes (CFM) are usually the first choice for ascorbate (Cammack, Ghasemzadeh et al. 1991, Cammack, Ghasemzadeh et al. 1992, Ferreira, Santos et al. 2013) and •NO measurements (Ledo, Barbosa et al. 2002, Ledo, Barbosa et al. 2005, Nuno R. Ferreira 2005, Barbosa, Lourenco et al. 2008, Santos, Lourenco et al. 2008, Lourenco, Santos et al. 2011), while platinum based microelectrode arrays (MEA) have been used to prepare glutamate biosensors (Burmeister and Gerhardt 2001, Day, Pomerleau et al. 2006, Kevin N. Hascup 2006, Hinzman, Thomas et al. 2010, Burmeister, Davis et al. 2013).

This work is highly focused in the use of microelectrodes (CFMs and MEAs) coupled to electrochemical techniques to perform real time and dynamic monitoring of ascorbate, glutamate and •NO. Both the CFMs and the Pt based MEAs have unique characteristics that give them an

advantage over other approaches. They have the ability to monitor in a subsecond time frame and record in real time when used with fast electrochemical techniques such as amperometry, high-speed chronoamperometry, square wave voltammetry (SWV) and fast cyclic voltammetry (FCV). Because they are so small, CFMs and MEAs are also able to sample very small environments, such as a single cell or vesicular volumes, where other devices cannot because they are too big (Gonon, Buda et al. 1980, Stamford, Kruk et al. 1984, Adams 1990, Malinski and Taha 1992, Burmeister and Gerhardt 2001, Hascup, Rutherford et al. 2007). Evidence has shown that CFMs appear to cause less disruptive tissue damage when implanted into a brain than other devices, for instance a microdialysis probe (Mitala, Wang et al. 2008, Jaquins-Gerstl and Michael 2009). On top of that, CFMs and MEAs are also excellent devices for those seeking greater sensitivity and selectivity by making electrode modifications tailored for the analyte of interest, providing a wider range of detectable species by simply making slight modifications (Crespi and Mobius 1992, Friedemann, Robinson et al. 1996, Gerhardt and Hoffman 2001, Nuno R. Ferreira 2005, Zhang, Liu et al. 2007, Ferreira, Santos et al. 2013). However, they also present some drawbacks. Since the neuronal environment consists of numerous electrochemically detectable targets of interest such as ascorbate, glutamate, $^{\bullet}$NO, glucose, lactate, urate, hydrogen peroxide, oxygen, simple inorganic ions, catecholamine and indolamine neurotransmitters and their metabolites, every one of these substances can be a potential interferent when one is aiming at monitoring a single species. The possible loss of sensitivity or fouling during the experiments is one aspect of concern when using microelectrodes for *in vivo* monitoring in the brain. Also, invasiveness and the development of inflammatory processes after implantation of the probe in the tissue implies that long term studies are still difficult to perform with this approach. It is therefore very important to analytically characterize each of the electrochemical probes used in this work.

1.7. *In vivo* electrochemistry

In vivo electrochemistry is a quite simple and powerful means to continuously monitor over flow of neurochemicals in the extracellular space. A key aspect relies in the use of an electrode that provides a surface or interface where some form of a charge-transfer process occurs. This charge-transfer process gives rise to potentials and/or currents that can be measured and related either by theory or by calibration to the concentration of substances in the solution that bathes the electrode. Broadly speaking, these methods can be divided into two groups: measurements that do not involve current, known generally as potentiometric methods, and measurements that involve current flow at an electrode under potential control, known as amperometry,

voltammetry, or polarography, depending upon the details of the experimental design (Michael 2006).

A potentiostat controls an applied potential at the working electrode versus an Ag/AgCl reference electrode. The working and reference electrodes must be in ionic contact. The working electrode is usually an inert material, such as platinum (Pt), iridium, or carbon that can readily act as a source or sink for electrons. If the potential is sufficient, molecules are either oxidized or reduced directly at the working electrode surface depending upon their intrinsic electrochemical properties. The currents generated from faradaic reactions are linear with respect to the concentration of the electroactive molecule(s) in the tissue surrounding the electrode (Michael and Wightman 1999). This basic principle allows for *in vitro* calibration methods for *in vivo* studies (Michael and Wightman 1999, Hascup, Rutherford et al. 2007).

1.7.1. Constant potential amperometry

One of the simplest and most widely used electrochemical techniques for monitoring rapid neurochemical events is constant potential amperometry, an elegant research tool, vital for studying exocytotic mechanisms from single cells or cell slice preparations. This technique involves the measurement of current at a constant fixed potential. Since the current can be continuously monitored, neurochemical events can be measured as quickly as 1 ms (Michael and Wightman 1999). Since the voltage is constantly applied to the working electrode and the current is directly proportional to the concentration at all times, the non-Faradaic background current recorded from the electrode is low, allowing for sensitive measurements of electrochemically active molecules (Hascup, Rutherford et al. 2007). Ultimately, the filtering, signal-to-noise ratio, sampling rate, and organic layer composition will determine the temporal resolution (Michael and Wightman 1999). While constant-potential amperometry provides the best temporal resolution of any electrochemical technique, it also has the worst chemical resolution. It is difficult to distinguish multiple electroactive molecules that are present *in vivo*. To further complicate matters, several interferent compounds also exist and can be measured at oxidation potentials similar to those of our analyte of interest. Thus, surface modifications are needed on the working electrode to improve its selectivity for the analyte of interest (Michael and Wightman 1999). Amperometry was the first choice technique used in this work.

1.7.1.1. Amperometric detection of ascorbate

The amperometric determination of ascorbate based on its electrochemical oxidation can be done at bare platinum or CFMs, operating at potential above +500 mV. In electrochemistry, ascorbate can be easily oxidized into DHA through a two-electron and one-proton process

followed by an irreversible hydrolysis to finally produce an electroinactive product of 2,3-diketo-1-gulonic acid. This product is readily adsorbed on the electrode surface, resulting in electrode fouling and thereby a high overpotential for ascorbate oxidation. The high-potential oxidation of ascorbate essentially renders difficulties in exploring the electrochemical property of ascorbate (Zhang, Liu et al. 2007). However, this overpotential is lowered substantially by using chemically modified electrodes. One disadvantage of current ascorbate detection methods is the interference of monoamines, especially catecholamines (Malinauskas, Garjonyt et al. 2004, Liu, Lin et al. 2009). Since selectivity is one of the most important characteristics of a sensor, it was proposed that the oxidation potential of ascorbate should be lowered by modifying the electrode using catalysts. A single wall carbon nanotube (SWNT) was found to be capable of lowering the oxidation potential of ascorbate to as low as 0 V compared with Ag/AgCl (Liu, Lin et al. 2008). Furthermore, most of the detection methods use cyclic voltammetry, differential pulse voltammetry or linear scanning voltammetry. These techniques lack the temporal resolution of amperometry, which is very important in neuroscience (Shi, Liu et al. 2012).

1.7.1.2. Amperometric detection of •NO

Direct detection of •NO has also been achieved with CFMs. The electrochemical detection of •NO proceeds via an electrochemical reaction that is followed by a chemical reaction. In the first step •NO transfers one electron to the electrode support being oxidized to NO^+, which in aqueous solution is converted to NO_2^- (Malinski, Mesaros et al. 1996). Due to its high reactivity, measuring •NO in biological systems can be difficult and the high oxidation potential needed for amperometric detection can lead to interference from other electroactive compounds. Carbon fibers modified with Nafion and o-phenylenediamine (*o*-PD) have been used to measure •NO concentrations by amperometry (Friedemann, Robinson et al. 1996, Nuno R. Ferreira 2005). The polymer acts as a molecular filter, keeping molecules larger than •NO away from the electrode. By this way, the selectivity of the microelectrodes against common interferents in the brain, like ascorbate and catecholamines is greatly increased. The Nafion also reduces side reactions such as nitrate oxidation, improving the sensitivity of the electrode. Improvement of microelectrode analytical performance has been also achieved by immobilization of electrocatalytic compounds at the electrode surface. Metalloporphyrins, metal phthalocyanines and other organometallic compounds with Ni, Fe, Co, Cu, and Mn centers have been used to lower •NO oxidation potential (Bedioui, Quinton et al. 2010). Deposition of platinum and carbon nanotubes has also been employed to reduce •NO oxidation potential and increase microelectrode sensitivity by increasing surface area and enabling faster electron-transfer kinetics between the electrode and •NO (Bedioui, Quinton et al. 2010, Jacobs, Vickrey et al. 2011).

Direct electrochemical detection of •NO has been used for many years to try to measure its concentration in cells and tissues, both basally and in response to various stimulators of •NO production. Direct determination of •NO concentrations would be expected to provide the best solution but the results have been somewhat disappointing (Hall and Garthwaite 2009).

Unfortunately, despite the numerous reports on microelectrode solutions for •NO measurement, only a few of them have been used to monitor •NO in the brain *in vivo.* The recorded •NO concentration increases following a stimulus *in vivo* range from few nanomolar to near micromolar levels (Buerk, Ances et al. 2003, Crespi and Rossetti 2004, Lourenco, Santos et al. 2011). This variability might be explained by a number of factors, including the type of microelectrode used, the brain region studied and the type of stimulus for •NO production (e. g. electrical stimulation, chemical stimulation and stimulus strength). Therefore, the recording of endogenous •NO signals *in vivo* and their relationship with its sources and spatial distribution in a given brain region, as well as the biological outcome of different •NO signals remain unclear.

1.7.1.3. Amperometric detection of glutamate

Electrochemical microelectrodes based on cyclic voltammetry or constant amperometry have been developed to measure neurotransmitters and modulators that are readily oxidized at electrodes. For analytes that are not intrinsically electrochemically active (such as glutamate) specific enzymes need to be immobilized onto the surface of electrodes. In this approach a neurotransmitter is detected by monitoring the consumption of an electroactive enzyme co-substrate, such as oxygen, or the formation of an electroactive product, such as hydrogen peroxide. A considerable number of enzymes, mainly oxidases and dehydrogenases, have been successfully incorporated into the design of electrochemical sensors. Glutamate biosensors are based on immobilized glutamate oxidase that converts glutamate into H_2O_2, which is then detected amperometrically at a constant electric potential. A range of immobilized enzyme-based electrochemical biosensors for glutamate detection, based on this principle, are now available for directly monitoring glutamate in the extracellular fluid (Hu, Mitchell et al. 1994, Kulagina, Shankar et al. 1999, Burmeister, Pomerleau et al. 2002, Rahman, Kwon et al. 2005, Schuvailo, Soldatkin et al. 2006). According to their working mechanisms and electrochemical mediators, the amperometric sensors are classified as first-generation sensors (using natural enzyme products, such as O_2 or H_2O_2) or second-generation sensors (using additional redox mediators (Wilson and Hu 2000, Schuhmann 2002). As shown in figure 1.9, glutamate first-generation sensors like the platinum based MEAs detect the produced H_2O_2 directly by applying a high potential (e.g., +700 mV) on the electrode (Burmeister, Moxon et al. 2000). Second-generation sensors, such as the hydrogel coated carbon fiber microelectrodes, contain an additional redox mediator (osmium

redox polymer) for detection of H_2O_2 (Oldenziel and Westerink 2005, Oldenziel, Dijkstra et al. 2006, Oldenziel, Dijkstra et al. 2006) . In this way, the H_2O_2 is reduced by the redox mediator and then the oxidized form of the redox mediator is electrochemically detected on the electrode surface at a relatively low potential (e.g., −150 mV). The latter approach results in sensors with less sensitivity for interfering compounds that are electrochemically active at higher potentials. However, the oxygen dependency could be an issue for this type of sensors, since the oxygen content of the brain may not be sufficiently applied for the continuous redox reactions. The difference in working principle and associated components as well as geometry and size of biosensor influence their performance and consequently the detection of glutamate in the brain.

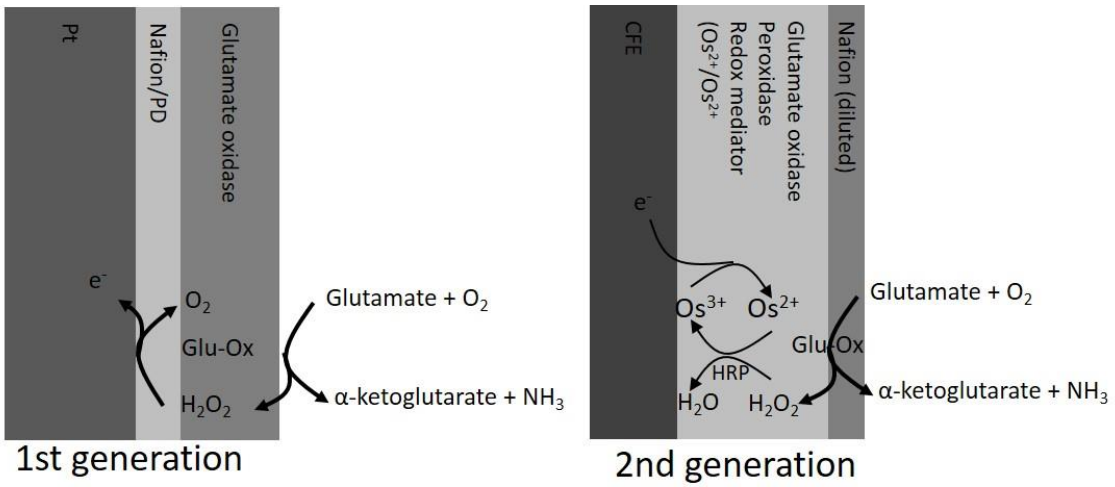

Figure 1.9. *First and second generation glutamate biosensors. Adapted from (Si Qin 2013).*

1.7.2. Voltammetry

Voltammetry is based on the measurement of current in an electrochemical cell under conditions of complete concentration polarization in which the rate of oxidation or reduction of the analyte is limited by the rate of mass transfer of the analyte to the electrode surface. In voltammetry, the voltage of the working electrode is varied systematically while the current response is measured. Several different voltage-time functions called excitation signals, can be applied to the electrode. The simplest of these is a linear scan, in which the potential of the working electrode is changed linearly with time. Typically, the potential of the working electrode is varied over a 1 or 2 V range. Other waveforms that can be applied are pulsed waveforms and triangular waveforms. The waveforms of four of the most common excitation signals used in voltammetry are shown in Figure 1.10. The classical voltammetric excitation signal is the linear scan shown in Figure 1.10 a, in which the dc voltage applied to the cell increases linearly as a function of time. The current that develops in the cell is then measured as a function of the applied voltage. Two pulse-type excitation signals are shown in Figure 1.10 b and 1.10c. Currents are measured at various times

during the lifetimes of these pulses. With the triangular waveform shown in Figure 1.10d, the potential is varied linearly between a maximum and a minimum value. This process may be repeated numerous times while the current is recorded as a function of potential. Cyclic voltammetry has found considerable application as a diagnostic tool that provides information about the mechanisms of oxidation reduction reactions under various conditions (Douglas A. Skoog 2014).

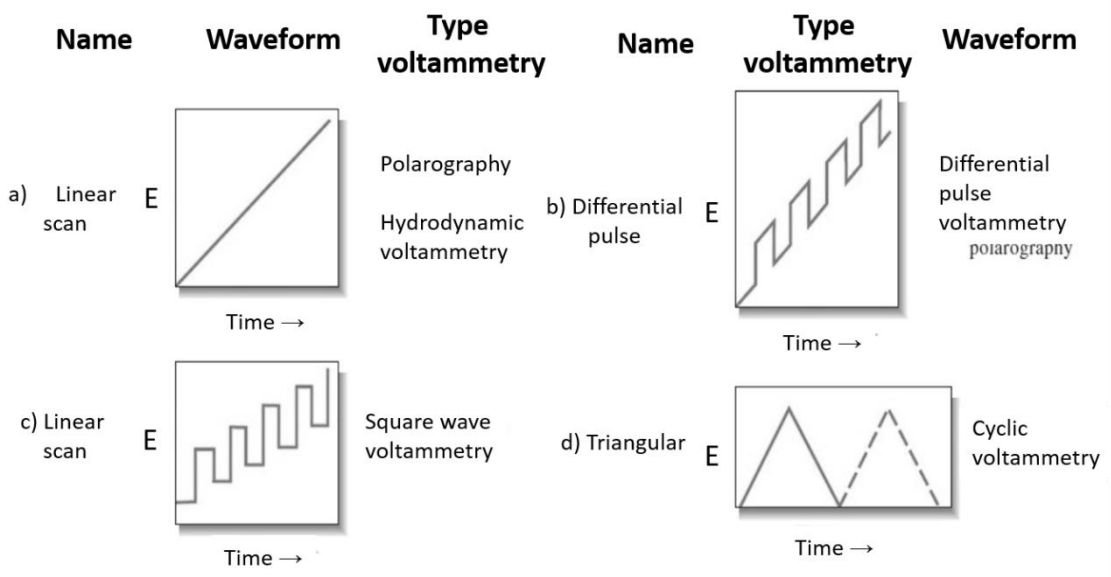

Figure 1.10. *Voltage versus time excitation signals used in voltammetry. From (Douglas A. Skoog 2014).*

1.7.2.1. Square wave voltammetry

Square wave voltammetry can be used to perform an experiment much faster than normal and differential pulse techniques, which typically run at scan rates of 1 to 10 mV/sec. Square wave voltammetry employs scan rates up to 1 V/sec or faster, allowing much faster determinations. A typical experiment requiring three minutes by normal or differential pulse techniques can be performed in a matter of seconds by square wave voltammetry. The scan rate for a square wave voltammetry experiment can be calculated from the equation 1.7:

Scan rate (mV/s) $=E_{step}$(mV) / T(s) **(equation 1.7)**

For example, if E_{step} is 2 mV and T is 0.01 sec (corresponding to a frequency of 100 Hz), the scan rate would be 200 mV/sec. This scan rate is considerably faster than the 1 to 10 mV/sec rate of other pulse techniques. The current is sampled twice during each square wave cycle, one at the end of the forward pulse, and again at the end of the reverse pulse. The technique discriminates against charging current by delaying the current measurement to the end of the pulse. The difference current between the two measurements is plotted *vs*. the potential staircase. Square

wave voltammetry yields peaks for faradaic processes, where the peak height is directly proportional to the concentration of the species in solution (Douglas A. Skoog 2014).

Aims and thesis outline

Ascorbate, being electrochemically active and highly concentrated in the extracellular space, is usually viewed as an interferent molecule when one wants to monitor neurochemicals using electrochemical methods. However, ascorbate itself is gaining growing interest as a modulator due to its association with glutamate signaling through the heteroexchange mechanism. Glutamate in turn, is the trigger for the neuronal production of •NO, an important neuromodulator that is also coupled to ascorbate dynamics in the brain. Moreover, •NO is implicated in a wide number of processes that range from memory and learning to NVC, via activation of nNOS. For this enzyme to work properly an adequate supply of O_2, among other cofactors, is required. In situations where this supply is compromised, •NO production is affected. In order to sustain •NO signaling under these circumstances of low O_2 availability, usually accompanied by a local drop in pH (brain acidosis), nitrite that is present in the extracellular space may sustain •NO signaling pathways through reduction to •NO by ascorbate in acidic media. Since these substances convey information associated to their concentration dynamics, it became necessary to use electrochemical methods since they allow for direct measurements of each one of the substances with a high degree of selectivity and a high spatio-temporal resolution to better understand their dynamic interplay in the brain.

Based on the previously presented notions, in this work we identified the following aims:

- Develop a microsensor that fulfills the criteria of size, speed, sensitivity and selectivity for *in vivo* measurements of ascorbate in the brain (chapter 3);
- Evaluate ascorbate dynamic concentration profile after glutamate stimulation with the previously developed microsensors (chapter 3);
- Verify the analytical performance of MEA glutamate biosensors and perform simultaneous measurements of ascorbate and glutamate in the brain of anesthetized rats in order to assess the dynamic interplay between these two molecules (chapter 4).
- Evaluate the coupling between •NO produced upon glutamate stimulation and ascorbate fluxes *in vivo* by following their concentration dynamics in real time (chapter 5);
- Verify if nitrite is reduced by ascorbate to •NO and maintain the balance between •NO production, oxygen consumption and NVC in the brain, especially in conditions where brain acidosis may occur (chapter 6).
- To investigate the impact of increasing circulating nitrate on •NO production and CBF, through the activation of the $NO_3^- \rightarrow NO_2^- \rightarrow$ •NO pathway (chapter 6).

To achieve the aforementioned goals this thesis was outlined as described next:

The first chapter gives a general overview of the different molecules to be studied and the way they interact with each other in the brain. Chapter 2 describes the used methodological procedures and materials used throughout the thesis.

Chapter 3 is dedicated to the development of CFMs modified with Nafion and CNTs composite films for *in vivo* measurement of ascorbate the rat brain. They were electrochemically characterized, namely the electrocatalytic oxidation of ascorbate and dopamine, the analytical performance in terms of sensitivity, L.O.D., selectivity, response time and active surface area. Furthermore, this chapter shows the *in vivo* application of the modified-microelectrodes for selective measures of both basal and glutamate-stimulated ascorbate release in the extracellular space. Having the CFMs for ascorbate developed, the next step was to perform simultaneous measurements of ascorbate and glutamate in order to evaluate their dynamic interaction. Chapter 4 was dedicated to this issue and the first set of experiments was made to characterize the analytical response of the biosensors of glutamate that were to be used in the in vivo experiments. Since the biosensors also showed good analytical properties for *in vitro* and *in vivo* measurements of glutamate signals, arrays consisting of these two types of microelectrodes were assembled and simultaneous measurements of ascorbate and glutamate were made, highlighting the interplay between these two molecules. Given that glutamate also leads to the production of •NO via activation of nNOS, in chapter 5 we investigated if •NO itself could act as a mediator of ascorbate release to the extracellular space. Arrays composed of CFMs selective for the measurement of •NO and ascorbate were assembled and simultaneous *in vivo* measurements were performed in the rat hippocampus. Chapter 6 was devoted to investigate the role of nitrite and ascorbate in the non-enzymatic production of •NO and to evaluate the impact on the regulation of blood flow. I this case, during *in vivo* experiments, CFMs were coupled a laser doppler probe in order to make measurements of •NO, ascorbate and CBF. The non-enzymatic production of •NO was evaluated during brain acidosis and after local stimulation with glutamate supplemented with nitrite and after local stimulation with glutamate preceded by systemic administration of nitrate.

Chapters 7 and 8 were used to present overall conclusions and used bibliography, respectively.

2. Materials and methods

2.1. Reagents and Solutions

All compounds were analytical grade and were used as received. Ascorbate, dopamine and DOPAC were obtained from Fluka. L-Glutamic acid sodium salt hydrate, H_2O_2 (30 wt.% in H_2O), DL-*threo*-β-Benzyloxyaspartic acid (TBOA) and noradrenaline were purchased from Sigma and Nafion (5 wt.% solution in a mixture of aliphatic alcohols and water) was purchased from Aldrich. Sodium nitrite was obtained from Riedel de Haen and ascorbate oxidase was obtained from AppliChem. Chemicals used for buffer solutions were obtained from Panreac (Barcelona, Spain). MWCNT and SWCNT were purchased from Nanolab (USA). Solutions were prepared in ultra-pure deionized water (Milli-Q, Millipore Company, Bedford, MA, USA) with a resistivity ≥ 18.2 Mohms cm. Ascorbate oxidase solutions were prepared by dissolving 1 mg (288 U) of the enzyme in 1.0 mL of 0.9% NaCl solution. 7-nitroindazole (7-NI) was purchased from Sigma and administered in a dose of 50 mg/kg via i.p. and it was prepared in dimethyl sulfoxide (DMSO).

2.1.1. Phosphate Saline buffer

The supporting electrolyte for microelectrode evaluation was phosphate saline buffer (PBS lite) 0.05 M (pH 7.4) with the following composition: (mM) 100 NaCl, 10 NaH_2PO_4 and 40 Na_2HPO_4.

2.1.2. $^{\bullet}$NO standard solution

A standard solution was prepared by bubbling $^{\bullet}$NO gas (Air Liquide, France) in MilliQ water until saturation in a fume hood. Due to the high reactivity between $^{\bullet}$NO and O_2, $^{\bullet}$NO solutions must be prepared from a gas tank is to avoid any contact between this gas and O_2. Otherwise, high nitrogen oxides ($^{\bullet}NO_2$, N_2O_3 and N_2O_4) resulting from the gas phase reaction between $^{\bullet}$NO and O_2 will lead to the formation of high concentrations of nitrite in these solutions. The system used to prepare $^{\bullet}$NO solutions was customized and consisted in the gas cylinder, one flask with NaOH pellets, another glass flask with NaOH 5 M and a glass Vacutainer tube where the solution was prepared. $^{\bullet}$NO was conducted through a stainless steel tubing until the apparatus. Connecting tubes and fittings were made of PFA (Bola, Germany) and reduced to the minimum to avoid gas exchange, according to the scheme represented in figure 2.1. The flow of $^{\bullet}$NO gas through NaOH pellets removes N_2O_3 and other N_xO_y impurities present in trace amounts in commercially available $^{\bullet}$NO gas cylinders. This procedure prevents these impurities to hydrolyze in aqueous solution to nitric and nitrous acids, thus lowering the pH of the solution and contaminating the final preparation with NO_2^-.

After bubbling the system with •NO for 5 minutes (to remove vestigial O_2 from inside), the vacutainer tube caped with a rubber septum containing ≈10 mL of previously deoxygenated MilliQ water (bubbled with Ar during 15 min) was plugged to the ending of the system, as depicted in figure 2.1, and •NO was bubbled for 15 minutes. At the end, the system was closed to avoid O_2 entrance. The resulting solution was then stored at 4 °C.

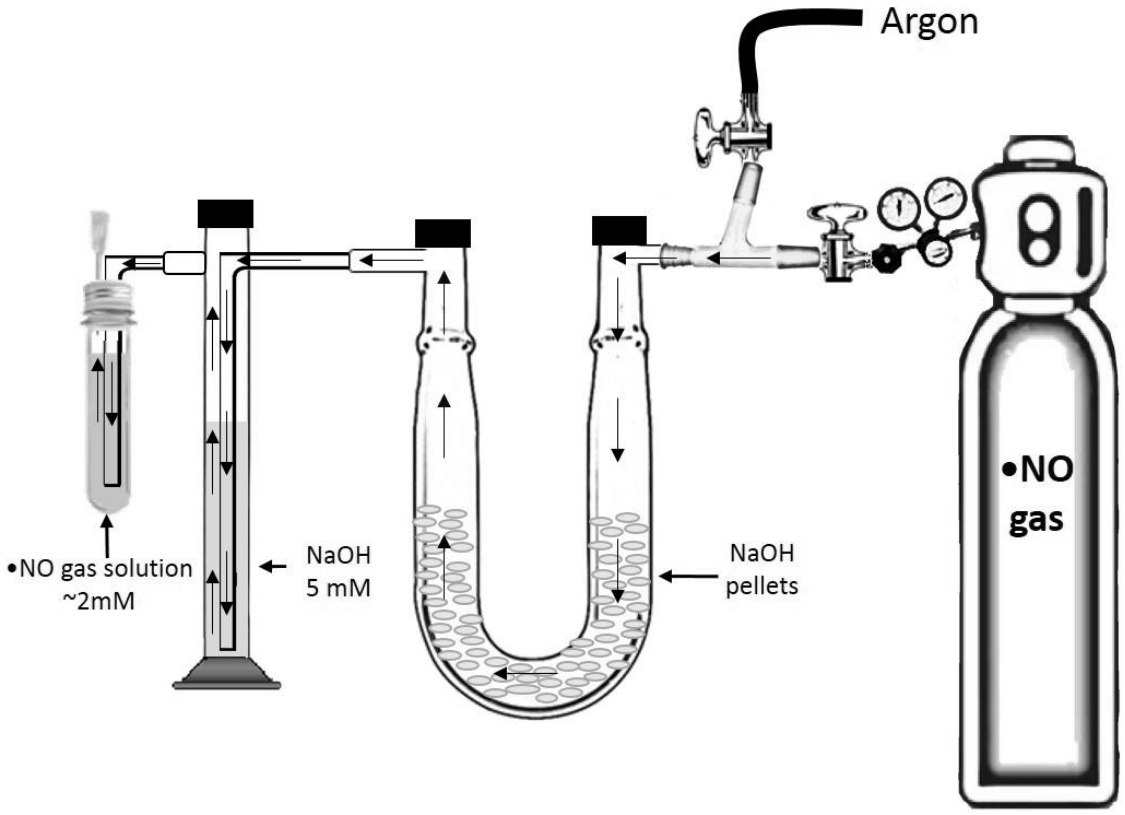

Figure 2.1. *Apparatus used to prepare •NO solutions from a •NO gas cylinder. Before bubbling into the tube containing the solution to be saturated, •NO from the gas cylinder passes through a series of washing flasks containing NaOH. The arrows indicate the direction of the gas flow. This operation must be performed in a fume hood.*

The concentration of •NO saturated solutions was checked before use with a ISO-NOP 2 mm Pt sensor connected to the amperometer ISO-NO Mark II (World Precision Instruments, Inc., USA). This commercial sensor contains a gas-permeable membrane and was calibrated by chemical generation of •NO from reaction of nitrite with an excess of iodide (0.1 M) and sulphuric acid (0.1 M) according to the reaction in Eq. 2.1:

$2NO_2^- + 2I^- + 2H^+ \rightarrow 2^{\bullet}NO + I_2 + H_2O$ (eq. 2.1)

The sensitivity was calculated based on three consecutive additions of a nitrite stock solution to the beaker (final concentration of 1 µM for each addition). After calibration, the sensor was allowed to stabilize for 10 min in PBS 0.05 M slowly stirred and at room temperature. Then, 10 µL of the •NO standard solution was added and the resulting increase in amperometric current used to estimate the •NO concentration. Typically, the concentration of the saturated •NO solution was *c.a.* 1.9 mM (Barbosa, Jesus et al. 2011).

2.1.3. Solutions for microelectrodes selectivity assessment

Ascorbic acid and nitrite were prepared in degassed milli Q water at a concentration of 20 mM. Dopamine, noradrenaline and serotonin were prepared at a concentration of 2 mM in 1% perchloric acid. The solutions were stored in aliquots at -20 ^{o}C.

2.1.4. Reference electrode platting solution

A solution of HCl 1M with saturated NaCl was used to electroplate the reference electrodes used for the *in vivo* experiments. This solution was stored at room temperature.

2.1.5. Drugs for local brain injection

All compounds used for local ejection in the brain were dissolved in NaCl 0.9% pH 7.4 and aliquots were stored at -20 ^{o}C.

2.1.6. Slides Subbing Solution

Solution chrome gelatin for subbing slides used in the histological studies was prepared by mixing aqueous solutions of gelatin and chromium potassium sulphate Gelatin solution was prepared by dissolving 0.1 g of gelatin in 95 mL of water under heating. Chromium potassium sulphate solution was prepared by dissolving 0.01 g in 10 mL of water. The two solutions were combined after the gelatin solution had cooled.

2.1.7. Cresyl Violet solution

Cresyl violet solution for brain slices staining was prepared by diluting 1 mL of a cresyl violet stock solution 2% (w/v) in water with 100 mL of a sodium acetate buffer (sodium acetate 0.2% (w/v) and glacial acetic acid 0.3% (w/v) in water).

2.2. Carbon fiber microelectrodes

2.2.1. Fabrication

Carbon fiber microelectrodes for monitoring •NO were fabricated essentially as previously described (Santos, Lourenco et al. 2008). Briefly, single carbon fibers (30 µm Specialty Materials, USA) were inserted into borosilicate glass capillaries (1.16 mm i.d x 2.0 mm o.d.; Harvard Apparatus Ltd, UK). The capillaries were then placed on a vertical puller (Harvard Apparatus Ltd, UK) and pulled, resulting two micropipettes one of which sealed on the surface of the carbon fiber. While the other was discarded, the micropipette containing the carbon fiber was placed under the microscope (Nikon, Japan) fitted with an eyepiece reticule and the protruding fiber was cut using a thin straight tip forceps, in order to obtain an exposed carbon surface with a tip length of 150-250 µm (Figure 2.2). Then, a small portion of conductive silver paint (RS, Northants, UK) was injected into the shank of the micropipette using a Teflon tube and a syringe. Then, a copper wire was introduced into the micropipette, placed in contact with the conductive silver paint and fixed to the capillary with standard cianoacrylate glue. To enable the connection to the recording system a gold connector pin was soldered at the end of the exposed copper wire. Finally, a small portion of a retractile sleeve was adjusted to the end where the copper wire was glued to the capillary since this is a fragile part of the microelectrode. Figure 2.3 shows a schematic representation (A) and a photograph (B) of a complete carbon fiber microelectrode.

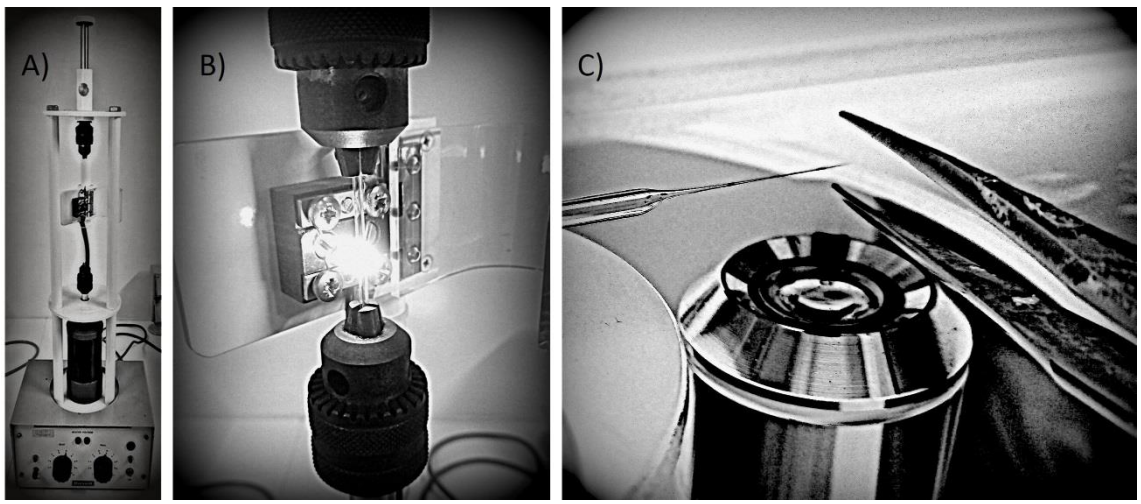

Figure 2.2. *Photographs illustrating the initial steps of the carbon fiber microelectrode fabrication.* ***(A-B)*** *Pulling of the glass capillary with a carbon fiber inside in a vertical puller.* ***(C)*** *Cutting of the fiber under the microscope, in order to obtain an exposed carbon surface with a tip length of 150-250 µm.*

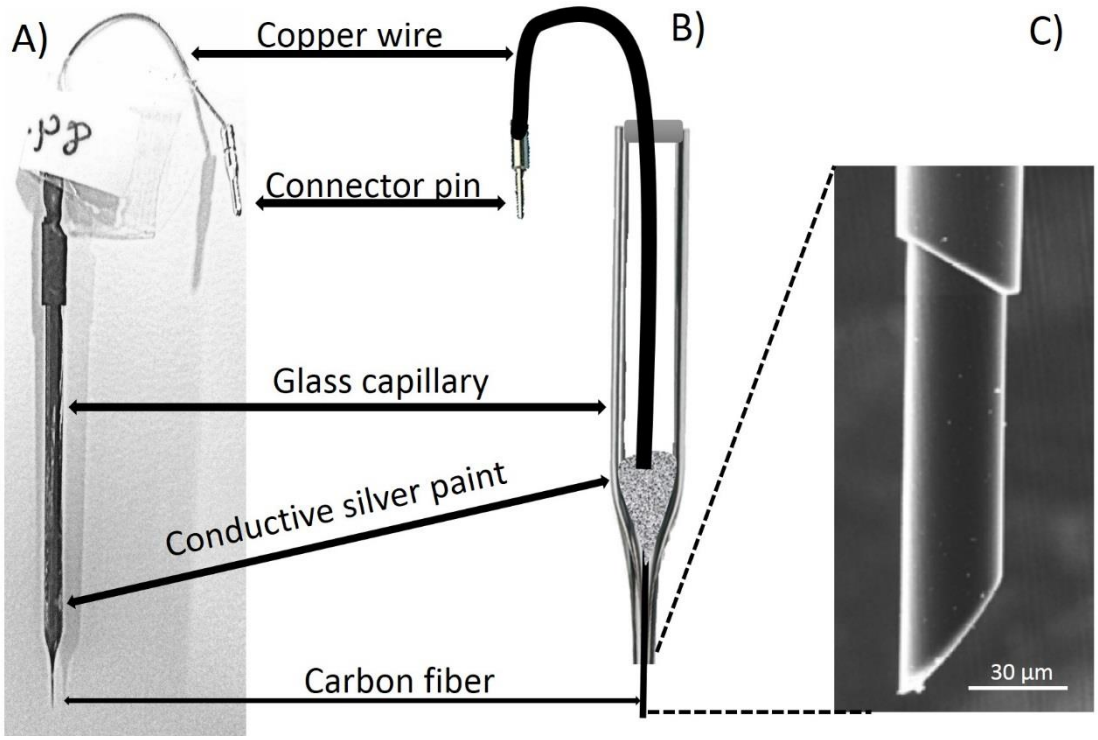

Figure 2.3. *Fully assembled carbon fiber microelectrode. A) Photograph of the microelectrode after fabrication. B) Schematic representation of the manufactured carbon fiber microelectrodes highlighting all its components. C) SEM photograph of the microelectrode carbon tip.*

When the fabrication process was completed, microelectrodes were tested for general recording properties in PBS lite prior to their surface modification. This was done by fast cyclic voltammetry (Ensman Instruments, USA) at a 200 V/s scan rate between -0.6 and +1.4 V for 30 s. A microelectrode with good electrical properties displays a more capacitive than resistive behavior (Stamford 1995), as result of a good glass-carbon fiber seal and an effective electric contact between the components of the microelectrode. The stability of the background current and sharp transients at reversal potentials were the hallmarks to consider the microelectrodes with good recording properties (Figure 2.4 A). When microelectrodes are more resistive and not suitable for electrochemical recordings they have the profile observed in figure 2.4 B. Microelectrodes that passed in FCV test were properly labeled and stored in racks at room temperature until use.

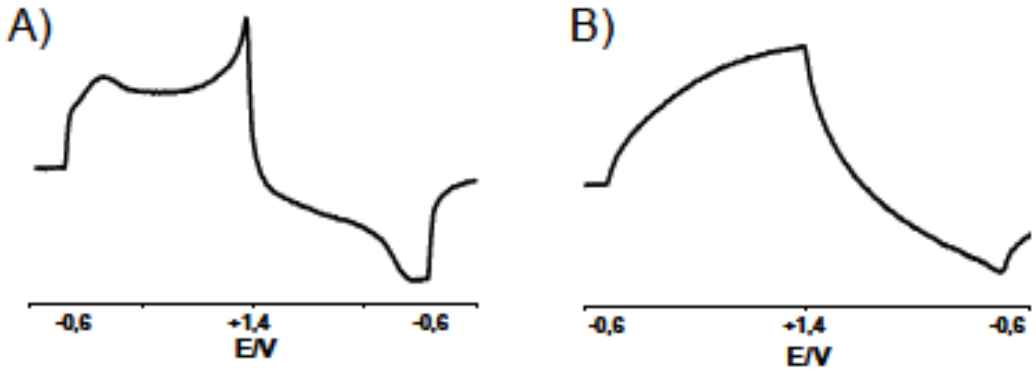

Figure 2.4. *FCV voltammograms recorded for bare microelectrodes. A) Microelectrodes with good redox profile. B) Microelectrodes with a poor redox profile (Ferreira 2006).*

2.2.2. Microelectrode modification for ascorbate measurements

SWCNTs and MWCNTs were used for coating the tip surface of CFMs. Both types of CNTs were suspended in 0.5% Nafion for a final concentration of 100 mg/mL. The 0.5 wt% Nafion solution was prepared by diluting the 5 wt% solution with isopropanol. A homogeneous suspension was obtained by sonication during at least 1/2 hour. A single drop of the suspension was applied onto a glassy plate, and the tip was immersed into the droplet for 30 s and then dried at 170°C for 5 minutes (Ferreira, Santos et al. 2013).

2.2.3. Microelectrode Modification for nitric oxide measurements

The chemical modification of the carbon fiber surface with exclusion layers has the intent to block or minimize undesirable electrochemically active compounds, found in high concentrations in CNS, to reach the carbon fiber surface, thus resulting carbon fiber microelectrodes with better selectivity towards •NO. The carbon fiber microelectrodes were modified in a two-step protocol with Nafion and *o*-PD (Figure 2.5).

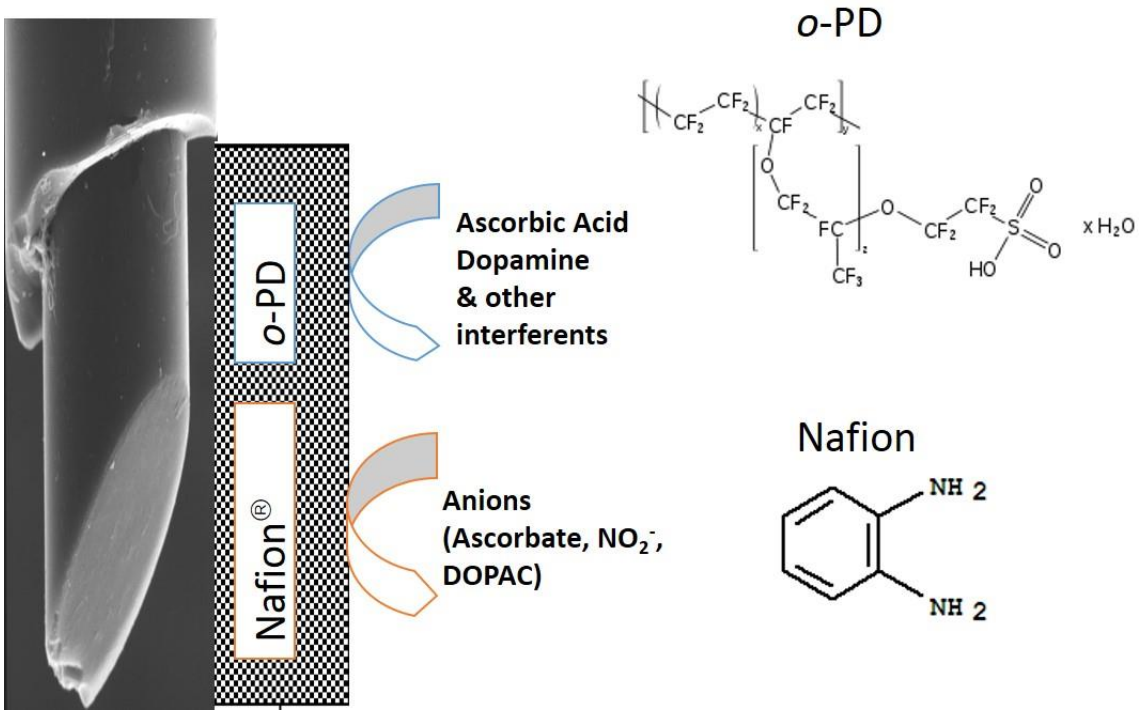

Figure 2.5. *SEM photograph of one microelectrode tip and representation of the two exclusion layers, Nafion and* o-PD. *Nafion blocks anionic substances such as ascorbic acid and nitrite. Larger molecules (>170 g/mol), such as dopamine, are blocked by the* o-PD *layer. Small uncharged molecules, such as •NO, can still diffuse through both exclusion layers and reach the active surface of the microelectrode. It is also possible to see the chemical structure of Nafion and* o-PD.

2.2.3.1.Nafion coating

The negatively charged sulfonic acid groups of Nafion make this anionic teflon derivative very useful to improve selectivity against ascorbic acid and anionic biogenic amine metabolites (Gerhardt, Oke et al. 1984). Prior to Nafion coating, microelectrodes were dried for 4 minutes in an oven at 180 ^{o}C to dry. Then, their tip was lowered halfway into the aliquot of Nafion solution (5% in aliphatic alcohols) and rotated in a circle five times lasting approximately 10 seconds per rotation. Next the tip was removed from the Nafion solution. This procedure was repeated 3 times. Then, microelectrodes were dried at 180 ^{o}C for 4 minutes to allow the Nafion layer to cure. After cooling, the procedure was repeated. Two layers of Nafion are described to be the optimal number of coatings to achieve selectivity against anions without compromising the sensitivity and response time (Friedemann, Robinson et al. 1996, Santos, Lourenco et al. 2008). Afterwards, microelectrodes were stored at 4 ^{o}C until they were used. Following coating with Nafion, microelectrodes must remain dry until use. In the day of use, when microelectrodes are soaked they must remain wet because when Nafion dries after soaking, it can crack and create areas that allow interferents to cross and compromise selectivity.

2.2.3.2.o-Phenylenediamine coating

The electropolymerization of the monomer *o*-phenylenediamine (*o*-PD) was always performed after Nafion coating. *o*-PD is used to create an exclusion layer at carbon fiber surface, acting as a molecular filter that prevents larger molecules such as dopamine, noradrenaline and serotonin from having contact with the carbon surface. Smaller molecules, such as $^{\bullet}NO$, are still able to pass through the matrix. The *o*-PD solution was freshly prepared in a degassed solution of 0.05 M PBS and immediately used. The film was deposited by electropolymerization at a constant potential of +0.7 V *vs* Ag/AgCl reference electrode for 30 min. After coating with *o*-PD, microelectrodes were kept in PBS until calibration and use. If they were not used in 24 hours after coating with *o*-PD, they were discarded.

2.3. Enzyme-based multisite microelectrode arrays

2.3.1. Fabrication

In this work, biosensors were made of ceramic based platinum microelectrode arrays (MEAs), a gift from Prof. Greg Gerhard from Center for Microelectrode Technology, University of Kentucky, USA.

The fabrication process of these MEAs was previously described (Burmeister, Moxon et al. 2000, Burmeister and Gerhardt 2001, Kevin N. Hascup 2006). Nevertheless, some important features must be highlighted.

Enzyme-based multisite microelectrode arrays are mass fabricated using photolithographic techniques. Photolithography presents several advantages such as:

- Mass production of reproducible recording surfaces as small as 5–10 µm.
- Multiple microelectrodes are patterned onto a single fabrication wafer substrate (usually 2.5 cm x 2.5 cm) allowing for increased fabrication number at a decreased cost.
- Finally, photolithographic techniques are used to manufacture numerous microelectrode designs with multiple recordings sites in well-defined, highly reproducible geometrical configurations (Kevin N. Hascup 2013).

Another important aspect is the ceramic material used for the MEA fabrication. This material reduces the cross-talk from adjacent connecting lines. Since ceramic is strong and rigid, it can be placed into tissues without flexing or breaking. The ceramic substrate may be polished or lapped down to achieve microelectrodes as thin as 37.5 µm.

Additionally, after the formation of the microelectrode on the ceramic wafer, a diamond saw or laser is used to "cut out" the individual microelectrodes. A major advantage of the diamond saw is that it produces highly polished edges for reduced tissue damage during implantation. The ceramic wafer with Pt recording sites is attached to a printed circuit board (PCB) holder for handling and connection to recording equipment. The PCB holder and fully constructed multisite microelectrode arrays are shown in Figure 2.6 A and B, respectively.

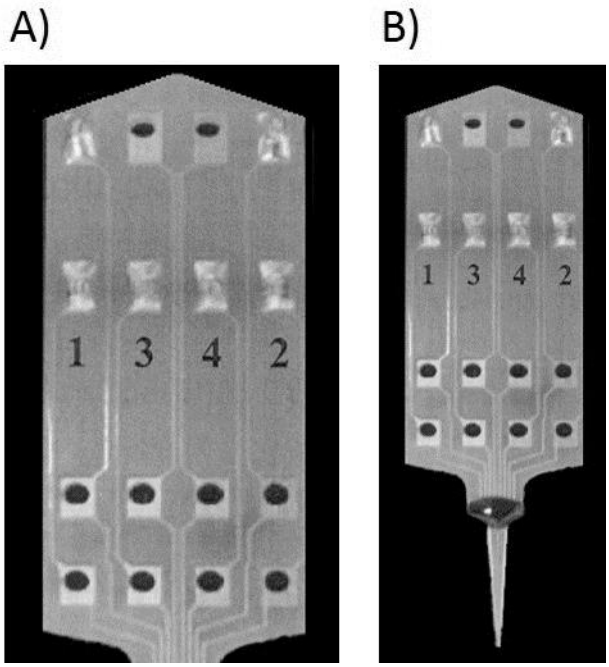

***Figure 2.6**. Photograph of the microelectrode PCB with and without attached ceramic microelectrode tip. (a) Close-up view of the PCB. Numbers beneath the pinholes indicate the specific Pt recording site connection. (b) Fully assembled microelectrode array. Black epoxy is used to insulate the wire bonding from the ceramic tip to the PCB as well as to provide stability.*

2.3.2. Multisite microelectrode array designs

Due to the flexibility of the fabrication process, these microelectrodes can be manufactured with different recording site geometric configurations. For this study, we used the configurations with four Pt recording sites. Figure 2.7 shows two popular four site configurations designated as the R1 (a row of four in-line sites, Figure 2.7 A) and S2 (two side-by-side site pairs, Figure 2.7 B). Individual microelectrodes are selected based on the type of recordings and brain regions of interest. The R1s provide a larger recording distance that is useful for large brain regions or layered structures, while the S2s provide dual detection in smaller brain structures. Furthermore, the advantage of multiple recording sites allows for self-referencing techniques and/or detection of multiple analytes (Kevin N. Hascup 2013).

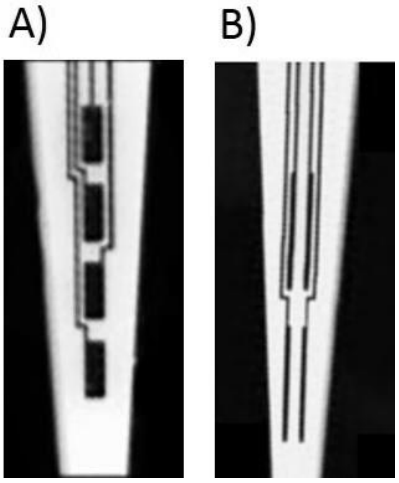

***Figure 2.7**. Photomicrographs of two ceramic-based Pt multisite microelectrode array designs. (A) Photomicrograph of an R1 microelectrode with a row of four Pt recording sites. Each site measures 50 x 150 µm with 50 µm spacing between sites. (B) A photomicrograph of a S2 microelectrode with two pairs of side-by-side Pt recording sites. Each site measures 333 x 15 µm with 30 µm between side-by-side sites and 100 µm separation among paired sites.*

2.3.3. Microelectrode preparation

Many CNS neurotransmitters are not inherently electrochemically active and therefore must be converted to a reporter molecule by cross-linking enzymes to the microelectrode surface. Below are the general procedures involved in preparing a microelectrode for use *in vitro or in vivo*.

2.3.3.1. Cleaning procedures

Microelectrodes were submitted to a cleaning procedure to remove any particulate matter or residue from the Pt recording sites that may have been deposited during the manufacturing process. New microelectrodes were placed into a stirred solution of Fisherbrand Citrisolv (Fisher Scientific) for 5 minutes followed by a 5 minutes rinse in purified H_2O, 5 minutes in isopropyl alcohol, and finally 5 more minutes in purified water H_2O. After the chemical cleaning procedure, a thin film can develop on the Pt recording sites, so a cotton swab was used to swipe delicately across the tip of the microelectrodes to remove this film and any excess of purified H_2O. Then microelectrodes were then placed in the oven at 180 ^oC for 5 minutes to dry. Typically, enzyme-based microelectrodes are reused for more than one experiment, provided they meet calibration criteria. Over prolonged use, applied enzyme layers (described below) may degrade analyte detection. A slightly different cleaning procedure is used for used for microelectrodes. In these cases, the enzyme layer must first be removed prior to re-use. The microelectrode tip is placed into a stirred solution of purified H_2O at 80 ^oC to soften the protein matrix on the Pt recording sites. Following 30 minutes of soaking, the microelectrodes are cleaned as described in the preceding paragraph and tested for response to hydrogen peroxide to ensure good sensitivity of the microelectrode recording surfaces (Kevin N. Hascup 2013).

2.3.3.2. Exclusion layer coatings – 1,3-Phenylenediamine

Following cleaning procedures, the MEAs are ready to receive different exclusion layers that will improve selectivity towards the analyte of interest. As described previously for carbon fiber microelectrodes, these layers will block or minimize undesirable electroactive compounds found in high concentrations in the CNS such as ascorbate or DOPAC. The planar geometry of the multisite microelectrodes often affects how materials adhere to the recording surfaces. It should be noted that exclusion and enzyme layer coatings can inhibit compounds from diffusing to the microelectrode surface by creating a diffusion barrier, thus limiting the response time of the microelectrode. For this reason, coating parametrics are performed to determine optimal coating procedures for both exclusion layer and enzyme layer coatings.

The organic molecule 1,3-phenylenediamine (*m*-PD) was the compound used to create an exclusion layer onto the Pt recording electrodes. A potential is applied in a triangular waveform to a solution of *m*-PD, thus causing its electropolymerization onto the Pt recording surfaces. Like *o*-PD, electropolymerized *m*-PD selectivity is achieved by forming a size exclusion layer that prevents larger molecules such as ascorbate, dopamine and DOPAC from reaching the recording surface. Smaller molecules, such as $^{\bullet}$NO and peroxide, are still able to pass through the matrix (Friedemann, Robinson et al. 1996). Since peroxide is a reporter molecule for oxidase enzymes, it makes *m*-PD an ideal exclusion layer for the enzyme-based multisite MEAs used in this work. The procedure for electropolymerizing *m*-PD (1,3-phenylenediamine dihydrochloride, 99% -Sigma-Aldrich) to the Pt recording sites is outlined below.

First, a solution of 5 mM *m*-PD was prepared in a degassed solution of 0.05 M PBS lite. Degassing was accomplished by bubbling nitrogen gas through the 0.05 M PBS solution for 20 minutes to remove O_2 before dissolving *m*-PD. Once the 5 mM *m*-PD was dissolved in the degassed 0.05 M PBS, the *m*-PD solution was stored in a brown glass bottle to prevent oxidation from light. If the solution turns yellow, it has oxidized and will no longer electropolymerize. Even with these storage methods, the 5 mM *m*-PD solution can oxidize in few hours so it is recommended using the solution immediately after preparation. When the *m*-PD solution was prepared, the microelectrode was connected to the FAST-16 MKIII recording system and approximately 40 ml of the 5 mM *m*-PD was placed into a 50 ml beaker. The microelectrode tip was lowered halfway into the solution along with a glass, Ag/AgCl reference electrode. The potential was applied a potential as a triangular wave with an offset of −0.5 V, peak to peak amplitude equal to ±0.25 V, at a frequency of 0.05 Hz, for a period of 20 minutes. Once electropolymerization was completed, MEAs were rinsed with purified H_2O to remove excess *m*-PD. The MEAs were cured for an

additional 24 h in a low-humidity environment at room temperature before *in vivo* use (Hinzman, Thomas et al. 2010).

This electropolymerization procedure with *m*-PD has four distinct advantages:

- The matrix formed by *m*-PD blocks dopamine, noradrenaline, and serotonin from reaching the Pt recording sites. This helps make the microelectrode more selective for measuring the analyte of interest;
- The *m*-PD is electropolymerized onto the microelectrode after the microelectrode is coated with an enzyme layer, forming the matrix. Since *m*-PD is electropolymerized after enzyme coating, additional coatings of *m*-PD can be applied to the microelectrode surface without having to clean the microelectrode. If the matrix degrades during an experiment, the microelectrode can be replated, recalibrated, and re-used to finish the experiment;
- Because a potential must be applied, Pt recording sites can also be selectively coated with *m*-PD. Removing the applied potential between a Pt recording site and the headstage prevents *m*-PD from being electropolymerized onto that site;
- Once *m*-PD has been successfully electropolymerized onto the Pt recording sites, the solution does not have to remain wet (Kevin N. Hascup 2013).

2.3.3.3. Enzyme coating with L-glutamate oxidase

Some molecules, like glutamate, are not electroactive and thus not measurable by electrochemical methods. In those cases, this difficulty is overcome with the use of enzymes that convert those substances into a reporter molecule such as peroxide that is oxidized at the Pt recording surfaces of the MEAs. The current measured from the oxidation of peroxide generated during the enzymatic breakdown is directly proportional to the analyte concentration. In the specific case of glutamate, the enzyme used is glutamate oxidase (Burmeister, Moxon et al. 2000, Burmeister and Gerhardt 2001, Burmeister, Pomerleau et al. 2002, Burmeister, Palmer et al. 2005, Day, Pomerleau et al. 2006, Burmeister, Davis et al. 2013). The O_2 dependence of oxidase enzyme-coated microelectrodes is also a concern. It is widely known that O_2 is required by the enzymes to measure the analyte, but with a low Km and also a portion is returned to the tissue by the oxidation of peroxide to O_2 and H^+ at the microelectrode surfaces (Hascup, Rutherford et al. 2007). A chemical cross-linking procedure is used to immobilize glutamate oxidase to the Pt recording surface. This helps to stabilize the enzymes and makes them active for longer periods of time. The process of enzyme immobilization is outlined below.

Prior to enzyme immobilization, MEAs were properly cleaned. A stock solution of L-glutamate oxidase, recombinant from US Biological (Swampscott, MA) was prepared by adding 50 µL of purified H_2O to the lyophilized, purified enzyme (25 units) to make a final concentration of 0.5 U/ µL. This stock solution is viable for approximately 6 months when stored at 4 °C. All proteins and enzymes were brought to room temperature prior to coating. Bovine serum albumin (BSA; 0.010 g) Fraction V, 99% (Sigma-Aldrich), was added to a 1.5 mL microcentrifuge tube. A 985 µL aliquot of purified H_2O was added and the BSA dissolved by manual agitation. Once dissolved, 5 µL of glutaraldehyde solution, Grade I, 25% (Sigma-Aldrich), was added to the BSA mixture and manually mixed by inversion five times. This solution, referred to as the protein matrix, was then kept aside for 5 minutes until it turned a faint yellow color. Glutaraldehyde cross-links proteins, which adhere to the microelectrode surface when cured. The BSA serves as a matrix to protect the oxidase enzyme activity during immobilization. Next, 4 µL of the BSA/glutaraldehyde mixture was removed and added to a 300 µL microcentrifuge tube and to this 1 µL of the L–glutamate oxidase stock solution (0.5 U/ µL) was added and mixed by micropipette agitation. This 5 µL solution had a final concentration of 1% BSA, 0.125% glutaraldehyde, and approximately 1% L–glutamate oxidase. Once the solutions were prepared, they were used immediately for MEA coating. All enzymes were applied to the Pt recording sites by hand. Solutions were drawn up into a 10 µL gastight Hamilton microsyringe (Hamilton Co.) and slowly dispensed to form a small

droplet of solution at the tip of the microsyringe. Using a dissecting microscope, the droplet was lightly brushed on to the Pt recording sites. The solution quickly dries, leaving behind a thin, translucent layer of enzyme that is visible underneath the microscope. Two additional coats of enzyme were applied in the same manner with one minute to dry between each coat. This procedure was complete once a visible film remained following coating. One pair of recording sites was coated with the enzyme mixture and the adjacent sites with the protein matrix (BSA and glutaraldehyde) in the same manner as applying the enzyme mixture. These two sites work as sentinels, since they had the same treatment of the sites coated with glutamate oxidase, except for the enzyme itself. With this procedure, two sites will respond to glutamate and the other two will not, and they can be used to determine if any interfering signal is present. This is called the self-referencing technique. Once the enzyme and/or inactive protein matrix was applied, microelectrodes were stored at room temperature. Enzyme-coated microelectrodes must cure at room temperature for 72 h prior to calibration and experimentation. Figure 2.8 presents a picture of the coated MEA as a schematic representation of the coating procedure of the MEAs biosensors for glutamate. The enzyme/protein layers on “uncured microelectrodes” can dissolve or lift off when put into solution. Complete curing increases enzyme layer adhesion to the microelectrode surface. This provides better sensitivity to L–glutamate and increases the shelf-life of the microelectrodes (Kevin N. Hascup 2013).

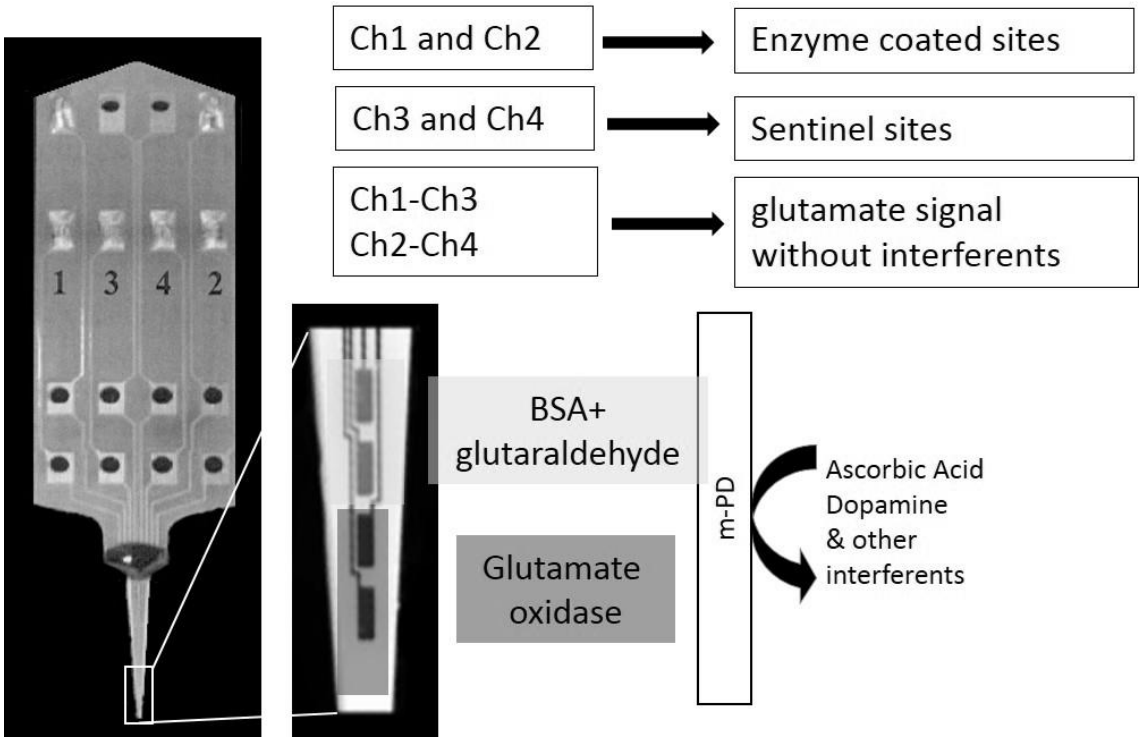

Figure 2.8. *Illustrations of the coating procedure. Close-up of a microelectrode array (MEA) tip and a schematic illustration of the selective coatings. Two of the platinum (Pt) sites (1 and 2) were used as recording sites and the other pair as reference (sentinel sites). The MEA recording sites were coated with a mixture of L-glutamate oxidase, bovine serum albumin (BSA) and glutaraldehyde, whereas the sentinel sites were only coated with BSA and glutaraldehyde. All MEA sites were coated with a protective layer of* m-*PD to block electroactive interferents commonly found in the brain, such as ascorbic acid and dopamine. Glutamate oxidase caused enzymatic breakdown of glutamate into α-ketoglutarate and peroxide (H_2O_2). Thus, the sentinel sites responded only to molecules not repelled by* m-*PD, except glutamate, and were used for self-referencing. Responses recorded at the sentinel sites were subtracted from those of the recording sites with the resulting signal representing glutamate measurements.*

2.4. Microelectrodes calibration

Calibrations were used to convert the current from the oxidation of the analyte of interest to concentration. A known amount of analyte was added to PBS lite to generate a current in picoamperes (pA) that was measured by the FAST16 mkIII system. The FAST16 mkIII system software recorded the current for each addition of analyte, creating a calibration curve for each recording site, and stored the sensitivity to analyte for each site. Also, known interferents with the measurement of the chemical substance of interest were added during the calibration to test the selectivity of the recording sites to the analyte versus interferents. Selectivity refers to a ratio of the sensitivity for the analyte over interferents on a molar basis, being calculated by dividing the analyte slope by the sensitivity to the interferents based on a single point calibration. A selectivity of 1000:1 means that a 1000 µM increase of the interferent results in an apparent 1 µM increase in the analyte. The calibration data was recalled and used to determine the concentration of analyte being measured from the change in current during *in vivo* experiments. The calibration parameters calculated were the slope (sensitivity), limit of detection (L.O.D) and linearity (R^2). The L.O.D is defined as the analyte concentration that yields an electrode response

that is equivalent to three times the background noise (baseline standard deviation) of the recording system:

L.O.D = 3 x (SD/m).

All microelectrodes used in this work were calibrated prior to *in vivo* recording. Post-calibration was also performed for most of the experiments. Pre-calibrations were used for $^{\bullet}$NO and glutamate and post-calibration was used for ascorbate.

2.4.1. Headstage/recording system

A headstage/potentiostat creates a potential difference between the microelectrode and a reference electrode to carryout electrochemical recordings. The recording system used also amplifies the electrochemical signal and is part of the Fast Analytical Sensing Technology (FAST-16 mkIII) system (Quanteon L.L .C, Nicholasville, KY). Figure 2.8 shows photographs of the FAST-16 mkIII recording system used (2.9 A) and of the calibration setup used for carbon fiber microelectrodes ($^{\bullet}$NO and ascorbate) and MEAs (Figure 2.9 B and 2.9 C respectively). In conjunction with other hardware elements, including the control box and a 16 bit A/D card in the computer, the FAST-16 mkIII system amplifies the electrical current generated by oxidation or reduction reactions and digitizes this current. A battery operated stir plate was used to eliminate the AC (50 Hz) power line interference.

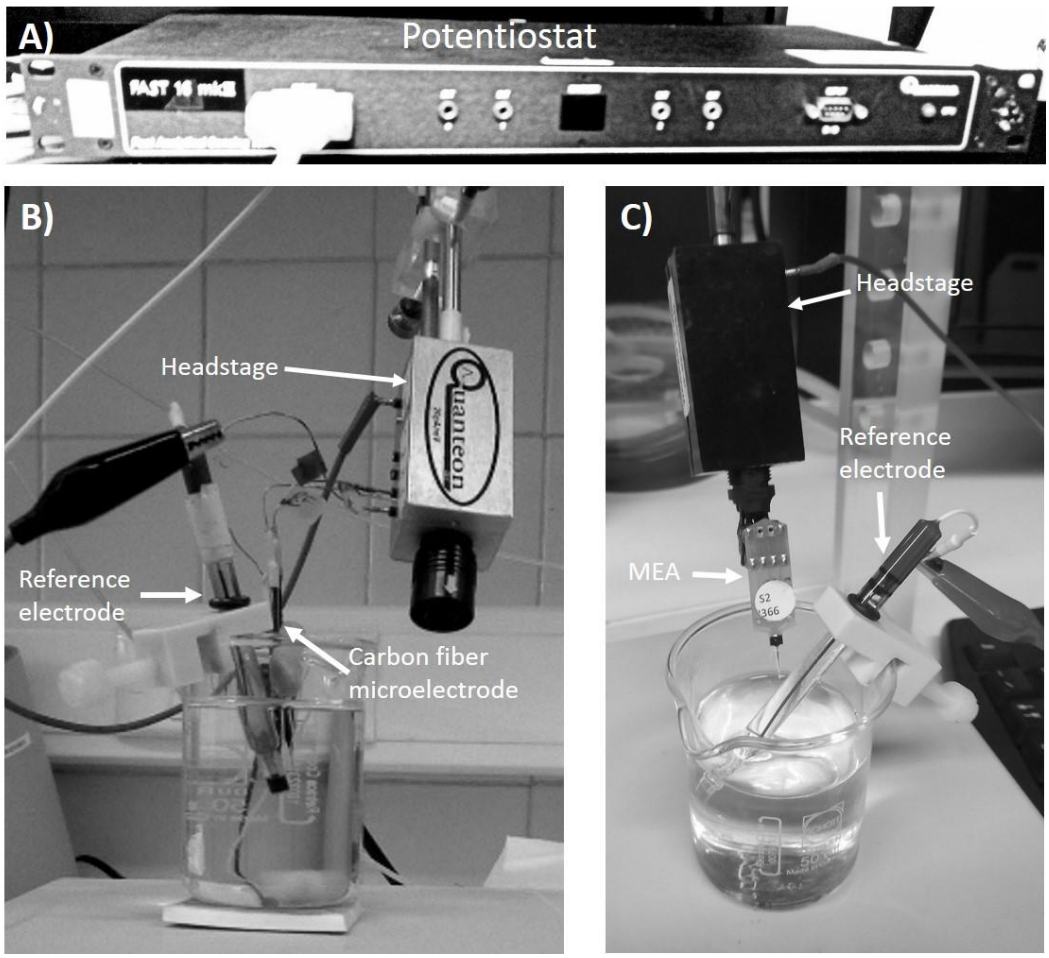

Figure 2.9. *Microelectrodes calibration setup. A) Fast 16 MKIII potentiostat. B) Calibration of a carbon fiber microelectrode. C) Calibration of a MEA. The microelectrodes connect to the FAST 16 potentiostat through a multi-channel headstage.*

The Windows based FAST-16 MKIII system software records, creates and displays second-by-second (1 Hz), or faster (1–40 Hz), data files (nominal 1–10 Hz). Recorded files were exported to other Windows based applications, such as Excel, for easier data processing. The low noise design and software oversampling allowed the FAST-16 mkIII recording system to be used without the need of a Faraday cage. In this work, measurements were carried out performing constant voltage amperometry in a two-electrode configuration mode using an Ag/AgCl reference electrode. A combination headstage gain of 20 nA/V and secondary gain stage of 2x gave a final gain of 10 nA/V. When using CFMs, the potential of the working microelectrode for ·NO measurement was held at +0.8 V *vs*. Ag/AgCl reference electrode. When CFM's were modified with SWCNT for ascorbate measurements, potential was held at +0.05 V *vs*. Ag/AgCl reference electrode. In the case of MEAs based biosensors of glutamate, we used a constant potential of +0.7 V *vs*. Ag/AgCl reference electrode.

2.4.2. Microelectrodes Calibration Procedure

Below there is a detailed description on the calibration procedures followed in the cases of CFM's modified with SWCNT for ascorbate measurements, CFM's chemically modified for •NO measurements and MEA's used for glutamate measurements.

2.4.2.1.CFM's modified with SWCNT for ascorbate measurements

1. Connect the computer, the potentiostat and run the software.
2. In the software window, set the potential for + 0.05V *vs*. Ag/AgCl.
3. Put 20 mL of PBS lite in a beaker cell at room temperature.
4. Insert a stirring bar in the PBS solution and place the beaker on top of a battery operated stirrer.
5. Place the microelectrode and the reference electrode (make sure the tip of both electrodes is immersed in PBS) in the beaker solution and plug them to the headstage.
6. Turn the stirring on (low velocity to avoid vortex formation).
7. Run the calibration procedure in the software.
8. Allow the background current to stabilize (5-10 minutes).
9. Start the recording and mark the baseline.
10. Add 20 μM of dopamine and observe if there is any change in background current. Do the same for noradrenaline (20 μM), DOPAC (50 μM) and nitrite (50 μM).
11. After the addition of the interferents, make three consecutive additions of ascorbate solution for a final concentration in the range of 100-300 μM. Wait for background current to stabilize between each addition.
12. Finish the recording and save the digital file.

2.4.2.2. CFM's modified with Nafion and o-PD for •NO measurements

The procedure is identical to the previously presented for ascorbate until point 9. When background current is stable and the baseline is marked in the software proceed as described next:

- Add 250 μM of ascorbate and observe if there is any change in background current.
- Make three consecutive additions of •NO solution with a gas tight syringe (Hamilton) for a final concentration in the range of 0.9-2.7 μM.
- Add 50 μM of nitrite and observe if there is any change in background current. Do the same for noradrenaline (20 μM) and dopamine (20 μM).
- Finish the recording and save the digital file.

2.4.2.3. MEAs biosensors for glutamate measurements

Despite the high reproducible Pt recording surfaces of MEAs, each Pt recording site on a MEA can respond differently to H_2O_2 and current enzyme coating procedures can result in different layer thicknesses. As a result, each MEA must be calibrated *in vitro* prior to experimentation to determine standard curves. The general procedure for calibrating an L-glutamate oxidase MEA is outlined below.

General calibration procedure:

1- Soak the MEA in a solution of PBS lite at 37°C for at least 1 hour prior to calibration. The soaking time allows for activation of the enzyme layer and better diffusion of molecules to the Pt recording site.
2- Connect the computer, the potentiostat and run the software.
3- In the software window, set the potential for + 0.7 V *vs*. Ag/AgCl.
4- Insert the MEA adaptor to the headstage.
5- Place the beaker in a recirculating water bath resting upon a battery operated, portable magnetic stir plate. Because the enzyme is temperature and pH dependent, the PBS is maintained at physiological temperature (37°C) and pH (7.4).
6- Place the microelectrode and the reference electrode in the beaker solution (make sure all sites are immersed in PBS) and plug them to the headstage.
7- Turn the stirring on (low velocity to avoid vortex formation).
8- Run the calibration procedure in the software.
9- Allow the background current to stabilize (5-10 minutes).
10- Start the recording and mark the baseline.
11- Add 250 µM of ascorbate and observe if there is any change in background current.
12- Then, make three consecutive additions of glutamate solution for a final concentration in the range of 20-60 µM. Wait for background current to stabilize between each addition.
13- Next, add 50 µM of nitrite and observe if there is any change in background current. Do the same for noradrenaline (20 µM) and dopamine (20 µM).
14- Finish the recording and save the digital file.

For MEAs calibrations, a FAST16mkIII recording system in combination with a headstage current-to-voltage converter of 2 nA/V was used.

2.5. Laser Doppler System

Laser Doppler Flowmetry (LDF), using the doppler shift of laser light as the signal, is established as an effective and reliable method for tissue blood flow monitoring in different tissues, providing continuous and real-time measurement capabilities (Steinmeier, Bondar et al. 2002, Tew, Klonizakis et al. 2011).

Laser doppler measures the total local microcirculatory blood perfusion including the perfusion in capillaries (nutritive flow), arterioles, venules and shunting vessels. The technique is based on the emission of a beam of laser light carried by a fiber-optic probe.

The light is scattered and partly absorbed by the tissue being studied. Light hitting moving blood cells undergoes a change in wavelength (Doppler shift) while light hitting static objects is unchanged. The magnitude and frequency distribution of these changes in wavelength are directly related to the number and velocity of the blood cells in the sample volume. The information is picked up by a returning fiber, converted into an electronic signal and analyzed (Oberg 1990, Perimed 2015).

Cerebral blood flow was monitored with the PeriFlux system 5000 equipped with one PF 5010 LDPM unit (Perimed, Sweden), connected to a probe designed for acute invasive measurements (needle probe 411). The needle probe 411 has an outer diameter of 450 µm, with two silica fibers with a core diameter of 125 µm, separated in 150 µm (Figure 2.10).

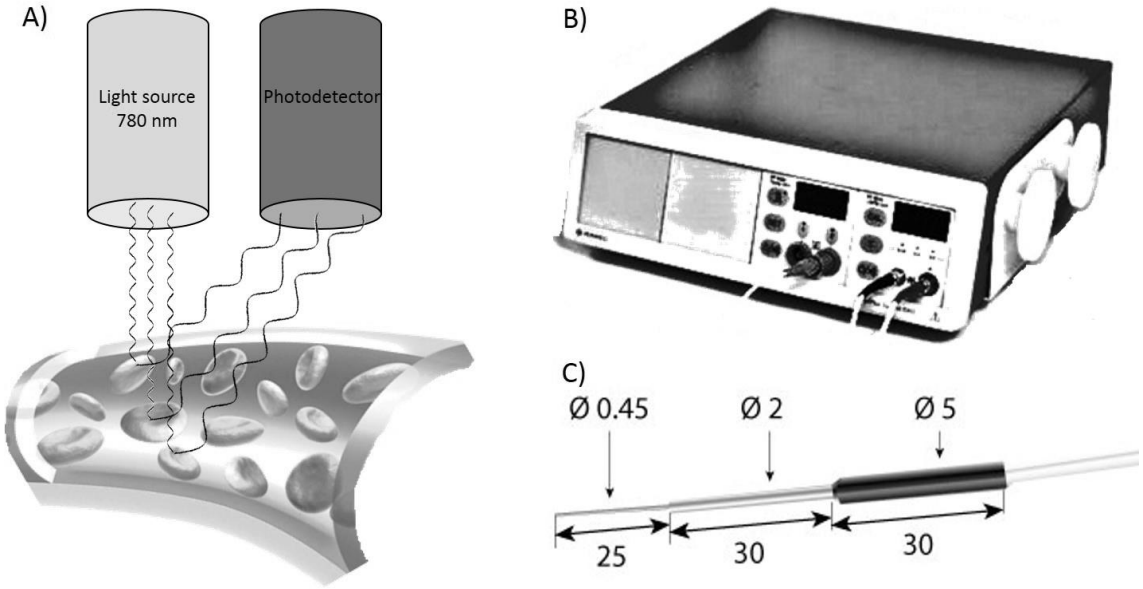

Figure 2.10. *A) Principle of laser Doppler flowmetry. A low intensity beam of light (780 nm) is emitted from a light source; if the light beam is scattered-off of stationary tissue or cells, there is no shift in the light spectrum. If, however, the light hits a moving cell in a blood vessel there is a shift in the light spectrum of the scattered light according to the Doppler flowmetry. The photodetector that is in the probe receives the scattered light and quantifies it. B) Periflux system 5000 from Perimed used for cerebral blood flow monitoring. C) Design of the needle probe used for the acute invasive measurements. The tip is thin (0.45 mm) for easy penetration of tissue such as animal brain.*

2.5.1. Laser Doppler probe calibration

The laser Doppler probe was calibrated before use using PF1001 motility standard (Perimed, Sweden) to equalize the perfusion values among the different recordings, accordingly to manufactured recommendation. Briefly, the probe tip was immersed (~5 mm) in the Motility Standard solution, avoiding bubbles around the tip and vibration of the solution. Unless the values recorded were within the interval of 250±15 PU, the device was calibrated automatically by pressing CAL button.

2.5.2. Data Acquisition

Laser Doppler Flowmeter was interfaced with a laptop computer and the signal analyzed using the Perisoft version 2.50 software (Perimed AB, Sweden). Signals were recorded using a time constant set to 0.03 s, in order to detect the heart synchronous pulsations, and the signal-processing unit used a bandwidth of 32 Hz. The perfusion represents the product of the concentration of moving blood cells and the mean velocity of these cells within the measuring volume. Measurements are expressed as Perfusion Units (PU), which are arbitrary. In that way, it only allows measurement of relative changes in cerebral blood flow (Perimed 2015).

2.6. Scanning electron microscopy

Scanning electron microscopy (SEM) was used to visualize the surface morphology of the carbon fiber microelectrodes (bare and surface modified with SWCNT). The scanning electron microscope uses a focused beam of high-energy electrons to generate a variety of signals at the surface of solid specimens. The signals that derive from electron-sample interactions reveal information about the sample including external morphology (texture), chemical composition, and crystalline structure and orientation of materials making up the sample. In most applications, data are collected over a selected area of the surface of the sample, and a 2-dimensional image is generated that displays spatial variations in these properties. Areas ranging from approximately 1 cm to 5 µm in width can be imaged in a scanning mode using conventional SEM techniques, with magnification ranging from 20X to approximately 30 000x, spatial resolution of 50 to 100 nm (Swapp 2015). A scanning electron microscope JEOL (JSM-5310) was used to visualize the surface morphology of the microelectrodes. Previously to visualization, microelectrodes were coated with a thin film of Au to confer sufficient conductivity and allow the image formation.

2.7. Setup for *in vivo* recordings

2.7.1. Animal models

Experiments were performed in accordance with the European Community Council Directive for the Care and Use of Laboratory Animals (2010/63/EU) and were approved by the local institutional animal care committee. Animals were handled and cared at the animal house facilities of the Center for Neurosciences and Cell Biology (Coimbra) under a 12:12 light dark cycle with free access to food and water.

All *in vivo* experiments were performed in male Wistar rats (8-12 weeks old, weight 250-390 g) from Charles River (Barcelona).

2.7.2. Reference electrode

Miniature Ag/AgCl reference electrodes were prepared at the beginning of each experiment from a teflon insulated silver wire (200 µm diameter, GoodFellow, UK). A small section of wire (few millimeters) was exposed at each ending of a segment of insulated wire. Then, one of the tips was coated with AgCl by applying a voltage of +9.0 V in the reference electrode plating solution previously described during 5 minutes. A new reference electrode was prepared for each experiment.

2.7.3. Micropipette/microelectrode/Laser doppler arrays

The drug delivery in the brain, particularly those related with local manipulations, was performed through a glass micropipette inserted in the brain attached to the microelectrode. Single barrel glass micropipettes (0.58 mm i.d x 1.0 mm o.d.; AM, Systems Inc., USA) were prepared in a vertical puller (Sutter Instrument Co, Model P30, USA). The tip of the pulled glass micropipette was bumped under a microscope, until the inner diameter of the tip was 15-20 µm. The glass micropipette was then attached to the microelectrode, MEA and/or microelectrode and Laser Doppler probe using sticky wax that was melted by flame (Kerr Brand Kerr Lab Corporation, Orange, CA). Precise visualization of the tip separation between the micropipette and the microelectrode was done using a microscope fitted with a reticule. According to the purpose of the experiment, several configurations were used and are represented in figure 2.11.

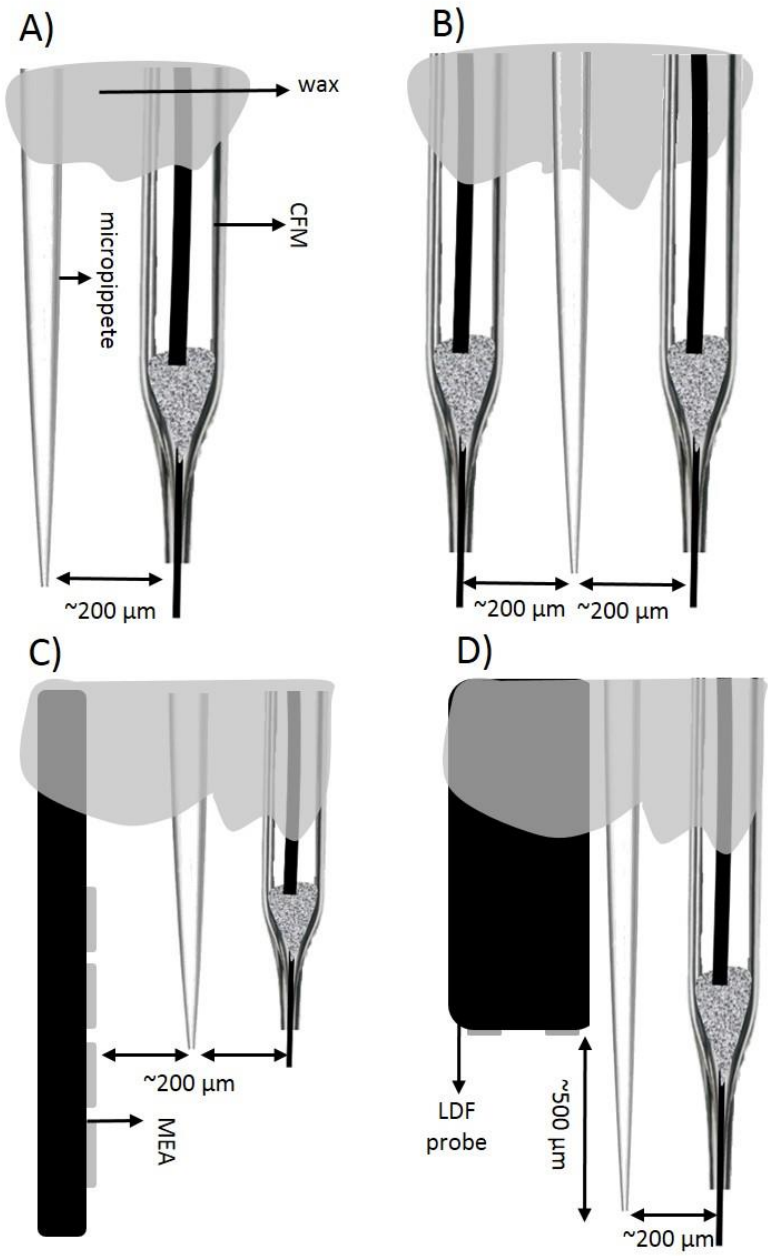

Figure 2.11. *Schematic representation of the arrays used in the* in vivo *recordings. (A) For the measurement of •NO or ascorbate a micropipette was assembled to the microelectrode. (B) For the simultaneous measurement of •NO and ascorbate the micropipette was placed in the middle of the two microelectrodes. C) For the simultaneous measurement of glutamate and ascorbate the micropipette was placed in the middle of the MEA biosensor and the ascorbate microelectrode. D) For the simultaneous measurement of •NO and CBF the microelectrode-micropipette array was attached to the laser doppler probe.*

Prior insertion in the brain, the glass micropipette was filled with the desired solution using a flexible microfilament (MicroFil, World Precision Instruments, UK) attached to a syringe.

2.7.4. Animals surgery

The stereotaxic surgery was performed essentially as previously described (Hoffman and Gerhardt 1999, Burmeister, Pomerleau et al. 2002, Barbosa, Lourenco et al. 2008). Rats were anesthetized using an intraperitoneal injection of urethane (1.25 g/Kg). Urethane was the anesthetic of choice since it produces a long-lasting steady level of surgical anesthesia, without significantly affecting neurotransmitter release. Additionally, it has minimal effects on cardiovascular and autonomic system and it consistently induces sleep-like brain state alternations (Maggi and Meli 1986, Maggi and Meli 1986, Maggi and Meli 1986, Pagliardini, Gosgnach et al. 2013).

Once completely anesthetized and not responsive to pinch in the hind foot (2-3 hours after urethane injection), the rat was placed in a stereotaxic frame (Stoelting, USA). A stereomicroscope (Meiji EMZ 13, Japan) was then positioned above the rat head to help visualizing the skull during the stereotaxic procedures. Body temperature was maintained using a T-pump from Gaymar (USA). The rectal temperature was regularly monitored by using a portable thermometer (model 470201, Jenway, Engand). The animals were placed onto the stereotaxic apparatus and the ear bars tightened into place. The mouth was fixed in the incisor bar and the nose clamp tightened. Then, a scalpel was used to make an incision on the midline of the scalp and the skin was reflected with the aid of forceps. The skull was then cleaned with 0.9% NaCl, the transparent pericranial tissues scrapped away, and then dried. With the aid of the microscope, the anatomical landmark bregma and lambda was identified and marked with a permanent marker. From bregma, the approximate location of the desired region was identified and a small portion of the skull (~3x4 mm) removed by using a drill tool (Dremel®, local retailer). Using forceps, the dura matter in that region was pulled laterally to expose the surface of the brain (the dura needs to be removed as it is strong enough to break the microelectrode tip). The Ag/AgCl reference electrode was inserted beneath the exposed skin and soaked with NaCl 0.9%. The representation of the animal head in the stereotaxic frame is shown in figure 2.12. Before the array insertion, the correct position of the skull was verified by fixing a needle onto the holder of the stereotactic frame and moving the tip of the needle with the micromanipulator of the stereotaxic frame to ensure that bregma and lambda were aligned along the antero-posterior axis. Similarly, the dorso-ventral positions of lambda and bregma should be the same, for which the position of the incision bar was moved if needed. During the course of the experiments

physiological conditions were recorded using a MouseOx oximeter (Starr Life Science, Allegheny Avenue Oakmont, PA, USA) and the following parameters were recorded:

Heart rate: 390-500 bpm

Oxygen saturation: 94-98%.

Breath rate: 84 - 118 per minute

Pulse Distention: 4.00 – 24.5 µm

Breath Distention: 2.70 – 10.1 µm

Pulse distension and breath distension are the amplitudes of the cardiac and breathing light absorption signals. Pulse distention is a measure of the local blood flow at the sensor location, while breath distention is proportional to intrathoracic pressure. At the end of the experiments the animals were sacrificed by cervical displacement while still under anesthesia.

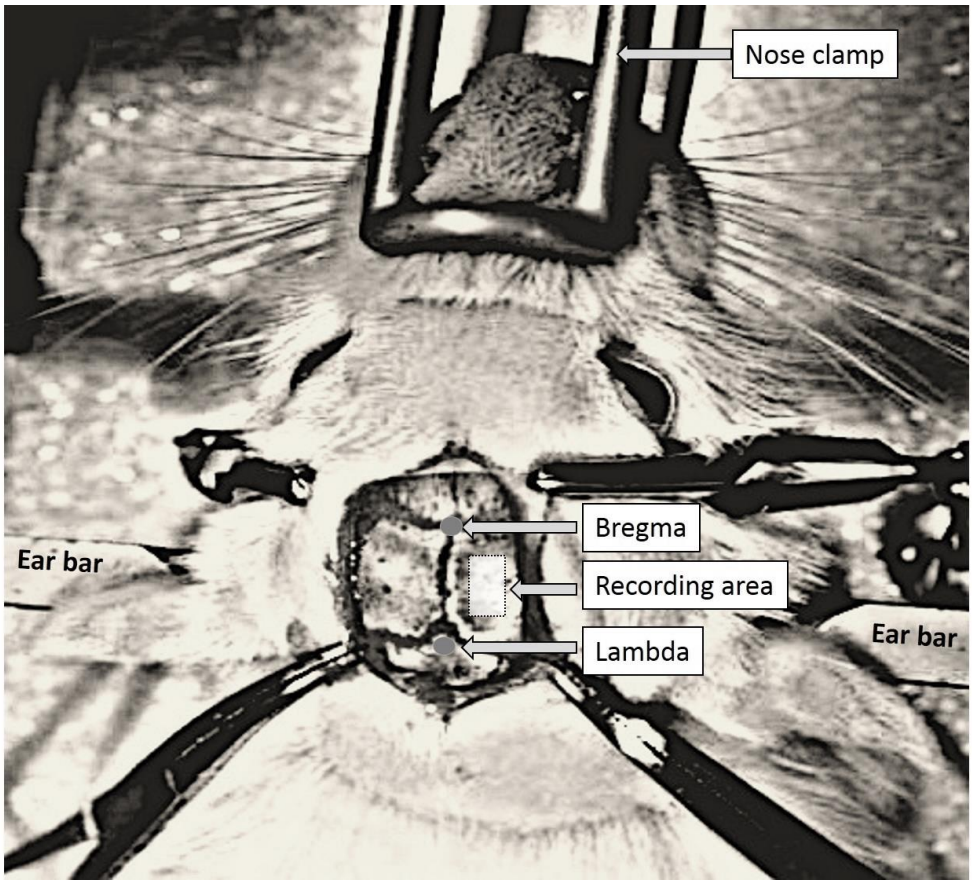

Figure 2.12. *Schematic representation of a dorsal view over the rat skull during the stereotaxic surgery. The rat was fixed to the stereotaxic frame by means of the ear, incisor and nose bars.*

2.7.5. Array insertion

In order to insert the microelectrode/micropipette array in the brain, the micropipette attached to the microelectrode was hold by a hydraulic micromanipulator (Narishige Scientific Instrument Lab, Japan) to ensure smooth vertical movements. Next, the tubing from the Picospritzer® III pressure system (Parker Hannifin Corp., General Valve Operation, USA) was plugged to the micropipette and the flow of the solution through the micropipette was tested with several pressure ejections. When ready, the microelectrode/micropipette array was inserted in the brain region of interest. Coordinates of the desired brain region, relative to bregma, were obtained from the rat brain atlas of Paxinos and Watson (Watson C. 2007). Coordinates used ranged from -3.2 to -4.1 (antero-posterior); -1.8 to -2.4 (medio-lateral); -2.4 to -3.2 (dorso-ventral). The recordings usually started after 15 minutes to allow stabilization of the baseline current. Locally ejected volumes of solution from the micropipette were measured using an eyepiece reticule that was fitted in the stereomicroscope. The measurements were based on the observation of the solution meniscus level before and after each pressure ejection, allowing a maximum precision of 12.5 nL. Different applied volumes were achieved by changing the pressure and/or the duration of the pulse.

2.8. Histology

2.8.1. Cresyl violet staining

In order to verify the microelectrode recording site, a lesion of the surrounding tissue was performed at the end of the experiment through the tip of the microelectrode by applying a DC pulse of +9.0 V. After euthanizing the animals by decapitation, the brain was rapidly removed and placed into freshly thawed 4% paraformaldehyde in PBS and soaked for at least 24 h at 4 ^{o}C. The brain was then transferred to a solution of 30% sucrose in PBS and stored until it sank to the bottom of the tube. Tissue was then frozen with cryospray (Thermo Electron Corporation, UK), mounted in OCT compound (VDR, UK) and 40 µm coronal sections along the brain region of interest were cut in a cryostat (Model CM1900, Leica, Germany). Sections were harvested in subbed slides, previously prepared by immersion for few seconds in the subbing solution previously described and allowed to dry. After harvested, the sections were allowed to dry overnight over slides and then stained with cresyl violet. Briefly, slides were immersed 2 minutes in MilliQ water, later subjected to several steps of dehydration and differentiation with ethanol solution at different concentrations (50%, 70%, 95% and 100% - 2 minutes each) and then immersed in the cresyl violet solution for 30 minutes. Finally, slides were immersed again in 95% ethanol solution and 100% ethanol, 2 minutes each and allowed to dry. Finally, they were analyzed under a light microscope to verify the exact location of the recording site. Figure 2.13

shows some sections of the brain after staining, highlighting the area of the lesion, that corresponds to the position of the array and correlates with the calculated position from the rat brain atlas.

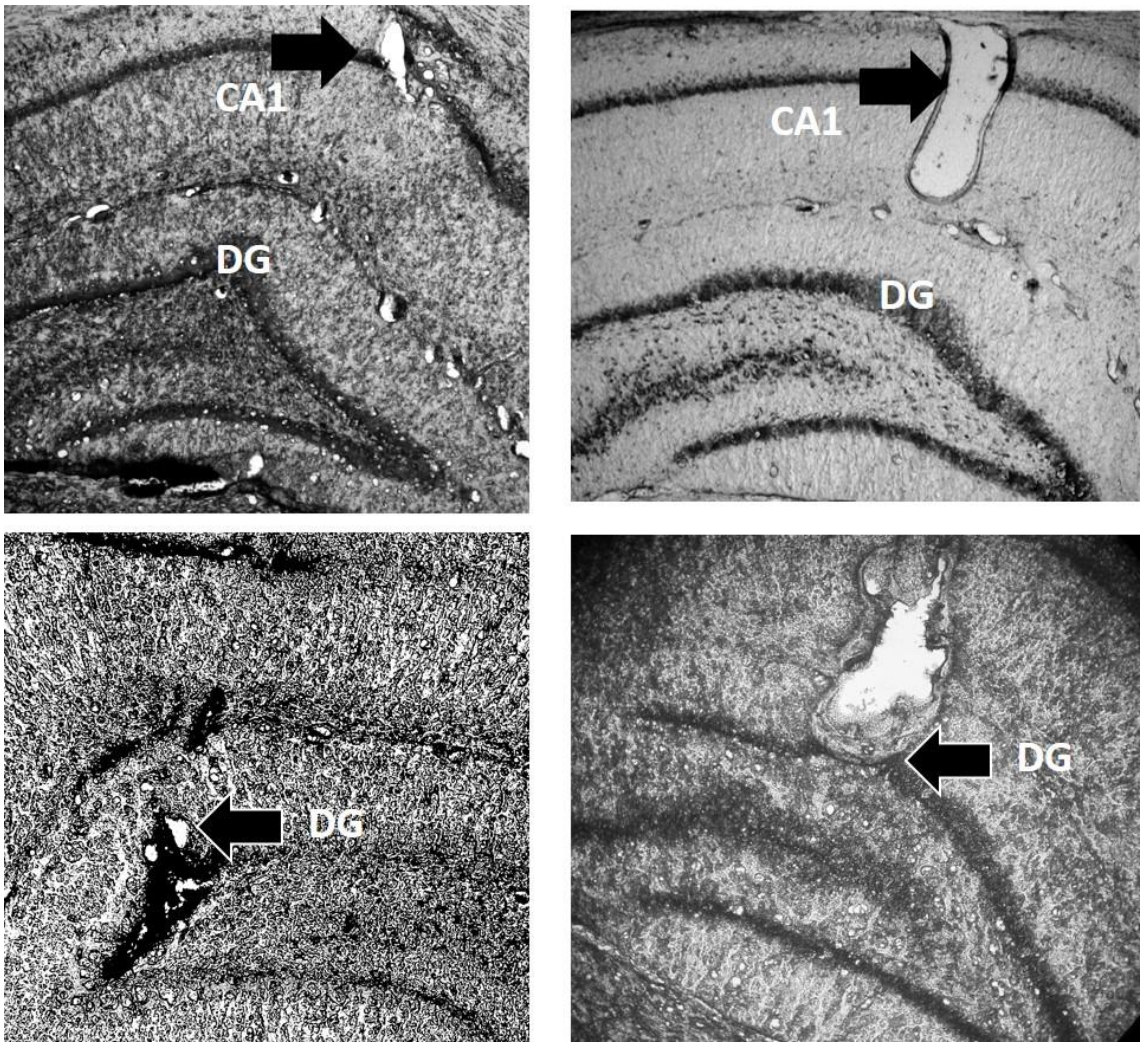

Figure 2.13. *Representative photographs of hippocampal coronal sections for confirmation of the recording site in the different subregions:* ***(A and B)*** CA1 *subregion,* ***(C and D)*** dentate gyrus*. Fixed tissue sections, 40 µm thickness, were stained with cresyl violet in order to visualize the lesion promoted by the current of 9.0 V applied through the active tip of the microelectrode.*

3. Real Time In vivo Measurement of Ascorbate in the Brain Using Carbon Nanotube- Modified Microelectrodes

Part of the work presented in this chapter was published in:

Ferreira, N. R., R. M. Santos, J. Laranjinha and R. M. Barbosa (2013). "Real Time *In vivo* Measurement of Ascorbate in the Brain Using Carbon Nanotube-Modified Microelectrodes." Electroanalysis 25(7): 1757-1763

3.1. Introduction

Ascorbate plays a modulator role in the brain, namely at the information processing and behavior functions linked to glutamate and dopamine-mediated neurotransmission, beyond its well-known function as an antioxidant and enzyme co-factor (Rebec and Pierce 1994, Rice 2000, Rebec 2007, Harrison and May 2009). In addition, ascorbate deficiency seems to be implicated in behavioral deficit in a transgenic mouse model of Huntington's disease (Rebec, Barton et al. 2002, Miller, Dorner et al. 2012). Although the brain tissue contains the highest concentration of ascorbate in the body, its regional distribution and concentration change in response to neuronal activation, raise the need for its real-time measurement upon neurotransmitter stimulation (Harrison and May 2009). Paradoxically, because of its high concentration in the brain extracellular space, (up to 500 μM), this molecule is usually viewed as an interferent molecule when major neurotransmitters (e.g. dopamine, noradrenaline and serotonine) are measured by electrochemical methods in combination with microelectrodes (Rebec, Barton et al. 2002).

A number of electrochemical methods have been described for the measurement of ascorbate in biological media but they suffer from major drawbacks. A major issue is that most of these methods do not allow the detection of ascorbate in brain tissue microenvironments in a real-time mode. Carbon fiber microelectrodes (CFMs) have been extensively used to study neurotransmitter release and uptake in association with fast electrochemical techniques such as amperometry, chronoamperometry and fast cyclic voltammetry. By virtue of its unique properties, such as favorable surface kinetics and biocompatibility, measurements can be performed with high spatial and temporal resolution and minimal damage to tissue (Barbosa, Lourenco et al. 2008, Huffman and Venton 2009, Lama, Charlson et al. 2012).

At physiological pH, ascorbate (first pKa = 4.10) is negatively charged whereas dopamine (pKa = 8.87) is positively charged. So far the most used approach to improve the selectivity of carbon fiber microelectrodes for measuring cathecolamine neurotransmitters *in vivo* is by coating the electrode surface with Nafion. This perfluorosulfonated polymer acts as an ion-exchange membrane highly permeable to cations but almost impermeable to anions (Gerhardt, Oke et al. 1984). Conversely, the use of polymers to improve the selectivity of CFMs for measuring ascorbate anion is very limited. Therefore, different approaches have been proposed which are based on the anodization treatment of CFMs in association with differential pulse voltammetry (Buda, Gonon et al. 1980, Pierce and Rebec 1993). Despite the fact that the anodization treatment allows the selective measurement of ascorbate, the sensitivity diminishes significantly after *in vivo* implantation of CFMs in the brain tissue. This problem has been partially solved by coating the

surface with a thin polymer film (Ghasemzadeh, Cammack et al. 1991). A further strategy to improve selectivity for ascorbate has been achieved by incorporating biochemical approaches with the electrochemical measurements. For instance, regional differences in extracellular ascorbate levels have also been reported by using a combination of FCV and ascorbate oxidase (Stamford, Kruk et al. 1984).

In recent years, carbon nanotubes (CNTs) have been extensively used for the fabrication of electrochemical sensors and biosensors due to their unique structural, mechanical, chemical and electronic properties. Usually found in two categories, single-wall (SWCNTs) and multiwall (MWCNTs), CNTs provide high surface-to-volume ratios, promote electron transfer reactions, decrease overpotentials of various electroactive compounds, increase sensitivity and reduce fouling (Agui, Yanez-Sedeno et al. 2008, Huffman and Venton 2009, Sarma, Vatsyayan et al. 2009, Vashist, Zheng et al. 2011).

To overcome the insolubility of CNTs in most solvents, Nafion can be used to make relatively stable suspensions via ultrasonication procedures (Wang, Musameh et al. 2003). In particular, the use of Nafion/CNT nanocomposite films offer an excellent matrix due to the chemical inertness, thermal stability, mechanical strength, antifouling property and good biocompatibility (Gerhardt, Oke et al. 1984, Gerhardt and Hoffman 2001, Brown and Lowry 2003). By using MWCNT modified microelectrodes (Hocevar, Wang et al. 2005) and carbon nanotube fiber microelectrode (Viry, Derre et al. 2010), dopamine has been measured in the presence of ascorbate. More recently, a polyaniline/polyacrylic/MWCNT modified Pt macrodisc electrode has been reported for measuring ascorbate in the presence of dopamine and uric acid (Ping, Wu et al. 2012, Tiwari, Singh et al. 2012). Furthermore, the simultaneous determination of ascorbate, dopamine and uric acid by using a screen-printed graphene electrode and chitosan-graphene modified electrodes has been reported (Han, Han et al. 2010).

Electrochemical methods *in vivo* require the use of fast techniques, such as constant potential amperometry, chronoamperometry or FCV, high sensitivity and selectivity and the use of ultra-small sensors (Lama, Charlson et al. 2012). To date, most of the studies reported in the literature concerning the measurement of ascorbate in biological media or tissues did not fulfill these criteria. The *in vivo* voltammetric measurement of ascorbate in the striatum of rat brain has been reported by using CFMs coated with a dimethylformamide/MWCNT film, but the use of a slow scanning technique such as differential pulse voltammetry did not allow the measurement of ascorbate in a real-time fashion (Zhang, Liu et al. 2007).

In this chapter, we have developed CFMs modified with Nafion and CNTs composite films for *in vivo* measurement of ascorbate the rat brain. The electrochemical characterization was studied, namely the electrocatalytic oxidation of ascorbate and dopamine, the analytical performance in terms of sensitivity, L.O.D., selectivity, response time and active surface area was also assessed. Furthermore, the modified-microelectrodes were stereotaxically inserted in the rat hippocampus for selective measures of both basal and glutamate-stimulated ascorbate release in the extracellular space.

3.2. Experimental

Calibration and *in vivo* experiments were performed by amperometry, (hold potential: +0.05 V *vs*. Ag/ AgCl) using a FAST-16 MK III high-speed electrochemical system Quanteon, L.L.C., KY, USA) in a two-electrode configuration. *In vivo* experiments were performed in the CA1 region of the hippocampus. All these procedures, as well as chemicals and solutions referred in this chapter have been described in chapter 2.

A scanning electron microscope JEOL (JSM-5310) was used to visualize the surface morphology of the microelectrodes. Ascorbate and dopamine oxidation potential was determined by square wave voltammetry (SWV), using an IVIUM Compactstat (Ivium Technologies, The Netherlands). This technique and equipment was also used for SWV experiments performed *in vivo*. Microelectrodes active surface area was determined by cyclic voltammetry using an Autolab potentiostat coupled to a GPES software version 4.9 (Eco Chemie, The Netherlands).

Data were analyzed for statistical significance defined at $p<0.05$ and were expressed as the mean $\pm$ standard deviation (S.D.). One-way analysis of variance (ANOVA) was performed to make comparisons between multiple groups followed by Dunnett pos-test. For each group of microelectrodes the confidence intervals (CI) at 95% were also calculated. Statistical analyses were performed using Origin Pro 7.5 and GraphPad Prism 5. Amperometric *in vivo* recordings were averaged and represented as black line (mean) with gray area (standard error).

3.3. Results and discussion

3.3.1. Scanning Electron Microscopy of Microelectrode Surface

Figure 3.1 illustrates SEM images of typical bare CFM tip surface (A) and after modification with SWCNT (100 mg/mL) in Nafion composite film (B). At low magnification, a very smooth surface was observed for bare CFM whereas a rugged surface was clearly seen at the CFM tip modified with the composite film. These surface morphologies obtained with SWCNT composite films are very similar to that obtained by MWCNTs (not shown). The roughness surface of the CNT-modified microelectrodes suggests an increase of the surface area of the active tip when compared with bare CFMs.

A)

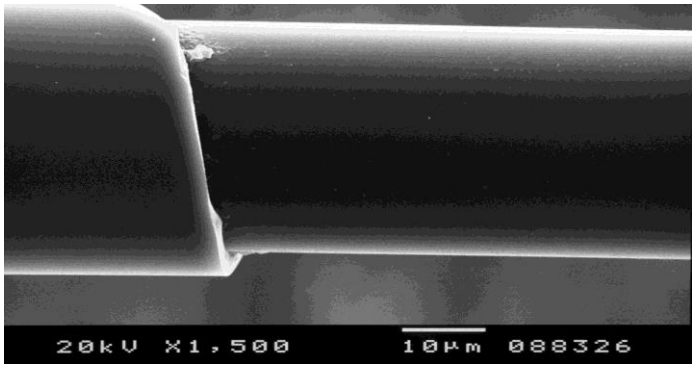

B)

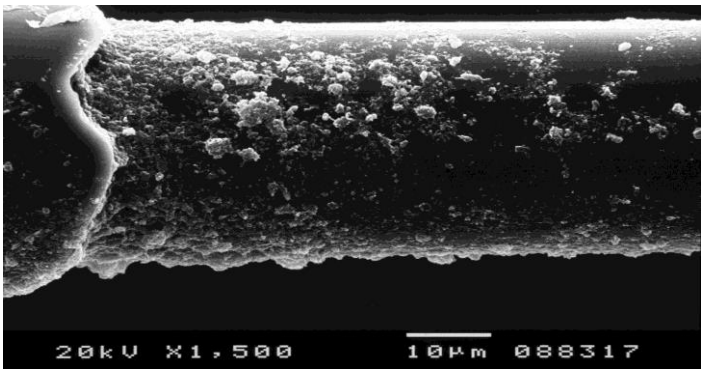

Figure 3.1. *Typical SEM images of the surface tip of bare carbon fiber microelectrodes (A) and modified with Nafion/SWCNT composite film (B) with same magnification 1500x.*

3.3.2. Microelectrode active surface area

As observed in figure 3.1, the deposition of carbon nanotubes onto the surface of the carbon fiber appears to increase the microelectrode tip active surface area. To study this increase we have carried out a cyclic voltammetric study of hexascorbatemmineruthenium (III) chloride (5 mM) in 1 M KNO_3 using bare CFMs and CFMs modified with Nafion/SWCNT. These experiments were performed using an autolab potentiostat from Echo Chemie (The Netherlands) and data acquisition was done with a GPES software. Potential was swept between -0.6 and +0.1 V *vs* Ag/AgCl reference. Results in figure 3.2 A and C clearly show the increase in current observed for CFMs modified with Nafion/SWCNT when compared with bare CFMs. The anodic and the cathodic peak heights as function of the square root of the scanning rate for bare and Nafion/SWCNT modified CFMs are shown in figure 3 B and D. The obtained linear relationship indicates clear diffusion character. The ratio of the anodic and cathodic current peak heights is close to one for both kinds of CFMs; this indicates the reversible character of the oxidation of hexascorbatemmineruthenium (III) chloride in both surfaces (N. S. Neghmouche 2013).

The apparent electroactive areas were calculated by using the Randles-Sevcik equation (eq 3.1).

$$A = I_p / (v^{1/2} K n^{3/2} D^{1/2} c)$$ **(equation 3.1)** (Randles 1947)

Here, I_p is the peak current (A), K is a constant (2.69 x 10^5), A is the surface area (cm^2), c is the concentration of the redox species (M), D is the diffusion coefficient of the redox species in $cm^2\ s^{-1}$ and v is the scan rate ($V\ s^{-1}$).

The values obtained were 1.4 ± 0.4 x 10^{-4} cm^2 and 15.6 ± 6.1 x 10^{-4} cm^2 (n= 8) for bare and Nafion/SWCNT modified CFMs, respectively. When assessed by paired Student's *t*-test a statistically significant difference between the two means ($p<0.01$) was observed. These results confirm that the roughness observed in SEM images for the CFMs modified with Nafion/SWCNT is correlated with an effective increase in their electroactive surface area, despite having Nafion blocking part of the surface.

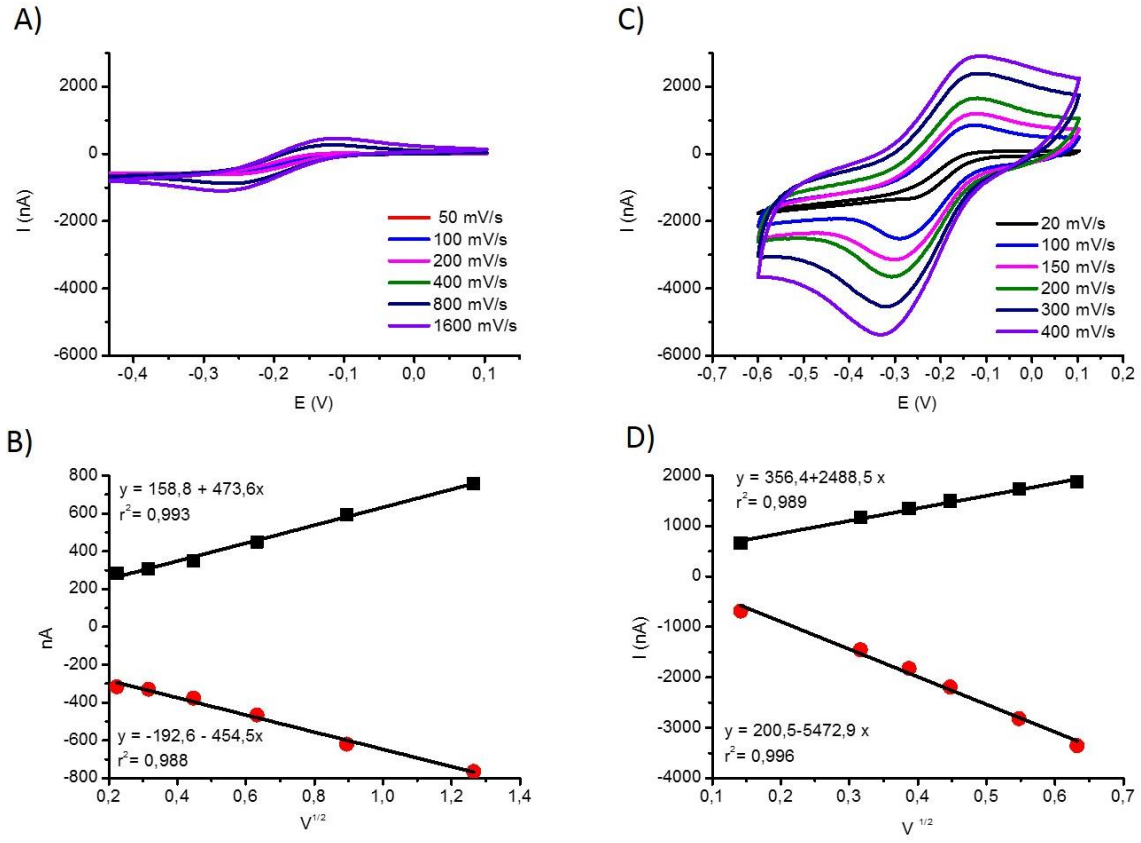

Figure 3.2. *Cyclic voltammograms of bare (A) and Nafion/SWCNT surface modified (C) CFM's in the presence of hexascorbatemmineruthenium (III) chloride (5 mM) in 1 M KNO_3. Linear regression plots of the oxidation and reduction peaks for a bare (C) and Nafion/SWCNT surface modified CFMs (D). Slopes are given in nA/V1/2.*

3.3.3. Electrocatalytic Oxidation of Ascorbate at Modified-Microelectrodes

It is well described that oxidation of ascorbate at bare electrodes is totally irreversible and requires high overpotentials because of the slow electron transfer kinetics and fouling of the electrode surface by the ascorbate oxidation products. At physiological pH, the oxidation of ascorbate involves the loss of a single proton and two electrons, yielding dehydroascorbate (Banhegyi, Braun et al. 1997, Raj and Ohsaka 2001, Liu, Honma et al. 2007). As shown in figure 3.3 A the anodic peak potential of ascorbate determined by SWV was +0.243 V *vs*. Ag/AgCl when using bare CFMs but, meaningfully, the peak was shifted negatively to -0.044 V in the case of Nafion/SWCNT modified CFMs, indicating a strong electrocatalytic effect of CNTs. This observation is in agreement with previous works describing the electrocatalytic effect on the ascorbate oxidation of MWCNTs-IL-Gel deposited on glassy carbon electrode (Zhao, Gao et al. 2005), of MWCNTs/Nafion modified carbon fiber electrode (Hocevar, Wang et al. 2005) and of MWCNTs/Nafion layer over platinum disc electrode on ascorbate oxidation (Tiwari, Singh et al. 2012). Noticeably, the electrocatalytic oxidation of dopamine at Nafion/SWCNT modified CFMs

suffered a less pronounced negative shift than ascorbate. The average oxidation potential for dopamine changed from +0.224 V in bare CFM to +0.196 V in Nafion/SWCNT modified CFMs (Figure 3.3 B). Thus, the peak resolution of both compounds was clearly visible by SWV as illustrated in figure 3.3 C.

Table 3.1 summarizes data of oxidation peak potential obtained by SWV for bare and surface-modified CFMs. When compared with bare CFM, both nanocomposite films evaluated exhibited an electrocatalytic effect on the ascorbate oxidation corresponding to a negative shift of ca. 0.3 V. Data analysis by One-way ANOVA followed by Dunnett pos-test, indicate that the differences are statistically significant ($p<0.001$) between bare (control) and modified-microelectrodes but not between Nafion/CNT modified microelectrodes ($p>0.05$).

Table 3.1. *Ascorbate peak oxidation potential of carbon fiber microelectrodes*

CFM	Oxidation peak potential (V)
Bare	+0.243 ± 0.050 (n=12)
Nafion/SWCNT	-0.044 ± 0.033 (n=10)
Nafion/MWCNT	-0.020± 0.006 (n=11)

The data are represented as mean ± S.D.

The number of microelectrodes is given in parenthesis.

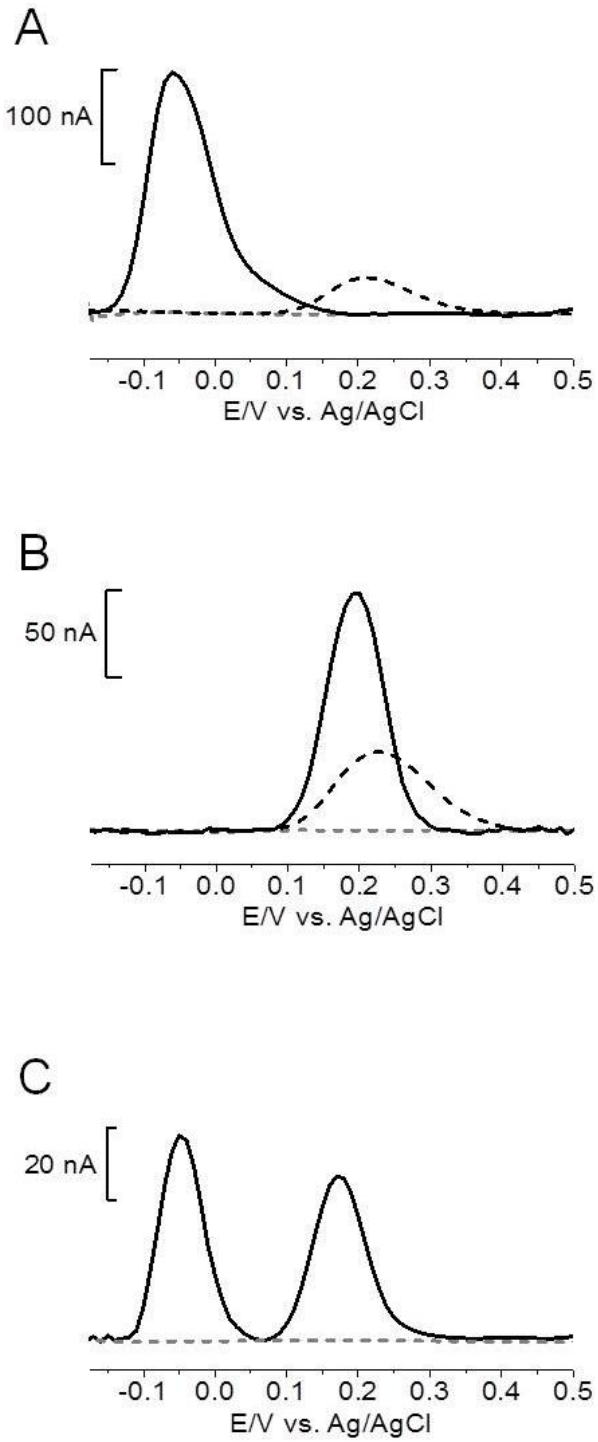

Figure 3.3. *(A) Ascorbate peak oxidation potential of bare (black dashed line; 1 mM; Ep = +0.243 V) and Nafion/SWCNT modified CFMs (solid line; 0.5 mM; Ep = -0.044 V). (B) Dopamine peak oxidation potential of bare (black dashed line; 20 µM; Ep = +0.224 V) and Nafion/SWCNT modified CFMs (solid line; 20 µM; Ep = +0.196 V). (C) Ascorbate (400 µM) and dopamine (20 µM) peak oxidation potential in Nafion/SWCNT modified CFM (Ep = -0.028 V and Ep = +0.178 V, respectively). Gray dashed lines represent baseline in each experiment. Square wave voltammetry parameters:* f*=10 Hz,* Es*=2 mV,* Esw*=10 mV.*

3.3.4. Linearity, Sensitivity and Detection Limit

Figure 3.4 shows a typical amperometric recording of the Nafion/SWCNT modified microelectrode at holding potential of +0.05 V *vs*. Ag/AgCl upon addition of 50 μM, 100 μM, 200 μM, 400 μM, and 800 μM ascorbate to a PBS buffer solution. At the beginning of the recording, dopamine, noradrenaline, DOPAC and nitrite were added to determine the corresponding selectivity ratios of the modified microelectrodes. Response time ($t_{50\%}$) was also calculated from the recordings and, typically, the modified microelectrode reached a steady-state in less than 0.5 s. The modified microelectrodes displayed a good linear response to ascorbate in the range of 50 μM up to 800 μM (R^2 = 0.998) as shown in figure 3.4 (inset). Calibration sensitivity was obtained from the linear regression of current peak height *vs*. concentration of ascorbate, giving a slope of 42.6 pA/μM and an intercept of 965 pA with a R^2= 0.998 for the recording presented.

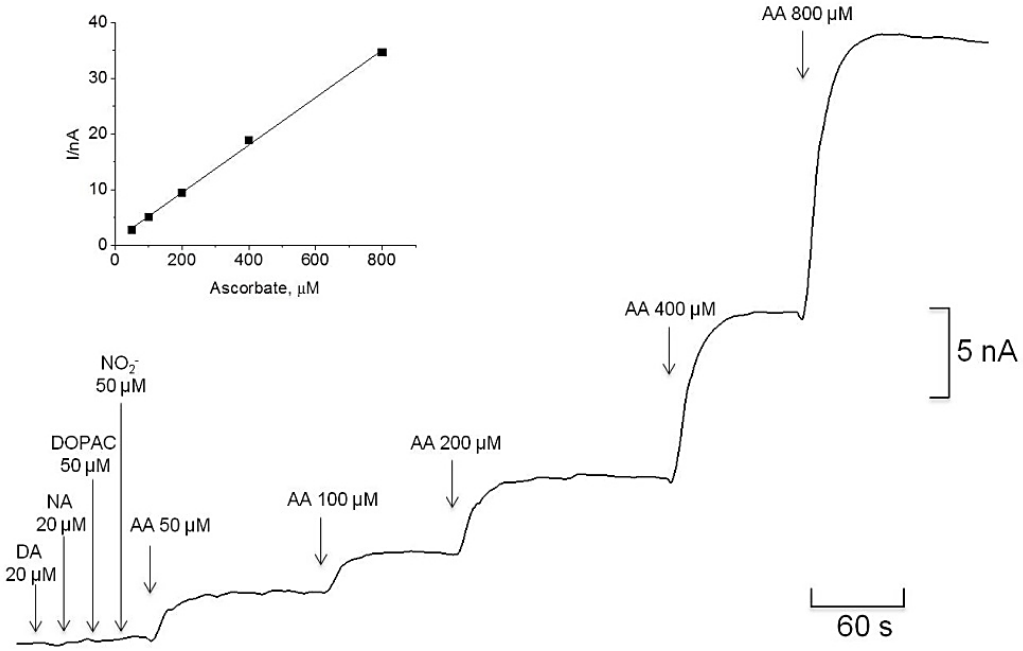

Figure 3.4. *Amperometric current recording at +0.05V vs. Ag/AgCl of a CFM/Nafion/SWCNT to successive additions of 50, 100, 200, 400 and 800 μM of ascorbate (represented in the figure as AA) and to the addition of potential interferents (DA – dopamine; NA – noradrenaline) present in the hippocampus. The calibration curve is shown as inset.*

Data in table 3.2 supports that the sensitivity of the Nafion/SWCNT microelectrodes is ca. 10 fold higher when compared with bare microelectrodes. Data analysis by One-way ANOVA followed by Dunnett pos-test, indicates that the differences between bare (control) and modified-microelectrodes are statistically significant ($p<0.05$). Likewise, the differences on L.O.D. are also statistically significant ($p<0.05$). These results emphasize the electrocatalytic properties of the Nafion/CNT composite in a way that allows a dramatic increase in sensitivity when working at

+0.05 V. These sensitivity and L.O.D. values compare favorably with previous reports (Kulagina, Shankar et al. 1999, Zhang, Liu et al. 2007), despite the use of different electrochemical techniques, experimental conditions and CFMs tip dimensions.

***Table 3.2**. Ascorbate calibration parameters obtained for carbon fiber microelectrodes modified with carbon nanotubes composite films at +0.05V vs. Ag/AgCl.*

Calibration parameter	**CFM Bare**	**CFM/Nafion/SWCNT**	**CFM/Nafion/MWCNT**
Sensitivity (pA/µM)	1.3±1.5 [0.5 – 2.1] (n=16)	37.5±34.9 [22.0-52.9] (n=22)	41.2±30.6 [20.7-61.8] (n=11)
L.O.D. (µM)	18.1±28.7 [2.9-33.5] (n=16)	2.6±3.1 [1.2-4.0] (n=22)	1.6±1.7 [0.5-2.7] (n=11)
Linearity (R^2)	0.995±0.002 [0.991-0.998] (n=16)	0.990±0.013 [0.985-0.996] (n=22)	0.992±0.012 [0.983-1.000] (n=11)
Response time (s)	0.35±0.25 [0.20-0.55] (n=12)	0.30±0.10 [0.25-0.40] (n=14)	0.50±0.25 [0.25-0.70] (n=6)

The data are represented as mean ± S.D. The confidence interval (CI) for sensitivity, limit of detection (L.O.D.) and response time is given in square brackets. The number of microelectrodes tested is given in parenthesis.

3.3.5. Selectivity

The oxidation potential of ascorbate at most common electrode materials (e.g. carbon, platinum) is very close to that of catecholamines (e.g. dopamine) and their metabolites (e.g. DOPAC), and by this reason the overlapping of the oxidation currents is a major problem.

Direct measurements of ascorbate by electrochemical methods in complex biological media such as brain tissue requires the use of microelectrodes with high selectivity against major compounds found in the extracellular space. Taking into consideration the relatively poor resolution power of the voltammetric techniques, one of the best experimental strategies that have been followed to improve selectivity is the modification of the microelectrode surface properties. This is an approach of utmost importance when the microelectrodes are associated with amperometry.

The CNT-modified CFMs, by shifting the oxidation potential of ascorbate negatively, allowed the measurement of anodic currents at very low potential (+0.05 V in this work). In addition, the electrocatalytic effect of the CNT-modified CFMs to dopamine was much less pronounced when compared with ascorbate. Therefore, a very high selectivity was expected against the majority of electroactive compounds present in the brain extracellular space. In fact, the recording depicted in figure 3.4 demonstrates that the interferents dopamine, noradrenaline, DOPAC, NO_2^- added sequentially did not induce measurable current changes, confirming the high selectivity of these modified-microelectrodes for ascorbate measurements.

3.3.6. *In vivo* fouling

Although sensitivity is of great importance in the characterization of the microelectrode response to ascorbate, its loss during *in vivo* exposure is always a major concern. Upon *in vivo* implantation of CFM/Nafion/SWCNT the decrease of sensitivity observed in a typically experiment lasting for 3-4 hours, was 82% (n=7) of their initial value. These values are in agreement with those obtained by others with electrochemical pre-treated microelectrodes (84%) (Ghasemzadeh, Cammack et al. 1991). It has been also reported a 66% decrease in sensitivity of a CFM coated with dimethylformamide and MWCNTs inserted in brain tissue during 10 minutes when assessed by differential pulse voltammetry (Zhang, Liu et al. 2007). These results emphasize the importance of performing calibrations after the *in vivo* experiments in order to get more accurate quantifications of ascorbate. In fact, this is agreed to be most representative of the *in vivo* measurement (Basse-Tomusk and Rebec 1990, Peter Capella 1990). The observed loss of sensitivity *in vivo* may be due to implantation and electrode fouling by interaction with the surrounding environment. Nevertheless, such loss of sensitivity is observed mainly during the first 20 minutes after implantation needed for stabilization of the background before starting the experiments.

Afterwards and throughout the time course of the *in vivo* recordings the sensitivity loss is much lower. Figure 3.5 shows local ejections of ascorbate (20 mM) at different time points of the experiment (400 s – black line, 2309 s - red line and 6480 s – blue line) and it is possible to observe that the intensity of the signal remains constant. Collectively, these results contribute to validate quantifications of ascorbate based on post calibration data and rule out a gradual decrease in sensitivity.

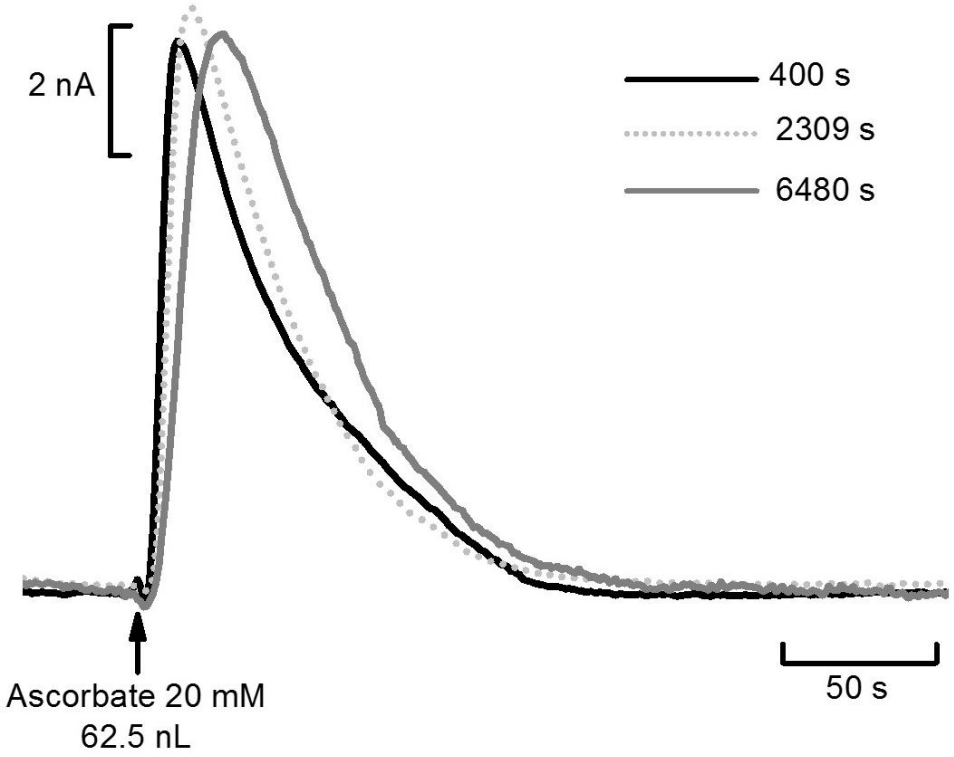

Figure 3.5. *Overlay of three amperometric recordings of ascorbate dynamics in rat hippocampus* in vivo *using CFM/Nafion/SWCNT following local pressure ejections of ascorbate 20 mM (65 nL) at different times. Black line – 400s, gray dotted line – 2309 s; gray full line – 6480 s. Arrow indicates the time of ejection.*

3.3.7. Real Time Measurements of Brain Extracellular Ascorbate

The Nafion/SWCNT microelectrodes coupled to amperometry were used for measuring rapid changes of extracellular ascorbate in the rat brain evoked by local stimulation with the excitatory neurotransmitter glutamate. The identity of the released compound was also assessed by SWV. Figure 3.6 shows a representative *in vivo* amperometric recording (hold potential: +0.05 V *vs*. Ag/AgCl) using a Nafion/SWCNT microelectrode following local pressure ejection of 20 mM L-Glutamate to induce the release of ascorbate in the hippocampal CA1 region of the rat hippocampus. Glutamate stimulation induced a rapid increase in the oxidation current corresponding to an ascorbate concentration change of 400 µM according to the post-calibration data.

The ascorbate concentration dynamics evoked by glutamate induced a biphasic signal, an observation that was not described in previous studies carried out in hippocampus, cortex and striatum (Cammack, Ghasemzadeh et al. 1991, Ghasemzadeh, Cammack et al. 1991, Kulagina, Shankar et al. 1999). In order to demonstrate that the current signal was derived from ascorbate oxidation, SWV has been performed before and after glutamate stimulation as depicted in Fig 3.6 (insets). On basis of pharmacological studies, the mechanism underlying glutamate evoked ascorbate efflux into brain extracellular space likely involves the glutamate/ascorbate heteroexchange (Cammack, Ghasemzadeh et al. 1991, Rebec and Pierce 1994, Yusa 2001).

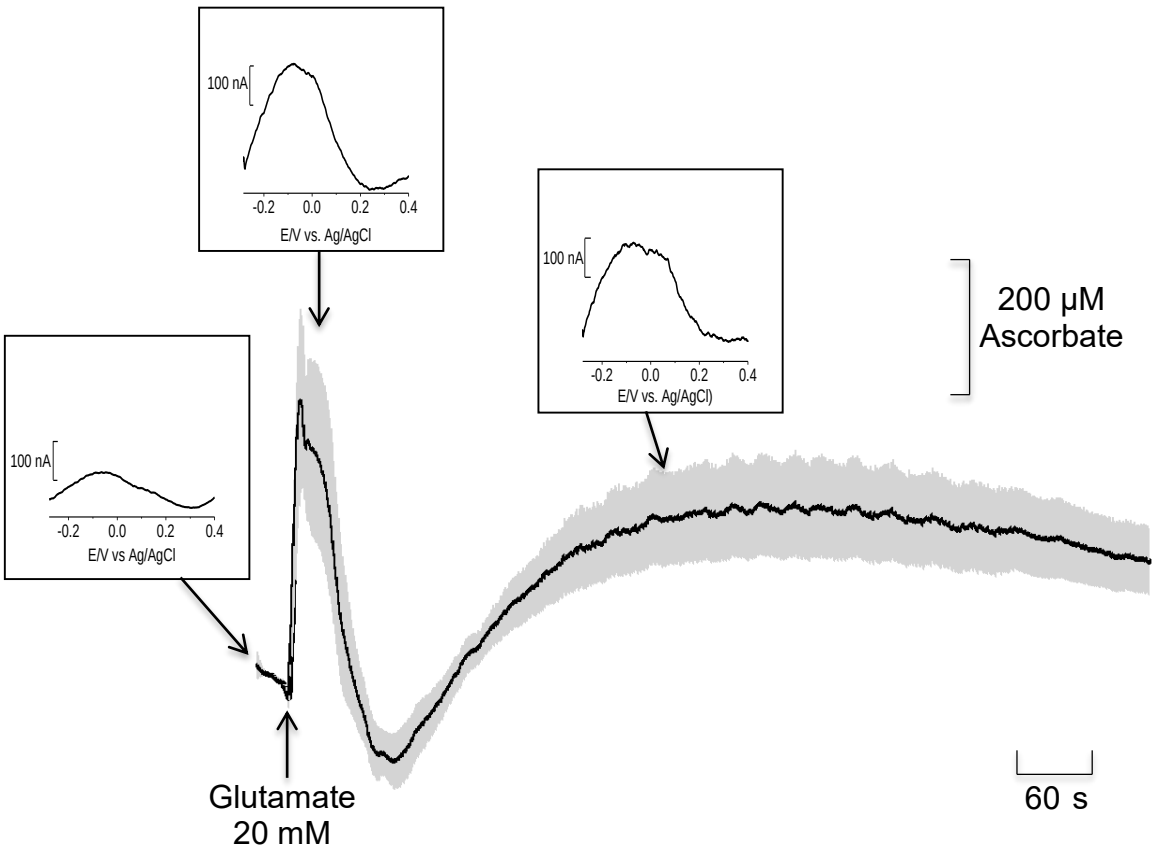

Figure 3.6. *Average amperometric recording of ascorbate dynamics in rat hippocampus* in vivo *using Nafion/SWCNT microelectrode following stimulation with glutamate 20 mM. Square wave voltammograms were carried out for each phase of the response (inset). Amperometric current was recorded at +0.05V vs. Ag/AgCl. SWV parameters:* f *= 50 Hz,* Es *=2 mV,* Esw *= 10 mV.*

SWV allows a relatively fast scan rate when compared with other voltammetric approaches. Taking advantage of this high temporal resolution (one scan each 2 s), we were able to collect several voltammograms during an *in vivo* experiment. Then, we used Origin 7.5 software to convert the conventional bi-dimensional plot into a false color representation to visualize the data with the applied potential as ordinate and time as abscissa with the current represented by color. Figure 3.7 shows the false color plot obtained during an *in vivo* experiment following a local stimulation with 20 mM L-glutamate. These results confirm the biphasic nature of the ascorbate signals, since it is possible to observe a biphasic increase in current (between 50-100 s and again after 130s) at the characteristic oxidation potential of ascorbate for the Nafion/SWCNT microelectrode.

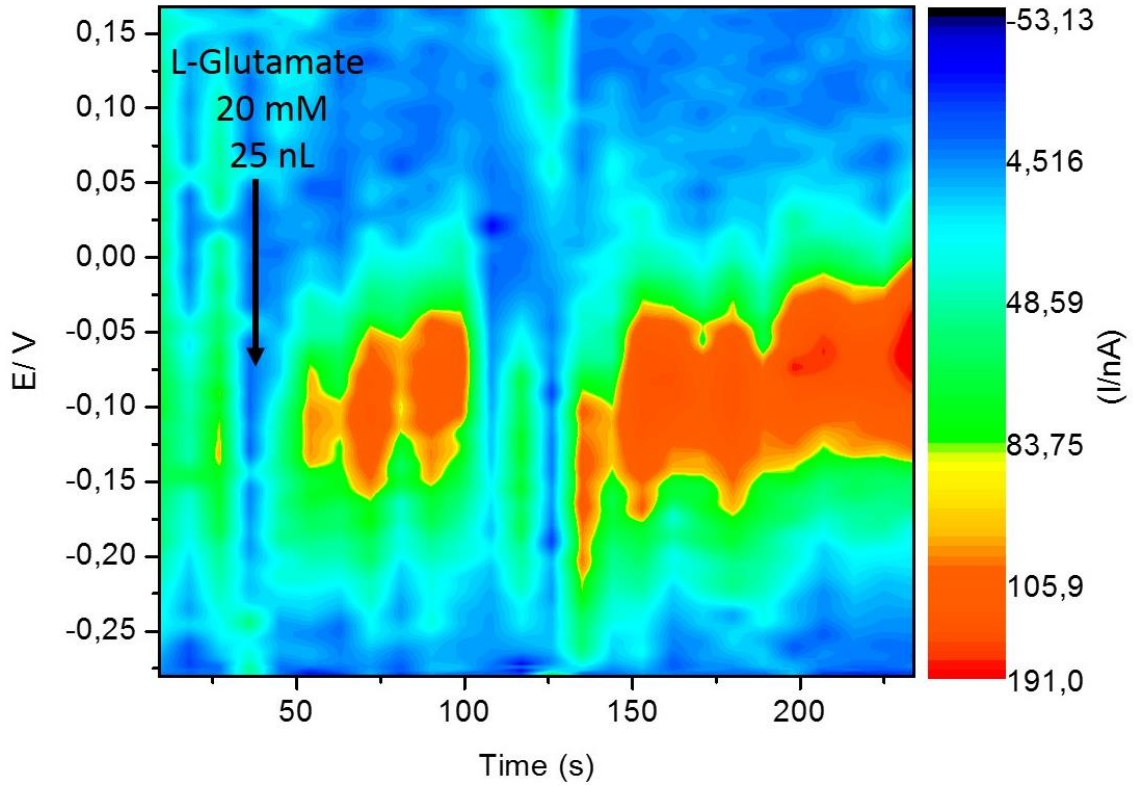

Figure 3.7. *Color representation of the voltammograms obtained during a local ejection of L-glutamate 20 mM (indicated in the arrow) in the CA1 region of the rat hippocampus. The abscissa is time, the ordinate is applied potential, and the current is shown in false color. SWV parameters:* f *= 50 Hz,* Es *=2 mV,* Esw *= 10 mV.*

Considering that extracellular ascorbate has been shown to be homeostatically regulated at the expense of intracellular stores (Grunewald, O'Neill et al. 1983, Grunewald and Fillenz 1984, Grunewald 1993, Rebec and Pierce 1994) a further strategy to provide a biologically relevant ascorbate measurement rely on its biochemical oxidation of ascorbate oxidase. Thus, basal ascorbate concentration in the CA1 region of the hippocampus was also assessed by measuring the decrease in current with Nafion/SWCNT microelectrodes following pressure ejection of ca. 50 nL of ascorbate oxidase (0.1 mg/mL) as shown in figure 3.8. The current change was converted to ascorbate concentration according to post-calibration, corresponding on average to 290 ± 130 µM (n=12), which is consistent with the value reported previously in rat hippocampus by using electrochemically pre-treated CFMs (Ghasemzadeh, Cammack et al. 1991). Local ejection of glutamate (20 mM) following ascorbate oxidase did not induce any measurable oxidation current (Figure 3.8).

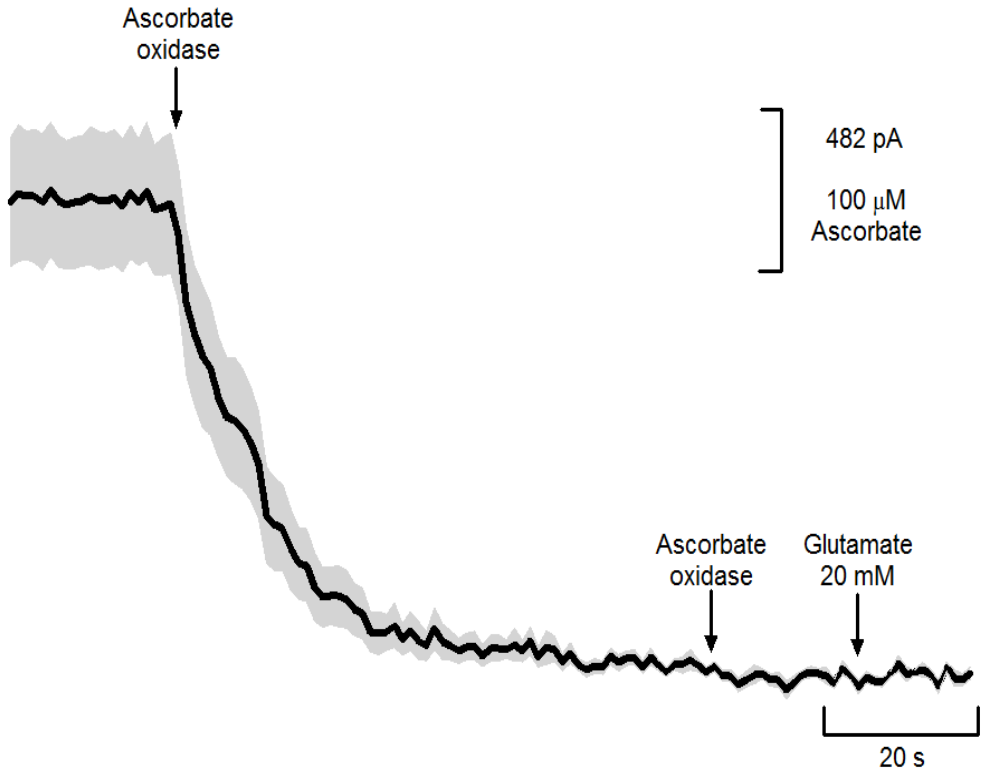

.

Figure 3.8. *Average amperometric current recording at +0.05 V of basal ascorbate in the CA1 region of the rat hippocampus following ejection of ascorbate oxidase (0.1 mg/ mL).*

3.4. Conclusions

Ascorbate has gained recognition as a neuromodulator linked to extracellular glutamate and other monoamines neurotransmitters. The fast and selective measurement of ascorbate in the brain extracellular space with CFMs has been a challenging task mainly because of the interference of uric acid, dopamine and its metabolite DOPAC among many other electroactive molecules. By using CFMs and a nanocomposite film based on CNTs and Nafion we have developed a novel ascorbate microsensor that fulfils the criteria of size, speed, selectivity and sensitivity required for directly probing *in vivo* the temporal and spatial dynamics of brain chemicals. Due to the electrocatalytic properties of CNTs, the modified-microelectrodes exhibited a very high selectivity against major interferents compounds present in the brain extracellular space, as well as high sensitivity and a low L.O.D for the measurement of ascorbate. Regardless of the observed decrease in sensitivity during *in vivo* implantation, the nanocomposite film prepared from Nafion provides excellent biocompatibility which is essential for chronic *in vivo* recordings in brain tissue. This study demonstrates that when combined with amperometry the modified microsensors allow the measurement of basal or tonic extracellular ascorbate in the rat hippocampus, and the phasic changes following stimulation with glutamate. Hence, the microsensor described in the present work could be of interest for assessing the role of ascorbate in brain physiology and pathophysiology like in Huntington's disease.

4. Simultaneous Measurements of Ascorbate and Glutamate *in vivo* in the Rat Brain

4.1. Introduction

As referred previously, ascorbate is known to play important roles in the brain. Besides being an antioxidant and enzyme co-factor, this molecule modulates information processes linked to glutamate, the major mediator of excitatory signals in the mammalian central nervous system and probably involved in most aspects of normal brain function including cognition, memory and learning. Glutamate also plays major roles in the development of the central nervous system, including synapse induction and elimination, cell migration, differentiation and death (Danbolt 2001). It has been suggested that changes in extracellular glutamate levels are coupled to fluctuations in extracellular ascorbate levels, via a heteroexchange mechanism involving the glutamate transporter proteins (O'Neill, Fillenz et al. 1984, Cammack, Ghasemzadeh et al. 1992, Miele, Boutelle et al. 1994, Walker, Galley et al. 1995). According to this model, glutamate uptake triggers the outward transport of ascorbate. In addition, ascorbate and glutamate have been implicated in neurodegenerative processes like Alzheimer or Huntington's disease (Rebec, Barton et al. 2003, Rebec 2007, Harrison, Hosseini et al. 2009, Harrison, Bowman et al. 2014). In this context, the idea of monitoring both neurochemicals dynamics *in vivo* with high spatial and temporal resolution could give new insights about the dynamic interplay between these two molecules during excitatory processes.

Intracranial microdialysis is the most widely used method for measuring L-glutamate and other amino acids in CNS tissues *in vivo* (Timmerman and Westerink 1997). Its strength involves identification of chemicals of interest in the dialysis sample by using powerful analytical techniques such as HPLC, with electrochemical detection or fluorescent detection. However, this approach can be damaging to the brain tissue (Clapp-Lilly, Roberts et al. 1999, Hascup, af Bjerken et al. 2009), may not detect synaptically derived neurotransmitters (Timmerman and Westerink 1997), and lacks the temporal resolution (>5 minute) to identify rapid synaptic-related events believed to occur to rapidly remove glutamate from the extracellular space by transporters located on neurons and glia in order to maintain low and non-toxic extracellular levels (Danbolt 2001).

To overcome some of the drawbacks of microdialysis technique, namely the spatio-temporal resolution and tissue damage, glutamate oxidase-coated ceramic microelectrode arrays (MEAs) have been developed (Burmeister, Moxon et al. 2000, Burmeister and Gerhardt 2001). These biosensors arrays have been successfully used for second-by-second, self-referencing measures of tonic and potassium-evoked glutamate levels both acutely and chronically within a variety of

brain structures and animal models (Day, Pomerleau et al. 2006, Quintero, Day et al. 2007, Hinzman, Thomas et al. 2010, Hascup, Hascup et al. 2011, Stephens, Quintero et al. 2011).

We have described in the previous chapter a novel ascorbate microsensor with the appropriate analytical properties for directly probing *in vivo* the temporal and spatial dynamics of ascorbate.

In this chapter we aimed at performing simultaneous measurements of ascorbate and glutamate in the brain of anesthetized rats in order to assess the dynamic interplay between these two molecules. For that purpose, we coupled the use of Nafion/SWCNT modified carbon fiber microelectrodes with MEAs biosensor for ascorbate and glutamate measurements, respectively. Since ascorbate sensors have already been characterized in the previous chapter, we started by performing *in vitro* experiments to assess the analytical performance of the MEA glutamate biosensors. Then, we used the MEAs to monitor glutamate release from the hippocampus of anesthetized rats and finally we recorded simultaneous signals of ascorbate and glutamate in the same animal model with composite-modified microsensors and MEAs glutamate biosensors. This approach revealed to be a valuable tool for future studies regarding the relationship of these two compounds in the brain in physiological and/or pathological pathways.

4.2. Experimental

Refer to Chapter 2 for detailed information regarding solutions, microelectrodes and *in vivo* experiments related procedures.

4.2.1. Microelectrodes

In these studies we have used Nafion/SWCNT carbon fiber microelectrodes and ceramic based platinum microelectrode arrays (MEAs) glutamate biosensors for ascorbate and glutamate measurements, respectively.

4.2.2. Ascorbate and glutamate measurements

The holding potential of the working microelectrode was +0.05 V *vs*. Ag/AgCl for ascorbate measurement and +0.7 V *vs*. Ag/AgCl for MEAs glutamate biosensors. For this purpose we used two potentiostats models: the FAST-16 MKIII for glutamate and FST-16 MKII for ascorbate measurements.

4.2.3. Animal and surgical procedures

In vivo experiments were performed in male Wistar rats (8-12 weeks old, weight 250-390 g), as described in chapter 2.

4.2.4. Electrochemical recordings

The arrays used are represented in figure 2.11 C. *In vivo* experiments were carried out in the rat hippocampus, using the coordinates (from bregma) indicated in the figures legend. Recordings with MEAs were done by lowering site 1 into the brain region of interest. Data acquisition rate was 2 Hz for CFMs and MEAs recordings. After baseline current stabilization (ca. 15 minutes), glutamate or KCl 70 mM solutions were locally pressure ejected from the micropipette. To study evoked glutamate release, a potassium solution (70 mM KCl, 79 mM NaCl, 2.5 mM $CaCl_2$) was locally applied. Volumes of the solutions were ejected from the micropipette using a Picospritzer III (Parker Hannifin Corp., General Value, Fairfield, NJ, USA, general valve operation, 30–300 kPa over 0.2–2.0 s) monitored using a stereomicroscope fitted with a reticule.

4.2.5. Data analysis

Recordings were analyzed using Microcal Origin Pro 7.5. Data are presented as mean ± Standard error mean (S.E.M.). Differences between two data sets were evaluated by a Students *t*-test. Statistical tests between multiple data sets were carried out using a one-way analysis of variance (ANOVA). Statistical analyses were performed using GraphPad Prism 5, as well as for the

determination of Vmax and Km of glutamate oxidase. For this purpose, the observed current was plotted as a function of the added concentration of glutamate (substrate) to the biosensor where the enzyme was immobilized. Then a Michaelis-Menten nonlinear fit was applied.

Each potassium-evoked glutamate signal was analyzed by the following parameters: peak amplitude (μM glutamate), rise time (T_R in seconds), the time from stimulus ejection to peak amplitude), and total signal duration (T_{Total} in seconds), the time from stimulus ejection until complete return to signal baseline) and uptake rate (μM/s), $k^{-1} \times$ maximum amplitude (where k^{-1} is the slope of the linear regression of the natural log transformation of the decay over time).

The current signal was converted into glutamate concentration using pre-calibration sensitivity obtained for each site.

4.3. Results and discussion

4.3.1. Analytical performance of glutamate biosensor microelectrode array (MEA)

4.3.1.1. Sensitivity, selectivity, L.O.D and response time

Even though the MEAs have already been used in previous works (Burmeister, Pomerleau et al. 2002, Day, Pomerleau et al. 2006, Kevin N. Hascup 2006, Parikh, Ji et al. 2010), in this chapter we started by performing an evaluation of the analytical performance of the MEAs based glutamate biosensors in order to validate its use *in vivo*. Figure 4.1 shows a typical amperometric recording of a S2 MEA glutamate biosensor at holding potential of +0.7 V *vs*. Ag/AgCl upon 3 successive additions of L-glutamate (20 μM) to a PBS buffer maintained at 37 ^{o}C. Before the addition of L-glutamate, 250 μM of ascorbate was added to evaluate the selectivity ratios. Dopamine (20 μM) was added after L-glutamate for the same purpose. Response time ($t_{50\%}$) was also calculated from the recordings and, typically, the modified microelectrode reached a steady-state response in less than 1.0 s. The MEA displayed a good linear response to glutamate in the range of 20-60 μM (R^2 = 0.997) as shown in figure 4.1 (inset). Calibration sensitivity was obtained from the linear regression of current peak height *vs*. concentration of glutamate, giving a slope of 3.4 pA/μM and an intercept of 6.33 pA with a R^2= 0.998 for channel 1 and a slope of 2.1 pA/μM and an intercept of -3.667 pA with a R^2= 0.999 for channel 2 of the MEA biosensor for the recording presented.

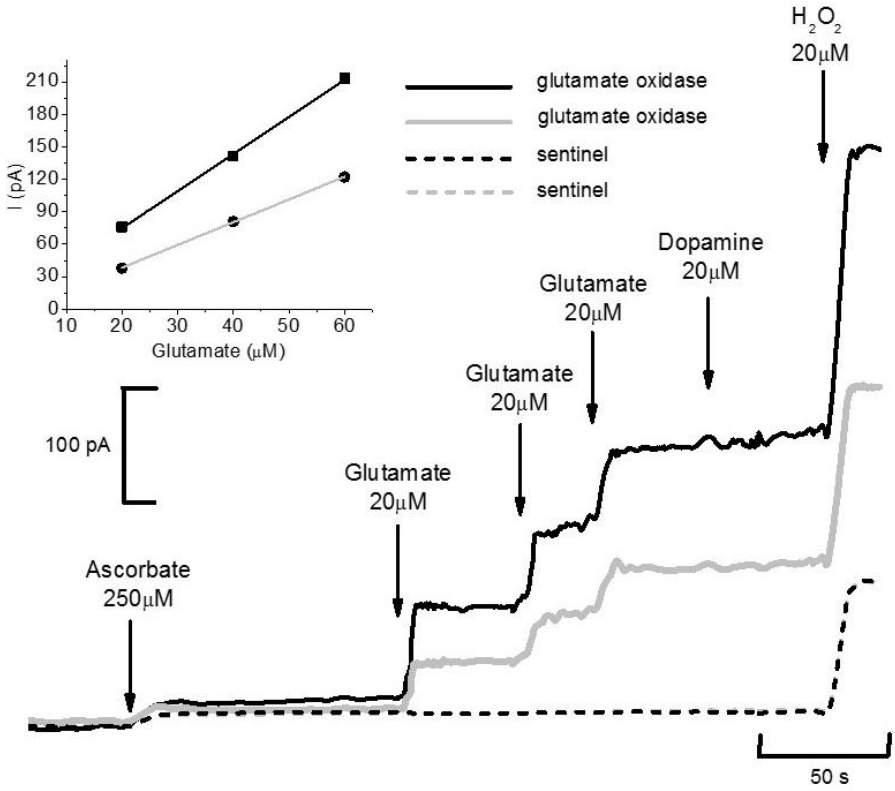

Figure 4.1. *Amperometric current recording at +0.7 V vs. Ag/AgCl of MEA (S2 design configuration) glutamate biosensor to successive additions of 20, 40 and 60 μM of glutamate and to the addition of interferents (ascorbate and dopamine). The calibration curve of each channel coated with glutamate oxidase is shown inset.*

Since two different MEA configurations were available, we performed a comparison of the analytical parameters (sensitivity, Linearity, response time, L.O.D and selectivity) between them. Figure 4.2 shows a typical recording of a calibration performed in R1 and S2 MEAs glutamate biosensors (black and gray lines, respectively). The average linear plot of each one of these MEAs configuration is also shown in figure 4.2 as inset. Both MEAs displayed a good linearity in the range of 20-60 μM as shown in figure 4.1 (inset).

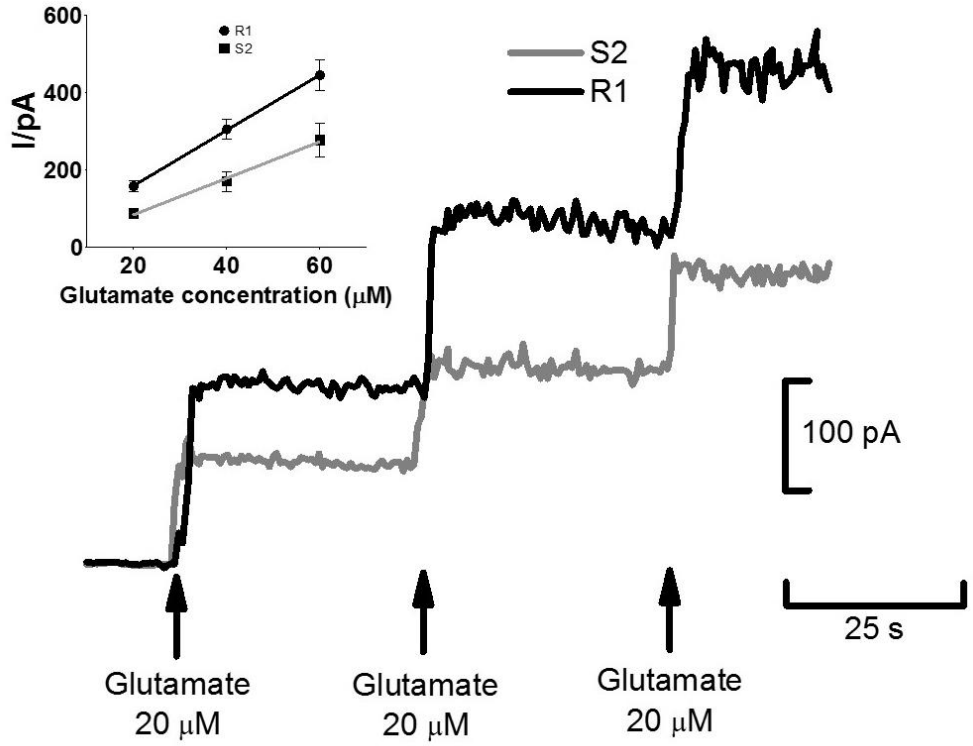

Figure 4.2. *Amperometric current recording at +0.7V vs. Ag/AgCl of S2 (gray line) and R1 (black line) MEA glutamate biosensors to three successive additions of 20 μM of glutamate. Average calibration curves (mean ± SEM) of each configuration of MEA glutamate biosensor is shown as inset (black line – R1, gray line – S2).*

Data in table 4.1 compares the analytical parameters of R1 and S2 MEA glutamate biosensors. It is possible to observe that both MEAs (R1 an S2) present good recording properties. These results are in agreement with previous reports even though sensitivity is lower (Burmeister and Gerhardt 2001, Burmeister, Pomerleau et al. 2002, Day, Pomerleau et al. 2006, Rutherford, Pomerleau et al. 2007, McLamore, Mohanty et al. 2010). It is interesting to observe that S2 MEA biosensors have a better sensitivity per area unit when compared to R1 MEAs, even though they present a lower absolute sensitivity. This means that in terms of recording surface, the S2 present a step forward in sensing capability when compared to the older R1 configuration MEAs. In terms of response time and L.O.D the values are very similar to what is found in the literature for the R1 configuration but the S2 MEAs have a significantly better performance in terms of L.O.D (~200 nM), suggesting that this design configuration is particularly suitable for measurements of very low levels of glutamate. In terms of selectivity, values here reported compare favorably with the literature, indicating that the electropolymerization with *m*-PD is an effective exclusion layer solution to obtain good selectivity ratios against major interferents in the brain.

Table 4.1. *Analytical parameters and selectivity ratios obtained for R1 and S2 MEAs glutamate biosensors.*

MEA configuration	Sensitivity (pA/µM)	Sensitivity (pA mm^{-2} $\mu M^{-1)}$	Linearity (R^2)	Response time $t_{50\%}$ (s)	L.O.D (nM)*	Selectivity ratio	
						Dopamine	Ascorbate
R1	7.1 ± 0.6 (n=18)	839.6 ±110.6 (n=18)	0.997 ±0.001 (n=18)	0.8 ±0.03 (n=12)	975 ± 251 (n=10)	423 ± 127 (n=6)	453 ± 34 (n=6)
S2	5.3 ± 0.8 (n=18)	1054.0 ± 166.1 (n=18)	0.998 ±0.001 (n=18)	0.9 ± 0.02 (n=6)	204 ± 32 (n=10)	438 ± 178 (n=6)	404 ± 84 (n=6)

*The data are represented as mean ± S.E.M. The number of microelectrodes tested is given in parenthesis. * p<0.05.*

4.3.1.2. Determination of Km and Vmax of glutamate biosensors

Due to the relatively low concentrations of glutamate in the extracellular space and high Km (values range from 0.3 to 5 mM) (System 2015), the kinetic parameters Km and Vmax for the enzyme glutamate oxidase are not usually of great concern. However, the efficiency of immobilized glutamate oxidase seems to be dependent of enzyme loading in the microelectrode surface (McMahon, Rocchitta et al. 2006). Given that the enzyme is applied manually in the MEAs surface by a drop-coating procedure which is a critical step in the preparation of the biosensor, we calculated glutamate oxidase Vmax and Km after the biosensor was fully constructed. With this additional information we can further validate the use of the biosensor for *in vivo* measurements. Figure 4.3 shows a calibration of the R1 and S2 MEA glutamate biosensors. The biosensor responds almost linearly in the range of concentrations (1-350 µM of L-glutamate). The average increase of current is higher for R1 biosensors when compared with S2. This was expected, due to its higher absolute sensitivity. The inset in figure 4.3 represents the Michaelis Menten nonlinear fit for R1 (black line) and S2 (gray line) biosensors, respectively.

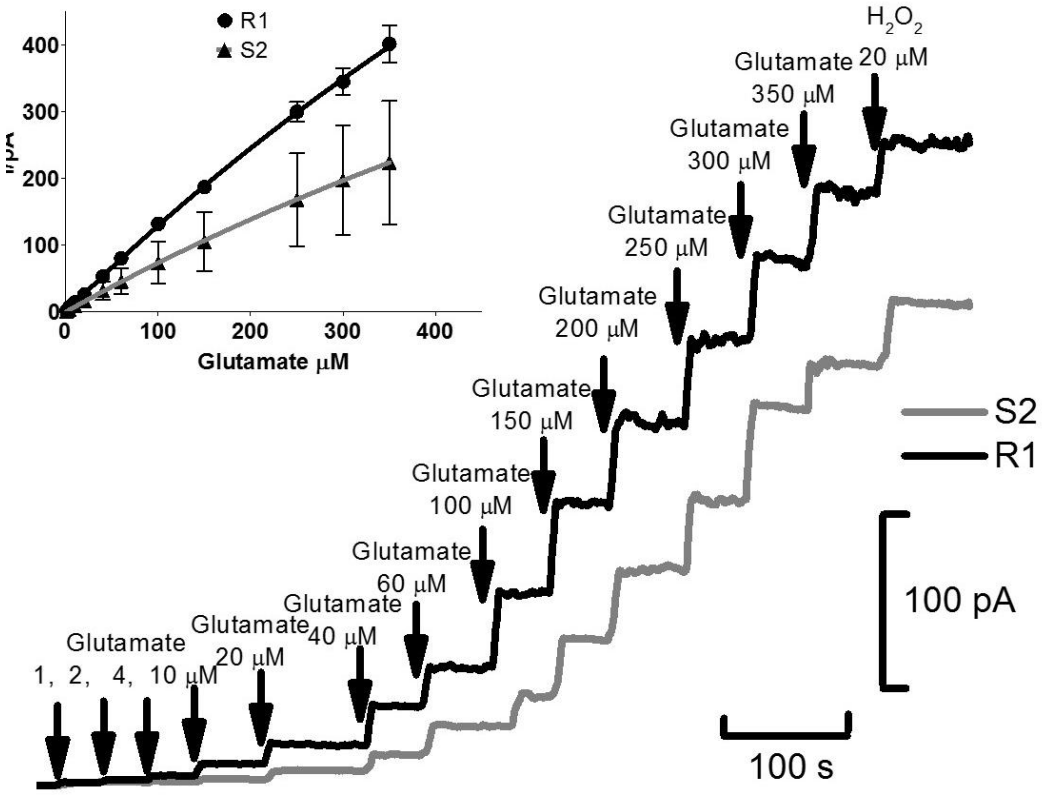

***Figure 4.3**. Amperometric response at +0.7 V vs. Ag/AgCl of R1 and S2 MEAs glutamate biosensors to successive additions up to 350 μM of glutamate. Inset: Michaelis-Menten fit (mean ± SEM; n=8 (R1) and n=6 (S2) of glutamate biosensors based on R1 and S2 MEAs.*

The nonlinear fit and data analysis was performed with GraphPad Prism 5.0 and the calculated values are presented in table 4.2. Reported values are in accordance with the literature (System 2015), for both Vmax and Km of the enzyme. S2 MEAs biosensors used in this study presented a high variability in terms of absolute current *vs* added concentration of glutamate, reflected in the high SEM present in table 4.2. One explanation for this fact may be related to the drop-coating deposition of the enzyme. As stated before, this is a hand-made process and reproducibility is still a problem with the manual deposition of the enzyme. It will be necessary to increase the number of tested biosensors to gather more accurate data for this MEA biosensor configuration regarding Km and Vmax values. In any case, Km and Vmax were calculated for each individual sensor and all of the present values well above the expected physiological concentrations of glutamate, suggesting that the coating is effective for immobilizing the enzyme.

Table 4.2. *Calculated Km and Vmax for R1 and S2 MEA glutamate biosensors.*

Michaelis Menten fit		
	R1 (n=8)	**S2 (n=6)**
Vmax (pA)	2329± 772	1233 ± 2950
Km (µM)	1699 ± 652	1579 ± 4439

Oxygen is a required cofactor of oxidase enzymes for the production of the reporter molecule, H_2O_2. The O_2 dependence of oxidase enzyme coated MEAs is a concern considering that O_2 levels in solutions (ca. 250 µM) are considerably higher than concentrations *in vivo* in the brain (ca. 50 µM) (Dixon, Lowry et al. 2002). The O_2 dependence of glutamate oxidase was not evaluated. However, others have examined if low O_2 concentrations would affect MEA performance with several different enzymes and they show that the enzymes tested (including glutamate oxidase) have a low O_2 dependence particularly at *in vivo* concentrations (50 µM) (Burmeister, Coates et al. 2004, Kevin N. Hascup 2013).

4.3.2. Real Time *in vivo* Measurement of Glutamate in the Rat Brain

Following the glutamate biosensor characterization its performance was tested *in vivo* in the rat hippocampus. Figure 4.4 illustrates the recording of a glutamate signal, following local application of 62.5 nL of a 70 mM KCl solution. A glutamate current signal was detected by the sites coated with glutamate oxidase, while the sentinel sites, coated only with glutaraldehyde and BSA were unresponsive to the stimulus. The glutamate signal increased rapidly following KCl depolarization lasting ca.10 s, and reaching a maximum peak concentration of 8 µM glutamate.

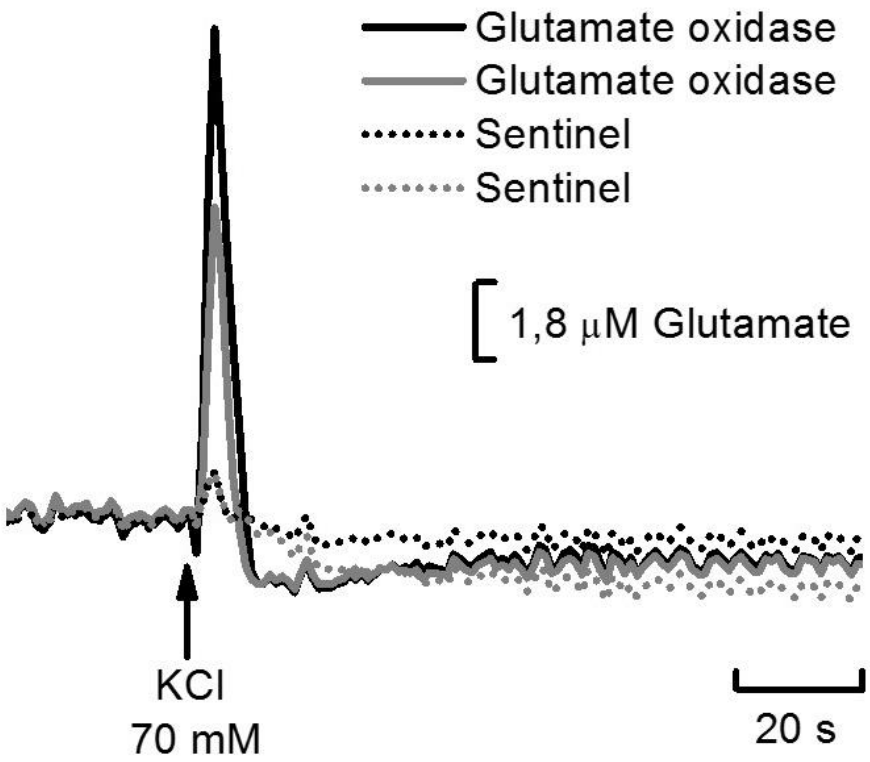

Figure 4.4. *Amperometric recording of glutamate in rat hippocampus* in vivo *using a MEA (S2) glutamate biosensor microarray following stimulation with KCl 70 mM. Black and gray (solid lines) represent sites 1 and 2 (coated with the enzyme glutamate oxidase) Black and gray dotted lines represent sites 3 and 4 (sentinel sites, without the enzyme). Amperometric current was recorded at +0.7 V vs. Ag/AgCl. Recording performed in the CA1 region of the hippocampus (AP: -3.8; ML: -2.2; DV: -2.4). Arrow indicates the time of KCl pressure-ejection.*

4.3.2.1. Self-referencing recordings

As described previously by Burmeister and Gerhardt (Burmeister and Gerhardt 2001), the development of a self-referencing technique allows the (1) enhancement of signal-to noise and (2) elimination of signal artifacts due to the detection of unknown substances. Figure 4.5 (upper solid gray trace) shows a typical recording active site coated with glutamate oxidase and a blank signal. The lower trace (black solid line) shows the resulting signal after offline current subtraction of site 3 (background) form site 1 (active site). The increase in signal to noise ratio is clear visible as shown in figure 4.5 (lower trace). This result demonstrates the ability of the self-referencing technique to enhance the signal to noise ratio.

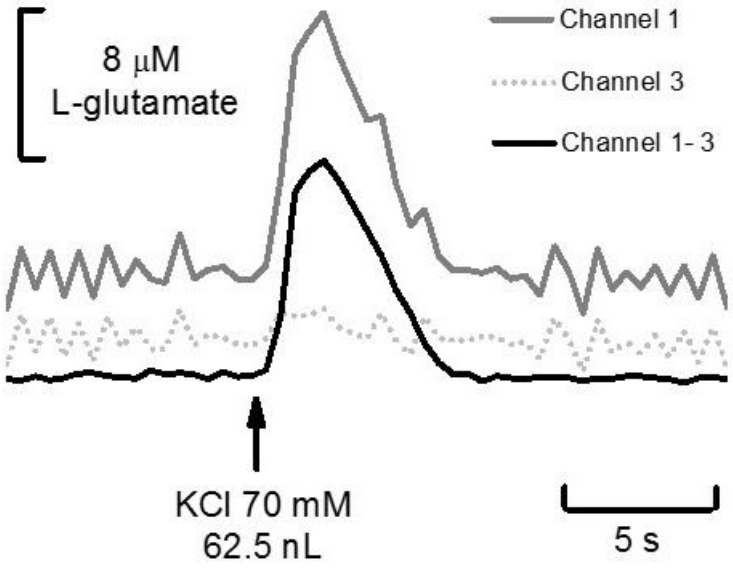

Figure 4.5. *Amperometric current of an active site coated with glutamate oxidase to 62.5 nL of a KCl 70 mM solution locally ejected (upper black solid trace). The background current measured at site 3 (gray dotted line) coated with BSA and glutaraldehyde was subtracted from active site. The lower trace (solid gray trace) is the result of the self-referencing method, yielding an enhanced signal-to-noise ratio. The recording was performed with a S2 MEA glutamate biosensor in the CA1 region of the hippocampus (AP – 3.8; ML:-2.2; DV: 2.4).*

4.3.2.2. In vivo measurements of glutamate release and uptake in the anesthetized rat brain

The first set of experiments involved the local application of KCl in the hippocampus to evoke release of L-glutamate. As shown in figure 4.6, local applications of KCl volumes ranging from 25 to 62.5 nL produced detectable and reproducible increases in extracellular levels of L-glutamate.

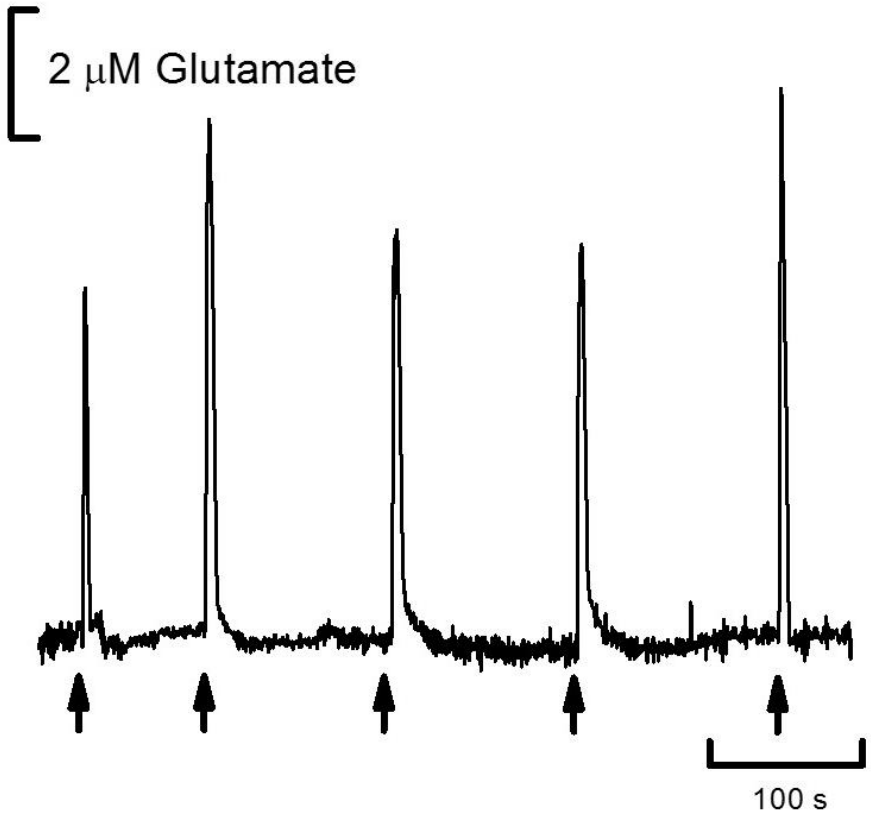

Figure 4.6. *Amperometric recording with a S2 MEA glutamate biosensor (+0.7 V vs. Ag/AgCl) of potassium-evoked release of L-glutamate in rat CA1 region of the hippocampus (AP: -3.8; ML: -2.2; DV: -2.4) induced with local ejection of a 70 mM KCl solution (volumes ranged from 25 to 62.5 nL).*

Additionally, L-glutamate was locally pressure-ejected to evaluate glutamate clearance and uptake rate. Glutamate uptake is the decrease in extracellular concentration by the action of glutamate transporters located on the membrane surface of neurons and astrocytes. Figure 4.7 demonstrates glutamate uptake studies in the CA1 region of the hippocampus of the anesthetized rat.

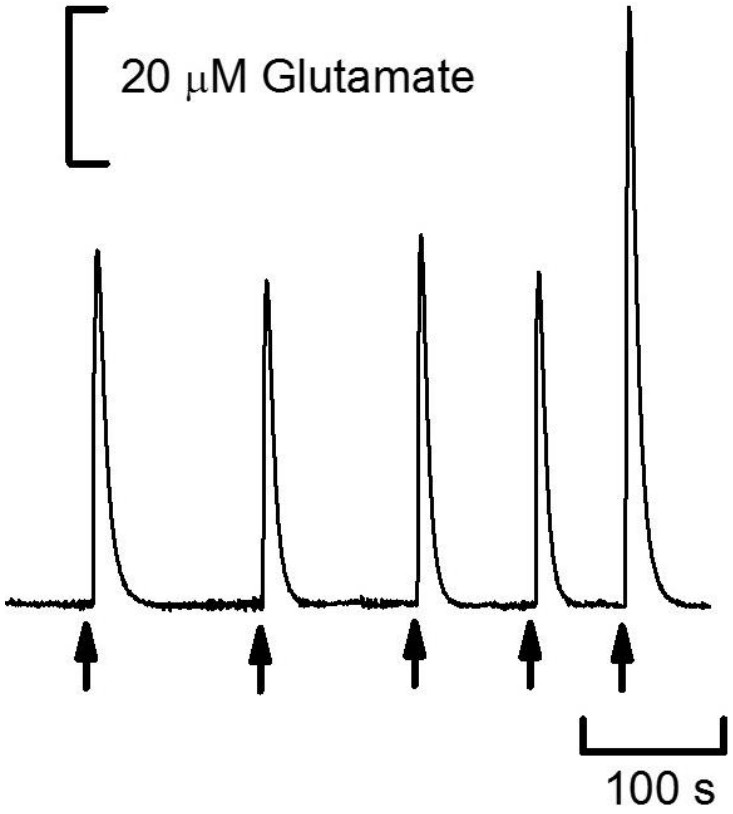

Figure 4.7. *Amperometric recording with a S2 MEA glutamate biosensor (+0.7 V vs. Ag/AgCl) of locally ejected of L-glutamate to study glutamate uptake in the hippocampus (AP: -3.8; ML: -2.2; DV: -3.2). Glutamate (20 mM) solution was applied via a micropipette at the time indicated by the arrows, in the range of 12.5 to 100 nL. Note the very rapid time course of the glutamate signals.*

The pressure ejection of L-glutamate solution elicited current signals that were similar to those seen from KCl stimulations and in both cases the signal returned rapidly to baseline, suggesting a rapid and complete uptake of glutamate. Both KCl-evoked and glutamate ejection-produced glutamate signals were analyzed and characterized by the parameters described previously in this chapter and results are presented in table 4.3.

Table 4.3. *Glutamate kinetics upon stimulation with KCl (70 mM), local ejection of glutamate (20 mM) and local ejection of a mixture of glutamate and TBOA (20 mM + 0.1 mM). Reported values for peak amplitude, T_R and T_{Total} and uptake rate represent the mean ± SEM. *p< 0.05.*

	Hippocampus (CA1)		
	KCl 70 mM	**Glutamate 20 mM**	**Glutamate 20 mM + TBOA 0.1 mM**
Number of rats	3	3	1
Number of responses	22	17	5
Average amplitude (µM)	9.6 ± 1.4	39.3 ± 8.4	11.3 ± 4.7 *
T_{rise}	3.0 ± 0.3	3.8 ± 0.2	7.3 ± 0.4 *
T_{total}	10.6 ± 0.7	21.3 ± 2.2	54.4 ± 12.4 *
Uptake rate (µM/s)	3.2 ± 1.0	5.8 ± 1.1	0.9 ± 0.6 *

The pressure ejection of L-glutamate solution produced current signals that were essentially similar to those seen from KCl stimulations, even though the peak amplitude of the 20 mM L-glutamate ejections was higher than what it was obtained for 70 mM KCl. This difference is expected due to the origin of glutamate in each case: KCl stimulates the release of endogenous glutamate while the local pressure-ejection of exogenous glutamate in a very high concentration (20 mM). By fitting the signal decay to a first-order exponential decay, the calculated average uptake rate was 5.8 µM/s for L-glutamate and 3.2 µM/s for KCl. The means were not statistically significant when assessed by student's *t*-test. The clearance of glutamate is very fast in the hippocampus and is comparable to other values reported in the literature (Quintero, Day et al. 2007). Interestingly, when TBOA, a known inhibitor of glutamate uptake (Shimamoto, Lebrun et al. 1998, Jabaudon, Shimamoto et al. 1999, Shigeri, Shimamoto et al. 2001) was co-ejected with glutamate, the kinetic parameters changed, namely the uptake rate, which decreased six fold, the glutamate uptake. Further studies are needed to get a better understanding about the dynamics of glutamate uptake in the brain.

4.3.3. Simultaneous and real time *in vivo* measurement of glutamate and ascorbate in the rat brain

The ultimate goal of this study was to perform simultaneous measurements of ascorbate and glutamate in the hippocampus of anesthetized rat combining MEA biosensors arrays and the Nafion/SWCNT modified-carbon fiber microelectrode developed in chapter 3. Figure 4.8 shows a simultaneous recording of ascorbate and glutamate upon stimulation with KCl 70 mM (A) and 20

mM glutamate (B). In both cases it was possible to observe a delay of c.a 1 s between the onset of the glutamate and ascorbate signals. Results also show that the onset of ascorbate signal initiates when glutamate signal is returning to the baseline. Furthermore, there is an apparent correlation between the intensity of both signals. When higher concentrations of glutamate are reached in the extracellular space, a higher release of ascorbate is observed (Figure 4.8). These dynamic measurements corroborate previous results indicating an interplay between these two compounds (Milby, Mefford et al. 1981, Ghasemzadeh, Cammack et al. 1991, John P. Lowry 1998, Wilson, Peters et al. 2000, Pomerleau, Day et al. 2003). A heteroexchange mechanism between ascorbate released and reuptake of glutamate could play a critical role (Milby, Mefford et al. 1981, Grunewald and Fillenz 1984). Another explanation is related to the fact that glutamate, when released into the synaptic cleft, is transported back into astrocytes through Na^+–glutamate cotransporters, leading to a swelling of astrocytes and to a consequent increase in membrane permeability to ascorbate thus accelerating its outward flux, since ascorbate is more concentrated inside the cells (Chan and Chu 1990, Shao, Enkvist et al. 1994, Wilson, Peters et al. 2000, Lane and Lawen 2012).

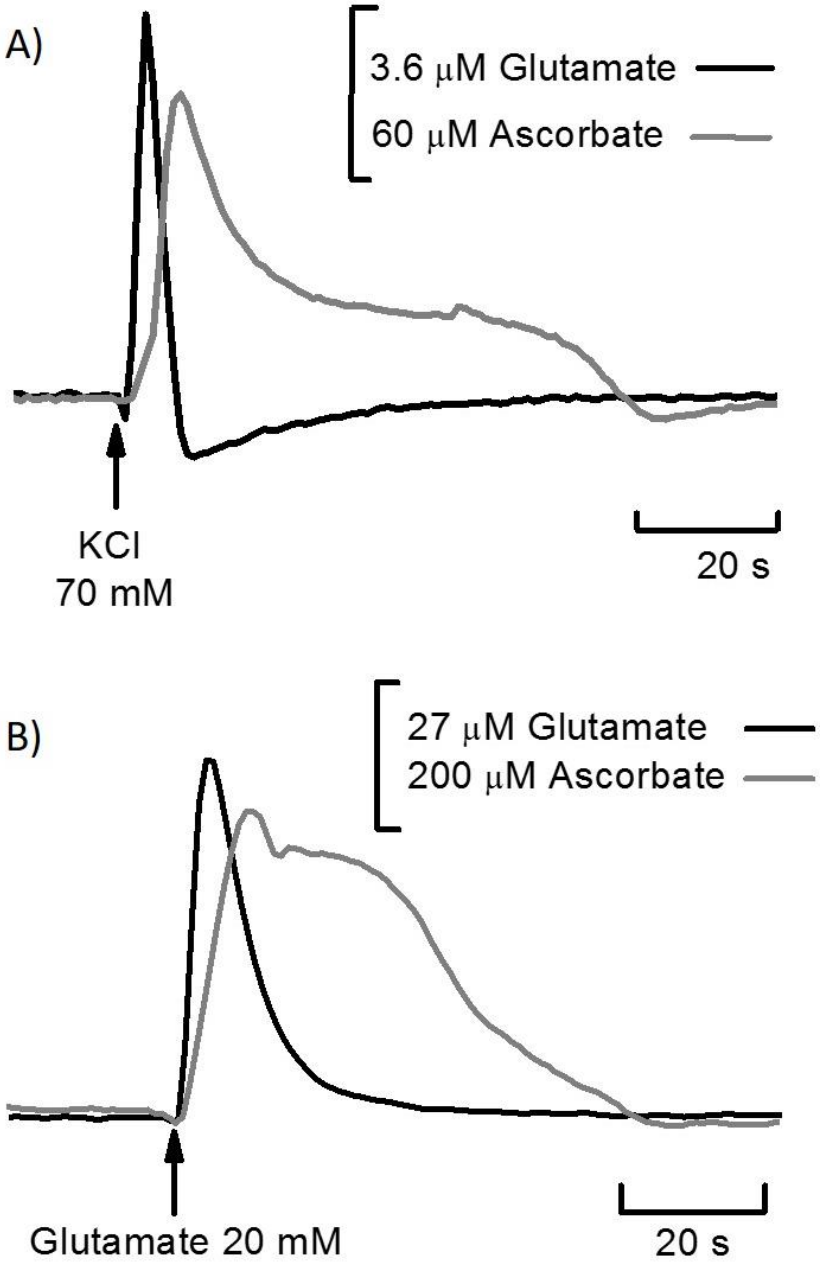

Figure 4.8. *A) Real-time and simultaneous amperometric recordings of glutamate and ascorbate upon stimulation with KCl 70 mM (25 nL) (panel A) with a MEA S2 glutamate biosensor array implanted in the in the CA1 region of the rat hippocampus (coordinates from Bregma: AP: -3.8, ML: -2.2, DV: -2.6) and with glutamate 20 mM (25 nL) (panel B) in the DG region of the rat hippocampus coordinates AP -3.8, ML -2.2, DV -3.2. Arrows indicate the time of pressure-ejection of each of the referred compounds*

To further understand how glutamate and ascorbate interact, an experiment was performed where ascorbate oxidase was locally ejected after a stimulus with KCl, as shown in figure 4.9. Results show that upon depolarization caused by the local increase in K^+, extracellular concentration of glutamate rises followed by an increase in extracellular ascorbate. Then, the local ejection of ascorbate oxidase rapidly depletes extracellular ascorbate and a subsequent

stimulus with KCl induces the release of a smaller concentration of glutamate, as no ascorbate signal was observed.

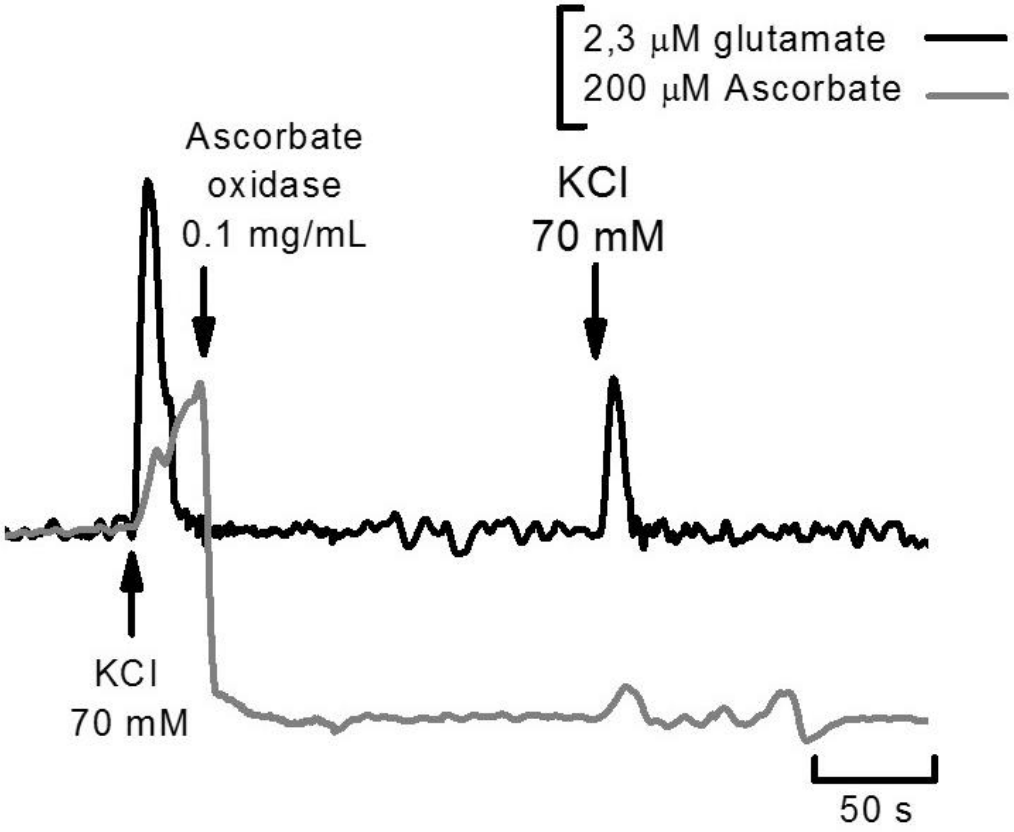

Figure 4.9. *Real-time and simultaneous amperometric recording of glutamate and ascorbate release upon stimulation with locally ejected KCl 70 mM (25 nL) with a MEA S2 glutamate biosensor and subsequent ejection of ascorbate oxidase 0.1 mg/mL (c.a. 100 nL). The repeated ejection of KCl induced the release of glutamate but the signal of ascorbate was almost completely abolished. The experiment was performed in the DG region of the rat hippocampus at coordinates AP: -3.8, ML: -2.5, DV: -3.6. Arrows indicate the time of ejection of each of the referred compounds.*

This experiment demonstrates that MEA biosensor remains unresponsive *in vivo* to high concentration changes of ascorbate (c.a. 500 µM) and somehow validates its use for *in vivo* experiments. Furthermore, depletion of ascorbate induced a lower glutamate current signal upon stimulation with KCl suggesting that ascorbate is able to modulate glutamatergic neurotransmission. It was previously reported that high concentrations of ascorbate may alter the redox state of the NMDA glutamate receptor thus blocking NMDA-gated channel function and act as a glutamate antagonist, preventing the overactivation of glutamate receptors and the associated excitotoxicity (Rebec and Pierce 1994, Kiyatkin and Rebec 1998, Rebec, Witowski et al. 2005, Sandstrom and Rebec 2007). When ascorbate is depleted this preventive effect is abolished and overactivation of the receptor may occur, leading to a generally increased state of oxidative stress. Also, depletion of ascorbate from the extracellular space may lead to an increased efflux of this substance from the cells. This will promote an imbalance in the redox status of the cells, increasing its oxidative stress status, with an impact in the intracellular regeneration of glutamate from glutamine, causing the observed decrease in the glutamate signal upon a depolarizing stimulus. Further studies are needed to validate this hypothesis by using this approach.

4.4. Conclusions

Increasing evidence links ascorbate with various aspects of glutamate neurotransmission. Glutamate reuptake is believed to promote the release of ascorbate via heteroexchange at the site of glutamate transport. Ascorbate release, in turn, may modulate the postsynaptic action by blocking NMDA receptors. Moreover, both ascorbate and glutamate have been associated with diseases like Alzheimer's or Huntington's. Taking this into account, it is very important to develop analytical tools that allow for real-time and direct measurements of these two compounds to get a better understanding about their dynamic interactions in brain function and dysfunction. In the present studies we aimed at construction an array of Nafion/SWCNT carbon fiber microelectrode for ascorbate measurements and MEA for extracellular glutamate measurements with a high spatial resolution and with minimal interference of catecholamines and other putative interferents with electrochemical measurements.

The MEA glutamate biosensor arrays used showed good recording characteristics in terms of sensitivity, L.O.D, response time for glutamate measurements *in vivo*. The use of *m*-PD as an exclusion layer greatly enhanced selectivity against major interferents such as ascorbate. The self-referencing technique allowed the subtraction of the background current at sentinel sites without the glutamate oxidase enzyme and cross-check the selectivity of the biosensors on a second-by-second time scale, increased the signal-to-noise ratio thus improving the sensitivity and L.O.D.

The presented studies using microelectrode arrays designs to record glutamate signals on a second-by-second basis contribute to a better understanding of basal (tonic) and potassium-evoked glutamate (phasic) release in hippocampus of anesthetized rat brain. Potassium-evoked glutamate release and uptake is robust, transient, and highly reproducible. The direct measurement and high spatio-temporal resolution of this bio-sensing technology is advantageous for these dynamic studies.

Finally, the simultaneous measurements of glutamate and ascorbate in the rat hippocampus in real-time allow to get insights about the dynamic interaction of these molecules in the rat hippocampus during normal brain function and how it may be disrupted in neurodegenerative processes such as Huntington's or Alzheimer's disease.

5. Coupling of ascorbate and nitric oxide dynamics *in vivo* in the rat hippocampus upon glutamatergic neuronal stimulation: a novel functional interplay

Part of the work presented in this chapter was published in:

Ferreira NR, Lourenço CF, Barbosa RM, Laranjinha J. "Coupling of ascorbate and nitric oxide dynamics *in vivo* in the rat hippocampus upon glutamatergic neuronal stimulation: a novel functional interplay". Brain Res Bull. 2015 May; 114: 13-9

Part of the work presented in this chapter was awarded with the young investigator award presented by Society for Free Radical Research-Europe in:

Nuno R. Ferreira, Cátia F. Lourenço, Ricardo M. Santos, Rui M. Barbosa, João Laranjinha. Nitric oxide and ascorbate dynamics *in vivo* in the rat hippocampus: a novel functional interplay? In Redox Signaling And Oxidative Stress In Health And Disease, Iv Spanish and Portuguese Meeting on Free Radicals, Valencia , Spain, 5-7th June 2012

5.1. Introduction

It is well established that ascorbate is a physiological reductant, enzyme co-factor and neuromodulator in the brain (Grunewald 1993, Rice 2000, Rebec 2007), with wide range impact, from cognitive functions to Alzheimer's disease (Bowman 2012). When analyzing these evidences and the underlying mechanisms supporting its different actions in the brain it is apparent that ascorbate compartmentalization and fluxes are critical issues inherent to its biological functions. In fact, ascorbate is actively transported into the brain and then into neurons via the sodium-dependent vitamin C transporters (SVCTs), causing its accumulation at very high concentrations that are estimated to be up to 10 mM in neurons and 1 mM in astrocytes. In the extracellular space of the brain, ascorbate concentration ranges between 250-500 µM (Rice 2000, Ferreira, Santos et al. 2013), a value that may increase by 250-500 µM following stimulation with glutamate (Cammack, Ghasemzadeh et al. 1991, Ferreira, Santos et al. 2013). However, the location and distribution of SVCTs transporters are not the sole critical features in maintaining a heterogeneous distribution of ascorbate in the brain as ascorbate fluxes between intra and extracellular compartments are functionally dependent on glutamatergic neuronal activation, as observed in the previous chapter and in other studies (Rice 2000). Looking at the data gathered in the last chapter regarding the simultaneous measures of glutamate and ascorbate in the brain and analyzing it in view of the available literature, it appears that an increase in extracellular ascorbate modulates glutamate dynamics and impacts in behavioral activity (Rebec and Pierce 1994, Sandstrom and Rebec 2007). In this regard, it is interesting to note that glutamate stimulation also triggers the production of nitric oxide (•NO), a diffusible intercellular messenger with a wide-range impact in the brain, ranging from neurotransmission to neurodegeneration and neurovascular coupling (Garthwaite and Boulton 1995, Dawson and Dawson 1998, Lindauer, Megow et al. 1999, Kitaura, Uozumi et al. 2007).

Mechanistic links between ascorbate and •NO metabolism have already been described. Indeed, ascorbate has been shown to potentiate •NO synthesis via a chemical stabilization of tetrahydrobiopterin (BH4) (Huang, Vita et al. 2000, Heller, Unbehaun et al. 2001, Kim 2005, Muller-Delp 2009), an important and easily oxidized co-factor involved in maintaining a functional NOS (Newaz, Yousefipour et al. 2005, Okazaki, Otani et al. 2011). Ascorbate has also been shown to augment •NO bioavailability in a BH4-independent manner, either by increasing NOS activity by changing its phosphorylation and S-nitrosylation status or by upregulating NOS expression (Ladurner, Schmitt et al. 2012, Mortensen and Lykkesfeldt 2013). These studies provide mechanistic insights that were largely obtained using *in vitro* cell systems but reveal little about the dynamics and compartmentalization of ascorbate and •NO upon glutamatergic stimulation *in*

vivo. It has been shown that glutamate is a trigger of both •NO production from the neuronal isoform of NOS via activation of NMDA receptors, and of ascorbate release through a putative heteroexchange mechanism, (O'Neill, Fillenz et al. 1984, Grunewald 1993, Yusa 2001), a process that, nevertheless, still remains controversial (Kulagina, Shankar et al. 1999, Portugal, Miya et al. 2009, Corti, Casini et al. 2010).

Given the above rationale, in this chapter we attempted to evaluate the coupling between •NO produced upon glutamate stimulation and ascorbate fluxes *in vivo* by following their respective dynamics in a second by second basis. For that purpose, we used carbon fiber microelectrodes coupled to electrochemical techniques for simultaneous and real time measurements of ascorbate and •NO in brain hippocampus.

The first part of the chapter is dedicated to an analytical characterization of the CFMs used for •NO measurements (the analysis of the Nafion/SWCNTCFMs used for ascorbate monitoring was done in chapter 3).

In vivo results strongly support a coupling between the two substances. We have established a link between the production of •NO derived from the activation of NMDA receptor for glutamate and the release of ascorbate to the extracellular fluid. The interplay between •NO and ascorbate points to a functional impact on the known activities of both compounds and lays the foundations for new regulatory mechanisms in the brain.

5.2. Experimental

Refer to Chapter 2 for detailed information regarding solutions, microelectrodes and *in vivo* experiments related procedures.

5.2.1. Microelectrodes

In these studies we have used Nafion/SWCNT and chemically modified carbon fiber microelectrodes with Nafion/*o*-PD for ascorbate and •NO measurements, respectively.

5.2.2. Ascorbate and •NO measurements

Measurements of •NO and ascorbate were made using amperometry, with a hold potential of +0.8 V and +0.05 V *vs* Ag/AgCl, respectively. A bipotentiostat Fast MK III (Quanteon, USA) was used for this purpose.

5.2.3. Animal and surgical procedures

In vivo experiments were performed in male Wistar rats (8-12 weeks old, weight 250-390 g), as described in chapter 2.

5.2.4. Electrochemical recordings

The used arrays are represented in figure 2.11 B. *In vivo* experiments were carried out in the hippocampus, and the used coordinates (from bregma) are indicated in the legend of each figure. Recordings were done by lowering the tip of the CFM used for •NO (used as reference) into the brain region of interest. Data collected from 27 animals was used in this chapter.

Data acquisition rate was 2 Hz. After baseline current stabilization (15 minutes), glutamate (20 mM) and the other solutions used for local application were pressure ejected from the micropipette using a Picospritzer III and ejected volumes monitored using a stereomicroscope fitted with a reticule.

5.2.5. Data analysis

The ascorbate and •NO signals were characterized in terms of (1) ascorbate or •NO peak amplitude, based on the conversion of the amperometric currents to fluxes according to Faraday's law ($I = n \cdot F \cdot \phi$), in which I corresponds to the amperometric current, n corresponds to the number of electrons involved in the electrochemical oxidation, F corresponds to the Faraday constant and ϕ is the flux); (2) area, calculated as the time integral of the signal; (3) T_{50}, the time in seconds from maximum amplitude to 50% decay of the signal; and (4) T_{total}, the time in seconds from the application of the stimulation to return to basal levels. Amperometric recordings were analyzed with OriginPro 7.5 and statistical analyses were performed with GraphPad Prism 5. Data are

presented as mean ± SEM. One-way analysis of variance (ANOVA) was performed to make comparisons between multiple groups followed by Dunnett post-test. When there were only two groups, statistical analyses of the data were performed using a Student's t-test. Differences were considered significant at $p < 0.05$.

5.3. Results

5.3.1. Analytical performance of •NO microelectrodes

5.3.1.1. Choosing the best chemical modification and working potential

Electrochemical oxidation of •NO on solid electrodes such as carbon fiber produces the nitrosonium cation (NO^+), which upon reaction with OH^- in aqueous solutions yields nitrite (NO_2^-) that, in turn, can be further oxidized to nitrate (NO_3^-) (Malinski and Taha 1992). The oxidation potential depends on electrode surface composition, electrochemical pre-treatment of the carbon fiber as well as chemical modifications of electrode surface. The first part of the chapter involved the study of the best chemical modification/working potential to maximize CFMs sensitivity for •NO measurements and selectivity towards potential interferents with its detection *in vivo*.

The oxidation potential of •NO was obtained from "hydrodynamic voltammograms" (HV) for three different kinds of chemical modifications (Nafion, Nafion/5 mM *o*-P and Nafion/ 100 mM *o*-PD) applied to the CFMs. This approach consists in the recording of the amperometric current for a given analyte concentration for different potential values. For each tested modification of the CFMs, an aliquot of •NO solution (1 µM) was added to 20 mL of PBS lite and the current recorded in the range of potentials (from + 0.3 to + 1.0 V with intervals of 0.1 V). The effect of varying the hold potential on the amperometric response of a chemically modified carbon fiber microelectrode is depicted in figure 5.1 A. While for potentials lower than + 0.5 V no response is observed, above this potential the amperometric current increases as a function of the hold potential in a sigmoid fashion from which the half-wave potential can be calculated (Figure 5.1 A). The value for •NO oxidation potential is indicated in figure 5.1 B and the reported values for the coatings with Nafion and 5 mM *o*-PD are in agreement with most of the reports found in the literature (Brunet, Pailleret et al. 2003). The biggest difference in half wave potentials was observed between CFMs coated only with Nafion (+ 0.583 V *vs*. Ag/AgCl) and CFMs coated with Nafion and 5 mM o-PD (+ 0.718 V *vs*. Ag/AgCl). Since coating with Nafion did not lower the oxidation potential of •NO to values below the oxidation potential of cathecolamines (approximately + 0.4 V), this coating is not sufficient to prevent the oxidation of these substances either *in vitro* or *in vivo* and was excluded for the remaining tests.

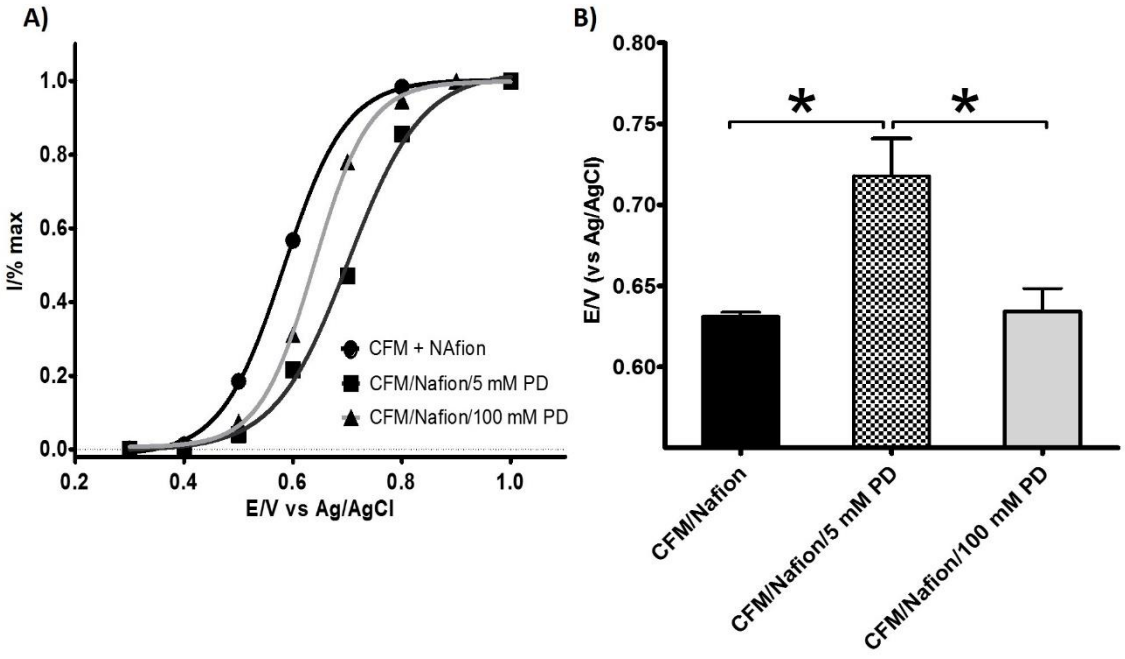

Figure 5.1. *A) Hydrodynamic voltammograms obtained with CFMs for 1 µM •NO in PBS solution. B) Calculated half-wave potential for each type of chemical modification (mean ± SEM). Values obtained were: + 0,583 ± 0,003 V for CFM/Nafion (n=3), + 0,718 ± 0,019 V for CFM/Nafion/5 mM o-PD (n=3), + 0,639 ± 0,002 V for CFM/Nafion/100 mM o-PD (n=7). * p<0.05.*

The sensitivity and selectivity of the *o*-PD coatings at different working potentials were also assessed. Results are depicted in table 5.1.

Table 5.1. *Average sensitivity, L.O.D and selectivity in CFMs at different potentials. Two different coatings were tested (Nafion/5 mM PD vs Nafion/100 mM PD). Results presented as mean ± SEM.*

	Sensitivity (pA µm^{-2} µM^{-1})		**L.O.D (nM)**		**Selectivity**					
					Nitrite		**Ascorbate**		**Dopamine**	
	5 mM o-PD	**100 mM o-PD**	**5 mM o-PD**	**100 mM o-PD**	**5 mM o-PD**	**100 mM o-PD**	**5 mM o-PD**	**100 mM o-PD**	**5 mM o-PD**	**100 mM o-PD**
0.5 V (n=3)	0.0013 ± 0.0004	0.00178 ± 0.0004	684.7 ± 84,54	565.2 ± 193.2	>10000	>10000	675 ± 525	767 ± 217	4.0 ± 2.0	1.2± 0.2
0.6 V (n=3)	0.0079 ± 0.0023	0.0089 ± 0.0020	125.9 ± 9.547	416.0 ± 149.6	>10000	8422 ± 1578	2445±6 85	1235 ± 635	15.0 ± 6.0	1.6 ± 0.2
0.7 V (n=3)	0.0323 ± 0.0096	0.0251 ± 0.0047	104.0 ± 13.45	80.69 ± 32.04	>10000	7078 ± 1809	4190±4 55	1000 ± 256	15.00 ± 6.0	3.9 ± 0.6
0.8 V (n=10)	0.0330 ± 0.0047	0.0263 ± 0.0050	33.98 ± 9.068	66.83 ± 23.27	9208 ± 791	5458 ± 2636	7282±9 84	1277 ± 397	86.9 ± 20.0	4.4 ± 0.7
0.9 V (n=4)	0.0320 ± 0.0058	0.0338 ± 0.0040	19.78 ± 3.961	49.40 ± 15.84	6663 ± 1630	460 ± 122	5838±1 347	922± 414	86.9 ± 7.0	4.7 ± 0.6

According to the results presented in table 5.1, the Nafion/5 mM *o*-PD coating and a working potential of + 0.8 V *vs* Ag/AgCl allowed the best overall analytical performance of the CFMs in terms of sensitivity, L.O.D and selectivity. The Nafion/ 5 mM *o*-PD coating at a working potential of + 0.9 V *vs* Ag/AgCl also showed good results in terms of sensitivity and L.O.D but the selectivity was lower. In fact, this chemical modification and working potential is used in several *in vivo* studies (Barbosa, Lourenco et al. 2008, Lourenco, Santos et al. 2011, Santos, Lourenco et al. 2011, Lourenco, Santos et al. 2014). However, the Nafion/ 5 mM *o*-PD coating and a working potential of + 0.8 V *vs* Ag/AgCl had substantially better performance in terms of selectivity and this is a very important parameter to account for when we aim at performing *in vivo* measurements. By this reason, +0.8 V *vs*. Ag/AgCl was the selected potential for the following studies and the selected coating was Nafion/ 5 mM *o*-PD.

5.3.1.2. In vitro characterization of •NO and ascorbate microelectrodes

Prior to use, each microelectrode was evaluated by amperometry, at a potential of + 0.8 V *vs* Ag/AgCl reference electrode (Bioanalytical Systems, RE-5), in terms of sensitivity for •NO and selectivity against some interferents in the brain, according to the procedures described in chapter 2 for microelectrodes calibration. A typical recording is shown in figure 5.2. •NO calibration of the microelectrode was performed on top of 250 µM of ascorbate to reproduce the *in vivo* conditions. Additionally, all chemicals intended to be used *in vivo,* particularly in local applications, were previously tested *in vitro* to confirm that they were not electrochemically active and did not contribute to the recorded currents associated to changes in •NO concentration.

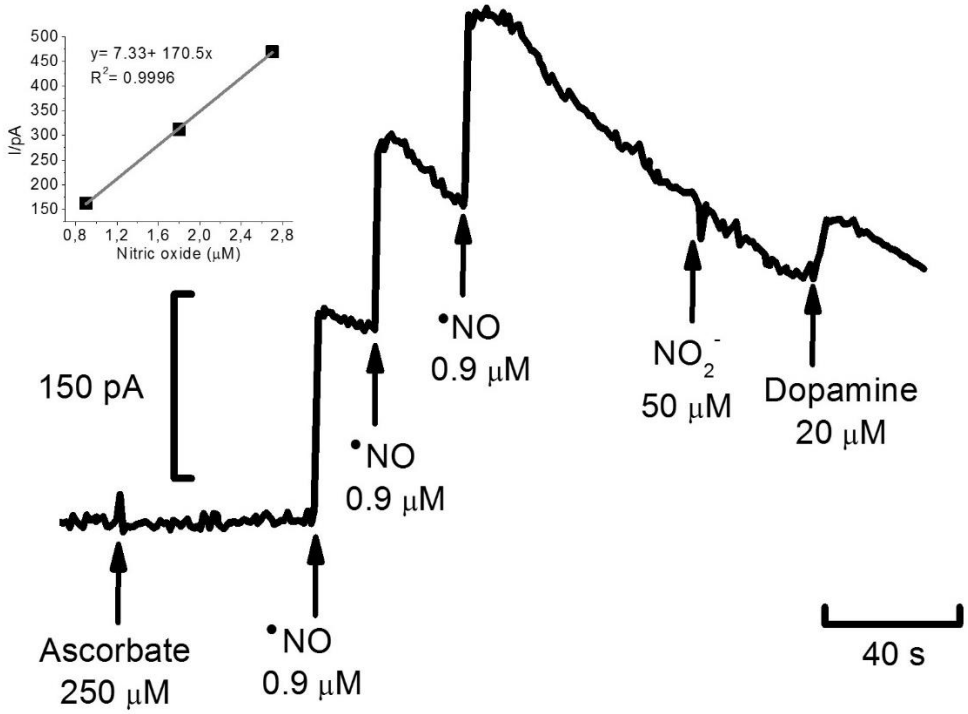

Figure 5.2. *Representative amperometric recording of microelectrode calibration for determination of sensitivity for •NO and selectivity against interferents. Compounds were added at the times indicated by the arrows. Linear regression applied to the correlation between the concentration of •NO added and the current change resulting from each addition is shown inset.*

In this study, CFMs for the detection of •NO had an average sensitivity of 138.5 ± 8.5 pA/ µM (n = 38) and a selectivity ratio (•NO: interferent) of 9517:1 ± 293:1 (n = 38) for nitrite, 8885 ± 473 (n = 38) for ascorbate, 5587 ± 807 (n = 38) for dopamine and 5136 ± 906 for noradrenaline. Microelectrodes used for ascorbate measurements were unresponsive to •NO, nitrite and dopamine at +0.05 V *vs* Ag/AgCl reference and had an average sensitivity of 40.8 ± 5.2 pA/ µM (n = 38).

5.3.1.3. In vivo verification of the interference of the vehicle

Drugs to be pressure-ejected locally in the brain were prepared in saline (NaCl 0.9%, pH 7.4). Figure 5.3 shows an amperometric recording performed upon local ejection of saline, to confirm that the vehicle had no interference in the recorded signals.

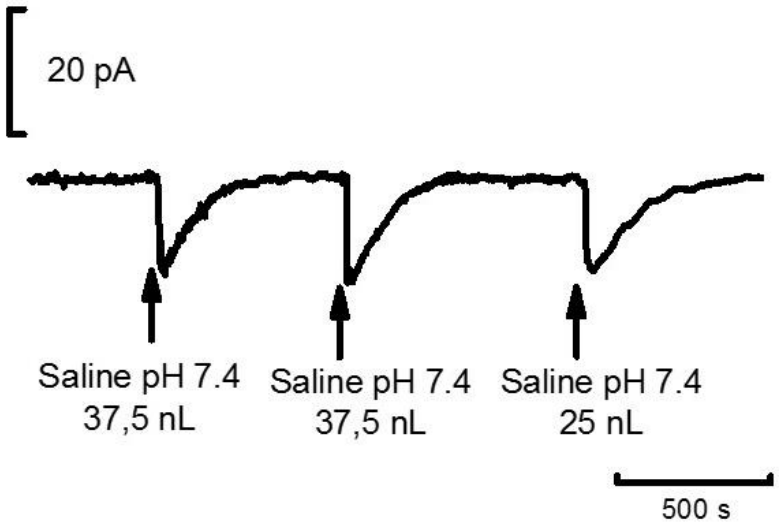

Figure 5.3. *Amperometric recording of the local ejection of saline in rat hippocampus* in vivo *using Nafion/* o*-PD CFM. Amperometric current was recorded at +0.8 V vs. Ag/AgCl. Recording performed in the DG region of the hippocampus (AP: -4.0; ML: -2.4; DV: -3.2). Arrow indicates the time of saline ejection.*

As illustrated, the local ejection of saline elicited a transient decrease in current, most likely due to a dilution effect. These results confirmed saline as a good vehicle for administration of solutions locally.

5.3.1.4. In vivo verification of •NO signal

As shown in figure 5.1 A, •NO doesn't oxidize at the CFM surface when a potential of +0.4 V *vs* Ag/AgCl is applied. However, this potential is high enough to oxidize other substances like ascorbate or catecholamines, in case they reach the electrode. To confirm the nature of the signal recorded using our standard stimulus (glutamate 20 mM) we performed experiments where signals were monitored by two Nafion/*o*-PD CFMs: in one of them a potential of +0.4 V *vs* Ag/AgCl was applied, while the other one was held at +0.8 V *vs* Ag/AgCl. Then, a stimulus with L-glutamate was applied and the result is illustrated in figure 5.4 A. The recording shows that the CFM recording at +0.4 V *vs* Ag/AgCl had a negligible current change when compared to the other. Then, applied voltages in the CFMs were shifted and the one that was recording at +0.4 V *vs* Ag/AgCl was changed to +0.8 V *vs* Ag/AgCl and vice-versa. Then, L-glutamate was locally administered. It was possible to observe that the current recorded in the CFM with a hold potential of +0.4 V *vs* Ag/AgCl was negligible when compared to the one that was recording at +0.8 V *vs* Ag/AgCl (Figure 5.4 B).

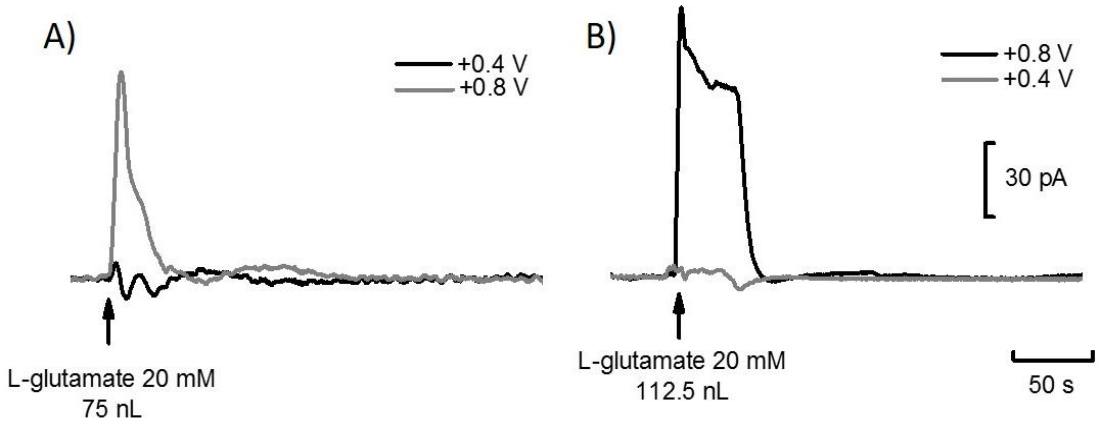

Figure 5.4. *A) Amperometric recording of the local ejection of L-glutamate (20 mM) in rat hippocampus* in vivo *using one array composed of two Nafion/* o*-PD CFMs and one micropipette. The CFMs were connected to a bipotentiostat and one of them was held at a holding potential of +0.4 V vs. Ag/AgCl and the other at +0.8 V vs. Ag/AgCl. B) Amperometric recording of the local ejection of L-glutamate (20 mM). In this case, the CFM that was recording previously at +0.4 v vs. Ag/AgCl was set to record at +0.8 V vs. Ag/AgCl and vice-versa. Recordings were performed in the DG region of the hippocampus (AP: -4.0; ML: -2.4; DV: -3.6). Arrow indicates the time of L-glutamate ejection.*

These results give two different kinds of important information for the remaining studies: first, it supports the idea that the current being measured is derived mostly from •NO oxidation, since the current change observed at +0.8 V *vs* Ag/AgCl is much higher than what is observed at +0.4 V *vs* Ag/AgCl, indicating that the species that is being recorded only oxidizes at higher potentials than + 0.4 V *vs* Ag/AgCl, like •NO. On this regard, we performed an additional hydrodynamic

voltammogram of •NO, but this time *in vivo*, as shown in figure 5.5. The calculated value for half wave potential was + 0.660 V *vs* Ag/AgCl, a value a value that differs approximately 60 mV from what it was obtained *in vitro* for the same type of modified CFM.

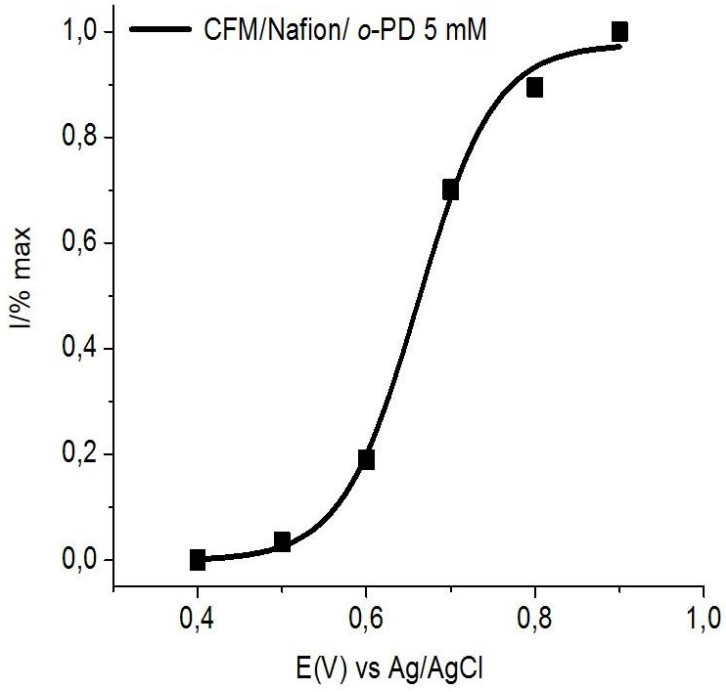

Figure 5.5. In vivo *hydrodynamic voltammogram obtained with one modified Nafion/o-PD CFM for •NO. Currents were recorded in the range of potentials (from + 0.4 to + 1.0 V with intervals of 0.1 V) and calculated half-wave potential was + 0.660 V vs Ag/AgCl. Recording performed in the DG region of the hippocampus (AP: -4.1; ML: -2.6; DV: -3.0).*

Second, these recordings provide good indications about the *in vivo* selectivity of the microelectrodes. At +0.4 V *vs* Ag/AgCl, a potential high enough to oxidize most of the potential interferents with •NO in the brain, the absence of a significant signal when compared to +0.8 V *vs* Ag/AgCl upon a stimulus with glutamate indicates the sensor was not measuring any of those substances. The *in vivo* selectivity will be further addressed in the following section.

5.3.1.5. In vivo selectivity of •NO microelectrodes

In order to further address the *in vivo* selectivity we performed experiments where one array composed of bare CFM and a CFM coated with Nafion/*o*-PD was inserted in the brain. Then, potential was held at +0.8 V *vs*. Ag/AgCl for both CFMs and, after a stable baseline was reached, some potential interferents with •NO detection in the brain were locally applied in the brain through a micropipette attached to the array. Figure 5.6 (A) shows the effect that the local ejection of ascorbate oxidase has on the recorded currents. Since reported values for extracellular ascorbate are about 250-500 µM (Stamford, Kruk et al. 1984, Rice 2000, Ferreira, Santos et al. 2013), the addition of ascorbate oxidase will represent a similar change in ascorbate extracellular concentration. As observed, only the bare CFM "sensed" this change, while the CFM coated with Nafion/*o*-PD remained practically unresponsive. The local addition of nitrite (B) and dopamine (C) in concentrations above the ones to be expected *in vivo* also evoked observable changes in current for the bare CFM, while the coated one remained unresponsive. These results don't rule out other possible interferents with •NO detection in the brain but strongly support the good selectivity performance obtained *in vitro*.

However, to keep high levels of selectivity and reproducible *in vivo* results, the following rules must be followed:

I. After the Nafion layer is soaked it must remain wet and the sensor must be inserted in the brain as soon as possible
II. Once coated with Nafion and *o*-PD, if the CFMs are not used, they should be discarded.
III. CFMs should be used *in vivo* only once. If it is necessary to remove the array out of the brain another CFM should be used, since the contact with blood degrades the coating.

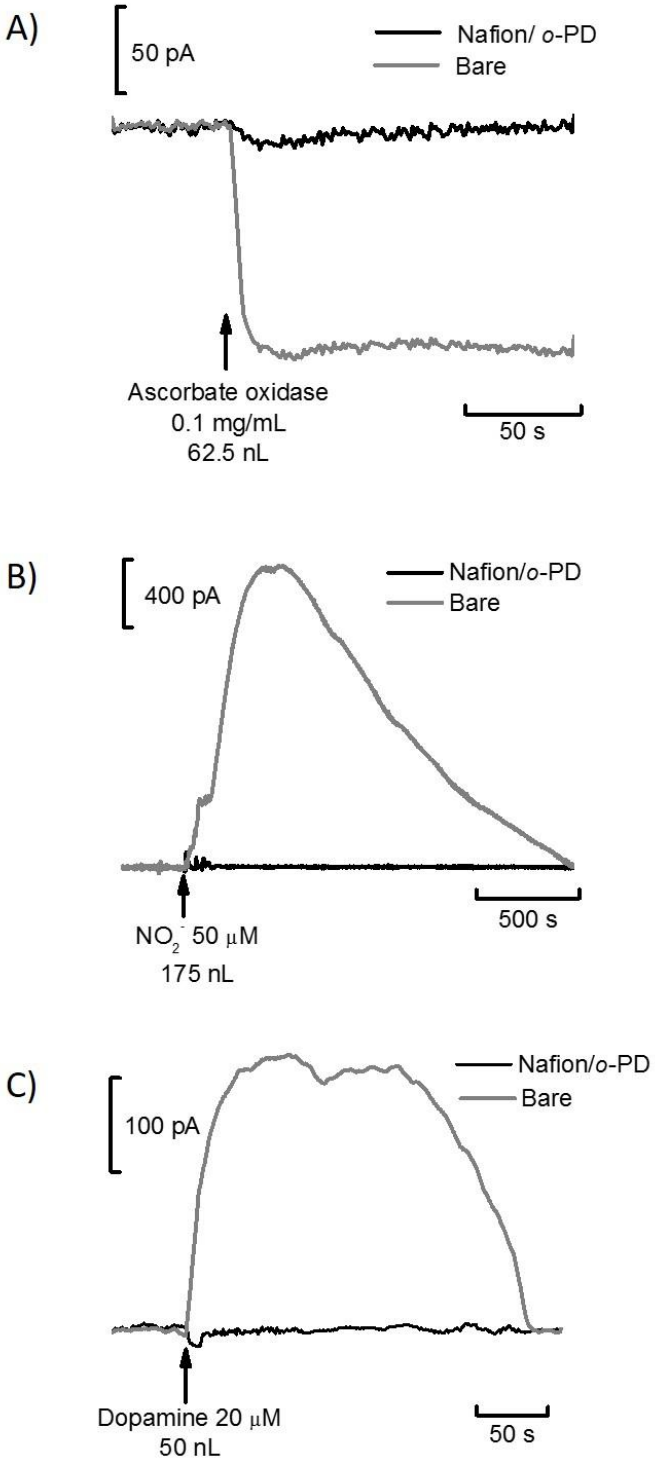

Figure 5.6. *A) Amperometric recordings in the rat hippocampus* in vivo *using one array composed of one bare CFM, one Nafion/o-PD CFM and one micropipette upon local ejections of ascorbate oxidase (A), nitrite (B) and dopamine (C). The CFMs were connected to a potentiostat and potential was held at +0.8 V vs. Ag/AgCl. Recordings performed in the DG region of the hippocampus (AP: -4.1; ML: -2.4; DV: -3.2). Arrow indicates the time when each substance to be tested was administered.*

5.3.2. Simultaneous Measurements of Nitric Oxide and Ascorbate in Hippocampus Evoked by Glutamate

The local ejection of glutamate in the rat hippocampus evoked transient signals in extracellular concentration of ascorbate and •NO. Ejections of vehicle (normal saline) produced no changes in baseline current or in some cases a small decrease of the oxidation current, likely due to a local dilution effect (as shown in figure 5.3). Figure 5.7 illustrates the average signals of ascorbate and •NO, recorded from the rat hippocampus upon a localized stimulation with 20 mM glutamate. The inset on the left shows a magnification of the first 10s of the recordings, where it is possible to observe a delay of 2-3 s between the onset of the signal of •NO and the signal of ascorbate. An analysis of the recorded signals (inset on the right) shows a good correlation between the maximum fluxes of both signals, ascorbate and •NO ($p<0.05$).

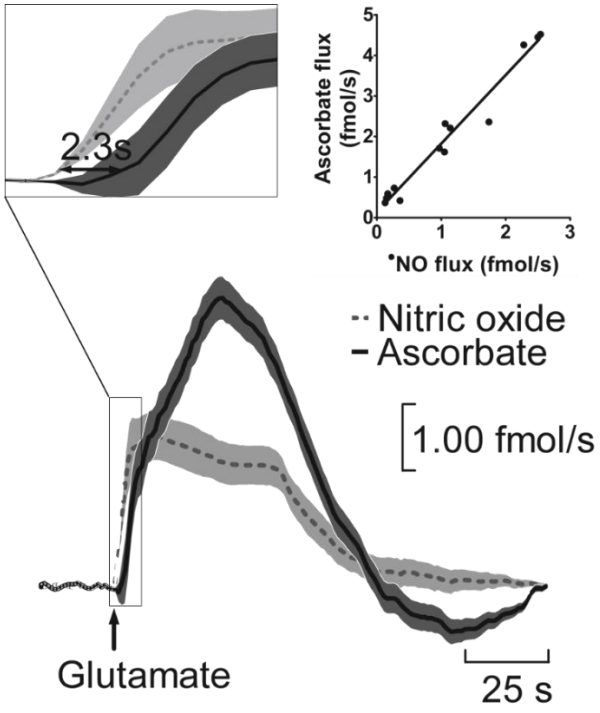

Figure 5.7. *Simultaneous measurement of •NO and ascorbate dynamics following a stimulation by local application of L-glutamate in the rat hippocampus. •NO (gray line) and ascorbate (black line) average signals (n=10). L-Glutamate (20 mM), was locally applied by pressure ejection (1s) at the time indicated by the arrow. Upper left corner inset: magnification of the first 10s after stimulation with L-glutamate. Upper right corner inset: Correlation analysis between •NO and AA signal in terms of maximum peak intensity (fmol/s).*

Data presented in table 5.2 shows the kinetic analysis of ascorbate and •NO signals obtained after a stimulation with glutamate 20 mM in the hippocampus. Since dynamic measures reflect a "concentration gradient" rather than a steady state concentration, amperometric currents were converted to fluxes by application of Faraday´s law. On average, •NO production in response to a first stimulation was characterized by a maximum peak amplitude of 2.6 ± 0.3 fmol/s, with a time rise of 19.6 ± 3.0 s and a total signal duration of 73.6 ± 5.9 s. Ascorbate response was characterized by a maximum peak amplitude of 4.2 ± 0.5 fmol/s, a time rise of 25.0 ± 3.8 s and a total signal duration of 64.2 ± 4.7 s.

Table 5.2. *Parameters calculated from glutamate-induced •NO and ascorbate signals in the rat hippocampus. Results presented as mean ± SEM.*

	Hippocampus	
	•NO	**Ascorbate**
Flux (fmol/s)	2.6 ± 0.3 (n=10)	4.2 ± 0.5 (n=10)
Signal area (fmol)	42.1 ± 8.8 (n=10)	136.6 ± 28.1 (n=10)
T rise (s)	19.6 ± 3.0 (n=10)	25.0 ± 3.8 (n=10)
T 50 (s)	42.0 ± 3.7 (n=10)	36.2 ± 5.3 (n=10)
T total (s)	73.6 ± 5.9 (n=10)	64.2 ± 4.7 (n=10)

5.3.3. Modulation of Nitric Oxide and Ascorbate Signals

5.3.3.1.Stimulation with NMDA and Exogenous Nitric Oxide

Transient signals were also observed when NMDA, a synthetic and specific agonist of the NMDA receptor, was used as a stimulus (Figure 5.8 A). Despite occasional minimal differences, overall the •NO and ascorbate signals were similar to those observed with glutamate, and it was possible to observe an identical delay between the onset of both signals (2.5 ± 0.6 s, n=6). The ejection of an exogenous solution of •NO (Figure 5.8 B) equally evoked a signal of ascorbate and in this case the delay between the onset of the signals of •NO and ascorbate was 2.4 ± 0.7 s (n=5). The ejection of increasing amounts of exogenous •NO solution had a linear correlation with ascorbate release, as illustrated in figure 5.9.

5.3.3.2.Inhibition of Nitric Oxide Synthase with 7-Nitroindazole

To further elucidate the relation between ascorbate release and •NO production induced by activation of glutamate receptors, 7-NI was used to selectively inhibit the neuronal isoform of NOS (Babbedge, Bland-Ward et al. 1993, Moore, Wallace et al. 1993, Moore and Bland-Ward 1996). This heterocyclic compound inhibits nNOS by competing with both L-arginine and BH4 and has been widely used as a selective inhibitor of nNOS *in vivo* (Bush and Pollack 2001, Lourenco, Santos et al. 2011). Figure 5.8 C illustrates the effect of 7-NI on •NO production induced by glutamate and the subsequent transitory increase of ascorbate. The recording was obtained following stimulation with glutamate, thirty minutes after the i.p. administration of 7-NI and it is possible to observe a significant reduction in both •NO and ascorbate signals. On average, the administration of 7-NI produced a decrease on •NO peak intensity of 71.4 ± 5.6% when compared to control stimulus (mean ± SEM, n= 11, $p < 0.05$) and a decrease on the signal area of 88.5 ± 3.0% (mean ± SEM, n= 11, $p < 0.05$). In the case of ascorbate signals, the decrease of signal peak intensity after the injection of 7-NI was 79.3 ±4.9% (mean ± SEM, n= 11, $p < 0.05$) and 75.2 ± 5% (mean ± SEM, n= 11, $p < 0.05$) for the signal area. Collectively, results suggest a relationship between •NO production by nNOS and the transitory increase of ascorbate in the extracellular space.

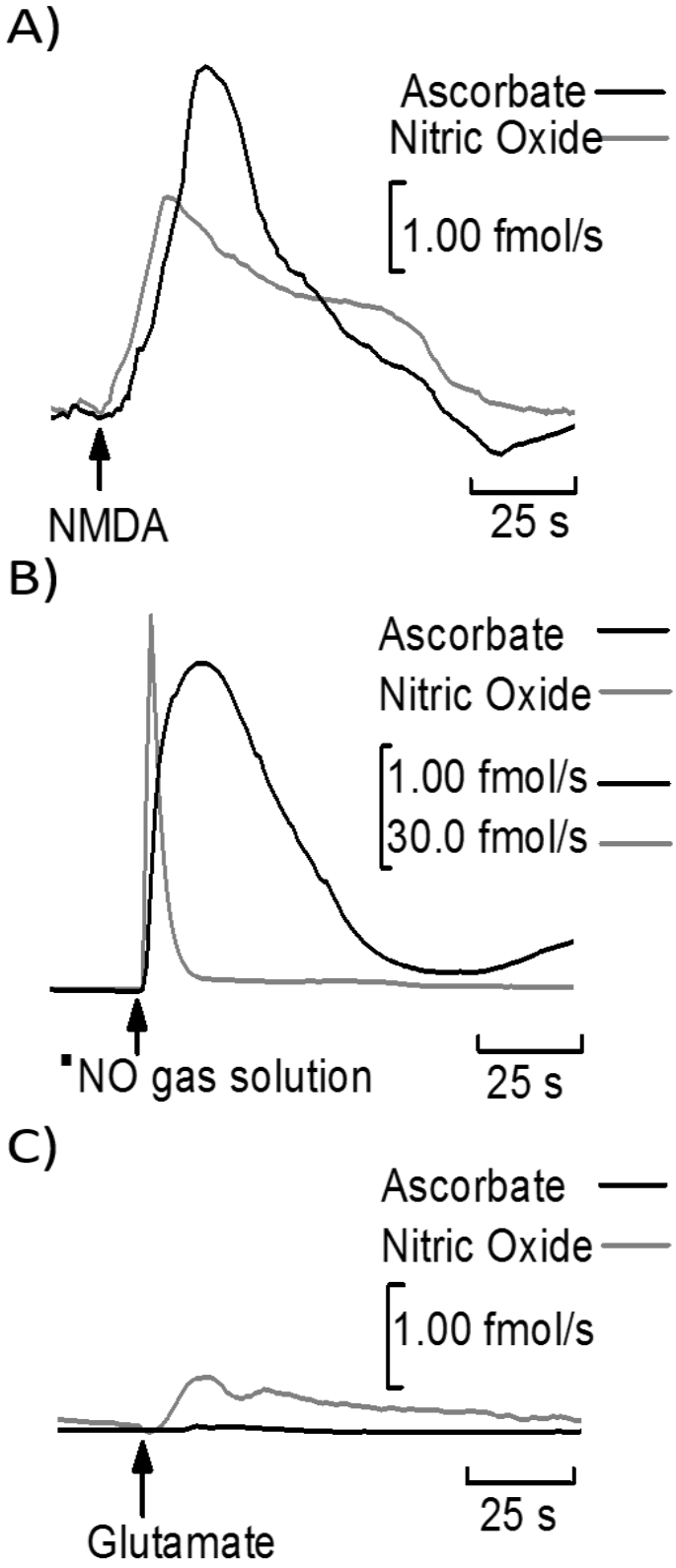

Figure 5.8. *(A) Simultaneous amperometric recordings of ascorbate (black line) and •NO (gray line) upon stimulation with NMDA (0.1 mM, 25 nL); (B) after local application of exogenous •NO (1.8 mM, 25 nL); (C) upon a stimulus with glutamate (20 mM, 12.5 nL) thirty minutes after the i.p. administration of 7-NI (50 mg/kg). Arrows indicate the time of ejection.*

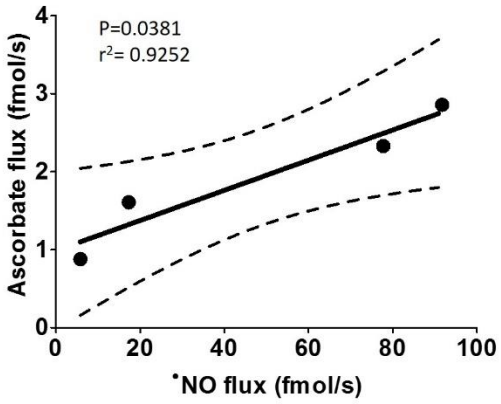

Figure 5.9. *Correlation analysis between ascorbate and •NO fluxes after local ejection of increasing volumes of • NO gas solution (2 mM). Experiment performed in the hippocampus.*

5.3.3.3. The effect of Ascorbate Oxidase on Ascorbate and Nitric Oxide signals

Ascorbate oxidase is an enzyme that is highly specific to ascorbate and it was used for modulation of ascorbate signals *in vivo* (Ghasemzadeh, Cammack et al. 1991, Rebec and Wang 2001, Ma, Rice et al. 2004) on basis of the following reaction (equation 5.1):

2 L-Ascorbate + O2 + 2H+ $\xrightarrow{\text{Ascorbate Oxidase}}$ 2-Dehydro-L-ascorbate+ 2 H2O (Akyilmaz and Dinckaya 1999) **(equation 5.1)**

When ascorbate oxidase was ejected locally on top of the signal it was possible to observe an immediate drop in the current that was being recorded with the CFMs used for ascorbate measurements, strongly supporting the presence of ascorbate (Figure 5.10 A). There is a change in •NO dynamics concomitant with a drop of ascorbate induced by administration of ascorbate oxidase. This is evident in figure 5.10 B under conditions when the stimulation with glutamate is performed in the presence of ascorbate oxidase. When the oxidase is added on top of ascorbate signal (Figure 5.10 A) the coupling involving •NO production and ascorbate release has been already established and, thus, little effect on •NO dynamics is expected, further supporting our hypothesis. Additionally, the ejection of ascorbate oxidase didn't have any measurable effect on the coated microelectrodes used for •NO measurements. Figures 5.10 B and 5.10 C compare the dynamics of •NO and ascorbate in the presence and absence of ascorbate oxidase. On average, the area of •NO signals decreased from 71.2 ± 17.4 fmol to 37.1 ± 15.2 fmol (mean ± SEM, n=10) and ascorbate signal area decreased from 146.8 ± 74.2 fmol to 17.8 ± 11.7 fmol (mean ± SEM, n=10). It was also possible to observe a change in the temporal dynamics of the •NO signal in the absence of ascorbate, with a faster decay (T_{50} decreased from 25 s to 9 s after the ejection of ascorbate oxidase).

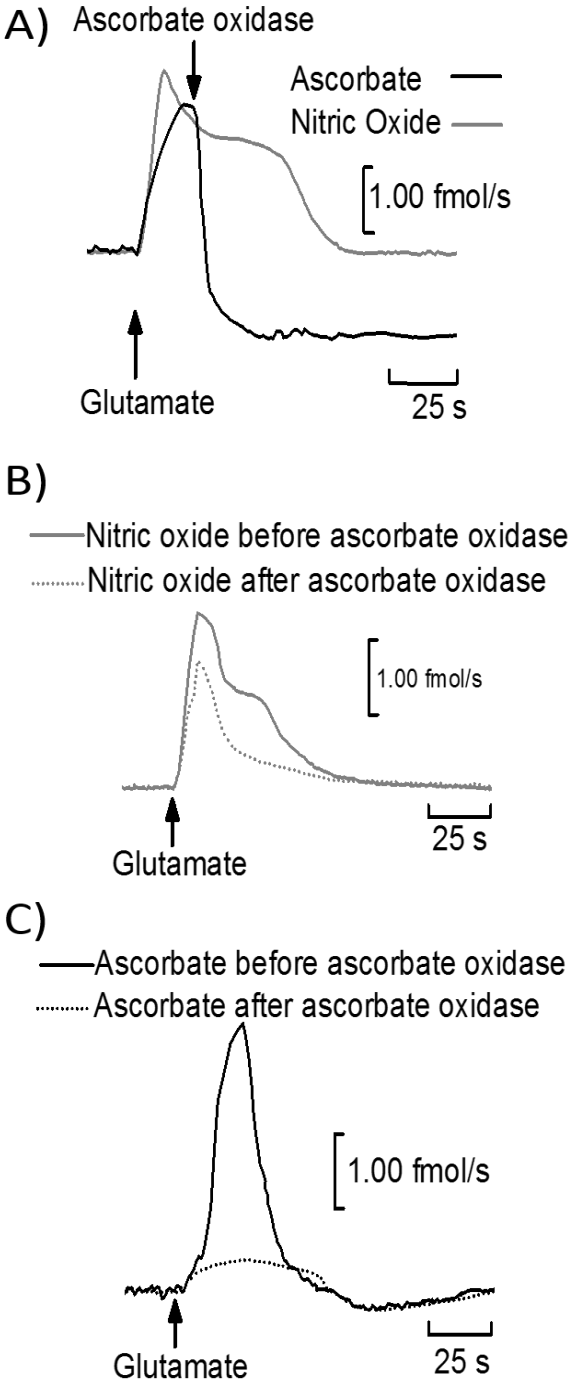

Figure 5.10. *A) Representative amperometric recording of the local ejection of ascorbate oxidase on top of ascorbate (black line) and •NO signals (gray line), after stimulation with L-glutamate. B) The effect of ascorbate oxidase on the dynamics of ascorbate and •NO signals evoked by the local ejection of L-glutamate (20 mM). The full gray line represents an average of •NO signals (n=10) and the full black line an average ascorbate signals (n=10) before the local application of ascorbate oxidase. The dotted gray line represents an average of •NO signals (n=10) and the dotted black line an average of ascorbate signals (n=10) after the local application of ascorbate oxidase (0.1 mg/mL, 87.5 nL). Arrow indicates the time of ejection.*

5.3.3.4. Inhibition of Glutamate Uptake

Usually, ascorbate release to the extracellular space is attributed to a glutamate/ascorbate heteroexchange mechanism (Ghasemzadeh, Cammack et al. 1991, Miele, Boutelle et al. 1994, Rebec, Witowski et al. 2005). According to this view, glutamate is the key player in the process of ascorbate release to the extracellular space. However, we have observed that in the presence of the TBOA, an inhibitor of glutamate uptake (Shimamoto, Lebrun et al. 1998, Jabaudon, Shimamoto et al. 1999, Shigeri, Shimamoto et al. 2001), the release of ascorbate still occurs and in a way subsequent to the increase of •NO (Figures 5.11 A and C). In fact, when compared with control stimulus, the co-ejection of glutamate and TBOA increased the area of •NO signal by 2.0 ± 0.3 fold (mean ± SEM, n=6, $P<0.05$) figure 5.11 B) and the same tendency was observed for ascorbate signal. When compared to control glutamate stimulus, the ascorbate total signal area increased 1.5 ± 0.3 fold (mean ± SEM, n=6, $P<0.05$) when glutamate was co-ejected with TBOA (Figure 5.11 D). Additionally, TBOA interfered with the time course of both, ascorbate and •NO (Figures 5.11 A and C, respectively).

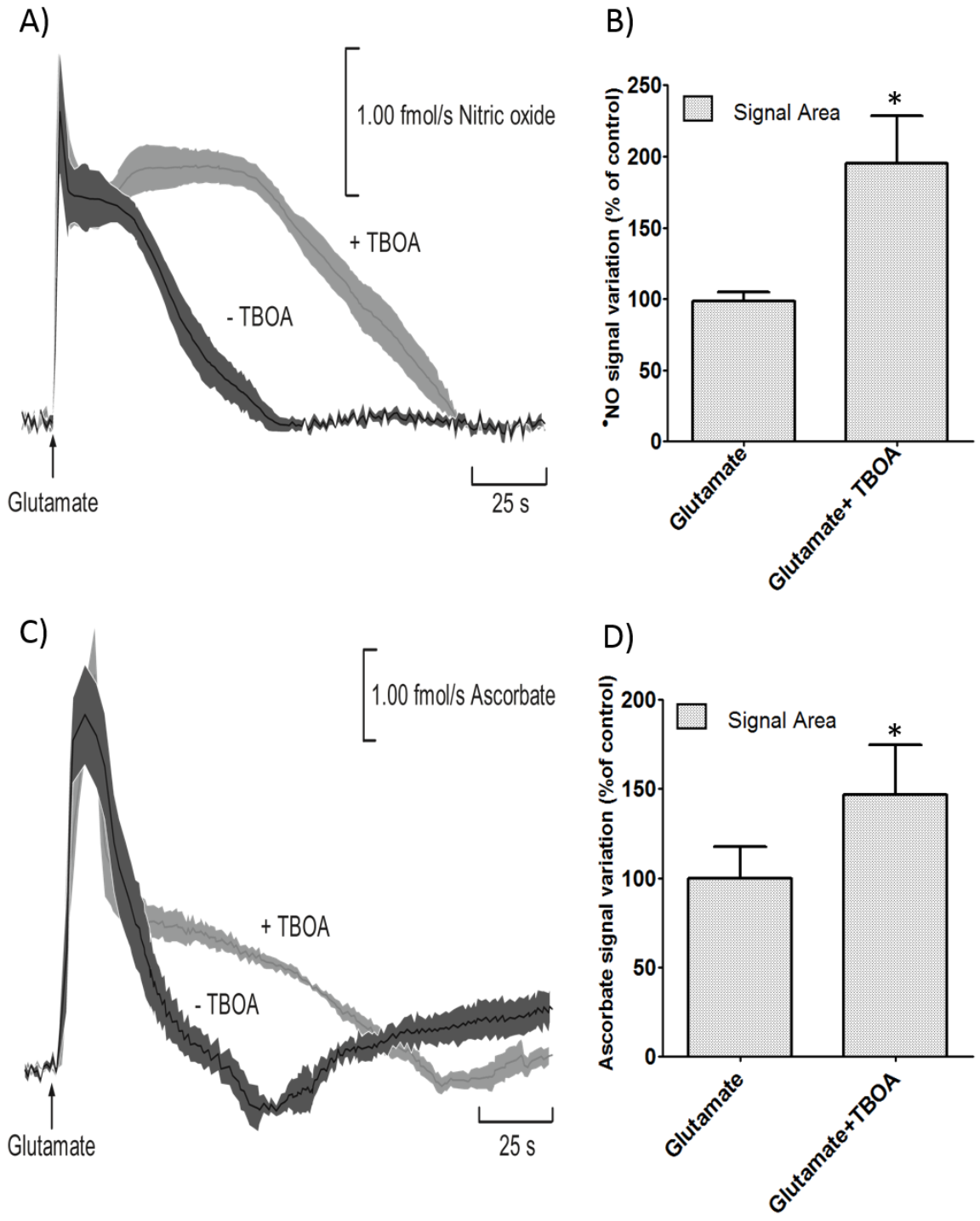

Figure 5.11. *Average recording of •NO (A) and ascorbate (C) signals upon a stimulus with glutamate 20 mM (black line, n=6), and after a stimulus with glutamate 20 mM and TBOA 0.1 mM (gray line, n=6). Quantification of the •NO (B) and ascorbate (D) signal area variation for the stimulus with glutamate and glutamate + TBOA (n=6, results presented as mean ± SEM). Arrows indicate the time of ejection of the stimulus. * p < 0.05.*

5.4. Discussion

Ascorbate is a highly prevalent molecule in the brain, especially in the cerebral cortex and hippocampus and, being accumulated at mM concentration in neurons, its release to the extracellular space has been linked to the activation of glutamatergic pathways (Rice 2000). Glutamate is also involved in •NO production by nNOS through activation of the NMDA receptor and considering the modulatory role of •NO in brain processes we have explored the possible connection between •NO production and ascorbate release upon glutamatergic stimulation *in vivo*. Given the nature of •NO molecule, a retrograde messenger that is diffusible, lacks specific interaction with targets and encodes information according to its spatiotemporal dynamic profile (Pacher, Beckman et al. 2007), it became critical to perform experiments in a way where ascorbate and •NO dynamics could be monitored independently and simultaneously, with enough spatial and temporal resolution to allow localized and real time measurements. The technological approach we used, consisting of two microelectrodes placed very close to each other (~250 µm), coated with specific films and polarized at two distinct potentials to enhance sensitivity and selectivity for each analyte, enabled us to perform such experiments. The identification tests confirmed that the major contributor to each signal was •NO and ascorbate, respectively. The ability to perform simultaneous measurements allowed us to follow the temporal dynamics of both compounds following stimulation and the reported values are in accordance to previous reports for each compound (Cammack, Ghasemzadeh et al. 1991, C.F. Lourenço 2014). A role for •NO in ascorbate uptake has been proposed in the retina in culture via the interference with the expression of sodium vitamin C transporter (SVCT2) (Portugal, da Encarnacao et al. 2012) but in this work several observations point to a more intricate role of neuronal •NO in ascorbate dynamics at glutamatergic synapses in hippocampus *in vivo*.

The simultaneous recordings point to a sequence of events whereby, following glutamate stimulation in the hippocampus, the increase in •NO production precedes the release of ascorbate to the extracellular space;

A quantitative correlation between the intensity of ascorbate and •NO signals is apparent;

The lag phase between •NO and ascorbate signals was similar when either glutamate or NMDA (the specific agonist of the receptor to which nNOS is physically and functionally bound at post-synaptic locations) were used and the local administration of •NO solution evoked the release of ascorbate and the length of lag-phase was maintained.

Collectively, these observations suggest a role for neuronal-derived •NO in ascorbate release from neural cells upon activation of glutamate NMDA receptors. According to this hypothesis, a glutamatergic stimulation in the presence of inhibitor of the neuronal isoform of NO synthase (nNOS) would decrease both, •NO and ascorbate signals. In fact, the use of 7-NI (a nNOS selective inhibitor) significantly decreased •NO signal (c.a 71%), a value that is in agreement with the results presented in a previous study, where an average decrease of 79% in peak amplitude was calculated after administration of 7-NI (Lourenco, Santos et al. 2011). Simultaneously, in the presence of 7-NI, the release of ascorbate was almost completely abolished.

The functional connection between •NO production and ascorbate release was further studied by using TBOA, an inhibitor of glutamate uptake that leads to a fast increase in extracellular glutamate concentration (Jabaudon, Shimamoto et al. 1999). Assuming that the heteroexchange glutamate/ascorbate mechanism is the primary path for the release of ascorbate, a significant decrease in ascorbate signal should be observed in the presence of the inhibitor, as previously reported (Cammack, Ghasemzadeh et al. 1991). The real time recordings *in vivo* showed that the inhibition of glutamate uptake was not accompanied by a reduction of ascorbate released. By the contrary, both ascorbate and •NO signals exhibited a tendency to increase their signal area, as a consequence of the rise in glutamate concentration in the extracellular space. These experiments do not exclude the glutamate-ascorbate heteroexchange mechanism since TBOA is a competitive inhibitor and can serve itself as substrate for the glutamate transporter (Rebec and Pierce 1994), but strongly suggest the occurrence of alternative pathways for ascorbate release following glutamate neurotransmission, in agreement with previous reports in the literature, that suggest other mechanisms different from the heteroexchange mechanism for ascorbate release (Wilson, Peters et al. 2000, May, Li et al. 2006, Portugal, Miya et al. 2009). In fact, it has been reported that •NO modulates glutamate uptake in synaptosomes and it may directly interfere with the transporter system for glutamate and therefore, modulate ascorbate release through the heteroexchange mechanism (Pogun, Dawson et al. 1994). Ascorbate release has also been attributed to occur through volume sensitive osmolyte anionic channels (*VS*OAC) in primary cultures of astrocytes (Wilson, Peters et al. 2000) and there is evidence in the literature that •NO can modulate these anionic channels and therefore, promote the release of ascorbate via activation of these channels in rabbit portal vein smooth muscle cells (Ellershaw, Greenwood et al. 2000). Results obtained in the previous chapter regarding the uptake rate of glutamate (see table 4.2) indicate that glutamate uptake is slower in the presence of TBOA. In this case, glutamate remains in the synaptic cleft for a longer period of time, and an overactivation of the NMDA receptor can occur, leading to an increase in •NO production and, subsequently, to an

increase in ascorbate release. Even though the mechanism responsible for this coupling is still to be elucidated, this work provides *in vivo* and real time recordings of •NO and ascorbate concentration dynamics in the extracellular that support a functional connection between glutamate-induced •NO production via the NMDA receptor and ascorbate release to the extracellular space.

In this regard, the observation that glutamate stimulation in the presence of ascorbate oxidase induced •NO production at lower fluxes than in the control (absence of ascorbate oxidase) suggests that extracellular ascorbate modulates •NO production, further strengthening the connection between •NO and ascorbate dynamics. Mechanistically, the effect of extracellular ascorbate may be interpreted on basis of its redox properties encompassing the modulation of the redox status of the NMDA receptor (Majewska, Bell et al. 1990, Kiyatkin and Rebec 1998, May, Li et al. 2006) and a reduction of potential oxidants, thus increasing •NO bioavailability or even in view of the influence that ascorbate has in the neurometabolic process that switch from glucose to lactate as the energy substrate of neurons and, ultimately, in the regeneration of glutamate through the enzymatic conversion of glutamine (Castro, Beltran et al. 2009). With this pathway compromised due to the lack of ascorbate, less glutamate will be released and probably less •NO will also be produced. However, a challenging hypothesis is the ascorbate-dependent reduction of circulating nitrite to •NO (Millar 1995), supporting nitrite as a potential source of •NO in the brain (Piknova, Kocharyan et al. 2011).

5.5. Conclusions

In order to improve therapies addressed to neurodegenerative diseases, it is crucial to better understand the different processes underlying brain function. In this chapter we demonstrated the existence of a coupling through which •NO produced upon glutamatergic stimulation triggers the release of ascorbate to the extracellular space. This conclusion relies mostly on the quantitative correlation between the intensity of ascorbate and •NO signals; the similar lag phase between •NO and ascorbate signals when either glutamate or NMDA were used and the observation that local administration of •NO solution evoked the release of ascorbate and the length of the lag-phase was maintained. The strong decrease of •NO and ascorbate signals after the injection of an inhibitor of nNOS like 7-NI further supported this idea. Released ascorbate modulates •NO signaling on basis of its redox properties, either by regulating the activity of the NMDA receptor or by interacting with other reactive species that may act as a "sink" for •NO and thus, increasing its half-life. Considering the importance of these compounds in the regulation of neurometabolic processes or neurovascular coupling, it seems clear that this is an important piece of knowledge towards a more integrated understanding of the brain and the neurological processes.

6. **Nitrite/ascorbate redox interaction leads to nitric oxide production in the brain hippocampus, supporting neurovascular coupling. An *in vivo* study in real-time**

Part of the work presented in this chapter was published in:

Pereira, C., Ferreira, N. R., Rocha, B. S., Barbosa, R. M., Laranjinha, J. (2013). "The redox interplay between nitrite and nitric oxide: From the gut to the brain." Redox biology 1: 276-84

6.1. Introduction

The brain has a very high energetic demand that requires a constant supply of oxygen and glucose. In fact, despite of comprising only 2% of the body's mass, brain accounts for 20% of resting O_2 consumption. A similar mismatch is observed for blood flow destined to the brain, which represents over 10% of cardiac output. (Magistretti, Pellerin et al. 1999, Magistretti 2006). At the same time, the brain has limited intracellular energy reserves, and therefore, proper functioning is highly dependent on cerebral blood supply and the continuous delivery of glucose and oxygen (Jackman and Iadecola 2015), and a well regulated blood flow within the brain is vital to maintain energy-dependent processes and to clear metabolic byproducts produced by neuronal activity, such as CO_2, excess lactate, other metabolites and heat. The dependence of the brain on blood flow is highlighted by the fact that even relatively small reductions in CBF can have deleterious effects on the brain (Drake and Iadecola 2007). In order to cope with this demand and to maximize energetic and metabolic efficiency, only a restricted number of neuronal cells fire at the same time and metabolic requirements are satisfied through the local and transient increase in cerebral blood flow (CBF) via a mechanism called functional hyperemia or neurovascular coupling (NVC), thus establishing a tight link between neuronal activity and blood flow. In fact, neurons, glia and blood vessels exhibit a close anatomical and functional coupling, forming the neurovascular unit (Woolsey, Rovainen et al. 1996, del Zoppo and Mabuchi 2003). A very important aspect of the NVC mechanism is the observed coupling in terms of space, time and amplitude between the increase in neuronal activity and CBF (Iadecola 2004). There is substantial evidence from studies of cerebellum, hippocampus and neocortex on how glutamate influences blood flow. Exogenous glutamate or selective glutamate receptor agonists dilate pial arterioles and/or precapillary microvessels. In contrast to cerebellum, this effect in hippocampus and neocortex does involve NMDA-type glutamate receptors (Fergus and Lee 1997, Lovick, Brown et al. 1999). Glutamate does not act directly on smooth muscle cells to produce vasodilation. Rather, this neurotransmitter increases CBF by inducing the release of vasoactive factors from other cells through several calcium- dependent mechanisms. Available evidence suggests that $^{\bullet}NO$ is an important mediator in the process of NVC. For example, the vasoactive actions of glutamate are attenuated by blocking NOS (Li and Iadecola 1994, Lovick, Brown et al. 1999, Yang, Chen et al. 1999) or in NOS null mice (Zhao, Ross et al. 2003). Moreover, it has been shown that neurovascular coupling in hippocampus is mediated via diffusion by neuronal-derived $^{\bullet}NO$ (Faraci and Breese 1993, Lourenco, Santos et al. 2014). Since the neuronal isoform of nitric oxide synthase (nNOS) requires oxygen as a substrate to work properly (Griffith and Stuehr 1995, Alderton, Cooper et al. 2001, Li and Poulos 2005), we would expect that, in situations where

oxygen supply is diminished (respiratory insufficiency, ischemia, stroke, ageing), the activity of nNOS is highly attenuated and, consequently, we would expect that the decreased production of •NO translates into subsequent impairment of blood flow and compromised vasodilation. Moreover, these situations are also characterized by a drop in pH, causing brain acidosis (Rehncrona 1985, Smith, von Hanwehr et al. 1986, von Hanwehr, Smith et al. 1986). Acidosis is also known to reduce the NMDA receptor-activated currents in cultured hippocampal neurons (Choi, Monyer et al. 1990, Tang, Dichter et al. 1990). However, apparently, hypoxic conditions don't block vasodilation (Millar 1995). This suggests the occurrence of alternative and/or complementary pathways to ensure that tissues get the needed amount of •NO, regardless of the functional state of the enzymes usually involved in its synthesis. It is known that •NO reacts in the extracellular space and it is converted to nitrite (Moncada and Higgs 1993). In addition, nitrate obtained from the diet or endogenously produced upon •NO oxidation, is mixed with saliva in the oral cavity and travels along the gut being absorbed in the small intestine. The salivary glands then recover c.a. 20% of circulating nitrate and secrete it into the oral cavity where it is reduced to nitrite by the local microflora and mixed with saliva, thus establishing the enterosalivar circulation of nitrate (Spiegelhalder, Eisenbrand et al. 1976, Wagner, Schultz et al. 1983). These different sources contribute to build up a pool of nitrite in the brain. The extracellular space is also rich in the powerful reducing agent ascorbate (250-500 µM) (Rice 2000). The reduction of nitrite promoted by univalent reductants such as dietary polyphenols and ascorbate is well established in the gastric environment where both reagents (nitrite and ascorbate) achieve optimal conditions (low pH, high concentration) for the reduction of nitrite to •NO occur (Gago, Lundberg et al. 2007, Rocha, Gago et al. 2011).

In this chapter we studied the role of nitrite in contributing to maintain the balance between •NO production, oxygen consumption and neurovascular coupling in the brain, in a process independent of enzymatic control, involving its univalent reduction to •NO by ascorbate, especially in conditions where brain acidosis may occur. Moreover, we also tested the impact that an increase in circulating nitrate could have on •NO production and on CBF, through the activation of the $NO_3^- \rightarrow NO_2^- \rightarrow$ •NO pathway. To achieve this, we performed dynamic and local measurements of ascorbate and •NO in the hippocampus using carbon fiber microelectrodes coupled to electrochemical techniques. These measurements were coupled to the dynamic and real time monitoring of CBF using Laser Doppler flowmetry. This technique is used for assessment of CBF changes in real-time in the CNS. Due to its small sample tissue volume (~ 1 mm^3), it has a reasonable spatial resolution to be used in the investigation of the mechanisms underlying the NVC (Steinmeier, Bondar et al. 2002).

6.2. Experimental

Refer to Chapter 2 for detailed information regarding solutions, microelectrodes and *in vivo* experiments related procedures.

For the *in vitro* determination of nitrite reduction to •NO by ascorbate, 20 mL of PBS lite were added to beaker and placed in a battery operated stirrer with gentle agitation. Then ascorbate and nitrite war added for a final concentration of 250 and 20 µM, respectively. Next, the ISO NO II sensor and the pH electrode (Crison, Barcelona, Spain) were inserted in the solution. The software (Duo 18) to record the current from the ISO NO II sensor was initiated and current monitoring started. After a stable baseline was reached, pH was registered (7.4) and it was then acidified through local addition of one HCl solution (1M) until a pH value of 6.5 was reached.

The $NaNO_3$ solution used during the experiments designed to study the impact of nitrate in •NO production and CBF was prepared in MiliQ water and injected intraperitoneally in a dose of 100 mg/kg.

6.2.1. Electrodes

In these studies we have used Nafion/SWCNT and chemically modified carbon fiber microelectrodes with Nafion/*o*-PD for ascorbate and •NO measurements, respectively. Bare CFMs were used to monitor nitrite clearance *in vivo*.

The commercial ISO-NOP 2 mm Pt sensor connected to the amperometer ISO-NO Mark II (World Precision Instruments, Inc., USA) was used for the *in vitro* test of nitrite reduction to •NO by ascorbate at a pH=6.5. The calibration procedure of this sensor is described in section 2.1.2 of the manuscript.

6.2.2. Ascorbate and •NO measurements

Measurements of •NO and ascorbate were made using amperometry, with a hold potential of +0.8 V and +0.05 V *vs* Ag/AgCl, respectively. A bipotentiostat Fast MK III (Quanteon, USA) was used for this purpose. The used array had the configuration illustrated in figure 2.11 B.

6.2.3. •NO and CBF measurements

•NO and CBF were simultaneously measured *in vivo* according using the array illustrated in figure 2.11 D. This consisted in a Nafion/*o*-PD coated CFM for a •NO, an injection micropipette for local application of stimulus and the laser Doppler flow probe for CBF measurements. The three components were assembled in a pre-defined geometry relatively to the others, thus permitting the microelectrode to be within the •NO diffusional spread.

6.2.4. Animal and surgical procedures

In vivo experiments were performed in male Wistar rats (8-12 weeks old, weight 250-390 g), as described in chapter 2. In brain acidosis experiments, a moderate gas flow of CO_2 was created in front of the rat nose by means of a funnel plugged to a gas tank containing 100% CO_2 and maintained for 60s. For some experiments, a local ejection of nitrite preceded the start of the gas flow. During the period of time that animals were breathing CO_2 the arterial oxygen was constantly monitored and values usually dropped to values around 30-40% when the CO_2 gas flow was stopped.

6.2.5. *In vivo* recordings

In vivo experiments were carried out in the hippocampus, and the used coordinates (from bregma) are indicated in the legend of each figure. Recordings were done by lowering the tip of the CFM used for •NO (used as reference) into the brain region of interest. Overall, data collected from 17 animals was used in this chapter.

Electrochemical data acquisition rate was 2 Hz. After baseline current stabilization (15 minutes), glutamate (20 mM) and the other solutions used for local application were pressure ejected from the micropipette using a Picospritzer III and ejected volumes monitored using a stereomicroscope fitted with a reticule.

Cerebral blood flow signals were recorded using a time constant set to 33.3 Hz. Measurements are expressed as Perfusion Units (PU), which are arbitrary.

6.2.6. Data analysis

Whenever necessary, the individual signals were characterized in terms of (1) peak amplitude, based on the conversion of the amperometric currents to fluxes according to Faraday's law ($I = n \cdot F \cdot \phi$), in which I corresponds to the amperometric current, n corresponds to the number of electrons involved in the electro-chemical oxidation, F corresponds to the Faraday constant and ϕ is the flux); (2) area, calculated as the time integral of the signal; (3) T_{50}, the time in seconds from maximum amplitude to 50% decay of the signal; and (4) T_{total}, the time in seconds from the application of the stimulation to return to basal levels. Recordings from CBF were exported from the Perisoft version 2.50 software, averaging one point per second, and synchronized with •NO recorded dynamics based on the markers added at the time of stimulations. CBF changes were analyzed in terms of 1) *CBF change*, relative change in CBF in respect to the basal levels (percentage); 2) signal area, calculated as the time integral of the signal. Recordings were analyzed with OriginPro 7.5 and statistical analyses were performed with GraphPad Prism 5. Data

are presented as mean ± SEM. One-way analysis of variance (ANOVA) was performed to make comparisons between multiple groups followed by Dunnett post-test. When there were only two groups, statistical analyses of the data were performed using a Student's t-test. Differences were considered significant at $p < 0.05$.

6.3. Results

6.3.1. *In vitro* nitrite nitric oxide production via reduction of nitrite by ascorbate

It is known that under the strong acidic conditions (pH 1.5-2) of the stomach nitrite is easily reduced to •NO (Benjamin, O'Driscoll et al. 1994, Gago, Lundberg et al. 2007). However, when the brain is submitted to hypoxic conditions, local pH drop is near 6.4 (van der Toorn, Sykova et al. 1996), a value higher than the stomach pH. The first task was to assess if nitrite reduction to •NO by ascorbate occurs at a pH similar to what is found in a situation of brain hypoxia. Figure 6.1 shows an amperometric recording at +0.9 V with the ISO-NOP (a sensor coated with a gas permeable sleeve that detects only gases) when ascorbate and nitrite were in solution and the pH of the buffer (PBS lite) was acidified from 7.4 to 6.5. The observed increase in current is attributable to •NO, confirming that, at a pH value similar to what is obtained in the hypoxic brain, nitrite is reduced to •NO by ascorbate. According to the previous calibration of the sensor, the increase in current corresponds to a •NO concentration of 118 nM.

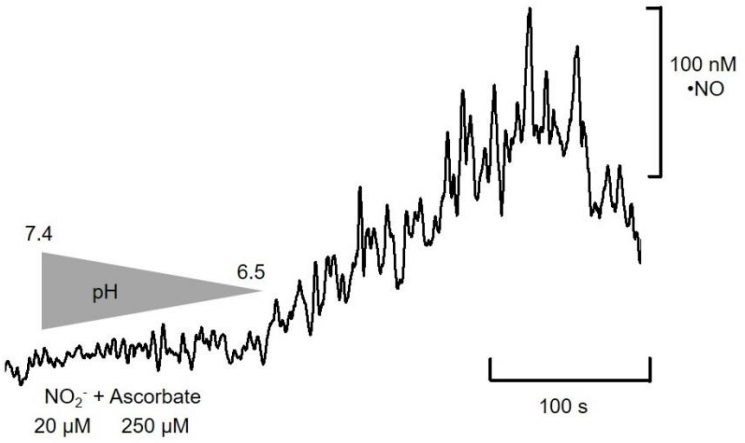

Figure 6.1. *•NO production from a mixture of ascorbate and nitrite as a function of pH. The reaction vessel was supplemented with 250 µM of ascorbate and 20 µM of nitrite at a pH of 7.4. The vessel was coupled to an ISO-NOP (selective for •NO measurements) and to a pH meter. Current was allowed to stabilize. Then, pH was slowly acidified until it reached the value of 6.51 (a value that can be reached* in vivo *under hypoxic conditions). At this pH value, current increased indicating that •NO was being produced. Maximum concentration of •NO obtained in these conditions was 118 nM.*

6.3.2. Measurement of •NO and CBF in the hippocampus during brain acidosis

Control experiments were performed to assess if the local ejection of nitrite produced any interference in the CFM used for •NO monitoring. Figure 6.2 A shows that a local application of nitrite (75 nL) didn't elicit any observable change in background current of the Nafion/ *o*-PD CFM used for •NO measurements.

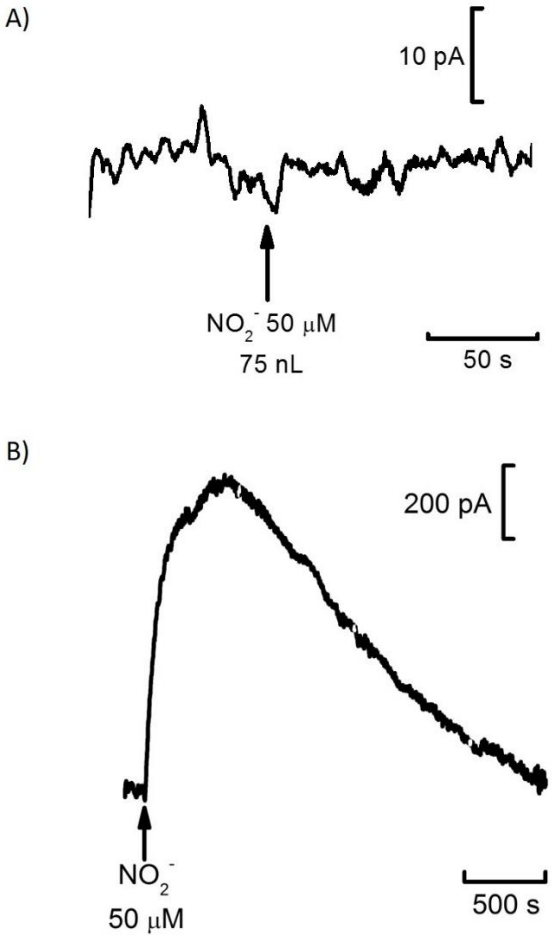

Figure 6.2 *A) Representative amperometric recording of the* in vivo *local ejection of 75 nL of nitrite (50 μM) at approximately 200 μm of a Nafion/* o*-PD CFM. No signal was measured, supporting the high selectivity of the microelectrodes for •NO measurements. Recording performed in the DG region of the hippocampus (AP: -4.1; ML: -2.3; DV: -3.0). Arrow indicates the time of nitrite ejection. B) Average amperometric (n=5) recording of a local ejection of nitrite next to a bare CFM (~200 μm) to evaluate nitrite clearance* in vivo*. Recordings performed in the CA1 region of the hippocampus (AP: -3.2; ML: -2.2; DV: -2.4). Arrow indicates the time of nitrite ejection. Volumes of ejected nitrite ranged from 50-75 nL.*

A further experiment (Figure 6.2 B) was made to evaluate nitrite clearance from the place where it was ejected, since it was necessary to confirm that it remained near the CFMs time enough to react with ascorbate in acidic conditions and produce •NO. Figure 6.2 B is an average recording (n=5) and lustrates that experiment. In this case bare CFMs were polarized at +0.8 V *vs*. Ag/AgCl to monitor nitrite. It is possible to observe that, when nitrite is locally ejected, the signal started to increase and the current peak was achieved at 298 ± 54 s after ejection. The total time of the

signal was 2074 ± 158 s and T_{50}, the time needed for the signal to decrease to half of the maximum peak, was 1163 ± 153 s. These values indicate that nitrite is present in the extracellular space during the time used for the acidosis protocol (60-70s).

Having performed the control experiments with nitrite, the following experiments were done to measure •NO and CBF signals obtained in a situation of brain acidosis and compare them to a situation where brain acidosis was preceded by a local ejection of nitrite. Brain acidosis was induced using a hypercapnia protocol that is known to decrease the pH to values around 6.7 (Siesjo, Folbergrova et al. 1972, Martoft, Stodkilde-Jorgensen et al. 2003). Simultaneous recordings of •NO and CBF were obtained. As illustrated in figure 6.3 A, submitting the animal to an atmosphere of CO_2 for 60 seconds elicited transient signals of •NO (gray line) and CBF (black line). It is possible to observe a delay of c.a. 30 seconds between the onset of CBF and •NO signals.

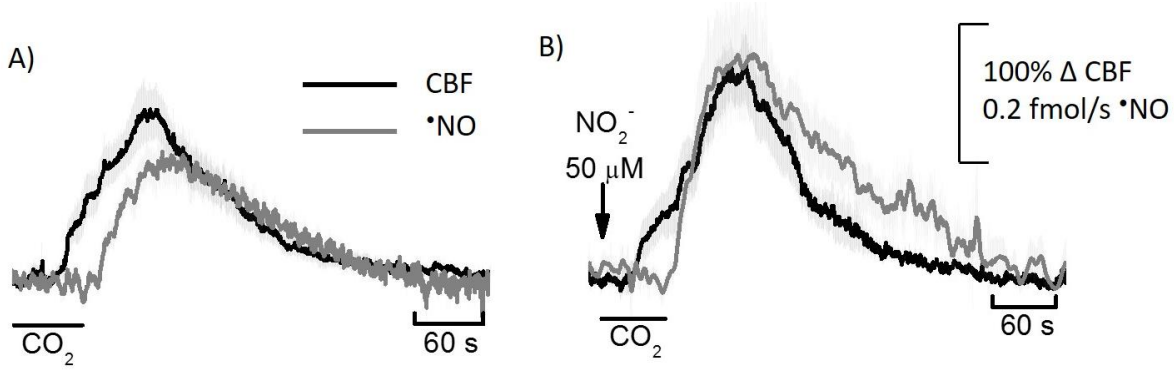

Figure 6.3 *A) Average amperometric measurements of •NO (gray line, n=13) and CBF (black line, n=10) signals after the induction of brain acidosis. B) Average amperometric measurements of •NO (gray line, n=20) and CBF (black line, n=10) signals after the induction of brain acidosis preceded by a local ejection of nitrite. Recordings performed in the DG region of the hippocampus (AP: -4.1; ML: -2.4; DV: -3.2). Arrow indicates the time of nitrite ejection. Volumes ranged from 50-75 nL.*

The previous ejection of nitrite before starting hypercapnia significantly increased •NO and CBF evoked signals in terms of peak maximum amplitude and signal area, as observed in figure 6.3 B. Tables 6.1 and 6.2 show some kinetic parameters and statistical analysis performed on the •NO and CBF signals obtained in both situations. Taking in consideration that the average sensitivity of the CFMs used in this study for •NO measurements was 158 ± 16 pA/µM (n=10, pre calibration data), the maximum peak amplitude corresponded to a •NO peak concentration near 119 nM for the acidosis condition and 227 nM for the acidosis condition with previous ejection of nitrite. This corresponded to an increase of 90% in the maximum •NO concentration when compared to the control situation. The maximum peak amplitude of CBF signals also increased 40% when nitrite was ejected locally before starting the CO_2 flow. Interestingly, the total duration of the signals (•NO and CBF) didn't change significantly in both conditions.

Table 6.1. *Statistical analysis of •NO signals obtained in terms of signal area, maximum peak amplitude and signal duration. Results are presented as mean ± SEM. * p< 0.05.*

	Nitric Oxide	
	Acidosis	**Nitrite+ acidosis**
Max amplitude Flux (fmol/s) *	0.220 ± 0.030 N=13	0.450 ± 0.033 N=20
Signal area * (fmol)	25.95 ± 3.264 N=13	58.91 ± 7.390 N=20
T total (s)	238.4 ± 14.17 N=13	247.1 ± 21.75 N=20

Table 6.2. *Statistical analysis of CBF signals obtained in terms of signal area, maximum peak amplitude and signal duration. Results are presented as mean ± SEM. * p< 0.05.*

	Cerebral Blood Flow	
	Acidosis	**Nitrite+ acidosis**
Max amplitude (% change P.U.) *	165.1 ± 13.08 N=10	231.2 ± 20.46 N=10
Signal area *	17350 ± 2064 N=10	24230 ± 1198 N=10
T total (s)	271.6 ± 17.94 N=10	298.4 ± 11.69 N=10

6.3.2.1. In vivo verification of •NO signal

Experiments were performed to confirm the nature of the recorded signal when using the brain acidosis protocol. Signals were monitored by one Nafion/*o*-PD CFM and two stimulations (local ejection of nitrite + 60 s of CO_2) were applied. During the first stimulation potential was held at +0.8 V *vs* Ag/AgCl and for the second one the potential was changed to +0.4 V *vs* Ag/ AgCl. The result is illustrated in figure 6.4 and shows that the CFM while recording at +0.4 V *vs* Ag/ AgCl had a negligible current change when compared to the recording obtained at +0.8 V *vs* Ag/ AgCl, indicating that the observed change in background current during the brain acidosis protocol is due to •NO.

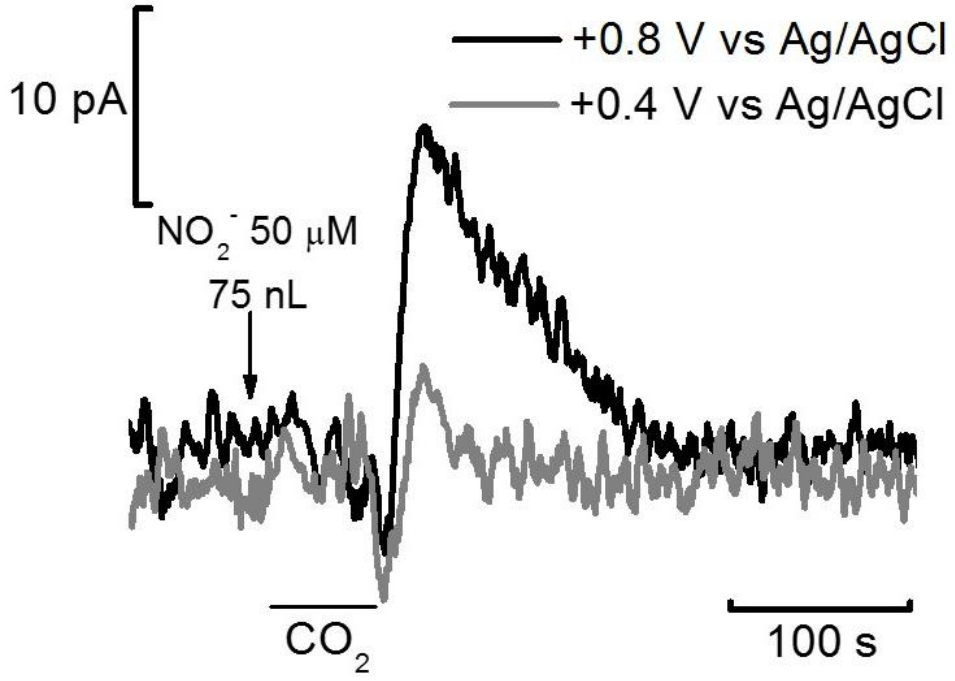

Figure 6.4. *Amperometric measurements of •NO signals at +0.8 V vs. Ag/AgCl (black line) and +0.4 V vs. Ag/AgCl (gray line) after the induction of brain acidosis preceded by a local ejection of nitrite. Recordings performed in the DG region of the hippocampus (AP: -4.1; ML: -2.4; DV: -3.2). Arrow indicates the time of nitrite ejection. When •NO is monitored at +0.4 V, a potential insufficient to oxidize this molecule, no signal is observed after the ejection of NO_2^- and induction of acidosis.*

6.3.3. Modulation of nitric oxide and cerebral blood flow signals in acidosis

6.3.3.1. Ascorbate role in nitrite reduction to •NO in the brain hippocampus

To assess the involvement of ascorbate in the production of •NO by reduction of nitrite in a situation of brain acidosis we performed experiments encompassing simultaneous measurements of •NO (with a nafion/*o*-PD CFM polarized at +0.8 V *vs*. Ag/AgCl) and ascorbate (with a Nafion/SWCNT CFM, polarized at +0.05 V *vs*. Ag/AgCl). As shown in figure 6.6, in a situation of acidosis there is a consumption of extracellular ascorbate (black line) previously to the increase in •NO signal (gray line). The observed dynamics of the two molecules suggests the involvement of ascorbate in the production of •NO in the induced situation of brain acidosis.

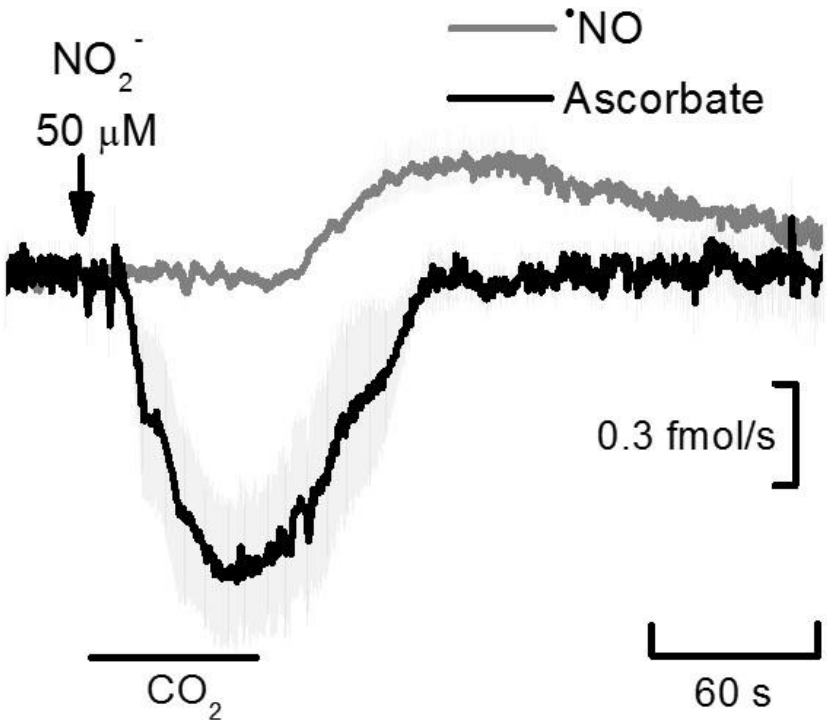

Figure 6.5. *Average amperometric recordings (n=7) of simultaneous measurements of ascorbate (black line line) and •NO (gray line) in the rat hippocampus* in vivo *after induction of brain acidosis with a previous local ejection of nitrite, as indicated by the arrow. Recordings performed in the DG region of the hippocampus (AP: -4.1; ML: -2.4; DV: -3.2). Arrow indicates the time of nitrite ejection. Volumes of ejected nitrite ranged from 50-75 nL.*

To further elucidate the relation between ascorbate release and •NO production, another set of experiments was designed. In this case, simultaneous measurements of •NO and CBF were performed before and after local ejection of ascorbate oxidase. As referred in the previous chapter, ascorbate oxidase is an enzyme that is highly specific to ascorbate and it was used to evaluate if the elimination of extracellular ascorbate had any influence in the observed •NO and CBF signals. Figure 6.7 shows the comparison between •NO and CBF signals obtained in the presence of ascorbate (left panel of the figure) and after ascorbate oxidase was locally ejected to eliminate extracellular ascorbate (right panel). It is possible to observe that, upon the local

ejection of ascorbate oxidase, •NO signals (gray line) of nitric oxide decreased 65% in terms of signal maximum amplitude, 90% in terms of signal area and 62% in terms of signal duration ($p < 0.05$). Simultaneously, CBF signals decreased 63% in terms of signal area and signal max amplitude and 30% in terms of signal duration ($p < 0.05$).

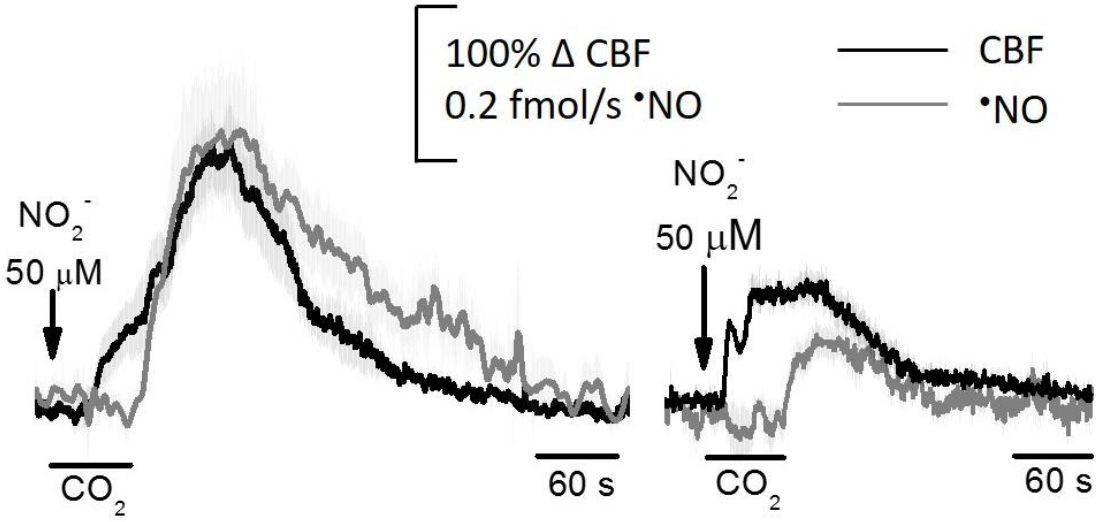

Figure 6.6. *Comparison of the average amperometric recording of •NO (gray line) and CBF (black line) signals (n=10) obtained after the induction of brain acidosis and upon a previous local ejection of nitrite in the presence of extracellular ascorbate (left panel) and in the absence of extracellular ascorbate (right panel). Ascorbate was eliminated from the extracellular space by locally ejecting ascorbate oxidase 0.1 mg/mL. Right panel represents the average of 8 signals. Recordings performed in the DG region of the hippocampus (AP: -4.1; ML: -2.4; DV: -3.2). Arrow indicates the time of nitrite ejection. Volumes of ejected nitrite ranged from 50-75 nL.*

Results suggest that ascorbate is implicated in the observed production of •NO in the brain in a situation of brain acidosis caused by hypercapnia. Since this is characterized by a pH that has been shown to be low enough for ascorbate to react with nitrite to yield •NO (Figure 6.1), we may suppose that this reaction is on the basis of the observed results.

6.3.3.2.Inhibition of nitric oxide synthase with 7-nitroindazole

In order to address the potential contribution of the enzymatic pathway for the observed •NO and CBF signals when the brain acidosis protocol is performed, we did an additional experiment. •NO and CBF were simultaneously measured and signals obtained in the situation of brain acidosis with a previous ejection of nitrite were compared before and after a systemic administration of 7-NI, a selective blocker of the enzyme n-NOS (Figure 6.8).

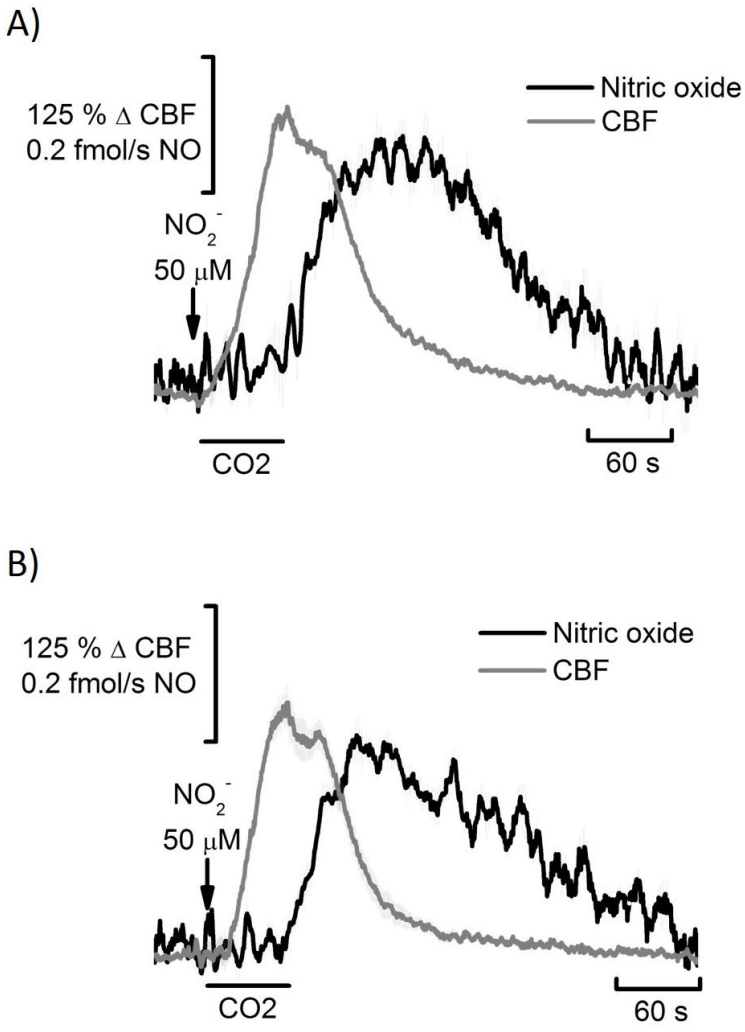

Figure 6.7. *Average amperometric recordings of •NO and CBF signals obtained after the local ejection of nitrite followed by the induction of brain before (A) and after (B) systemic administration of 7-NI. Recordings performed in the DG region of the hippocampus (AP: -4.1; ML: -2.4; DV: -3.2). Arrow indicates the time of nitrite ejection. Volumes of ejected nitrite ranged from 50-75 nL. 7-NI was administered intraperitoneally in a dose of 50 mg/kg.*

For these experiments, an additional micropippete was added to the array and filled with L-glutamate, that was used to locally stimulate the enzymatic production of •NO through the activation of n-NOS. When glutamate evoked signals were obtained, we changed to the acidosis protocol and recorded •NO and CBF signals. Then, 7-NI was administered and, thirty minutes later,

we confirmed with another stimulation with L-Glutamate that n-NOS was blocked by the absence of •NO signal. Then, the protocol of brain acidosis was performed again and results collected while 7-NI was exerting its effect on the enzyme. Another stimulus with L-Glutamate was applied 90-100 minutes after the administration of 7-NI, and we got a signal of •NO and CBF, confirming that nNOS was active again. As shown in figure 6.8, results collected while nNOS was inhibited by 7-NI (n=9) did not significantly change neither •NO nor CBF dynamics under brain acidosis situation preceded by local nitrite ejection when compared to the results collected before the administration of 7-NI (n=8), suggesting that this is not a major pathway for •NO production during brain acidosis, thus supporting the idea that the observed •NO signals during brain acidosis have a non-enzymatic source.

6.3.4. Modulation of •NO and CBF signals with nitrite and nitrate – a possible role for diet in brain perfusion

We have shown in the previous chapter that the removal of ascorbate from the extracellular space has a significant effect on the dynamics of •NO signals. In this chapter we have observed a correlation between local ejection of nitrite and the increase in •NO and CBF signals in a situation of brain acidosis. Considering that upon glutamatergic stimulus local oxygen drops to a very low tension, reaching a "hypoxia like" transient status, it can be hypothesized that during this time period pH will drop sufficiently to locally promote nitrite reduction to •NO by the ascorbate hence released during the stimulation. Under these circumstances, an increase in nitrite basal levels in the extracellular space should promote an increase in •NO and in CBF via non enzymatic production of •NO. This pathway to improve NVC assumes particular relevance in situations where it is compromised (ageing, hypertension, neurodegenerative diseases). In this section we have explored that possibility by performing experiments where animals were submitted to stimulus with L-glutamate and then to L-glutamate supplemented with nitrite. We monitored •NO and CBF signals in both conditions. Results are shown in figures 6.9 and 6.10. Figure 6.9 shows the effect that nitrite has on glutamate evoked •NO signals. Total signal area increased from 45.5 ± 7.3 fmol (n=18) when glutamate was used as stimulus to 74.4 ± 6.7 fmol (n=18) when glutamate was supplemented with nitrite, representing an increase of 63.5% of the signal area ($p< 0.05$). This suggests that nitrite is potentiating •NO production, possibly via reduction by extracellular ascorbate that is also released during a glutamatergic stimulus.

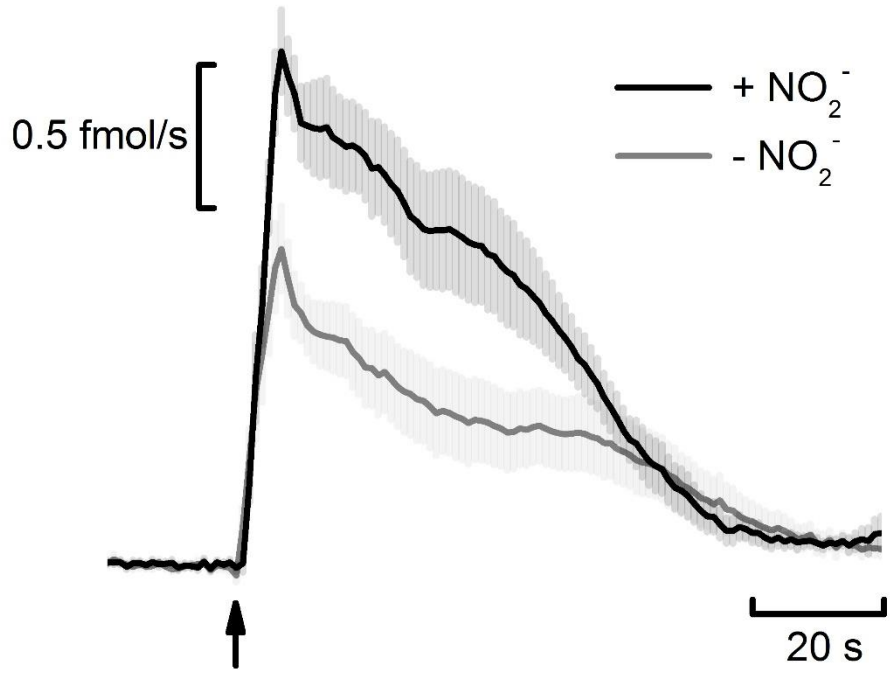

Figure 6.8. *Average amperometric recordings (n= 18) of •NO dynamics following a stimulation by local application of 20 mM L-glutamate (gray line) and 20 mM L-glutamate supplemented with 50 µM of nitrite in the rat hippocampus (black line). Stimulus were locally applied by pressure ejection at the time indicated by the arrow. Volumes ejected ranged from 12.5 to 75 nL. Experiments performed in the CA1 and DG regions of the hippocampus.*

When analyzing CBF signals obtained using the same experimental approach (Figure 6.10) it is possible to observe that, when compared to the control stimulus with L-glutamate only, the stimulus supplemented with nitrite increased the signal area from 97.2 ± 5.8 % (n=8) to 135.3 ± 14.5 % (n=8), representing an increase of 39% ($p < 0.05$). Taking these two observations together it seems that the increase in •NO signals translates to an increase in CBF signals, as expected in NVC.

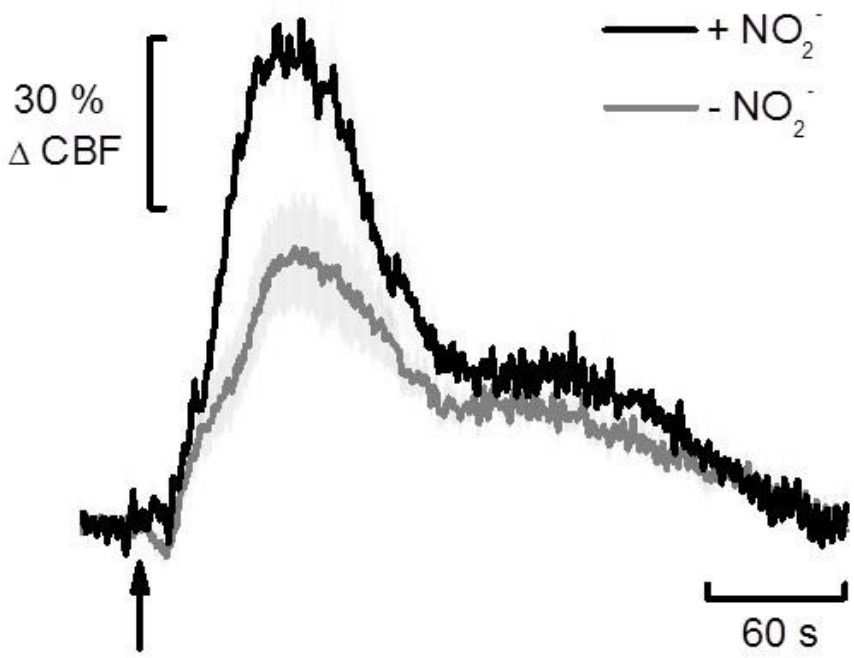

***Figure 6.9**. Average Laser Doppler recordings (n=8) of CBF dynamics following a stimulation by local application of L-glutamate (gray line) and glutamate supplemented with nitrite (black line) in the rat hippocampus. Stimulus were locally applied by pressure ejection at the time indicated by the arrow. Volumes ejected ranged from 12.5 to 75 nL. Experiments performed in the DG region of the hippocampus (AP: -3.6; ML: -2.2; DV: -3.2).*

Finally, we wanted to explore the $NO_3^- \rightarrow NO_2^- \rightarrow$ •NO pathway and evaluate if modulation of dietary nitrate can increase blood flow. For that purpose we performed one experiment where we collected glutamate evoked •NO and CBF recordings simultaneously. Then, an intraperitoneal injection of $NaNO_3$ (10 mg/kg) was given to the anesthetized rat and. thirty minutes later, new glutamate evoked •NO and CBF recordings were collected. The comparison of •NO signals before and after administration of $NaNO_3$ is shown in figure 6.11 and the same comparison for CBF signals is shown in figure 6.12. Figure 6.11 shows the effect that the increased circulating nitrate/nitrite has on glutamate evoked •NO signals. Total signal area slightly increased from 32.7 ± 1.4 fmol (n=3) before the administration of $NaNO_3$ to 33.1 ± 0.8 fmol (n=3) when glutamate was supplemented with nitrite, representing an increase of less than 2% of the signal area ($p > 0.05$). Despite the slight tendency for the signal area to increase, these results were not statistically significant.

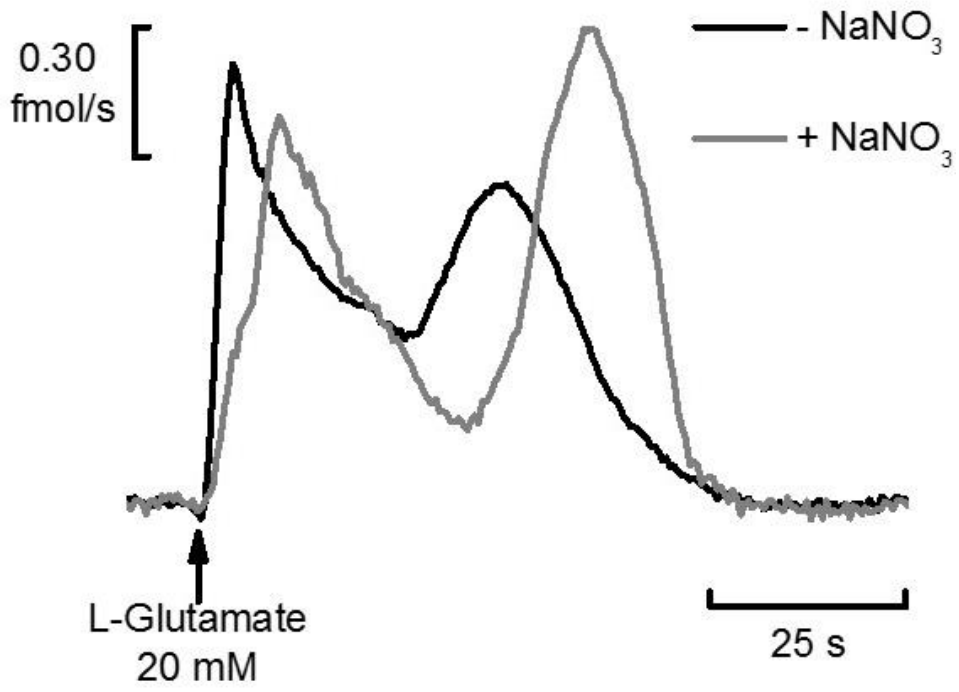

Figure 6.10. *Representative amperometric recording of glutamate evoked •NO signals before (black line) and after (gray line) an i.p administration of $NaNO_3$ (10 mg/kg). Recordings performed in the DG region of the hippocampus (AP: -4.1; ML:-3.0; DV: -3.6). L-Glutamate was applied by pressure ejection at the time indicated by the arrow. Volume ejected – 25 nL.*

When analyzing CBF signals obtained using the same experimental approach (Figure 6.12), it is possible to observe that, when compared to the signals obtained before the i.p. administration of $NaNO_3$, CBF signal area increased from 99.9 ± 28.93 (n=3) to 164.2 ± 15.1 (n=4), representing an increase of 64% ($p > 0.05$). These results show a tendency for both •NO and CBF signals to increase upon a systemic administration of $NaNO_3$ but they also lack statistical significance, due to the limited number of animals used and recordings collected (one animal, 3 and 4 recordings before and after $NaNO_3$ administration, respectively).

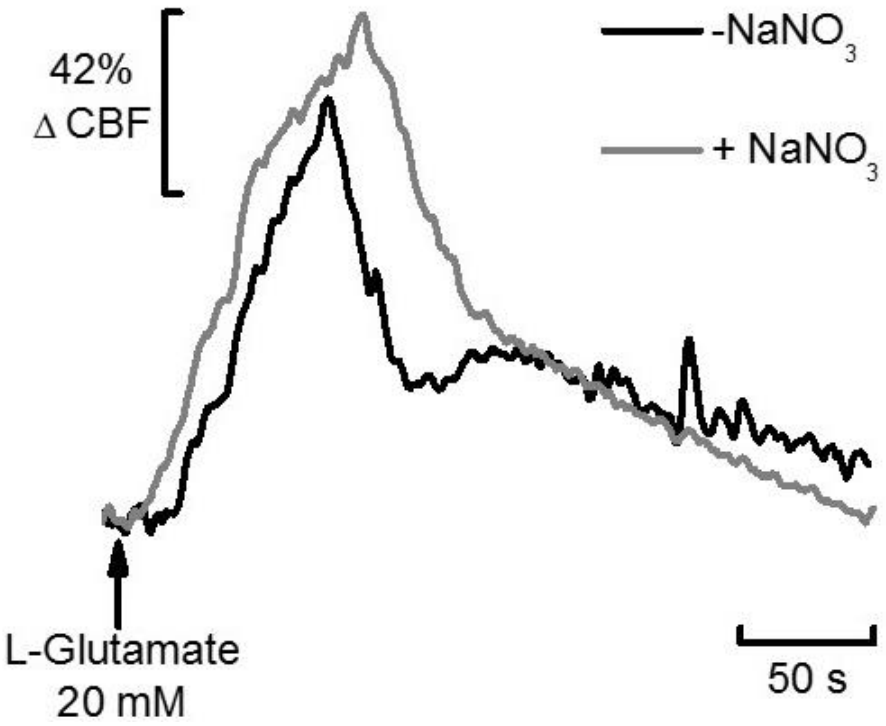

Figure 6.11. *Representative Laser Doppler recording of glutamate evoked CBF dynamics before (black line) and after (gray line) an i.p administration of $NaNO_3$ (10 mg/kg). Recordings performed in the DG region of the hippocampus (AP: -4.1; ML:-3.0; DV: -3.6). L-Glutamate was applied by pressure ejection (1s) at the time indicated by the arrow. Volume ejected – 25 nL.*

Even though more experiments are needed to confirm the observed tendency, these are promising results and they seem to indicate that the activation of the $NO_3^- \rightarrow NO_2^- \rightarrow {}^{\bullet}NO$ pathway also leads to increases of ${}^{\bullet}NO$ signal following stimulation with glutamate. This increase is followed by an increase in local cerebral blood flow. The observed coupling between the supplementation with NO_2^- and NO_3^- and the increase in ${}^{\bullet}NO$ and CBF signals suggests that the intake of food rich in NO_3^- (vegetables and fruit) may have a beneficial impact in brain perfusion, especially in ageing and other disorders that impair NVC.

6.4. Discussion

The reversible redox conversion of nitrite and •NO in a physiological setting is now widely accepted. Nitrite has long been identified as a stable intermediate of •NO oxidation but several lines of evidence support the reduction of nitrite to •NO *in vivo* (Zweier, Samouilov et al. 1999, Gago, Lundberg et al. 2007, Lundberg, Weitzberg et al. 2008, Lundberg 2009, Lundberg, Gladwin et al. 2009, Lundberg and Weitzberg 2010). In the brain, nitrite was found to have a direct effect on resting CBF in a rat model (Rifkind, Nagababu et al. 2007) and in NVC (Piknova, Kocharyan et al. 2011). In older adults high nitrate diet increased cerebral perfusion in white matter of the frontal lobe, presumably via $NO_3^- \rightarrow NO_2^- \rightarrow$ •NO conversion pathway (Presley, Morgan et al. 2011). In this chapter we have tested the hypothesis that the redox interplay between nitrite and •NO may participate in maintaining the balance between •NO production, oxygen consumption and neurovascular coupling in the brain, in a process independent of enzymatic control, involving the univalent reduction of nitrite to •NO by ascorbate, especially in conditions of where brain acidosis may occur, like in hypercapnia (Siesjo, Folbergrova et al. 1972, Rehncrona 1985). We also tested the impact of activating the $NO_3^- \rightarrow NO_2^- \rightarrow$ •NO pathway on •NO mediated processes (e.g. NVC) upon neuronal glutamatergic stimulation in a process facilitated by ascorbate and a localized and transient decrease of oxygen tension.

The technological approach we used consisted in using arrays with specific geometry that enabled performing simultaneous recordings of •NO and ascorbate (two CFMs placed very close to each other (~250 µm), coated with specific films and polarized at two distinct potentials to enhance sensitivity and selectivity for each analyte) or •NO and CBF (one Nafion/*o*-PD CFM for •NO attached to the laser doppler flow probe for CBF measurements). We used a commercial laser doppler probe with satisfactory features (notably with small size) that allow real-time measurement of CBF in brain deep structures, such as the hippocampus. The ability to perform simultaneous measurements enabled us to follow the temporal dynamics of these compounds following stimulation.

Supported by the *in vitro* findings where nitrite was reduced to •NO by ascorbate at a pH of 6.5, *in vivo* experiments performed in this chapter show that brain acidosis that occurs during hypercapnia leads to a non-enzymatic production of •NO and CBF transient increase, presumably through the reduction of nitrite to •NO by ascorbate in the extracellular space. These findings are based on the following observations:

I- Inducing brain acidosis with hypercapnia leads to transient increases in •NO and CBF signals, and the previous local ejection of NO_2^- significantly increases both;

II- The maximum peak amplitude of •NO signals, when converted into concentration, is 119 nM under a situation of acidosis, similar to what was obtained *in vitro* (118 nM) and correlates to the hypothetical concentrations that can be reached for situations *in vivo* where pH can drop to values between 4-7 (Zweier, Samouilov et al. 1999);

III- The simultaneous recordings of •NO and ascorbate point to a sequence of events whereby, following acidosis, the increase in •NO production is preceded by a transient decrease of ascorbate in extracellular space, indicating that ascorbate is consumed previously to •NO is produced;

IV- When extracellular ascorbate is depleted by the local ejection of ascorbate oxidase, •NO and CBF signals decrease remarkably.

The information collected with these dynamic measurements allowed us to monitor how two key players change during the induction of acidosis (•NO and ascorbate) and couple them to a functional measurement (CBF). Even though it was not possible to measure neither nitrite nor pH dynamics during the protocol of acidosis, it was possible to see nitrite's effect in the production of •NO and in the increase of cerebral when its concentration was locally increased. The non-enzymatic source of the recorded •NO signals was confirmed with the use of 7-NI. Results showed that the use of this inhibitor of nNOS didn't have any significant effect in •NO and CBF signals elicited with hypercapnia. It can be argued how much this nNOS independent pathway for •NO production is truly enzyme independent. It is known that NO_2^- is reduced to bioactive •NO through acidification or via reaction with a number of proteins possessing NO_2^- reductase activity, including hemeglobins (Cosby, Partovi et al. 2003, Shiva, Huang et al. 2007), molybdenum-containing enzymes (Li, Samouilov et al. 2003, Li, Kundu et al. 2009) or even cytochrome C oxidase (Wharton and Weintraub 1980, Basu, Azarova et al. 2008).

In considering the role of other enzymes, it is questionable whether cytochrome oxidase or other enzymes would be able to function at the very low pH values observed during hypercapnia. In addition, nitrite itself is readily converted to •NO at these values of pH and it has been shown elsewhere that as pH decreases, the rat of nitrite conversion to •NO increases and, in the pH range 4-7 it follows a first order kinetics in $[H^+]$ (Zweier, Samouilov et al. 1999). Therefore, one does not have to invoke the presence of any enzyme to explain the marked •NO generation which occurs. Moreover, the experiment performed *in vitro* indicates that nitrite is able to be reduced by ascorbate to •NO without the need for any enzyme and just by decreasing pH and the

maximum •NO concentration reached during the *in vitro* experiment (where nitrite and ascorbate concentrations used tried to mimic an *in vivo* situation) was identical to the maximum concentration obtained *in vivo* when the hypercapnia protocol to induce brain acidosis was performed, suggesting a similar mechanism to produce •NO in both situations.

However, one cannot completely exclude the possibility of other enzymes be catalyzing the conversion of nitrite to •NO. The existence of •NO signals after ascorbate depletion (Figure 6.7) from the extracellular space, even though they are significantly decreased suggest that other alternative pathways may also contribute to the observed •NO signals, but in a much lesser extent than the direct reduction of nitrite by ascorbate.

One puzzling finding was the fact that the simultaneous measurements of •NO and CBF showed that CBF starts to increase even before the increase in •NO signals. Considering that •NO is an important mediator in the process of NVC (Lourenco, Santos et al. 2014) the signal of •NO should precede the CBF signal and results show the opposite. It has been reported that in hypercapnia •NO may act as a permissive factor by facilitating the action of other vasodilators, whereas in the vascular response initiated by glutamatergic or cholinergic stimulation •NO is likely to be the major mediator of smooth muscle relaxation (Iadecola and Zhang 1996). This helps to explain the inverted lag phase between the onset of the two signals when we compare the temporal coupling between •NO and CBF when glutamate is used as stimulus (Lourenco, Santos et al. 2014) with the presented situation of hypercapnia. With this experimental model we may be activating other pathways that also lead to the increase in CBF (Wagerle, DeGiulio et al. 1991, Iadecola and Zhang 1994, Parfenova, Hsu et al. 1995, Faraci and Sobey 1998). In any case, results clearly show that in the acidic conditions associated with hypercapnia, •NO is produced and even increased when nitrite is added, as well as CBF. So, this experimental model may not be ideal to observe the characteristic coupling in time of NVC but we were able to see the coupling in amplitude between •NO on CBF signals, also characteristic of the NVC process.

Finally, we evaluated the impact of activating the $NO_3^- \rightarrow NO_2^- \rightarrow$ •NO pathway on •NO -mediated processes (e.g. NVC) upon neuronal glutamatergic stimulation in a process facilitated by ascorbate. These experiments revealed that an increase in extracellular nitrite, either by local application or by activation of the $NO_3^- \rightarrow NO_2^- \rightarrow$ •NO pathway through a systemic administration of NO_3^- leads to an increased production of •NO upon glutamatergic stimulation. The increased production of •NO is then translated into an increased CBF when compared to the control situation. These findings support the concept that dietary intake of NO_3^- has a beneficial impact on the improvement of cerebral perfusion, especially in situations where the process of NVC may

be compromised, as observed in ageing, ischemic events or hypertension (Iadecola and Davisson 2008, Presley, Morgan et al. 2011). The last section of the chapter regarding the systemic administration of NO_3^- is preliminary data and lacks robustness in terms of results and more experiments are needed to achieve statistical significance. However, experiments where nitrite was locally applied concomitantly the stimulus with glutamate clearly show the increase in both •NO and CBF signals when compared to the control situation. In fact, a role for nitrite in neurovascular coupling has been previously proposed (Piknova, Kocharyan et al. 2011) but they failed to give the direct measures of •NO that we show in this chapter and support the proposed mechanism by which nitrite can serve as an additional source of •NO to sustain the hemodynamic response to functional brain stimulation.

Whatever the exact mechanism, NO_2^- reduction represents a physiological mechanism by which •NO production is sustained in hypoxic conditions, during which catalytic •NO generation by NOS, which relies on oxygen as a substrate, is compromised and the improvement of these studies can ultimately lead to the development of new or alternative therapeutic approaches to improve the observed impairment in NVC observed in several diseases (Alzheimer, Parkinson, hypertension, stroke) and in ageing.

6.5. Conclusions

In conclusion, neurotransmission alters blood flow through several processes working in concert. Synaptic activity triggers neurons and astrocytes to release vasoactive mediators. These mediators act on local blood vessels to produce vasodilation of arterioles, and perhaps capillaries, at the site of activation. When oxygen and nutrients required supply for a harmonious function of the neurovascular unit is compromised, alternative pathways to maintain a proper blood flow arise. In this chapter we showed that in situations where oxygen supply is diminished and brain pH decreases (hypercapnia) nitrite is reduced to •NO by ascorbate in the extracellular space and supports the process of NVC. This conclusion is supported by the observed transient increases in •NO and CBF signals in a situation of brain acidosis induced with hypercapnia, and by the confirmation that a previous local ejection of NO_2^- significantly increases both signals. The important role of ascorbate in this process was highlighted by the simultaneous recordings of •NO and ascorbate that strongly suggest the latter is consumed previously to •NO production; moreover, when extracellular ascorbate is depleted by locally ejecting ascorbate oxidase, •NO and CBF signals decrease remarkably. The absence of changes in the recorded •NO and CBF signals after the injection of an inhibitor of nNOS like 7-NI excluded the involvement of the enzyme in the observed •NO production, further supporting this idea.

Finally, we collected evidence (even though additional experiments are needed to obtain more robust results) that the activation of the $NO_3^- \rightarrow NO_2^- \rightarrow$ •NO pathway has a beneficial impact in cerebral perfusion, through this non-enzymatic production of •NO with the correspondent coupling to cerebral blood flow.

Thus, it seems clear that NO_2^- reduction by ascorbate represents a physiological mechanism by which •NO production is sustained in hypoxic/acidic conditions, during which catalytic •NO generation by NOS, which relies on oxygen as a substrate, is compromised. Ultimately, this line of investigation gives an important insight to help in the development of new or alternative therapeutic approaches to improve the observed impairment in NVC observed in several disorders (aging, neurodegenerative diseases, hypertension, diabetes).

7. Final conclusions

The work presented in this document is based in the development and implementation of methodological approaches encompassing the use of a laser doppler flow probe and microelectrodes based on carbon fibers and ceramic based platinum microelectrode arrays coupled to electrochemical techniques for studying the dynamic interplay between ascorbate, glutamate and NO, three substances with high relevance in neurotransmission and signaling in the brain and their impact in regulation of cerebral blood flow.

Taking into account the data that was collected and analyzed throughout this thesis, the following conclusions can be summarized:

I. By using CFMs and a novel nanocomposite film based on the CNTs and Nafion we have developed a novel ascorbate microsensor that fulfils the criteria of size, speed, selectivity and sensitivity required for directly probing *in vivo* the temporal and spatial dynamics of brain ascorbate.
II. When combined with amperometry the modified microsensors allow not only the measurement of basal extracellular ascorbate in the rat hippocampus but also the real-time changes following stimulation with glutamate with high selectivity, sensitivity and spatio-temporal resolution.
III. The MEA glutamate biosensor arrays used showed good recording characteristics (sensitivity, L.O.D, response time, Km and Vmax) for glutamate measurements and the use of *m*-PD as an exclusion layer greatly enhanced selectivity against major interferents such as ascorbate and dopamine.
IV. The self-referencing technique allowed the subtraction of the background current at sentinel sites without the glutamate oxidase enzyme and cross-check the selectivity of the sensors on a second-by-second time scale and increased the signal to noise ratio, improving sensitivity and L.O.D.
V. The observed potassium-evoked glutamate release and uptake was robust, transient, and highly reproducible.
VI. Combining the use of the MEAs and Nafion/SWCNT CFMs allowed performing simultaneous measurements of glutamate and ascorbate in the rat hippocampus in real time and observe the dynamic interaction of these molecules in the rat hippocampus.
VII. This approach emerges as a very powerful tool for the study of the dynamic interplay between these two molecules and how it may be altered in the case of neurodegenerative diseases such as Huntington's or Alzheimer's disease.

VIII. We demonstrated the existence of a coupling through which •NO produced upon glutamatergic stimulation triggers the release of ascorbate to the extracellular space.

IX. In situations where oxygen supply is diminished and brain pH decreases (hypercapnia) nitrite is reduced to •NO by ascorbate in the extracellular space and supports the process of NVC.

X. The activation of the $NO_3^- \rightarrow NO_2^- \rightarrow$ •NO pathway has a beneficial impact in cerebral perfusion, through this non-enzymatic production of •NO with the correspondent coupling to cerebral blood flow.

8. BIBLIOGRAPHY

(1993). "A novel gene containing a trinucleotide repeat that is expanded and unstable on Huntington's disease chromosomes. The Huntington's Disease Collaborative Research Group." Cell **72**(6): 971-983.

Adams, R. N. (1990). "In vivo electrochemical measurements in the CNS." Prog Neurobiol **35**(4): 297-311.

Agui, L., P. Yanez-Sedeno and J. M. Pingarron (2008). "Role of carbon nanotubes in electroanalytical chemistry: a review." Anal Chim Acta **622**(1-2): 11-47.

Akyilmaz, E. and E. Dinckaya (1999). "A new enzyme electrode based on ascorbate oxidase immobilized in gelatin for specific determination of l-ascorbic acid." Talanta **50**(1): 87-93.

Alderton, W. K., C. E. Cooper and R. G. Knowles (2001). "Nitric oxide synthases: structure, function and inhibition." Biochem J **357**(Pt 3): 593-615.

Andersen, P., Morris, R., Amaral, D., Bliss, T. & O‟Keefe, J. (2007). The hippocampus book, Oxford University Press, Inc., New York.

Atlante, A., S. Gagliardi, G. M. Minervini, M. T. Ciotti, E. Marra and P. Calissano (1997). "Glutamate neurotoxicity in rat cerebellar granule cells: a major role for xanthine oxidase in oxygen radical formation." J Neurochem **68**(5): 2038-2045.

Attwell, D., A. M. Buchan, S. Charpak, M. Lauritzen, B. A. Macvicar and E. A. Newman (2010). "Glial and neuronal control of brain blood flow." Nature **468**(7321): 232-243.

Attwell, D. and C. Iadecola (2002). "The neural basis of functional brain imaging signals." Trends Neurosci **25**(12): 621-625.

Babbedge, R. C., P. A. Bland-Ward, S. L. Hart and P. K. Moore (1993). "Inhibition of rat cerebellar nitric oxide synthase by 7-nitro indazole and related substituted indazoles." Br J Pharmacol **110**(1): 225-228.

Banhegyi, G., L. Braun, M. Csala, F. Puskas and J. Mandl (1997). "Ascorbate metabolism and its regulation in animals." Free Radic Biol Med **23**(5): 793-803.

Barbosa, R. M., A. J. L. Jesus, R. M. Santos, C. L. Pereira, C. F. Marques, B. S. Rocha, N. R. Ferreira, A. Ledo and J. Laranjinha (2011). "Preparation, standardization and measurement of nitric oxide solutions." GLOBAL JOURNAL OF ANALYTICAL CHEMISTRY **2**(6): 13.

Barbosa, R. M., C. F. Lourenco, R. M. Santos, F. Pomerleau, P. Huettl, G. A. Gerhardt and J. Laranjinha (2008). "In vivo real-time measurement of nitric oxide in anesthetized rat brain." Methods Enzymol **441**: 351-367.

Basse-Tomusk, A. and G. V. Rebec (1990). "Corticostriatal and thalamic regulation of amphetamine-induced ascorbate release in the neostriatum." Pharmacol Biochem Behav **35**(1): 55-60.

Basse-Tomusk, A. and G. V. Rebec (1991). "Regional distribution of ascorbate and 3,4-dihydroxyphenylacetic acid (DOPAC) in rat striatum." Brain Res **538**(1): 29-35.

Basu, S., N. A. Azarova, M. D. Font, S. B. King, N. Hogg, M. T. Gladwin, S. Shiva and D. B. Kim-Shapiro (2008). "Nitrite reductase activity of cytochrome c." J Biol Chem **283**(47): 32590-32597.

Bedioui, F., D. Quinton, S. Griveau and T. Nyokong (2010). "Designing molecular materials and strategies for the electrochemical detection of nitric oxide, superoxide and peroxynitrite in biological systems." Phys Chem Chem Phys **12**(34): 9976-9988.

Benjamin, N., F. O'Driscoll, H. Dougall, C. Duncan, L. Smith, M. Golden and H. McKenzie (1994). "Stomach NO synthesis." Nature **368**(6471): 502.

Berger, U. V., X. C. Lu, W. Liu, Z. Tang, B. S. Slusher and M. A. Hediger (2003). "Effect of middle cerebral artery occlusion on mRNA expression for the sodium-coupled vitamin C transporter SVCT2 in rat brain." J Neurochem **86**(4): 896-906.

Bernath, S. (1992). "Calcium-independent release of amino acid neurotransmitters: fact or artifact?" Prog Neurobiol **38**(1): 57-91.

Bigelow, J. C., D. S. Brown and R. M. Wightman (1984). "Gamma-aminobutyric acid stimulates the release of endogenous ascorbic acid from rat striatal tissue." J Neurochem **42**(2): 412-419.

Blanke, M. L. and A. M. J. VanDongen (2009). Activation Mechanisms of the NMDA Receptor. Biology of the NMDA Receptor. A. M. Van Dongen. Boca Raton (FL).

Bode, A. M., L. Cunningham and R. C. Rose (1990). "Spontaneous decay of oxidized ascorbic acid (dehydro-L-ascorbic acid) evaluated by high-pressure liquid chromatography." Clin Chem **36**(10): 1807-1809.

Bon, C. L. and J. Garthwaite (2003). "On the role of nitric oxide in hippocampal long-term potentiation." J Neurosci **23**(5): 1941-1948.

Bowman, G. L. (2012). "Ascorbic acid, cognitive function, and Alzheimer's disease: a current review and future direction." Biofactors **38**(2): 114-122.

Brahma, B., R. E. Forman, E. E. Stewart, C. Nicholson and M. E. Rice (2000). "Ascorbate inhibits edema in brain slices." J Neurochem **74**(3): 1263-1270.

Brenman, J. E., D. S. Chao, S. H. Gee, A. W. McGee, S. E. Craven, D. R. Santillano, Z. Wu, F. Huang, H. Xia, M. F. Peters, S. C. Froehner and D. S. Bredt (1996). "Interaction of nitric oxide synthase with the postsynaptic density protein PSD-95 and alpha1-syntrophin mediated by PDZ domains." Cell **84**(5): 757-767.

Brown, F. O. and J. P. Lowry (2003). "Microelectrochemical sensors for in vivo brain analysis: an investigation of procedures for modifying Pt electrodes using Nafion." Analyst **128**(6): 700-705.

Brunet, A., A. Pailleret, M. A. Devynck, J. Devynck and F. Bedioui (2003). "Electrochemical sensing of nitric oxide for biological systems: methodological approach and new insights in examining interfering compounds." Talanta **61**(1): 53-59.

Buda, M., F. Gonon, R. Cespuglio, M. Jouvet and J. F. Pujol (1980). "[In vivo voltametric measurement of ascorbic acid and DOPAC in the striatum of the rat and guinea-pig]." C R Seances Acad Sci D **290**(5): 431-434.

Buerk, D. G., B. M. Ances, J. H. Greenberg and J. A. Detre (2003). "Temporal dynamics of brain tissue nitric oxide during functional forepaw stimulation in rats." Neuroimage **18**(1): 1-9.

Buettner, G. R. (1988). "In the absence of catalytic metals ascorbate does not autoxidize at pH 7: ascorbate as a test for catalytic metals." J Biochem Biophys Methods **16**(1): 27-40.

Buettner, G. R. (1990). "Ascorbate oxidation: UV absorbance of ascorbate and ESR spectroscopy of the ascorbyl radical as assays for iron." Free Radic Res Commun **10**(1-2): 5-9.

Buettner, G. R. (1993). "The pecking order of free radicals and antioxidants: lipid peroxidation, alpha-tocopherol, and ascorbate." Arch Biochem Biophys **300**(2): 535-543.

Buettner, G. R. and B. A. Jurkiewicz (1993). "Ascorbate free radical as a marker of oxidative stress: an EPR study." Free Radic Biol Med **14**(1): 49-55.

Buettner, G. R. and B. A. Jurkiewicz (1996). "Catalytic metals, ascorbate and free radicals: combinations to avoid." Radiat Res **145**(5): 532-541.

Burette, A., U. Zabel, R. J. Weinberg, H. H. Schmidt and J. G. Valtschanoff (2002). "Synaptic localization of nitric oxide synthase and soluble guanylyl cyclase in the hippocampus." J Neurosci **22**(20): 8961-8970.

Burgess, N., E. A. Maguire and J. O'Keefe (2002). "The human hippocampus and spatial and episodic memory." Neuron **35**(4): 625-641.

Burmeister, J. J., T. D. Coates and G. A. Gerhardt (2004). "Multisite microelectrode arrays for measurements of multiple neurochemicals." Conf Proc IEEE Eng Med Biol Soc **7**: 5348-5351.

Burmeister, J. J., V. A. Davis, J. E. Quintero, F. Pomerleau, P. Huettl and G. A. Gerhardt (2013). "Glutaraldehyde cross-linked glutamate oxidase coated microelectrode arrays: selectivity and resting levels of glutamate in the CNS." ACS Chem Neurosci **4**(5): 721-728.

Burmeister, J. J. and G. A. Gerhardt (2001). "Self-referencing ceramic-based multisite microelectrodes for the detection and elimination of interferences from the measurement of L-glutamate and other analytes." Anal Chem **73**(5): 1037-1042.

Burmeister, J. J., K. Moxon and G. A. Gerhardt (2000). "Ceramic-based multisite microelectrodes for electrochemical recordings." Anal Chem **72**(1): 187-192.

Burmeister, J. J., M. Palmer and G. A. Gerhardt (2005). "L-lactate measures in brain tissue with ceramic-based multisite microelectrodes." Biosens Bioelectron **20**(9): 1772-1779.

Burmeister, J. J., F. Pomerleau, M. Palmer, B. K. Day, P. Huettl and G. A. Gerhardt (2002). "Improved ceramic-based multisite microelectrode for rapid measurements of L-glutamate in the CNS." J Neurosci Methods **119**(2): 163-171.

Bush, M. A. and G. M. Pollack (2001). "Pharmacokinetics and pharmacodynamics of 7-nitroindazole, a selective nitric oxide synthase inhibitor, in the rat hippocampus." Pharm Res **18**(11): 1607-1612.

C.F. Lourenço, N. R. F., R.M. Santos, N. Lukacova, R.M. Barbosa, J. Laranjinha (2014). "The pattern of glutamate-induced nitric oxide dynamics in vivo and its correlation with nNOS expression in rat hippocampus, cerebral cortex and striatum " Brain Research.

Cammack, J., B. Ghasemzadeh and R. N. Adams (1991). "The pharmacological profile of glutamate-evoked ascorbic acid efflux measured by in vivo electrochemistry." Brain Res **565**(1): 17-22.

Cammack, J., B. Ghasemzadeh and R. N. Adams (1992). "Electrochemical monitoring of brain ascorbic acid changes associated with hypoxia, spreading depression, and seizure activity." Neurochem Res **17**(1): 23-27.

Carlsson, S., N. P. Wiklund, L. Engstrand, E. Weitzberg and J. O. Lundberg (2001). "Effects of pH, nitrite, and ascorbic acid on nonenzymatic nitric oxide generation and bacterial growth in urine." Nitric Oxide **5**(6): 580-586.

Castro, M. A., C. Angulo, S. Brauchi, F. Nualart and Concha, II (2008). "Ascorbic acid participates in a general mechanism for concerted glucose transport inhibition and lactate transport stimulation." Pflugers Arch **457**(2): 519-528.

Castro, M. A., F. A. Beltran, S. Brauchi and Concha, II (2009). "A metabolic switch in brain: glucose and lactate metabolism modulation by ascorbic acid." J Neurochem **110**(2): 423-440.

Castro, M. A., M. Pozo, C. Cortes, L. Garcia Mde, Concha, II and F. Nualart (2007). "Intracellular ascorbic acid inhibits transport of glucose by neurons, but not by astrocytes." J Neurochem **102**(3): 773-782.

Chan, P. H. and L. Chu (1990). "Mechanisms underlying glutamate-induced swelling of astrocytes in primary culture." Acta Neurochir Suppl (Wien) **51**: 7-10.

Choi, D. W. (1988). "Glutamate neurotoxicity and diseases of the nervous system." Neuron **1**(8): 623-634.

Choi, D. W., H. Monyer, R. G. Giffard, M. P. Goldberg and C. W. Christine (1990). "Acute brain injury, NMDA receptors, and hydrogen ions: observations in cortical cell cultures." Adv Exp Med Biol **268**: 501-504.

Ciani, E., L. Groneng, M. Voltattorni, V. Rolseth, A. Contestabile and R. E. Paulsen (1996). "Inhibition of free radical production or free radical scavenging protects from the excitotoxic cell death mediated by glutamate in cultures of cerebellar granule neurons." Brain Res **728**(1): 1-6.

Ciszewski, A. and G. Milczarek (2003). "Electrochemical detection of nitric oxide using polymer modified electrodes." Talanta **61**(1): 11-26.

Clapp-Lilly, K. L., R. C. Roberts, L. K. Duffy, K. P. Irons, Y. Hu and K. L. Drew (1999). "An ultrastructural analysis of tissue surrounding a microdialysis probe." J Neurosci Methods **90**(2): 129-142.

Coassin, M., A. Tomasi, V. Vannini and F. Ursini (1991). "Enzymatic recycling of oxidized ascorbate in pig heart: one-electron *vs* two-electron pathway." Arch Biochem Biophys **290**(2): 458-462.

Contestabile, A., B. Monti, A. Contestabile and E. Ciani (2003). "Brain nitric oxide and its dual role in neurodegeneration/neuroprotection: understanding molecular mechanisms to devise drug approaches." Curr Med Chem **10**(20): 2147-2174.

Cooper, C. E. (1999). "Nitric oxide and iron proteins." Biochim Biophys Acta **1411**(2-3): 290-309.

Cooper, C. E. and C. Giulivi (2007). "Nitric oxide regulation of mitochondrial oxygen consumption II: Molecular mechanism and tissue physiology." Am J Physiol Cell Physiol **292**(6): C1993-2003.

Corti, A., A. F. Casini and A. Pompella (2010). "Cellular pathways for transport and efflux of ascorbate and dehydroascorbate." Arch Biochem Biophys **500**(2): 107-115.

Cosby, K., K. S. Partovi, J. H. Crawford, R. P. Patel, C. D. Reiter, S. Martyr, B. K. Yang, M. A. Waclawiw, G. Zalos, X. Xu, K. T. Huang, H. Shields, D. B. Kim-Shapiro, A. N. Schechter, R. O. Cannon, 3rd and M. T. Gladwin (2003). "Nitrite reduction to nitric oxide by deoxyhemoglobin vasodilates the human circulation." Nat Med **9**(12): 1498-1505.

Coyle, J. T. and P. Puttfarcken (1993). "Oxidative stress, glutamate, and neurodegenerative disorders." Science **262**(5134): 689-695.

Crespi, F. and C. Mobius (1992). "In vivo selective monitoring of basal levels of cerebral dopamine using voltammetry with Nafion modified (NA-CRO) carbon fibre micro-electrodes." J Neurosci Methods **42**(3): 149-161.

Crespi, F. and Z. L. Rossetti (2004). "Pulse of nitric oxide release in response to activation of N-methyl-D-aspartate receptors in the rat striatum: rapid desensitization, inhibition by receptor antagonists, and potentiation by glycine." J Pharmacol Exp Ther **309**(2): 462-468.

Danbolt, N. C. (2001). "Glutamate uptake." Prog Neurobiol **65**(1): 1-105.

Dawson, V. L. and T. M. Dawson (1998). "Nitric oxide in neurodegeneration." Prog Brain Res **118**: 215-229.

Day, B. K., F. Pomerleau, J. J. Burmeister, P. Huettl and G. A. Gerhardt (2006). "Microelectrode array studies of basal and potassium-evoked release of L-glutamate in the anesthetized rat brain." J Neurochem **96**(6): 1626-1635.

de Angelis, L. and C. Furlan (1995). "The effects of ascorbic acid and oxiracetam on scopolamine-induced amnesia in a habituation test in aged mice." Neurobiol Learn Mem **64**(2): 119-124.

del Zoppo, G. J. and T. Mabuchi (2003). "Cerebral microvessel responses to focal ischemia." J Cereb Blood Flow Metab **23**(8): 879-894.

Demestre, M., M. Boutelle and M. Fillenz (1997). "Stimulated release of lactate in freely moving rats is dependent on the uptake of glutamate." J Physiol **499 (Pt 3)**: 825-832.

Diliberto, E. J., Jr. and P. L. Allen (1980). "Semidehydroascorbate as a product of the enzymic conversion of dopamine to norepinephrine. Coupling of semidehydroascorbate reductase to dopamine-beta-hydroxylase." Mol Pharmacol **17**(3): 421-426.

Diliberto, E. J., Jr. and P. L. Allen (1981). "Mechanism of dopamine-beta-hydroxylation. Semidehydroascorbate as the enzyme oxidation product of ascorbate." J Biol Chem **256**(7): 3385-3393.

Dirnagl, U., U. Lindauer and A. Villringer (1993). "Role of nitric oxide in the coupling of cerebral blood flow to neuronal activation in rats." Neurosci Lett **149**(1): 43-46.

Dixon, B. M., J. P. Lowry and R. D. O'Neill (2002). "Characterization in vitro and in vivo of the oxygen dependence of an enzyme/polymer biosensor for monitoring brain glucose." J Neurosci Methods **119**(2): 135-142.

Douglas A. Skoog, D. M. W., F. James Holler, Stanley R. Crouch (2014). Fundamentals of Analytical Chemistry, Mary Finch.

Drake, C. T. and C. Iadecola (2007). "The role of neuronal signaling in controlling cerebral blood flow." Brain Lang **102**(2): 141-152.

Du, J., J. J. Cullen and G. R. Buettner (2012). "Ascorbic acid: Chemistry, biology and the treatment of cancer." Biochim Biophys Acta.

Duncan, C., H. Dougall, P. Johnston, S. Green, R. Brogan, C. Leifert, L. Smith, M. Golden and N. Benjamin (1995). "Chemical generation of nitric oxide in the mouth from the enterosalivary circulation of dietary nitrate." Nat Med **1**(6): 546-551.

Dykens, J. A., A. Stern and E. Trenkner (1987). "Mechanism of kainate toxicity to cerebellar neurons in vitro is analogous to reperfusion tissue injury." J Neurochem **49**(4): 1222-1228.

Ebadi, M. and S. K. Sharma (2003). "Peroxynitrite and mitochondrial dysfunction in the pathogenesis of Parkinson's disease." Antioxid Redox Signal **5**(3): 319-335.

Ellershaw, D. C., I. A. Greenwood and W. A. Large (2000). "Dual modulation of swelling-activated chloride current by NO and NO donors in rabbit portal vein myocytes." J Physiol **528 Pt 1**: 15-24.

Faraci, F. M. and K. R. Breese (1993). "Nitric oxide mediates vasodilatation in response to activation of N-methyl-D-aspartate receptors in brain." Circ Res **72**(2): 476-480.

Faraci, F. M. and C. G. Sobey (1998). "Role of potassium channels in regulation of cerebral vascular tone." J Cereb Blood Flow Metab **18**(10): 1047-1063.

Fergus, A. and K. S. Lee (1997). "Regulation of cerebral microvessels by glutamatergic mechanisms." Brain Res **754**(1-2): 35-45.

Ferreira, N. R. (2006). Detecção electroquímica de óxido nítrico em fatias de hipocampo de rato com microeléctrodos de fibra de carbono. Master in Sciences, University of Coimbra.

Ferreira, N. R., R. M. Santos, J. Laranjinha and R. M. Barbosa (2013). "Real Time In Vivo Measurement of Ascorbate in the Brain Using Carbon Nanotube-Modified Microelectrodes." Electroanalysis **25**(7): 1757-1763.

Ferris, D. C., J. Kume-Kick, I. Russo-Menna and M. E. Rice (1995). "Gender differences in cerebral ascorbate levels and ascorbate loss in ischemia." Neuroreport **6**(11): 1485-1489.

Fillenbaum, G. G., M. N. Kuchibhatla, J. T. Hanlon, M. B. Artz, C. F. Pieper, K. E. Schmader, M. W. Dysken and S. L. Gray (2005). "Dementia and Alzheimer's disease in community-dwelling elders taking vitamin C and/or vitamin E." Ann Pharmacother **39**(12): 2009-2014.

Fonnum, F. (1984). "Glutamate: a neurotransmitter in mammalian brain." J Neurochem **42**(1): 1-11.

Fowler, J. C. (1993). "Glucose deprivation results in a lactate preventable increase in adenosine and depression of synaptic transmission in rat hippocampal slices." J Neurochem **60**(2): 572-576.

Friedemann, M. N., S. W. Robinson and G. A. Gerhardt (1996). "o-Phenylenediamine-modified carbon fiber electrodes for the detection of nitric oxide." Anal Chem **68**(15): 2621-2628.

Gago, B., J. O. Lundberg, R. M. Barbosa and J. Laranjinha (2007). "Red wine-dependent reduction of nitrite to nitric oxide in the stomach." Free Radic Biol Med **43**(9): 1233-1242.

Garthwaite, J. (2008). "Concepts of neural nitric oxide-mediated transmission." Eur J Neurosci **27**(11): 2783-2802.

Garthwaite, J. and C. L. Boulton (1995). "Nitric oxide signaling in the central nervous system." Annu Rev Physiol **57**: 683-706.

Garthwaite, J., S. L. Charles and R. Chess-Williams (1988). "Endothelium-derived relaxing factor release on activation of NMDA receptors suggests role as intercellular messenger in the brain." Nature **336**(6197): 385-388.

Gerhardt, G. A. and A. F. Hoffman (2001). "Effects of recording media composition on the responses of Nafion-coated carbon fiber microelectrodes measured using high-speed chronoamperometry." J Neurosci Methods **109**(1): 13-21.

Gerhardt, G. A., A. F. Oke, G. Nagy, B. Moghaddam and R. N. Adams (1984). "Nafion-coated electrodes with high selectivity for CNS electrochemistry." Brain Res **290**(2): 390-395.

Ghasemzadeh, B., J. Cammack and R. N. Adams (1991). "Dynamic changes in extracellular fluid ascorbic acid monitored by in vivo electrochemistry." Brain Res **547**(1): 162-166.

Gijsbertsen, A., W. Siu, M. F. Kling, P. Johnsson, P. Jansen, S. Stolte and M. J. Vrakking (2007). "Direct determination of the sign of the NO dipole moment." Phys Rev Lett **99**(21): 213003.

Giraldez, R. R., A. Panda, Y. Xia, S. P. Sanders and J. L. Zweier (1997). "Decreased nitric-oxide synthase activity causes impaired endothelium-dependent relaxation in the postischemic heart." J Biol Chem **272**(34): 21420-21426.

Girouard, H. and C. Iadecola (2006). "Neurovascular coupling in the normal brain and in hypertension, stroke, and Alzheimer disease." J Appl Physiol (1985) **100**(1): 328-335.

Gonon, F., M. Buda, R. Cespuglio, M. Jouvet and J. F. Pujol (1980). "In vivo electrochemical detection of catechols in the neostriatum of anaesthetized rats: dopamine or DOPAC?" Nature **286**(5776): 902-904.

Gordon, G. R., S. J. Mulligan and B. A. MacVicar (2007). "Astrocyte control of the cerebrovasculature." Glia **55**(12): 1214-1221.

Greenberg, J. H., N. W. Sohn and P. J. Hand (1999). "Nitric oxide and the cerebral-blood-flow response to somatosensory activation following deafferentation." Exp Brain Res **129**(4): 541-550.

Griffith, O. W. and D. J. Stuehr (1995). "Nitric oxide synthases: properties and catalytic mechanism." Annu Rev Physiol **57**: 707-736.

Grunewald, R. A. (1993). "Ascorbic acid in the brain." Brain Res Brain Res Rev **18**(1): 123-133.

Grunewald, R. A. and M. Fillenz (1984). "Release of ascorbate from a synaptosomal fraction of rat brain." Neurochem Int **6**(4): 491-500.

Grunewald, R. A., R. D. O'Neill, M. Fillenz and W. J. Albery (1983). "The origin of circadian and amphetamine-induced changes in the extracellular concentration of brain ascorbate." Neurochem Int **5**(6): 773-778.

Guix, F. X., I. Uribesalgo, M. Coma and F. J. Munoz (2005). "The physiology and pathophysiology of nitric oxide in the brain." Prog Neurobiol **76**(2): 126-152.

Hall, C. N. and J. Garthwaite (2009). "What is the real physiological NO concentration in vivo?" Nitric Oxide **21**(2): 92-103.

Han, D. X., T. T. Han, C. S. Shan, A. Ivaska and L. Niu (2010). "Simultaneous Determination of Ascorbic Acid, Dopamine and Uric Acid with Chitosan-Graphene Modified Electrode." Electroanalysis **22**(17-18): 2001-2008.

Harrison, F. E., G. L. Bowman and M. C. Polidori (2014). "Ascorbic acid and the brain: rationale for the use against cognitive decline." Nutrients **6**(4): 1752-1781.

Harrison, F. E., A. H. Hosseini, S. M. Dawes, S. Weaver and J. M. May (2009). "Ascorbic acid attenuates scopolamine-induced spatial learning deficits in the water maze." Behav Brain Res **205**(2): 550-558.

Harrison, F. E. and J. M. May (2009). "Vitamin C function in the brain: vital role of the ascorbate transporter SVCT2." Free Radic Biol Med **46**(6): 719-730.

Harrison, F. E., S. S. Yu, K. L. Van Den Bossche, L. Li, J. M. May and M. P. McDonald (2008). "Elevated oxidative stress and sensorimotor deficits but normal cognition in mice that cannot synthesize ascorbic acid." J Neurochem **106**(3): 1198-1208.

Hascup, E. R., S. af Bjerken, K. N. Hascup, F. Pomerleau, P. Huettl, I. Stromberg and G. A. Gerhardt (2009). "Histological studies of the effects of chronic implantation of ceramic-based microelectrode arrays and microdialysis probes in rat prefrontal cortex." Brain Res **1291**: 12-20.

Hascup, K. N., E. R. Hascup, M. L. Stephens, P. E. Glaser, T. Yoshitake, A. A. Mathe, G. A. Gerhardt and J. Kehr (2011). "Resting glutamate levels and rapid glutamate transients in the prefrontal cortex of the Flinders Sensitive Line rat: a genetic rodent model of depression." Neuropsychopharmacology **36**(8): 1769-1777.

Hascup, K. N., E. C. Rutherford, J. E. Quintero, B. K. Day, J. R. Nickell, F. Pomerleau, P. Huettl, J. J. Burmeister and G. A. Gerhardt (2007). Second-by-Second Measures of L-Glutamate and Other Neurotransmitters Using Enzyme-Based Microelectrode Arrays. Electrochemical Methods for Neuroscience. A. C. Michael and L. M. Borland. Boca Raton (FL).

Headley, P. M. and S. Grillner (1990). "Excitatory amino acids and synaptic transmission: the evidence for a physiological function." Trends Pharmacol Sci **11**(5): 205-211.

Heller, R., A. Unbehaun, B. Schellenberg, B. Mayer, G. Werner-Felmayer and E. R. Werner (2001). "L-ascorbic acid potentiates endothelial nitric oxide synthesis via a chemical stabilization of tetrahydrobiopterin." J Biol Chem **276**(1): 40-47.

Hill, B. G., B. P. Dranka, S. M. Bailey, J. R. Lancaster, Jr. and V. M. Darley-Usmar (2010). "What part of NO don't you understand? Some answers to the cardinal questions in nitric oxide biology." J Biol Chem **285**(26): 19699-19704.

Hinzman, J. M., T. C. Thomas, J. J. Burmeister, J. E. Quintero, P. Huettl, F. Pomerleau, G. A. Gerhardt and J. Lifshitz (2010). "Diffuse brain injury elevates tonic glutamate levels and potassium-evoked glutamate release in discrete brain regions at two days post-injury: an enzyme-based microelectrode array study." J Neurotrauma **27**(5): 889-899.

Hocevar, S. B., J. Wang, R. P. Deo, M. Musameh and B. Ogorevc (2005). "Carbon nanotube modified microelectrode for enhanced voltammetric detection of dopamine in the presence of ascorbate." Electroanalysis **17**(5-6): 417-422.

Hoffman, A. F. and G. A. Gerhardt (1999). "Differences in pharmacological properties of dopamine release between the substantia nigra and striatum: an in vivo electrochemical study." J Pharmacol Exp Ther **289**(1): 455-463.

Hu, Y., K. M. Mitchell, F. N. Albahadily, E. K. Michaelis and G. S. Wilson (1994). "Direct measurement of glutamate release in the brain using a dual enzyme-based electrochemical sensor." Brain Res **659**(1-2): 117-125.

Huang, A., J. A. Vita, R. C. Venema and J. F. Keaney, Jr. (2000). "Ascorbic acid enhances endothelial nitric-oxide synthase activity by increasing intracellular tetrahydrobiopterin." J Biol Chem **275**(23): 17399-17406.

Huang, J. and J. M. May (2006). "Ascorbic acid protects SH-SY5Y neuroblastoma cells from apoptosis and death induced by beta-amyloid." Brain Res **1097**(1): 52-58.

Huffman, M. L. and B. J. Venton (2009). "Carbon-fiber microelectrodes for in vivo applications." Analyst **134**(1): 18-24.

Iadecola, C. (1993). "Regulation of the cerebral microcirculation during neural activity: is nitric oxide the missing link?" Trends Neurosci **16**(6): 206-214.

Iadecola, C. (2004). "Neurovascular regulation in the normal brain and in Alzheimer's disease." Nat Rev Neurosci **5**(5): 347-360.

Iadecola, C. and R. L. Davisson (2008). "Hypertension and cerebrovascular dysfunction." Cell Metab **7**(6): 476-484.

Iadecola, C. and F. Zhang (1994). "Nitric oxide-dependent and -independent components of cerebrovasodilation elicited by hypercapnia." Am J Physiol **266**(2 Pt 2): R546-552.

Iadecola, C. and F. Zhang (1996). "Permissive and obligatory roles of NO in cerebrovascular responses to hypercapnia and acetylcholine." Am J Physiol **271**(4 Pt 2): R990-1001.

Ito, A., S. Hayashi and T. Yoshida (1981). "Participation of a cytochrome b5-like hemoprotein of outer mitochondrial membrane (OM cytochrome b) in NADH-semidehydroascorbic acid reductase activity of rat liver." Biochem Biophys Res Commun **101**(2): 591-598.

Jabaudon, D., K. Shimamoto, Y. Yasuda-Kamatani, M. Scanziani, B. H. Gahwiler and U. Gerber (1999). "Inhibition of uptake unmasks rapid extracellular turnover of glutamate of nonvesicular origin." Proc Natl Acad Sci U S A **96**(15): 8733-8738.

Jackman, K. and C. Iadecola (2015). "Neurovascular regulation in the ischemic brain." Antioxid Redox Signal **22**(2): 149-160.

Jacobs, C. B., T. L. Vickrey and B. J. Venton (2011). "Functional groups modulate the sensitivity and electron transfer kinetics of neurochemicals at carbon nanotube modified microelectrodes." Analyst **136**(17): 3557-3565.

Jaquins-Gerstl, A. and A. C. Michael (2009). "Comparison of the brain penetration injury associated with microdialysis and voltammetry." J Neurosci Methods **183**(2): 127-135.

John P. Lowry, M. R. R. a. R. D. O. N. (1998). "Behaviourally induced changes in extracellular levels of brain glutamate monitored at 1 s resolution with an implanted biosensor " Analytical Communications **35**(3): 3.

Kevin N. Hascup, E. C. R., Jorge E. Quintero, B. Keith Day, Justin R. Nickell, Francois Pomerleau, Peter Huettl, Jason J. Burmeister, and Greg A. Gerhardt (2006). Second-by-Second Measures of L-Glutamate and Other Neurotransmitters Using Enzyme-Based Microelectrode Arrays Electrochemical methods for neuroscince. L. M. B. Adrian C. Michael, Taylor & Francis Group**:** 408-450.

Kevin N. Hascup, E. R. H., O. Meagan Littrell, Jason M. Hinzman, Catherine E. Werner, Verda A. Davis, Jason J. Burmeister, Francois Pomerleau, Jorge E. Quintero, Peter Huettl, and Greg A. Gerhardt (2013). Microelectrode Array Fabrication and Optimization for Selective Neurochemical Detection. Microelectrode Biosensors. N. D. Stéphane Marinesco, Humana Press**:** 27-55.

Kharitonov, V. G., A. R. Sundquist and V. S. Sharma (1994). "Kinetics of nitric oxide autoxidation in aqueous solution." J Biol Chem **269**(8): 5881-5883.

Kim, J. W. (2005). "Ascorbic acid enhances nitric oxide production in trabecular meshwork cells." Korean J Ophthalmol **19**(3): 227-232.

Kiss, J. P. and E. S. Vizi (2001). "Nitric oxide: a novel link between synaptic and nonsynaptic transmission." Trends Neurosci **24**(4): 211-215.

Kitaura, H., N. Uozumi, M. Tohmi, M. Yamazaki, K. Sakimura, M. Kudoh, T. Shimizu and K. Shibuki (2007). "Roles of nitric oxide as a vasodilator in neurovascular coupling of mouse somatosensory cortex." Neurosci Res **59**(2): 160-171.

Kiyatkin, E. A. and G. V. Rebec (1998). "Ascorbate modulates glutamate-induced excitations of striatal neurons." Brain Res **812**(1-2): 14-22.

Knott, A. B. and E. Bossy-Wetzel (2009). "Nitric oxide in health and disease of the nervous system." Antioxid Redox Signal **11**(3): 541-554.

Kulagina, N. V., L. Shankar and A. C. Michael (1999). "Monitoring glutamate and ascorbate in the extracellular space of brain tissue with electrochemical microsensors." Anal Chem **71**(22): 5093-5100.

Ladurner, A., C. A. Schmitt, D. Schachner, A. G. Atanasov, E. R. Werner, V. M. Dirsch and E. H. Heiss (2012). "Ascorbate stimulates endothelial nitric oxide synthase enzyme activity by rapid modulation of its phosphorylation status." Free Radic Biol Med **52**(10): 2082-2090.

Lafon-Cazal, M., S. Pietri, M. Culcasi and J. Bockaert (1993). "NMDA-dependent superoxide production and neurotoxicity." Nature **364**(6437): 535-537.

Lama, R. D., K. Charlson, A. Anantharam and P. Hashemi (2012). "Ultrafast detection and quantification of brain signaling molecules with carbon fiber microelectrodes." Anal Chem **84**(19): 8096-8101.

Lane, D. J. and A. Lawen (2012). "The Glutamate Aspartate Transporter (GLAST) Mediates L: -Glutamate-Stimulated Ascorbate-Release Via Swelling-Activated Anion Channels in Cultured Neonatal Rodent Astrocytes." Cell Biochem Biophys.

Ledo, A., R. M. Barbosa, J. Frade and J. Laranjinha (2002). "Nitric oxide monitoring in hippocampal brain slices using electrochemical methods." Methods Enzymol **359**: 111-125.

Ledo, A., R. M. Barbosa, G. A. Gerhardt, E. Cadenas and J. Laranjinha (2005). "Concentration dynamics of nitric oxide in rat hippocampal subregions evoked by stimulation of the NMDA glutamate receptor." Proc Natl Acad Sci U S A **102**(48): 17483-17488.

Ledo, A., J. Frade, R. M. Barbosa and J. Laranjinha (2004). "Nitric oxide in brain: diffusion, targets and concentration dynamics in hippocampal subregions." Mol Aspects Med **25**(1-2): 75-89.

Li, H., T. K. Kundu and J. L. Zweier (2009). "Characterization of the magnitude and mechanism of aldehyde oxidase-mediated nitric oxide production from nitrite." J Biol Chem **284**(49): 33850-33858.

Li, H. and T. L. Poulos (2005). "Structure-function studies on nitric oxide synthases." J Inorg Biochem **99**(1): 293-305.

Li, H., A. Samouilov, X. Liu and J. L. Zweier (2003). "Characterization of the magnitude and kinetics of xanthine oxidase-catalyzed nitrate reduction: evaluation of its role in nitrite and nitric oxide generation in anoxic tissues." Biochemistry **42**(4): 1150-1159.

Li, J. and C. Iadecola (1994). "Nitric oxide and adenosine mediate vasodilation during functional activation in cerebellar cortex." Neuropharmacology **33**(11): 1453-1461.

Lindauer, U., D. Megow, H. Matsuda and U. Dirnagl (1999). "Nitric oxide: a modulator, but not a mediator, of neurovascular coupling in rat somatosensory cortex." Am J Physiol **277**(2 Pt 2): H799-811.

Liu, A., I. Honma and H. Zhou (2007). "Simultaneous voltammetric detection of dopamine and uric acid at their physiological level in the presence of ascorbic acid using poly(acrylic acid)-multiwalled carbon-nanotube composite-covered glassy-carbon electrode." Biosensors & Bioelectronics **23**(1): 74-80.

Liu, K., Y. Lin, L. Xiang, P. Yu, L. Su and L. Mao (2008). "Comparative study of change in extracellular ascorbic acid in different brain ischemia/reperfusion models with in vivo microdialysis combined with on-line electrochemical detection." Neurochem Int **52**(6): 1247-1255.

Liu, K., Y. Lin, P. Yu and L. Mao (2009). "Dynamic regional changes of extracellular ascorbic acid during global cerebral ischemia: studied with in vivo microdialysis coupled with on-line electrochemical detection." Brain Res **1253**: 161-168.

Liu, X., M. J. Miller, M. S. Joshi, D. D. Thomas and J. R. Lancaster, Jr. (1998). "Accelerated reaction of nitric oxide with O2 within the hydrophobic interior of biological membranes." Proc Natl Acad Sci U S A **95**(5): 2175-2179.

Lourenco, C. F., R. Santos, R. M. Barbosa, G. Gerhardt, E. Cadenas and J. Laranjinha (2011). "In vivo modulation of nitric oxide concentration dynamics upon glutamatergic neuronal activation in the hippocampus." Hippocampus **21**(6): 622-630.

Lourenco, C. F., R. M. Santos, R. M. Barbosa, E. Cadenas, R. Radi and J. Laranjinha (2014). "Neurovascular coupling in hippocampus is mediated via diffusion by neuronal-derived nitric oxide." Free Radic Biol Med **73**: 421-429.

Lovick, T. A., L. A. Brown and B. J. Key (1999). "Neurovascular relationships in hippocampal slices: physiological and anatomical studies of mechanisms underlying flow-metabolism coupling in intraparenchymal microvessels." Neuroscience **92**(1): 47-60.

Luchsinger, J. A., M. X. Tang, S. Shea and R. Mayeux (2003). "Antioxidant vitamin intake and risk of Alzheimer disease." Arch Neurol **60**(2): 203-208.

Lundberg, J. O. (2009). "Cardiovascular prevention by dietary nitrate and nitrite." Am J Physiol Heart Circ Physiol **296**(5): H1221-1223.

Lundberg, J. O., M. T. Gladwin, A. Ahluwalia, N. Benjamin, N. S. Bryan, A. Butler, P. Cabrales, A. Fago, M. Feelisch, P. C. Ford, B. A. Freeman, M. Frenneaux, J. Friedman, M. Kelm, C. G. Kevil, D. B. Kim-Shapiro, A. V. Kozlov, J. R. Lancaster, Jr., D. J. Lefer, K. McColl, K. McCurry, R. P. Patel, J. Petersson, T. Rassaf, V. P. Reutov, G. B. Richter-Addo, A. Schechter, S. Shiva, K. Tsuchiya, E. E. van Faassen, A. J. Webb, B. S. Zuckerbraun, J. L. Zweier and E. Weitzberg (2009). "Nitrate and nitrite in biology, nutrition and therapeutics." Nat Chem Biol **5**(12): 865-869.

Lundberg, J. O. and M. Govoni (2004). "Inorganic nitrate is a possible source for systemic generation of nitric oxide." Free Radic Biol Med **37**(3): 395-400.

Lundberg, J. O. and E. Weitzberg (2010). "The biological role of nitrate and nitrite: the times they are a-changin'." Nitric Oxide **22**(2): 61-63.

Lundberg, J. O., E. Weitzberg and M. T. Gladwin (2008). "The nitrate-nitrite-nitric oxide pathway in physiology and therapeutics." Nat Rev Drug Discov **7**(2): 156-167.

Lundberg, J. O., E. Weitzberg, J. M. Lundberg and K. Alving (1994). "Intragastric nitric oxide production in humans: measurements in expelled air." Gut **35**(11): 1543-1546.

Lyrer, P., H. Landolt, A. Kabiersch, H. Langemann and H. Kaeser (1991). "Levels of low molecular weight scavengers in the rat brain during focal ischemia." Brain Res **567**(2): 317-320.

M DAVIES, J. A., D PARTRIDGE (1991). Vitamin C: Its Chemistry and Biochemistry, The Royal Society of Chemistry.

Ma, Y. L., M. E. Rice, M. L. Chao, P. M. Rivera, H. W. Zhao, A. P. Ross, X. Zhu, M. A. Smith and K. L. Drew (2004). "Ascorbate distribution during hibernation is independent of ascorbate redox state." Free Radic Biol Med **37**(4): 511-520.

Maellaro, E., B. Del Bello, L. Sugherini, A. Santucci, M. Comporti and A. F. Casini (1994). "Purification and characterization of glutathione-dependent dehydroascorbate reductase from rat liver." Biochem J **301 (Pt 2)**: 471-476.

Maggi, C. A. and A. Meli (1986). "Suitability of urethane anesthesia for physiopharmacological investigations in various systems. Part 1: General considerations." Experientia **42**(2): 109-114.

Maggi, C. A. and A. Meli (1986). "Suitability of urethane anesthesia for physiopharmacological investigations in various systems. Part 2: Cardiovascular system." Experientia **42**(3): 292-297.

Maggi, C. A. and A. Meli (1986). "Suitability of urethane anesthesia for physiopharmacological investigations. Part 3: Other systems and conclusions." Experientia **42**(5): 531-537.

Magistretti, P. J. (2006). "Neuron-glia metabolic coupling and plasticity." J Exp Biol **209**(Pt 12): 2304-2311.

Magistretti, P. J., L. Pellerin, D. L. Rothman and R. G. Shulman (1999). "Energy on demand." Science **283**(5401): 496-497.

Majewska, M. D., J. A. Bell and E. D. London (1990). "Regulation of the NMDA receptor by redox phenomena: inhibitory role of ascorbate." Brain Res **537**(1-2): 328-332.

Malinauskas, A., R. Garjonyt, R. Mazeikien and I. Jureviciut (2004). "Electrochemical response of ascorbic acid at conducting and electrogenerated polymer modified electrodes for electroanalytical applications: a review." Talanta **64**(1): 121-129.

Malinski, T., S. Mesaros and P. Tomboulian (1996). "Nitric oxide measurement using electrochemical methods." Methods Enzymol **268**: 58-69.

Malinski, T. and Z. Taha (1992). "Nitric oxide release from a single cell measured in situ by a porphyrinic-based microsensor." Nature **358**(6388): 676-678.

Marques, C. F. L. (2011). In vivo Nitric Oxide Concentration Dynamics Induced by Glutamatergic Neuronal Activation in Rat Brain and Its Role In Neurovascular Coupling. PhD, Universidade de Coimbra.

Martoft, L., H. Stodkilde-Jorgensen, A. Forslid, H. D. Pedersen and P. F. Jorgensen (2003). "CO2 induced acute respiratory acidosis and brain tissue intracellular pH: a 31P NMR study in swine." Lab Anim **37**(3): 241-248.

May, J. M. (2012). "Vitamin C transport and its role in the central nervous system." Subcell Biochem **56**: 85-103.

May, J. M., C. E. Cobb, S. Mendiratta, K. E. Hill and R. F. Burk (1998). "Reduction of the ascorbyl free radical to ascorbate by thioredoxin reductase." J Biol Chem **273**(36): 23039-23045.

May, J. M., L. Li, K. Hayslett and Z. C. Qu (2006). "Ascorbate transport and recycling by SH-SY5Y neuroblastoma cells: response to glutamate toxicity." Neurochem Res **31**(6): 785-794.

May, J. M., Z. Qu and C. E. Cobb (2000). "Extracellular reduction of the ascorbate free radical by human erythrocytes." Biochem Biophys Res Commun **267**(1): 118-123.

Mayer, M. L. and N. Armstrong (2004). "Structure and function of glutamate receptor ion channels." Annu Rev Physiol **66**: 161-181.

McLamore, E. S., S. Mohanty, J. Shi, J. Claussen, S. S. Jedlicka, J. L. Rickus and D. M. Porterfield (2010). "A self-referencing glutamate biosensor for measuring real time neuronal glutamate flux." J Neurosci Methods **189**(1): 14-22.

McMahon, C. P., G. Rocchitta, P. A. Serra, S. M. Kirwan, J. P. Lowry and R. D. O'Neill (2006). "The efficiency of immobilised glutamate oxidase decreases with surface enzyme loading: an electrostatic effect, and reversal by a polycation significantly enhances biosensor sensitivity." Analyst **131**(1): 68-72.

Mefford, I. N., A. F. Oke and R. N. Adams (1981). "Regional distribution of ascorbate in human brain." Brain Res **212**(1): 223-226.

Mehlhorn, R. J. (1991). "Ascorbate- and dehydroascorbic acid-mediated reduction of free radicals in the human erythrocyte." J Biol Chem **266**(5): 2724-2731.

Michael, D. J. and R. M. Wightman (1999). "Electrochemical monitoring of biogenic amine neurotransmission in real time." J Pharm Biomed Anal **19**(1-2): 33-46.

Michael, L. M. B. a. A. C. (2006). An Introduction to Electrochemical Methods in Neuroscience Electrochemical methods for neuroscience, Taylor & Francis Group.

Miele, M., M. G. Boutelle and M. Fillenz (1994). "The physiologically induced release of ascorbate in rat brain is dependent on impulse traffic, calcium influx and glutamate uptake." Neuroscience **62**(1): 87-91.

Milby, K. H., I. N. Mefford, W. Chey and R. N. Adams (1981). "In vitro and in vivo depolarization coupled efflux of ascorbic acid in rat brain preparations." Brain Res Bull **7**(3): 237-242.

Millar, J. (1995). "The nitric oxide/ascorbate cycle: how neurones may control their own oxygen supply." Med Hypotheses **45**(1): 21-26.

Millar, T. M., C. R. Stevens, N. Benjamin, R. Eisenthal, R. Harrison and D. R. Blake (1998). "Xanthine oxidoreductase catalyses the reduction of nitrates and nitrite to nitric oxide under hypoxic conditions." FEBS Lett **427**(2): 225-228.

Miller, B. R., J. L. Dorner, K. D. Bunner, T. W. Gaither, E. L. Klein, S. J. Barton and G. V. Rebec (2012). "Up-regulation of GLT1 reverses the deficit in cortically evoked striatal ascorbate efflux in the R6/2 mouse model of Huntington's disease." J Neurochem **121**(4): 629-638.

Milsom, A. B., B. O. Fernandez, M. F. Garcia-Saura, J. Rodriguez and M. Feelisch (2012). "Contributions of nitric oxide synthases, dietary nitrite/nitrate, and other sources to the formation of NO signaling products." Antioxid Redox Signal **17**(3): 422-432.

Mitala, C. M., Y. Wang, L. M. Borland, M. Jung, S. Shand, S. Watkins, S. G. Weber and A. C. Michael (2008). "Impact of microdialysis probes on vasculature and dopamine in the rat striatum: a combined fluorescence and voltammetric study." J Neurosci Methods **174**(2): 177-185.

Moller, M., H. Botti, C. Batthyany, H. Rubbo, R. Radi and A. Denicola (2005). "Direct measurement of nitric oxide and oxygen partitioning into liposomes and low density lipoprotein." J Biol Chem **280**(10): 8850-8854.

Moncada, S. and A. Higgs (1993). "The L-arginine-nitric oxide pathway." N Engl J Med **329**(27): 2002-2012.

Montine, T. J., M. D. Neely, J. F. Quinn, M. F. Beal, W. R. Markesbery, L. J. Roberts and J. D. Morrow (2002). "Lipid peroxidation in aging brain and Alzheimer's disease." Free Radic Biol Med **33**(5): 620-626.

Moore, P. K. and P. A. Bland-Ward (1996). "7-nitroindazole: an inhibitor of nitric oxide synthase." Methods Enzymol **268**: 393-398.

Moore, P. K., P. Wallace, Z. Gaffen, S. L. Hart and R. C. Babbedge (1993). "Characterization of the novel nitric oxide synthase inhibitor 7-nitro indazole and related indazoles: antinociceptive and cardiovascular effects." Br J Pharmacol **110**(1): 219-224.

Moriyama, Y., M. Hayashi, H. Yamada, S. Yatsushiro, S. Ishio and A. Yamamoto (2000). "Synaptic-like microvesicles, synaptic vesicle counterparts in endocrine cells, are involved in a novel regulatory mechanism for the synthesis and secretion of hormones." J Exp Biol **203**(Pt 1): 117-125.

Morris, M. C., L. A. Beckett, P. A. Scherr, L. E. Hebert, D. A. Bennett, T. S. Field and D. A. Evans (1998). "Vitamin E and vitamin C supplement use and risk of incident Alzheimer disease." Alzheimer Dis Assoc Disord **12**(3): 121-126.

Mortensen, A. and J. Lykkesfeldt (2013). "Does vitamin C enhance nitric oxide bioavailability in a tetrahydrobiopterin-dependent manner? In vitro, in vivo and clinical studies." Nitric Oxide.

Muller-Delp, J. M. (2009). "Ascorbic acid and tetrahydrobiopterin: looking beyond nitric oxide bioavailability." Cardiovasc Res **84**(2): 178-179.

Mungrue, I. N., D. S. Bredt, D. J. Stewart and M. Husain (2003). "From molecules to mammals: what's NOS got to do with it?" Acta Physiol Scand **179**(2): 123-135.

N. S. Neghmouche, T. L. (2013). "Calculation of electrochemical parameters starting from the polarization curves of ferrocene at glassy carbon electrode." International Letters of Chemistry, Physics and Astronomy **4**: 9.

Nagayama, H., M. Hamamoto, M. Ueda, C. Nito, H. Yamaguchi and Y. Katayama (2004). "The effect of ascorbic acid on the pharmacokinetics of levodopa in elderly patients with Parkinson disease." Clin Neuropharmacol **27**(6): 270-273.

Newaz, M. A., Z. Yousefipour and N. N. Nawal (2005). "Modulation of nitric oxide synthase activity in brain, liver, and blood vessels of spontaneously hypertensive rats by ascorbic acid: protection from free radical injury." Clin Exp Hypertens **27**(6): 497-508.

Nuno R. Ferreira, A. L., Joao G. Frade, Greg A. Gerhardt,Joao Laranjinha, Rui M. Barbosa (2005). "Electrochemical measurement of endogenously produced nitric oxide in brain slices using Nafion/o-phenylenediamine modified carbon fiber microelectrodes." Analytica Chimica Acta **535**(1-2): 1-7.

O'Neill, R. D., M. Fillenz, L. Sundstrom and J. N. Rawlins (1984). "Voltammetrically monitored brain ascorbate as an index of excitatory amino acid release in the unrestrained rat." Neurosci Lett **52**(3): 227-233.

Oberg, P. A. (1990). "Laser-Doppler flowmetry." Crit Rev Biomed Eng **18**(2): 125-163.

Okazaki, T., H. Otani, T. Shimazu, K. Yoshioka, M. Fujita and T. Iwasaka (2011). "Ascorbic acid and N-acetyl cysteine prevent uncoupling of nitric oxide synthase and increase tolerance to ischemia/reperfusion injury in diabetic rat heart." Free Radic Res.

Oke, A. F., L. May and R. N. Adams (1987). "Ascorbic acid distribution patterns in human brain. A comparison with nonhuman mammalian species." Ann N Y Acad Sci **498**: 1-12.

Oldenziel, W. H., G. Dijkstra, T. I. Cremers and B. H. Westerink (2006). "Evaluation of hydrogel-coated glutamate microsensors." Anal Chem **78**(10): 3366-3378.

Oldenziel, W. H., G. Dijkstra, T. I. Cremers and B. H. Westerink (2006). "In vivo monitoring of extracellular glutamate in the brain with a microsensor." Brain Res **1118**(1): 34-42.

Oldenziel, W. H. and B. H. Westerink (2005). "Improving glutamate microsensors by optimizing the composition of the redox hydrogel." Anal Chem **77**(17): 5520-5528.

Pacher, P., J. S. Beckman and L. Liaudet (2007). "Nitric oxide and peroxynitrite in health and disease." Physiol Rev **87**(1): 315-424.

Pagliardini, S., S. Gosgnach and C. T. Dickson (2013). "Spontaneous sleep-like brain state alternations and breathing characteristics in urethane anesthetized mice." PLoS One **8**(7): e70411.

Parfenova, H., P. Hsu and C. W. Leffler (1995). "Dilator prostanoid-induced cyclic AMP formation and release by cerebral microvascular smooth muscle cells: inhibition by indomethacin." J Pharmacol Exp Ther **272**(1): 44-52.

Parikh, V., J. Ji, M. W. Decker and M. Sarter (2010). "Prefrontal beta2 subunit-containing and alpha7 nicotinic acetylcholine receptors differentially control glutamatergic and cholinergic signaling." J Neurosci **30**(9): 3518-3530.

Parle, M. and D. Dhingra (2003). "Ascorbic Acid: a promising memory-enhancer in mice." J Pharmacol Sci **93**(2): 129-135.

Patneau, D. K. and M. L. Mayer (1990). "Structure-activity relationships for amino acid transmitter candidates acting at N-methyl-D-aspartate and quisqualate receptors." J Neurosci **10**(7): 2385-2399.

Pellerin, L., A. K. Bouzier-Sore, A. Aubert, S. Serres, M. Merle, R. Costalat and P. J. Magistretti (2007). "Activity-dependent regulation of energy metabolism by astrocytes: an update." Glia **55**(12): 1251-1262.

Pellerin, L. and P. J. Magistretti (1994). "Glutamate uptake into astrocytes stimulates aerobic glycolysis: a mechanism coupling neuronal activity to glucose utilization." Proc Natl Acad Sci U S A **91**(22): 10625-10629.

Pelligrino, D. A., R. L. Gay, 3rd, V. L. Baughman and Q. Wang (1996). "NO synthase inhibition modulates NMDA-induced changes in cerebral blood flow and EEG activity." Am J Physiol **271**(3 Pt 2): H990-995.

Pereira, C., N. R. Ferreira, B. S. Rocha, R. M. Barbosa and J. Laranjinha (2013). "The redox interplay between nitrite and nitric oxide: From the gut to the brain." Redox Biol **1**: 276-284.

Perimed. (2015). "Laser Doppler Monitoring." 2015, from http://www.perimed-instruments.com/laser-doppler-monitoring.

Peter Capella, B. G., Kim Mitchell, Ralph N. Adams (1990). "Nafion-coated carbon fiber electrodes for neurochemical studies in brain tissue." Electroanalysis **2**(3): 175–182.

Pierce, R. C. and G. V. Rebec (1993). "Intraneostriatal administration of glutamate antagonists increases behavioral activation and decreases neostriatal ascorbate via nondopaminergic mechanisms." J Neurosci **13**(10): 4272-4280.

Piknova, B., A. Kocharyan, A. N. Schechter and A. C. Silva (2011). "The role of nitrite in neurovascular coupling." Brain Res **1407**: 62-68.

Ping, J. F., J. Wu, Y. X. Wang and Y. B. Ying (2012). "Simultaneous determination of ascorbic acid, dopamine and uric acid using high-performance screen-printed graphene electrode." Biosensors & Bioelectronics **34**(1): 70-76.

Pogun, S., V. Dawson and M. J. Kuhar (1994). "Nitric oxide inhibits 3H-glutamate transport in synaptosomes." Synapse **18**(1): 21-26.

Pomerleau, F., B. K. Day, P. Huettl, J. J. Burmeister and G. A. Gerhardt (2003). "Real time in vivo measures of L-glutamate in the rat central nervous system using ceramic-based multisite microelectrode arrays." Ann N Y Acad Sci **1003**: 454-457.

Portugal, C. C., T. G. da Encarnacao, R. Socodato, S. R. Moreira, D. Brudzewsky, A. F. Ambrosio and R. Paes-de-Carvalho (2012). "Nitric oxide modulates sodium vitamin C transporter 2 (SVCT-2) protein expression via protein kinase G (PKG) and nuclear factor-kappaB (NF-kappaB)." J Biol Chem **287**(6): 3860-3872.

Portugal, C. C., V. S. Miya, C. Calaza Kda, R. A. Santos and R. Paes-de-Carvalho (2009). "Glutamate receptors modulate sodium-dependent and calcium-independent vitamin C bidirectional transport in cultured avian retinal cells." J Neurochem **108**(2): 507-520.

Pratico, D. (2002). "Alzheimer's disease and oxygen radicals: new insights." Biochem Pharmacol **63**(4): 563-567.

Presley, T. D., A. R. Morgan, E. Bechtold, W. Clodfelter, R. W. Dove, J. M. Jennings, R. A. Kraft, S. B. King, P. J. Laurienti, W. J. Rejeski, J. H. Burdette, D. B. Kim-Shapiro and G. D. Miller (2011). "Acute effect of a high nitrate diet on brain perfusion in older adults." Nitric Oxide **24**(1): 34-42.

Quintero, J. E., B. K. Day, Z. Zhang, R. Grondin, M. L. Stephens, P. Huettl, F. Pomerleau, D. M. Gash and G. A. Gerhardt (2007). "Amperometric measures of age-related changes in glutamate regulation in the cortex of rhesus monkeys." Exp Neurol **208**(2): 238-246.

Rahman, M. A., N. H. Kwon, M. S. Won, E. S. Choe and Y. B. Shim (2005). "Functionalized conducting polymer as an enzyme-immobilizing substrate: an amperometric glutamate microbiosensor for in vivo measurements." Anal Chem **77**(15): 4854-4860.

Raj, C. R. and T. Ohsaka (2001). "Electroanalysis of ascorbate and dopamine at a gold electrode modified with a positively charged self-assembled monolayer." Journal of Electroanalytical Chemistry **496**(1-2): 44-49.

Randles, J. E. B. (1947). "Kinetics of rapid electrode reactions." Discuss. Faraday Society **1**(11-19).

Rebec, G. V. (2007). From Interferant Anion to Neuromodulator: Ascorbate Oxidizes its Way to Respectability. Electrochemical Methods for Neurscience. Boca Raton (FL), CRC Press.

Rebec, G. V., S. J. Barton and M. D. Ennis (2002). "Dysregulation of ascorbate release in the striatum of behaving mice expressing the Huntington's disease gene." J Neurosci **22**(2): RC202.

Rebec, G. V., S. J. Barton, A. M. Marseilles and K. Collins (2003). "Ascorbate treatment attenuates the Huntington behavioral phenotype in mice." Neuroreport **14**(9): 1263-1265.

Rebec, G. V. and R. C. Pierce (1994). "A vitamin as neuromodulator: ascorbate release into the extracellular fluid of the brain regulates dopaminergic and glutamatergic transmission." Prog Neurobiol **43**(6): 537-565.

Rebec, G. V. and Z. Wang (2001). "Behavioral activation in rats requires endogenous ascorbate release in striatum." J Neurosci **21**(2): 668-675.

Rebec, G. V., S. R. Witowski, M. I. Sandstrom, R. D. Rostand and R. T. Kennedy (2005). "Extracellular ascorbate modulates cortically evoked glutamate dynamics in rat striatum." Neurosci Lett **378**(3): 166-170.

Rehncrona, S. (1985). "Brain acidosis." Ann Emerg Med **14**(8): 770-776.

Rice, M. E. (2000). "Ascorbate regulation and its neuroprotective role in the brain." Trends Neurosci **23**(5): 209-216.

Rice, M. E., E. J. Lee and Y. Choy (1995). "High levels of ascorbic acid, not glutathione, in the CNS of anoxia-tolerant reptiles contrasted with levels in anoxia-intolerant species." J Neurochem **64**(4): 1790-1799.

Rice, M. E. and I. Russo-Menna (1998). "Differential compartmentalization of brain ascorbate and glutathione between neurons and glia." Neuroscience **82**(4): 1213-1223.

Rifkind, J. M., E. Nagababu, E. Barbiro-Michaely, S. Ramasamy, R. M. Pluta and A. Mayevsky (2007). "Nitrite infusion increases cerebral blood flow and decreases mean arterial blood pressure in rats: a role for red cell NO." Nitric Oxide **16**(4): 448-456.

Riviere, S., I. Birlouez-Aragon, F. Nourhashemi and B. Vellas (1998). "Low plasma vitamin C in Alzheimer patients despite an adequate diet." Int J Geriatr Psychiatry **13**(11): 749-754.

Rocha, B. S., B. Gago, C. Pereira, R. M. Barbosa, S. Bartesaghi, J. O. Lundberg, R. Radi and J. Laranjinha (2011). "Dietary Nitrite in Nitric Oxide Biology: A Redox Interplay with Implications for Pathophysiology and Therapeutics." Curr Drug Targets **12**(9): 1351-1363.

Roy, C. S. and C. S. Sherrington (1890). "On the Regulation of the Blood-supply of the Brain." J Physiol **11**(1-2): 85-158 117.

Rutherford, E. C., F. Pomerleau, P. Huettl, I. Stromberg and G. A. Gerhardt (2007). "Chronic second-by-second measures of L-glutamate in the central nervous system of freely moving rats." J Neurochem **102**(3): 712-722.

Sandstrom, M. I. and G. V. Rebec (2007). "Extracellular ascorbate modulates glutamate dynamics: role of behavioral activation." BMC Neurosci **8**: 32.

Santhanam, L., H. K. Lim, H. K. Lim, V. Miriel, T. Brown, M. Patel, S. Balanson, S. Ryoo, M. Anderson, K. Irani, F. Khanday, L. Di Costanzo, D. Nyhan, J. M. Hare, D. W. Christianson, R. Rivers, A. Shoukas and D. E. Berkowitz (2007). "Inducible NO synthase dependent S-nitrosylation and

activation of arginase1 contribute to age-related endothelial dysfunction." Circ Res **101**(7): 692-702.

Santos, R. M., C. F. Lourenco, A. P. Piedade, R. Andrews, F. Pomerleau, P. Huettl, G. A. Gerhardt, J. Laranjinha and R. M. Barbosa (2008). "A comparative study of carbon fiber-based microelectrodes for the measurement of nitric oxide in brain tissue." Biosens Bioelectron **24**(4): 704-709.

Santos, R. M., C. F. Lourenco, F. Pomerleau, P. Huettl, G. A. Gerhardt, J. Laranjinha and R. M. Barbosa (2011). "Brain nitric oxide inactivation is governed by the vasculature." Antioxid Redox Signal **14**(6): 1011-1021.

Sarma, A. K., P. Vatsyayan, P. Goswami and S. D. Minteer (2009). "Recent advances in material science for developing enzyme electrodes." Biosens Bioelectron **24**(8): 2313-2322.

Sato, K., H. Saito and H. Katsuki (1993). "Synergism of tocopherol and ascorbate on the survival of cultured brain neurones." Neuroreport **4**(10): 1179-1182.

Sayed, N., P. Baskaran, X. Ma, F. van den Akker and A. Beuve (2007). "Desensitization of soluble guanylyl cyclase, the NO receptor, by S-nitrosylation." Proc Natl Acad Sci U S A **104**(30): 12312-12317.

Schaus, R. (1957). "The ascorbic acid content of human pituitary, cerebral cortex, heart, and skeletal muscle and its relation to age." Am J Clin Nutr **5**(1): 39-41.

Schuhmann, W. (2002). "Amperometric enzyme biosensors based on optimised electron-transfer pathways and non-manual immobilisation procedures." J Biotechnol **82**(4): 425-441.

Schuvailo, O. M., O. O. Soldatkin, A. Lefebvre, R. Cespuglio and A. P. Soldatkin (2006). "Highly selective microbiosensors for in vivo measurement of glucose, lactate and glutamate." Anal Chim Acta **573-574**: 110-116.

Shao, Y., M. O. Enkvist and K. D. McCarthy (1994). "Glutamate blocks astroglial stellation: effect of glutamate uptake and volume changes." Glia **11**(1): 1-10.

Sharma, P. (1997). "Consequences of hypoxia on the cell size of neuropeptide-Y neurons and the role of ascorbate in cultured neurons from chick embryo." Neurochem Int **30**(3): 337-344.

Shi, W., C. Liu, Y. Song, N. Lin, S. Zhou and X. Cai (2012). "An ascorbic acid amperometric sensor using over-oxidized polypyrrole and palladium nanoparticles composites." Biosens Bioelectron **38**(1): 100-106.

Shigeri, Y., K. Shimamoto, Y. Yasuda-Kamatani, R. P. Seal, N. Yumoto, T. Nakajima and S. G. Amara (2001). "Effects of threo-beta-hydroxyaspartate derivatives on excitatory amino acid transporters (EAAT4 and EAAT5)." J Neurochem **79**(2): 297-302.

Shimamoto, K., B. Lebrun, Y. Yasuda-Kamatani, M. Sakaitani, Y. Shigeri, N. Yumoto and T. Nakajima (1998). "DL-threo-beta-benzyloxyaspartate, a potent blocker of excitatory amino acid transporters." Mol Pharmacol **53**(2): 195-201.

Shiva, S., Z. Huang, R. Grubina, J. Sun, L. A. Ringwood, P. H. MacArthur, X. Xu, E. Murphy, V. M. Darley-Usmar and M. T. Gladwin (2007). "Deoxymyoglobin is a nitrite reductase that generates nitric oxide and regulates mitochondrial respiration." Circ Res **100**(5): 654-661.

Si Qin, M. v. d. Z. E., Ngabi Wahono,Thomas I. F. H. Cremers, and Ben H. C. Westerink (2013). Monitoring Extracellular Glutamate in the Brain by Microdialysis and Microsensors. Microelectrode Biosensors. N. D. Stéphane Marinesco, Humana Press**:** 153-177.

Siesjo, B. K., J. Folbergrova and V. MacMillan (1972). "The effect of hypercapnia upon intracellular pH in the brain, evaluated by the bicarbonate-carbonic acid method and from the creatine phosphokinase equilibrium." J Neurochem **19**(11): 2483-2495.

Siushansian, R., S. J. Dixon and J. X. Wilson (1996). "Osmotic swelling stimulates ascorbate efflux from cerebral astrocytes." J Neurochem **66**(3): 1227-1233.

Smith, M. L., R. von Hanwehr and B. K. Siesjo (1986). "Changes in extra- and intracellular pH in the brain during and following ischemia in hyperglycemic and in moderately hypoglycemic rats." J Cereb Blood Flow Metab **6**(5): 574-583.

Sotiriou, S., S. Gispert, J. Cheng, Y. Wang, A. Chen, S. Hoogstraten-Miller, G. F. Miller, O. Kwon, M. Levine, S. H. Guttentag and R. L. Nussbaum (2002). "Ascorbic-acid transporter Slc23a1 is essential for vitamin C transport into the brain and for perinatal survival." Nat Med **8**(5): 514-517.

Spiegelhalder, B., G. Eisenbrand and R. Preussmann (1976). "Influence of dietary nitrate on nitrite content of human saliva: possible relevance to in vivo formation of N-nitroso compounds." Food Cosmet Toxicol **14**(6): 545-548.

Squire, L. R. (1992). "Memory and the hippocampus: a synthesis from findings with rats, monkeys, and humans." Psychol Rev **99**(2): 195-231.

Stamford, J. A., Z. L. Kruk and J. Millar (1984). "Regional differences in extracellular ascorbic acid levels in the rat brain determined by high speed cyclic voltammetry." Brain Res **299**(2): 289-295.

Stamford, J. A., P., P., Davidson, C., C.M., J., and Phillips P.E.M. (1995). Fast Cyclic Voltammetry in Brain Slices. Neuromethods. R. N. Adams, Humana Press Inc. **27:** 81-116.

Staub, F., J. Peters, O. Kempski, G. H. Schneider, L. Schurer and A. Baethmann (1993). "Swelling of glial cells in lactacidosis and by glutamate: significance of Cl(-)-transport." Brain Res **610**(1): 69-74.

Steinert, J. R., C. Kopp-Scheinpflug, C. Baker, R. A. Challiss, R. Mistry, M. D. Haustein, S. J. Griffin, H. Tong, B. P. Graham and I. D. Forsythe (2008). "Nitric oxide is a volume transmitter regulating postsynaptic excitability at a glutamatergic synapse." Neuron **60**(4): 642-656.

Steinmeier, R., I. Bondar, C. Bauhuf and R. Fahlbusch (2002). "Laser Doppler flowmetry mapping of cerebrocortical microflow: characteristics and limitations." Neuroimage **15**(1): 107-119.

Stephens, M. L., J. E. Quintero, F. Pomerleau, P. Huettl and G. A. Gerhardt (2011). "Age-related changes in glutamate release in the CA3 and dentate gyrus of the rat hippocampus." Neurobiol Aging **32**(5): 811-820.

Stone, J. R. and M. A. Marletta (1994). "Soluble guanylate cyclase from bovine lung: activation with nitric oxide and carbon monoxide and spectral characterization of the ferrous and ferric states." Biochemistry **33**(18): 5636-5640.

Stone, J. R. and M. A. Marletta (1995). "The ferrous heme of soluble guanylate cyclase: formation of hexacoordinate complexes with carbon monoxide and nitrosomethane." Biochemistry **34**(50): 16397-16403.

Swapp, S. (2015). "Scanning Electron Microscopy (SEM)." 2015.

Sydow, K. and T. Munzel (2003). "ADMA and oxidative stress." Atheroscler Suppl **4**(4): 41-51.

System, B.-T. c. E. I. (2015). "Information on EC 1.4.3.11 - L-glutamate oxidase." 2015, from http://www.brenda-enzymes.org/enzyme.php?ecno=1.4.3.11.

Tang, C. M., M. Dichter and M. Morad (1989). "Quisqualate activates a rapidly inactivating high conductance ionic channel in hippocampal neurons." Science **243**(4897): 1474-1477.

Tang, C. M., M. Dichter and M. Morad (1990). "Modulation of the N-methyl-D-aspartate channel by extracellular H+." Proc Natl Acad Sci U S A **87**(16): 6445-6449.

Tatoyan, A. and C. Giulivi (1998). "Purification and characterization of a nitric-oxide synthase from rat liver mitochondria." J Biol Chem **273**(18): 11044-11048.

Tew, G. A., M. Klonizakis, J. Moss, A. D. Ruddock, J. M. Saxton and G. J. Hodges (2011). "Reproducibility of cutaneous thermal hyperaemia assessed by laser Doppler flowmetry in young and older adults." Microvasc Res **81**(2): 177-182.

Thomas, D. D., L. A. Ridnour, J. S. Isenberg, W. Flores-Santana, C. H. Switzer, S. Donzelli, P. Hussain, C. Vecoli, N. Paolocci, S. Ambs, C. A. Colton, C. C. Harris, D. D. Roberts and D. A. Wink (2008). "The chemical biology of nitric oxide: implications in cellular signaling." Free Radic Biol Med **45**(1): 18-31.

Timmerman, W. and B. H. Westerink (1997). "Brain microdialysis of GABA and glutamate: what does it signify?" Synapse **27**(3): 242-261.

Tiwari, I., K. P. Singh, M. Singh and C. E. Banks (2012). "Polyaniline/polyacrylic acid/multi-walled carbon nanotube modified electrodes for sensing ascorbic acid." Analytical Methods **4**(1): 118-124.

Toth, M., Z. Kukor and S. Valent (2002). "Chemical stabilization of tetrahydrobiopterin by L-ascorbic acid: contribution to placental endothelial nitric oxide synthase activity." Mol Hum Reprod **8**(3): 271-280.

Trussell, L. O. and G. D. Fischbach (1989). "Glutamate receptor desensitization and its role in synaptic transmission." Neuron **3**(2): 209-218.

Tsukaguchi, H., T. Tokui, B. Mackenzie, U. V. Berger, X. Z. Chen, Y. Wang, R. F. Brubaker and M. A. Hediger (1999). "A family of mammalian Na+-dependent L-ascorbic acid transporters." Nature **399**(6731): 70-75.

van der Toorn, A., E. Sykova, R. M. Dijkhuizen, I. Vorisek, L. Vargova, E. Skobisova, M. van Lookeren Campagne, T. Reese and K. Nicolay (1996). "Dynamic changes in water ADC, energy metabolism, extracellular space volume, and tortuosity in neonatal rat brain during global ischemia." Magn Reson Med **36**(1): 52-60.

VanDuijn, M. M., K. Tijssen, J. VanSteveninck, P. J. Van Den Broek and J. Van Der Zee (2000). "Erythrocytes reduce extracellular ascorbate free radicals using intracellular ascorbate as an electron donor." J Biol Chem **275**(36): 27720-27725.

Vashist, S. K., D. Zheng, K. Al-Rubeaan, J. H. Luong and F. S. Sheu (2011). "Advances in carbon nanotube based electrochemical sensors for bioanalytical applications." Biotechnol Adv **29**(2): 169-188.

Villalba, J. M., A. Canalejo, J. C. Rodriguez-Aguilera, M. I. Buron, D. J. Moore and P. Navas (1993). "NADH-ascorbate free radical and -ferricyanide reductase activities represent different levels of plasma membrane electron transport." J Bioenerg Biomembr **25**(4): 411-417.

Viry, L., A. Derre, P. Poulin and A. Kuhn (2010). "Discrimination of dopamine and ascorbic acid using carbon nanotube fiber microelectrodes." Phys Chem Chem Phys **12**(34): 9993-9995.

von Hanwehr, R., M. L. Smith and B. K. Siesjo (1986). "Extra- and intracellular pH during near-complete forebrain ischemia in the rat." J Neurochem **46**(2): 331-339.

Wagerle, L. C., P. A. DeGiulio, O. P. Mishra and M. Delivoria-Papadopoulos (1991). "Effect of dexamethasone on cerebral prostanoid formation and pial arteriolar reactivity to CO2 in newborn pigs." Am J Physiol **260**(4 Pt 2): H1313-1318.

Wagner, D. A., D. S. Schultz, W. M. Deen, V. R. Young and S. R. Tannenbaum (1983). "Metabolic fate of an oral dose of 15N-labeled nitrate in humans: effect of diet supplementation with ascorbic acid." Cancer Res **43**(4): 1921-1925.

Walker, M. C., P. T. Galley, M. L. Errington, S. D. Shorvon and J. G. Jefferys (1995). "Ascorbate and glutamate release in the rat hippocampus after perforant path stimulation: a "dialysis electrode" study." J Neurochem **65**(2): 725-731.

Wang, J., M. Musameh and Y. Lin (2003). "Solubilization of carbon nanotubes by Nafion toward the preparation of amperometric biosensors." J Am Chem Soc **125**(9): 2408-2409.

Wang, Q., T. Kjaer, M. B. Jorgensen, O. B. Paulson, N. A. Lassen, N. H. Diemer and H. C. Lou (1993). "Nitric oxide does not act as a mediator coupling cerebral blood flow to neural activity following somatosensory stimuli in rats." Neurol Res **15**(1): 33-36.

Washburn, M. P. and W. W. Wells (1999). "Identification of the dehydroascorbic acid reductase and thioltransferase (Glutaredoxin) activities of bovine erythrocyte glutathione peroxidase." Biochem Biophys Res Commun **257**(2): 567-571.

Watson C., P. G. (2007). The Rat Brain in stereotaxic coordinates, 6th edition, Elsevier Inc.

Wharton, D. C. and S. T. Weintraub (1980). "Identification of nitric oxide and nitrous oxide as products of nitrite reduction by Pseudomonas cytochrome oxidase (nitrate reductase)." Biochem Biophys Res Commun **97**(1): 236-242.

Wilson, G. S. and Y. Hu (2000). "Enzyme-based biosensors for in vivo measurements." Chem Rev **100**(7): 2693-2704.

Wilson, J. X., C. E. Peters, S. M. Sitar, P. Daoust and A. W. Gelb (2000). "Glutamate stimulates ascorbate transport by astrocytes." Brain Res **858**(1): 61-66.

Wink, D. A. and J. B. Mitchell (1998). "Chemical biology of nitric oxide: Insights into regulatory, cytotoxic, and cytoprotective mechanisms of nitric oxide." Free Radic Biol Med **25**(4-5): 434-456.

Winkler, B. S. (1987). "In vitro oxidation of ascorbic acid and its prevention by GSH." Biochim Biophys Acta **925**(3): 258-264.

Winkler, B. S., S. M. Orselli and T. S. Rex (1994). "The redox couple between glutathione and ascorbic acid: a chemical and physiological perspective." Free Radic Biol Med **17**(4): 333-349.

Woolsey, T. A., C. M. Rovainen, S. B. Cox, M. H. Henegar, G. E. Liang, D. Liu, Y. E. Moskalenko, J. Sui and L. Wei (1996). "Neuronal units linked to microvascular modules in cerebral cortex: response elements for imaging the brain." Cereb Cortex **6**(5): 647-660.

Yang, G., G. Chen, T. J. Ebner and C. Iadecola (1999). "Nitric oxide is the predominant mediator of cerebellar hyperemia during somatosensory activation in rats." Am J Physiol **277**(6 Pt 2): R1760-1770.

Yang, G., Y. Zhang, M. E. Ross and C. Iadecola (2003). "Attenuation of activity-induced increases in cerebellar blood flow in mice lacking neuronal nitric oxide synthase." Am J Physiol Heart Circ Physiol **285**(1): H298-304.

Yusa, T. (2001). "Increased extracellular ascorbate release reflects glutamate re-uptake during the early stage of reperfusion after forebrain ischemia in rats." Brain Res **897**(1-2): 104-113.

Zacharia, I. G. and W. M. Deen (2005). "Diffusivity and solubility of nitric oxide in water and saline." Ann Biomed Eng **33**(2): 214-222.

Zhang, M., K. Liu, L. Xiang, Y. Lin, L. Su and L. Mao (2007). "Carbon nanotube-modified carbon fiber microelectrodes for in vivo voltammetric measurement of ascorbic acid in rat brain." Anal Chem **79**(17): 6559-6565.

Zhang, S. M., M. A. Hernan, H. Chen, D. Spiegelman, W. C. Willett and A. Ascherio (2002). "Intakes of vitamins E and C, carotenoids, vitamin supplements, and PD risk." Neurology **59**(8): 1161-1169.

Zhao, X., M. E. Ross and C. Iadecola (2003). "L-Arginine increases ischemic injury in wild-type mice but not in iNOS-deficient mice." Brain Res **966**(2): 308-311.

Zhao, Y. F., Y. Q. Gao, D. P. Zhan, H. Liu, Q. Zhao, Y. Kou, Y. H. Shao, M. X. Li, Q. K. Zhuang and Z. W. Zhu (2005). "Selective detection of dopamine in the presence of ascorbic acid and uric acid by a carbon nanotubes-ionic liquid gel modified electrode." Talanta **66**(1): 51-57.

Zweier, J. L., A. Samouilov and P. Kuppusamy (1999). "Non-enzymatic nitric oxide synthesis in biological systems." Biochim Biophys Acta **1411**(2-3): 250-262.

Zweier, J. L., P. Wang, A. Samouilov and P. Kuppusamy (1995). "Enzyme-independent formation of nitric oxide in biological tissues." Nat Med **1**(8): 804-809.